HELSINKI UNIVERSITY OF TECHNOLOGY
Faculty of Engineering and Architecture
Department of Structural Engineering and Building Technology

Matias Remes

# SOUND INSULATION OF WOODEN DOUBLE-LEAF PARTITIONS

This Master`s Thesis has been submitted for official examination for the degree of Master of Science in Espoo, Finland, 7th September 2009.

Supervisor: Professor Martti Viljanen

Instructors: M.Sc. Heikki Helimäki, Helimäki Acoustics Ltd

M.Sc. Janne Pynnönen, Stora Enso Timber Ltd

## HELSINKI UNIVERSITY OF TECHNOLOGY
## ABSTRACT OF THE MASTER`S THESIS

| | |
|---|---|
| **Author:** | Matias Remes |
| **Name:** | Sound Insulation of Wooden Double-leaf Partitions |
| **Date:** | 7th September 2009 |
| **Number of pages:** | 99 + 49 |
| **Faculty:** | Faculty of Engineering and Architecture |
| **Professorship:** | Structural Engineering and Building Physics, Rak-43 |
| **Supervisor:** | Professor Martti Viljanen |
| **Instructors:** | M.Sc. (Eng.) Heikki Helimäki, Helimäki Acoustics Ltd<br>M.Sc. (Eng.) Janne Pynnönen, Stora Enso Timber Ltd |
| **Keywords:** | Airborne sound insulation, double-leaf partition, wood, flanking transmission, perforated panel, office, noise |

The main goal of the study was to develop three solutions of wooden partitions that could be used in, for example, office buildings for providing sound insulation between work rooms. Three classes of target values were set for the apparent sound reduction index that should be achieved with the new partitions: class 1 $R`_w \geq 55$ dB, class 2 $R`_w \geq 45$ dB, class 3 $R`_w \geq 35$ dB. Additionally, the effect of perforated panels on the sound reduction index of a double-leaf partition was investigated with measurements.

As a starting point, the apparent sound reduction index was measured between rooms separated by a typical partition system. The measurement result was $R`_w = 28$ dB. The results indicated that achieving the target values would require improving the sound reduction indexes of the partitions and sealing of joints as well as diminishing sound transmission via flanking structures. Two literature-based prediction models are presented in the study: one for calculating the sound reduction index of a double-leaf partition and one for estimating the effect of flanking transmission on sound insulation. The models were used for evaluating the means to achieve the target values with the new partition structures.

The new partitions were measured in a test room, yielding the following values of the apparent weighted sound reduction index: class 1 $R`_w = 50$ dB, class 2 $R`_w = 47$ dB, class 3 $R`_w = 43$ dB. The corresponding modelling results in classes 1 – 3 were 48 dB, 47 dB and 40 dB, respectively. The highest target value could not be achieved most likely because of flanking transmission via a continuous plate structure of the test room side wall. Modelling results indicated that it would be possible to achieve the target value by diminishing flanking transmission via the side wall junction. The measurement results of perforated panels suggested that a sound insulation level of $R`_w \geq 35$ dB can be achieved with a double-leaf partition, even if over half of one of the partition surfaces consisted of perforated panels.

The prediction models proved as a valuable tool for product development. Compared to measurement results, the sound insulation level that could be achieved with the partitions could be modelled to good accuracy. In the light of the results, flanking transmission via tangential structures should be taken into consideration especially when a high level of sound insulation is striven for. Future research should consider how the sound reduction index of a wooden double-leaf partition could be improved by diminishing sound transmission via stiff wooden studs. The effect of perforated panels on sound insulation should be investigated more extensively.

**TEKNILLINEN KORKEAKOULU**
**DIPLOMITYÖN TIIVISTELMÄ**

| | |
|---|---|
| **Tekijä:** | Matias Remes |
| **Työn nimi:** | Sound Insulation of Wooden Double-leaf Partitions |
| **Päivämäärä:** | 7.9.2009 |
| **Sivumäärä:** | 99 + 49 |
| **Tiedekunta:** | Insinööritieteiden ja arkkitehtuurin tiedekunta |
| **Professuuri:** | Talonrakennustekniikka, Rak-43 |
| **Työn valvoja:** | Professori Martti Viljanen |
| **Työn ohjaajat:** | DI Heikki Helimäki, Helimäki Akustikot Oy<br>DI Janne Pynnönen, Stora Enso Timber Ltd |
| **Avainsanat:** | Ilmaääneneristys, kaksinkertainen levyseinä, puurakenne, sivutiesiirtymä, rei`itetty levy, toimisto, melu |


Tutkimuksen tavoitteena oli kehittää kolme puurakenteista väliseinäratkaisua, jotka soveltuvat käytettäväksi esimerkiksi toimistorakennuksissa ääneneristykseen työhuoneiden välillä. Väliseinillä saavutettavalle ilmaääneneristysluvulle asettiin tavoitearvot kolmessa luokassa: luokka 1 $R`_w \geq 55$ dB, luokka 2 $R`_w \geq 45$ dB, luokka 3 $R`_w \geq 35$ dB. Työssä selvitettiin lisäksi mittauksien avulla, miten rei`itetyt rakennuslevyt vaikuttavat kaksinkertaisen levyseinän ääneneristävyyteen.

Tutkimuksen lähtökohtana oli huoneiden välillä tyypillisellä väliseinäjärjestelmällä saavutettava ilmaääneneristysluku, jonka arvoksi mitattiin $R`_w = 28$ dB. Tavoitearvojen saavuttamiseksi tuli mittaustulosten perusteella parantaa väliseinien ääneneristävyyttä ja rakenteiden kokonaistiiviyttä sekä vähentää äänen kulkeutumista ympäröivien rakenteiden kautta sivutiesiirtymänä. Työssä esitetään kirjallisuuslähteisiin perustuen mallit, joilla voidaan laskea kaksinkertaisen levyseinän ilmaääneneristävyys sekä arvioida sivutiesiirtymän vaikutusta ääneneristävyyteen. Mallien avulla haettiin keinoja, joilla riittävä ääneneristävyys voitaisiin saavuttaa uusilla rakenneratkaisuilla eri tavoiteluokissa.

Kehitetyt väliseinärakenteet mitattiin testihuoneessa, ja mittauksissa saatiin seuraavat tulokset: luokka 1 $R`_w = 50$ dB, luokka 2 $R`_w = 47$ dB, luokka 3 $R`_w = 43$ dB. Laskentamalleilla saatiin tavoiteluokissa 1 – 3 vastaavat ilmaääneneristyluvut 48 dB, 47 dB ja 40 dB. Todennäköisin syy siihen, että korkeinta tavoitearvoa ei saavutettu testihuoneessa oli ääneneristystä heikentävä sivutiesiirtymä huoneen sivuseinän jatkuvan levyrakenteen kautta. Mallinnustuloksien perusteella tavoitearvo olisi mahdollista saavuttaa vähentämällä sivutiesiirtymää sivuseinäliitoksen kautta. Reikälevyjä sisältävän seinän mittaustulokset osoittivat, että luokkaa $R`_w \geq 35$ dB oleva ääneneristystaso voidaan saavuttaa, vaikka yli puolet huoneita erottavan kaksinkertaisen levyseinän toisesta seinäpuoliskosta koostuisi rei`itetyistä rakennuslevyistä.

Laskentamallit olivat hyödyllinen työkalu tuotekehityksessä ja niillä saatiin mittaustuloksiin verrattuna hyviä arvioita seinärakenteiden ääneneristävyydestä. Saatujen tulosten valossa sivutiesiirtymä väliseiniä ympäröivien rakenteiden kautta tulisi ottaa huomioon varsinkin korkeaa ääneneristystasoa tavoiteltaessa. Jatkotutkimuksessa tulisi selvittää keinoja vähentää äänen kulkeutumista kytketyn kaksinkertaisen levyseinän puurungon kautta. Rei`itettyjen levyjen vaikutusta väliseinien ääneneristävyyteen tulisi tutkia nykyistä laajemmin.

# FOREWORD

The writing work for the Master`s Thesis was carried out at Helsinki University of Technology, Department of Structural Engineering and Building Technology, during spring and early autumn of 2009. The acoustical measurements were conducted at the premises of Idea-Puu Oy in Nummela. The supervisor of the Master`s Thesis was professor Martti Viljanen from the Faculty of Engineering and Architecture, Laboratory of Structural Engineering and Building Physics at TKK and the instructors were M.Sc. Heikki Helimäki from Helimäki Acoustics Ltd and M.Sc. Janne Pynnönen from Stora Enso Timber Ltd.

First of all, I would like to thank the companies who financed the Master`s Thesis project – Stora Enso Timber Ltd and Idea-Puu Oy. Special thanks to Mr Duncan Mayes, Mr Janne Pynnönen and Mr Jouko Silen at Stora Enso Timber as well as Mr Aimo Schroderus and Mr Rami Piipponen at Idea-Puu Oy for creating a pleasant working atmosphere and making the interesting project possible. I would also like to express my thanks to professor Matti Kairi, Department of Forest Products Technology at TKK, for all the valuable organizational efforts during the project.

I would like to give my special thanks to Mr Heikki Helimäki for his expert advise as well as for kindly lending the measurement equipment. Thanks also to Lic.Sc. (Tech.) Mikko Kylliäinen at Helimäki Acoustics Ltd for useful comments and feedback.

I wish to thank professor Martti Viljanen for his valuable advise concerning the text and structure of the thesis. For proofreading and language revisions I would like to thank Mr William Martin at TKK.

I owe my sincere thanks to my family and friends for all the support during my studies.

In Espoo, Finland, 7th September 2009

Matias Remes

# TABLE OF CONTENTS

# LIST OF SYMBOLS

| | | |
|---|---|---|
| $b$ | [m] | Centres distance of studs |
| $b_g$ | [m] | Centres distance of partition gables |
| $c_0$ | [m/s] | Phase velocity of sound in air |
| $c_B$ | [m/s] | Phase velocity of bending waves |
| $c_d$ | [m/s] | Sound velocity in cavity material |
| $c_S$ | [m/s] | Phase velocity of transverse shear waves |
| $d$ | [m] | Distance, cavity thickness of double-leaf partition |
| $f$ | [Hz] | Frequency |
| $f_{br}$ | [Hz] | Bridge frequency |
| $f_c$ | [Hz] | Critical frequency |
| $f_{c1}$ | [Hz] | Lowest resonance frequency of cavity |
| $f_d$ | [Hz] | Resonance frequency of cavity |
| $f_h$ | [Hz] | Transition frequency of bending and shear waves |
| $f_{mam}$ | [Hz] | Mass-air-mass resonance frequency |
| $f_{mn}$ | [Hz] | Natural frequency |
| $f_s$ | [Hz] | Schroeder frequency |
| $f_{11}$ | [Hz] | Lowest natural frequency |
| $h$ | [m] | Plate thickness |
| $m$` | [kg/m$^2$] | Surface density |
| $n$ | [-] | Number of point couplings per unit area, relative impedance |
| | | |
| $A$ | [m$^2$-Sab] | Absorption area |
| $B$ | [Nm] | Bending stiffness per unit width of a plate |
| $C$ | [dB] | Spectrum adaptation term no. 1 in standard ISO 717-1 [27] |
| $C_{tr}$ | [dB] | Spectrum adaptation term no. 2 in standard ISO 717-1 [27] |
| $D$ | [m] | Slit depth |
| $E$ | [N/m$^2$], [-] | Modulus of elasticity, end correction |
| $F_n$ | [dB] | Characteristic sound radiation via flanking structure |
| $FR$ | [-] | Filling ratio |
| $G$ | [Pa] | Modulus of rigidity |
| $K$ | [-] | $K = 2\pi f/c_0$ in the equation of $R_{slit}$ |
| $K_{ij}$ | [dB] | Vibration reduction index |
| $L$ | [m], [-] | Ratio of slit depth to slit width |
| $L_{A,eq}$ | [dB] | A-weighted equivalent sound level |
| $L_{A,eq,T}$ | [dB] | A-weighted equivalent sound level using averaging time $T$ |
| $L_{p,1}$ | [dB] | Sound pressure level in source room |
| $L_{p,2}$ | [dB] | Sound pressure level in receiving room |
| $L_{p\_tot}$ | [dB] | Total sound pressure level |
| $L_x$ | [m] | Plate width |
| $L_y$ | [m] | Plate height |
| $L_{x,c}$ | [m] | Cavity width |
| $L_{y,c}$ | [m] | Cavity height |
| $R$ | [dB] | Sound reduction index |
| $R$` | [dB] | Apparent sound reduction index |

| | | |
|---|---|---|
| $R_0$ | [dB] | Sound reduction index for normal incidence |
| $R_{br}$ | [dB] | Sound reduction index of double-leaf partition with stiff studs |
| $R_f$ | [dB] | Sound reduction index for field incidence |
| $R_{fn}$ | [dB] | Sound reduction index of flanking structure *n* |
| $R_{ideal}$ | [dB] | Ideal sound reduction index |
| $R_{sum}$ | [dB] | Logarithmic sum of sound reduction indexes |
| $R_{real}$ | [dB] | Sound reduction index of double-leaf partition with absorbing cavity |
| $R`_w$ | [dB] | Apparent weighted sound reduction index |
| $R_w$ | [dB] | Weighted sound reduction index |
| $R_{slit}$ | [dB] | Sound reduction index of slit |
| $R_{struct}$ | [dB] | Sound reduction index of solid structure |
| $R_{total}$ | [dB] | Total sound reduction index of combined structure |
| $S$ | [m$^2$] | Area |
| $S_{slit}$ | [m$^2$] | Area of slit |
| $S_{sn}$ | [m$^2$] | Area of flanking structure *n* in source room |
| $S_{rn}$ | [m$^2$] | Area of flanking structure *n* in receiving room |
| $S_{struct}$ | [m$^2$] | Area of solid structure |
| $T$ | [s], [°C] | Reverberation time, temperature |
| $V$ | [m$^3$] | Volume |
| $V_a$ | [m$^3$] | Volume of air in cavity |
| $W$ | [m] | Width of slit |
| $W_i$ | [W] | Incident sound power |
| $W_r$ | [W] | Reflected sound power |
| $W_t$ | [W] | Transmitted sound power |

| | | |
|---|---|---|
| $\alpha$ | [-] | Absorption coefficient |
| $\alpha_c$ | [-] | Absorption coefficient of cavity material |
| $\alpha_{eff}$ | [-] | Effective absorption coefficient of cavity material |
| $\eta$ | [-] | Loss factor |
| $\eta_{int}$ | [-] | Internal loss factor |
| $\lambda_B$ | [m] | Bending wavelength of plate |
| $\mu$ | [-] | Poisson`s ratio |
| $\rho$ | [kg/m$^3$] | Density |
| $\rho_0$ | [kg/m$^3$] | Density of air |
| $\sigma_0$ | [m/s] | Radiation factor for diffuse incidence |
| $\tau$ | [-] | Transmission coefficient |
| $\omega$ | [rad/s] | Angular frequency |
| $\Delta R_{abs}$ | [dB] | Deterioration of ideal sound reduction index |
| $\Delta R_h$ | [dB] | Correction term |
| $\Delta R_M$ | [dB] | Improvement in sound reduction index above bridge frequency |

# List of Abbreviations

| | |
|---|---|
| A | A-weighting |
| ANSI | American National Standards Institute |
| EN | Council of Europe (Euroopan neuvosto) |
| HVAC | Heating, ventilation and air conditioning |
| ISO | International Organization for Standardization |
| MDF | Medium density fiberboard |
| OSB | Oriented strandboard |
| SFS | The Finnish Standards Association |
| SPL | Sound pressure level |
| SRI | Sound reduction index |
| STI | Speech transmission index |

# 1 INTRODUCTION

## 1.1 Background and Scope of Research

Acoustic conditions and noise constitute one of the factors of the indoor climate – along with thermal conditions, air quality and lighting [36]. According to research results, people in Finnish office buildings consider noise as one of the most important indoor climate qualities [6]. Noise has various negative effects in the office working environment: it can disturb concentration and cause distraction, annoyance, stress and impairment in work performance [10] [30]. As about half of the working population in the world works in offices [22], sound insulation and noise control clearly constitute an important area of modern office design.

Architectural layout significantly affects the acoustical conditions in offices and, thus, also the means of noise control. This study concentrates on a closed office layout, where noise abatement between adjacent work rooms essentially requires adequate sound insulation of the intervening partitions. In contrast, the means for noise control in spatially open layouts – the open plan and landscape office – are mostly room acoustical requiring sound absorbing surfaces [10]. Regardless of office layout, the fundamental goal of sound insulation is to attenuate noises – such as unwanted speech and ringing phones – to a level that no longer causes distraction or, at best, to total inaudibility.

Sound insulation is one of the fundamental fields of acoustics which has been studied from the early 20$^{th}$ century. From the early days of acoustical research, there has been a need for developing structures and building products with optimal properties relating to sound insulation and noise control. This demand continues to occupy acoustical researchers of today. As people have become more and more aware of the acoustical aspects in built environment – not the least because of increased noise problems caused by urbanization – sound insulation and noise control are as topic subjects as ever.

Measurements are an essential tool for acoustical research and development. Sound insulation measurements can be conducted in a laboratory, yielding information essentially on the sound reduction properties of single building elements. However, in field conditions the acoustical environment is altogether different: sound traverses from room to room also via tangential structures as a result of which sound insulation deteriorates. In real buildings it is also common that structures contain holes or poorly sealed joints – due to deficient design or careless construction work – which further compromise sound insulation.

In this study, partitions were investigated in field conditions where sound insulation between rooms is a sum of various components. The essential research problem was how to achieve a sufficient level of sound insulation between two office rooms with partition structures that are both lightweight and made of wood or wood-based materials. Possible solutions were limited to double-leaf partitions, consisting of plates over studding and intervening cavity. The secondary research problem related to perforated panels and their effect on sound insulation. Although perforated panels are often used in partitions for room acoustical purposes, little is generally known about the extent to which perforations deteriorate the sound reduction index of a solid partition structure.

The requirement of light weight was set for practical and functional reasons. The easiest solution in offices is to implement the walls between adjacent rooms as lightweight partitions [10]. Indeed, such partitions posses many features that are advantageous compared to massive masonry structures, not the least significant of which relate to easiness of construction and cost-effectiveness. Furthermore, as spatial flexibility is a growing trend in modern office buildings, it is desirable that partitions can be assembled and reassembled with as little effort as possible.

The reason for concentrating on wooden partitions was an intention to show that wood and wood-based building products can be successfully applied to sound insulating structures. While wood has many known favourable qualities – building physical, aesthetical and ecological – acoustically wood is a material somewhat burdened with misconceptions [41].

## 1.2 Goals

The primary goal of the study was to develop three solutions of wooden, lightweight partitions that are suitable for different applications based on their sound insulation properties. The secondary goal was to gain information of how perforated panels affect the sound reduction index of a double-leaf partition.

As a boundary condition, it was required that the new partitions use wooden studs and wood-based building boards – as opposed to steel studs and gypsum boards – but still have good sound insulation properties. Due to economic and practical reasons, it was also desired that the partitions should have a total thickness below about 200 mm.

The new partitions were divided into three target classes according to the intended application and soundproofing level:

- **Class 1 partitions**
  - Suitable to spaces with high requirements for acoustical privacy
  - Target value for the apparent weighted sound reduction index between adjacent rooms: $R`_w \geq 55$ dB
  - Example of application in offices: between customer-, conference- or management rooms, high requirements for confidentiality
- **Class 2 partitions**
  - Suitable to spaces with increased requirements for sound insulation
  - Target value for the apparent weighted sound reduction index between adjacent rooms: $R`_w \geq 45$ dB
  - Example of application in offices: between single person work rooms, high requirements for sound insulation
- **Class 3 partitions**
  - Suitable to spaces with normal sound insulation requirements

- Target value for the apparent weighted sound reduction index between adjacent rooms: $R`_w \geq 35$ dB
- Example of application in offices: between single person work rooms, moderate requirements for sound insulation

The selection and definition of the three sound insulation levels was based on standard *SFS 5907*, *Acoustical Classification of Buildings* [40]. The standard provides acoustical guidelines for different spaces and building types concerning, for example, airborne sound insulation between adjacent office rooms.

## 1.3 Research Method

The method for developing the partitions consisted of theoretical modelling and field measurements of the apparent sound reduction index. A typical partition system, consisting of two interconnected lightweight partitions, was used as a starting point. The sound insulation properties of these partitions were charted with measurements of the apparent sound reduction index. The purpose of the measurements was to find out the extent to which sound insulation would have to be improved in order to achieve the target values set for the new structures.

Two prediction models were drafted based on literature sources: one for calculating the sound reduction index of a double-leaf partition and one for estimating the apparent sound reduction index between two rooms in the presence of flanking transmission. The prediction models were used for investigating the various means – structural configurations and material parameters – by which the target values could be achieved.

The new partitions were built in a test room and measurements of the apparent sound reduction index were conducted for each partition type. The effect of perforated panels on sound insulation was investigated empirically in the same test room, also utilizing measurements of the apparent sound reduction index.

# 2 NOISE IN THE OFFICE

## 2.1 Effects of Noise on People and Office Working Conditions

In a series of questionnaire studies conducted between 2002 - 2007 in Finnish office buildings, noise was found to be the most important factor of indoor climate affecting work satisfaction in open-plan offices and the second most important factor in a closed office layout with individual work rooms. Extraneous speech overheard from adjacent work places was found to be the single most distracting and annoying noise source in open-plan offices, while other distracting sounds were caused by, for example, ringing phones and people moving in the corridors. [6]

The typical definition of noise found in many textbooks is “unwanted sound”. However, as pointed out by Kryter [31, p. 270], this is a slightly misleading definition since the unwantedness does not necessarily refer to the sound itself but rather to its information content which is strongly affected by the past experiences of each individual. Speech, for example, can hardly be classified as noise in a lecture hall where the information it provides is of crucial importance. In offices, on the other hand, overheard speech often causes distraction if it is considered as redundant by the hearer. Research results indicate that it is not the level, but intelligibility of speech that generally makes it distracting [28]. Steady “meaningless” broadband noise, such as ventilation humming, rarely has any significant effect on work performance [12].

The main health risks of noise are listed by the *World Health Organization*, *WHO* [23]. These include various physiological effects, such as hearing fatigue and impairment, as well as psychological effects and interferences with social behaviour. From the viewpoint of office working conditions, the most important factors on the list relate to annoyance and work performance. In offices, the primary effects of noise relate to disturbances in concentration and reduced working comfort; office-related noises very rarely cause hearing damage because average noise levels are generally low [28].

When considering the effects of noise on people, subjective and objective factors have to be discerned. The physical properties of noise, such as sound level and spectrum, can be measured objectively. Although the physical factors play an important role, the subjective characteristics of the observer ultimately determine how noise is perceived [15]. The amount of distraction or annoyance caused by noise is highly subjective – for example, even silent background music from a nearby radio in an office work room can be irritating to one worker and cause enjoyment to the other. The factors that affect how noise is perceived by an observer include, for example, the requirement of performed work task on concentration, psychological factors such as observer`s attitudes and information content of the noise as well as observer`s social orientation and other individual characteristics [12] [15].

It has been shown that work performance is most likely to be reduced due to noise if the task is complex, has a high information-load and is cognitively demanding [12]. According to questionnaire studies conducted in Finnish offices, such tasks include word processing, studying, creative thinking and phone conversations [6]. For this reason, persons performing cognitively demanding work tasks should always be situated in well sound-isolated work rooms [10].

There is also evidence that the individual characteristics of the observer, such as personality and temperament, affect noise perception [12]. Although individual characteristics can be difficult to take account of in acoustical design of offices, individually-experienced noise defects can be minimized by designing versatile spaces with more peaceful working rooms for the noise-sensitive individuals [15].

In addition to various psychological and physiological effects, distracting noise in offices also has economic consequences. The more intelligible overheard speech is, the more it causes distraction, decrement in work performance and, ultimately, working time and economic losses [10]. Studies indicate that losses in working time associated with noise distractions are typically most significant in open-plan offices but can be notable in closed work rooms as well [7] [28].

The nature of work task greatly affects the amount of distraction and decrement in work efficiency caused by noise. The location of individual work centres in an office is, thus, an essential design consideration. Work tasks requiring uninterrupted industrial peace, such as tasks of an expert or demanding planning work, should be located in a single work room which is separated from its surroundings with ceiling height partitions. Work tasks involving confidentiality, such as managerial duties, always require an acoustically well-isolated single work room, since none of the conversation is to be distinguished by outsiders. Short-term work tasks, on the other hand, do not necessary require a separate work room, but can be performed in open plan or landscaped offices. [10]

The primary goal of acoustical design in closed work rooms and various open-plan office layouts is essentially the same: providing speech privacy between adjacent work places. However, it is notable that closed work rooms always provide a better standing point for sound insulation, because effective isolation against distracting speech is much easier to achieve with floor to ceiling height partitions than with screens [10].

## 2.2 Evaluation of Speech Distraction

In offices, privacy against obtrusive speech is an essential acoustical design criterion. The general goal is to reduce speech intelligibility between spaces which require good speech privacy and confidentiality as efficiently as possible.

The sound level of speech is one of the significant parameters that affects speech privacy – the louder a voice is used, the more distraction speech causes at the neighbouring work place. A standardized level of speech according to its volume – normal, raised or loud – is given in standard *ANSI S3.5* [9]. The A-weighted sound level of normal speech at a distance of 1 m from the listener in a free field is about 60 dB.

A characteristic of speech is that it does not contain very low or high frequencies, the sound level of speech being greatest at a frequency range of 200 – 5000 Hz [39]. Notably, the sensitivity of the human hearing system is also greatest within this frequency range [39]. Voice communication by speech involves frequencies of about 200 – 8000 Hz, while the frequency range of about 1000 – 3000 Hz is the most important for understanding [30]. The building acoustical frequency range in which sound insulation measurements are typically conducted, 100 – 3150 Hz or 50 – 5000 Hz [10], covers these important frequencies.

The intelligibility of speech between adjacent rooms can be objectively estimated with three factors: sound reduction index, background noise level in the receiving room and speech transmission index [9]. Table 1 illustrates the subjective impression of speech intelligibility between adjacent rooms with different values of apparent weighted sound reduction index, $R`_w$ [dB]. Background noise level in the receiving room is assumed to be $L_{A,eq}$ = 35 dB, which is a typical value in offices [9].

**Table 1.** The subjective impression of the sound reduction index. [9]

| $R`_w$ [dB] | Subjective perception of speech intelligibility in the receiving room |
|---|---|
| > 60 | Loud shout audible, words undistinguishable |
| > 55 | Loud speech not audible |
| > 50 | Loud speech audible, words undistinguishable |
| > 45 | Normal speaking voice not audible |
| > 40 | Normal speaking voice audible, words undistinguishable |
| > 35 | Normal speaking voice audible but not distracting, words distinguishable |
| < 30 | Conversation in the neighbouring room can be heard effortlessly |

The speech transmission index, STI, is a measurable quantity describing the intelligibility of speech. STI has single number values between 0,00…1,00; the higher the value, the better is speech intelligibility. A value of STI = 1,00 indicates that all the syllables in speech are distinguishable, while STI = 0,00 corresponds to totally incomprehensible speech. The speech transmission index depends on the difference of speech and background noise level, reverberation time, the distance between speaker and observer as well as on the directivity of the speaker`s voice and direction in relation to the observer. Figure 1 presents how the STI is associated with background noise level and the apparent weighted sound reduction index when the sound source is speech with normal volume, $L_{A,eq}$ = 65 dB. [9]

Table 2 presents the connection between objective STI-values and subjective impression. It should be noted that, while a high value of the STI is striven for in spaces requiring good speech distinction, such as auditoria and classrooms, in offices the STI should be as low as possible between adjacent work places, since speech privacy is the main goal. It is also notable that even a value of STI = 0,00 does not guarantee that speech is totally inaudible – only that it is undistinguishable [15]. In offices, a value of STI = 0,00 should be achieved between spaces requiring utmost confidentiality [40].

The values of speech transmission index given in Table 2 illustrate the principled difference between closed work rooms and open-plan office space: speech privacy between two closed work rooms is characteristically better than between adjacent work places in an open-plan office. This is due to the fact that effective sound insulation is more difficult to achieve with screens and sound absorbing surface treatments than with full-height partitions [10]. However, the STI increases rapidly increases – and speech privacy deteriorates – as the value of the sound reduction index decreases. Problems related to insufficient speech privacy begin to emerge when background noise level is low, $L_{A,eq} < 35$ dB, and the apparent weighted sound reduction index is below about 30…35 dB [9]. If proper measures are not taken to ensure adequate sound insulation, speech privacy can thus be an issue in closed work rooms as well.

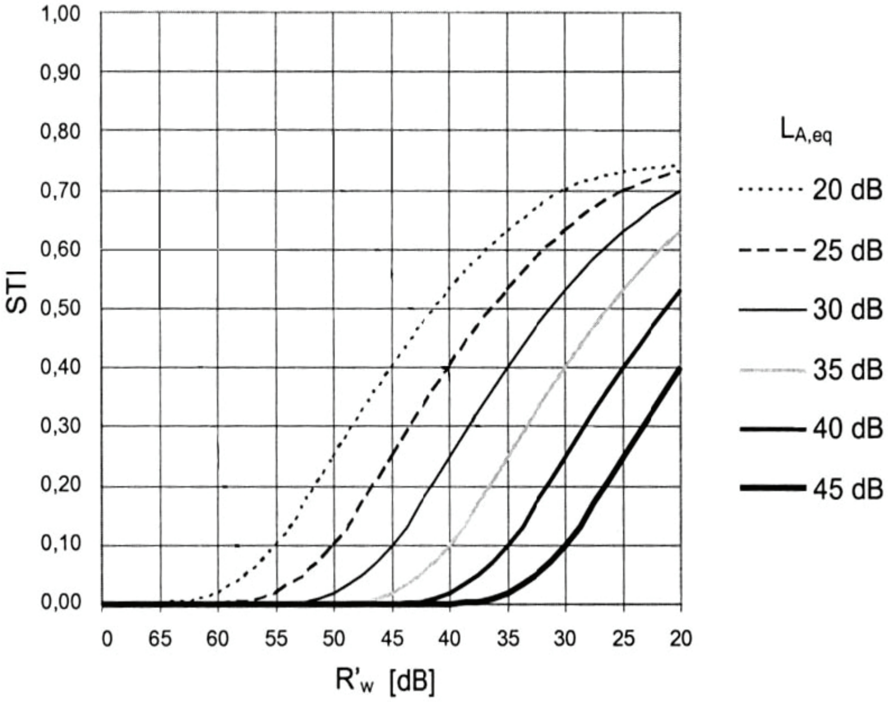


**Figure 1.** Connection between the speech transmission index, STI, the apparent weighted sound reduction index, $R`_w$, and background noise level, $L_{A,eq}$ [40].

**Table 2.** Connection between the speech transmission index and subjective impressions. [9] [40]

| STI | Speech privacy | Example in offices |
|---|---|---|
| < 0.05 | Complete | Between acoustically well-isolated work rooms, doors closed |
| 0.05 – 0.20 | Sufficient | Between work rooms, normal sound insulation, doors closed |
| 0.20 – 0.40 | Good | Between work rooms, doors open to the hallway |
| 0.40 – 0.55 | Reasonable | Open-plan office, acoustically well-designed |
| 0.55 – 0.70 | Tolerable | Open-plan office, small deficiencies in acoustical planning |
| 0.70 – 0.85 | Poor | Open-plan office, notable deficiencies in acoustical planning |
| > 0.85 | Non existent | Open-plan office, no acoustical design |

# 3 Basic Concepts of Sound Insulation and Absorption

## 3.1 Sound Insulation

### 3.1.1 Definition of airborne sound insulation

The purpose of airborne sound insulation is to decrease the amount of sound traversing between adjacent rooms. The basic quantity describing airborne sound insulation is the sound reduction index, *R* [dB], abbreviated as SRI: [16]

$$R = 10\log\frac{1}{\tau} = 10\log_{10}\frac{W_i}{W_t} \tag{1}$$

where $\tau$ is the transmission coefficient, $W_i$ is the sound power incident on a structure and $W_t$ is the transmitted sound power. Equation (1) presupposes that a diffuse sound field is created in the source room [18], which virtually means that sound waves impinge on the surface of the separating partition at myriad, discrete angles of incidence, θ. In reality, the sound reduction index also depends on the incidence angle, reaching the highest value at perpendicular incidence, θ = 0°. The sound reduction index for grazing incidence, θ = 90°, is theoretically zero, although such a case does not exist in practice but the sound reduction index always has non-zero values. [16]

The sound reduction index can be measured in a laboratory or in the field. The measurements are conducted in third-octave- or octave bands at minimum in a frequency range of 100 – 3150 Hz [10]. An extended frequency range of 50 – 5000 Hz can also be used. The apparent sound reduction index between adjacent rooms can be measured by the so-called pressure method described in standard *ISO 140-4* [25] for field measurements. In the pressure method, sound reduction index is determined by Equation [10]

$$R = L_{p,1} - L_{p,2} + 10\log_{10}\frac{S}{A} \tag{2}$$

where $L_{p,2}$ is the sound pressure level in the receiving room and $L_{p,1}$ that in the source room [dB re 20 µPa], *S* is the area of the separating partition [m$^2$] and *A* is the absorption area of the receiving room [m$^2$-Sab]. The absorption area can be determined by the volume *V* [m$^3$] and reverberation time *T* [s] of a room according a formula developed by Wallace Sabine [10]:

$$T = 0{,}16\frac{V}{A} \Leftrightarrow A = 0{,}16\frac{V}{T} \tag{3}$$

### 3.1.2 Measurement of apparent sound reduction index

The field measurement of airborne sound insulation between rooms is described in standard *ISO 140-4*. Assuming that the sound fields in source and receiving rooms are, according to the standard, “sufficiently diffuse”, the apparent sound reduction index, $R`$ [dB], is given by Equation (2). The equation can be applied to both laboratory and field measurements of the sound reduction index. In the case of field measurements, a comma is used in the superscript of *R*. [25]

According to standard *ISO 140-4*, the area of the separating element *S* appearing in Equation (2) is taken as the area common to both rooms. In the case of *S* being less than 10 m$^2$, a value of *max(S, V/7,5)* is used, where *V* is the volume of the receiving room [m$^3$]. The room with larger volume should be chosen as the source room. [25]

The sound source – typically a loudspeaker – in the receiving room should be placed so as to provide as diffuse a sound field in the source room as possible and, according to standard *ISO 140-4*, “at such a distance from the separating element and the flanking elements…that the direct transmission upon them is not dominant”. The minimum number of discrete loudspeaker positions is two if a single sound source is used, and the minimum number of microphone positions is five. The standard also gives instructions on how the microphone positions should selected in relation to room boundaries. [25]

According to *ISO 140-4*, sound insulation measurements are to be conducted at least in third-octave bands of 100 – 3150 Hz, while additional information can be obtained by extending the frequency range to 50 – 5000 Hz. The receiving room absorption area is determined using Equation (3) and reverberation time is measured according to standard *ISO 354* [26]. The sound pressure level in the receiving room should be at least 10 dB higher than the background noise level in all frequency bands. [25]

Standard *ISO 717-1* [27] provides a method for converting the results of sound insulation measurements, conducted in frequency bands according to *ISO 140-4*, into a single-number quantity. For field measurements, the resulting quantity is called the apparent weighted sound reduction index, denoted as $R`_w$, and the corresponding value for laboratory measurements is called the weighted sound reduction index, $R_w$.

According to the method described in *ISO 717-1*, the single-number value of the sound reduction index is determined by comparing the measurement results to the values of a reference curve. The reference curve is shifted in 1 dB steps to the highest possible position, at which the sum of unfavourable deviations between reference and measured values is as large as possible but does not exceed 32,0 dB. Unfavourable deviation means that the measured value of the sound reduction index at a certain frequency band is lower than the corresponding reference value. When the *ISO 717-1* reference curve has been shifted to the correct position, the sound reduction index, $R`_w$ or $R_w$, can be read from the reference curve at 500 Hz. The procedure is illustrated in Figure 2. [26]

The weighted sound reduction index is originally intended for describing how a structure, such as a partition wall, attenuates the A-weighted sound level of speech [10]. If the spectrum of sound to be attenuated differs considerably from the speech spectrum – as is the case with, for example, traffic noise and music – the correlation between the conventional sound reduction index and the subjective impression of sound insulation deteriorates [10]. Spectrum adaptation terms can be used to improve this correlation. The two generally used spectrum adaption terms are denoted as $C$ and $C_{tr}$. The first can be applied to, for example, noise caused by living activities while the latter is mostly used with traffic noise [25]. The equations for calculating the spectrum adaptation terms are given in *ISO 717-1*. It is a common procedure to state the results of sound insulation measurements using the spectrum adaptation terms. In the case of field measurements, the standardized formulation is $R`_w(C; C_{tr})$ [25].

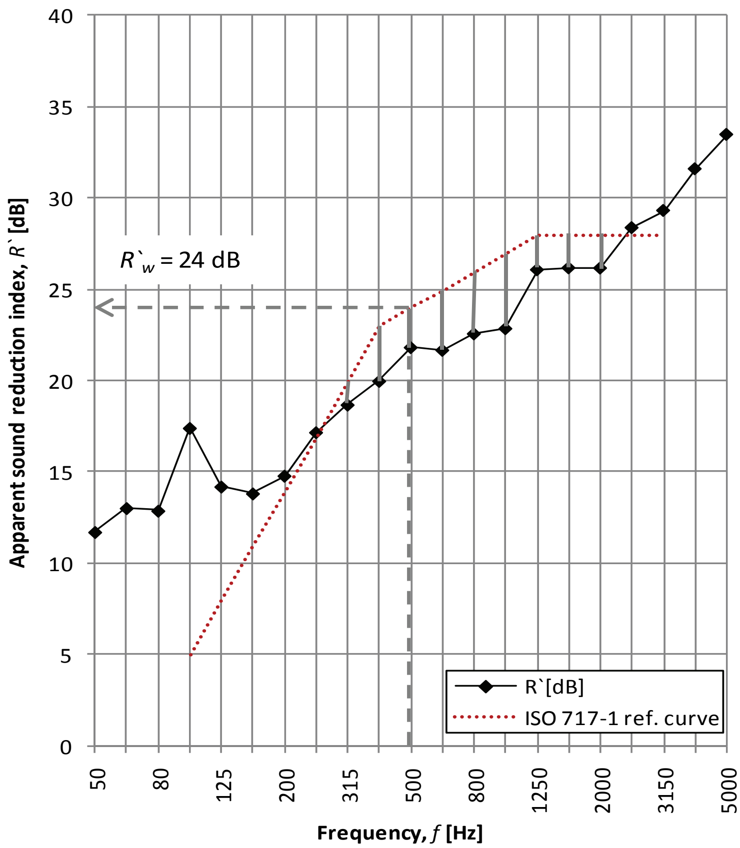


**Figure 2.** The procedure for determining the apparent weighted sound reduction index, $R`_w$, from measurement values. ISO 717-1 reference curve is shifted to a position where the sum of unfavourable deviations does not exceed 32,0 dB. The value of $R`_w$ can then be read from the reference curve at 500 Hz. [25]

### 3.1.3 Sound insulation in offices – general issues

Figure 3 presents a schematic diagram of the factors that generally affect the apparent sound reduction index between two spaces, such as office work rooms. In field conditions, sound insulation depends on, not only the intervening partition, but flanking transmission and possible slits and other sound leaks. Sound insulation is also affected by workmanship and structural details; for example, carelessly sealed junctions or lead-ins penetrating an otherwise compact structure may considerably deteriorate sound insulation. Optimizing the structural section of the separating partition is a fundamental starting point for achieving good sound insulation, but it can only improve the apparent sound reduction index up to a certain point. Achieving a high value of apparent sound reduction index requires taking account of the deteriorating effects of slits and flanking transmission as well.

Flanking transmission means that sound traverses between adjacent rooms via other paths than directly through the separating partition. In the case of structural flanking transmission, the flanking paths consist of tangential structures. Flanking can also occur via air shafts and HVAC lead-ins. As a result of flanking transmission, sound insulation between two rooms in field conditions depends on, not only the separating partition, but also on the tangential structures and their junctions to the separating partition element. [9]

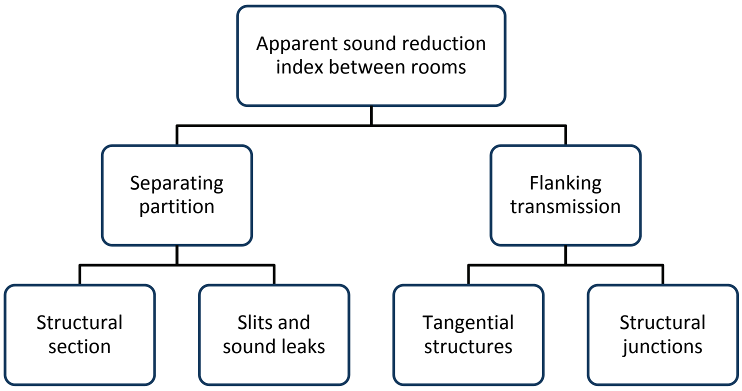


**Figure 3.** Sound reduction index between two rooms depends, not only on the separating partition, but also on flanking transmission and slits.

A clear distinction should be made between two measures of sound insulation: the apparent weighted sound reduction index, $R`_w$, measured in the field, and the corresponding laboratory value weighted sound reduction index, $R_w$. Due to flanking transmission and slits, the first has virtually always a lower value. The apparent sound reduction index is the crucial parameter by which the acoustical quality of buildings should be ultimately judged – a structure which has a poor sound insulation capability in the field is of little use, no matter how high a value of $R_w$ is achieved in the laboratory. [9]

The difference between the values of $R`_w$ and $R_w$ is typically about 3 – 6 dB, but can exceed even 20 dB if the structure contains severe sound leaks. Poorly designed flanking structures can cause a deterioration of 5 – 10 dB to the $R`_w$-value. Nevertheless, the difference between $R`_w$ and $R_w$ can be less than 1 dB if the structural joints are carefully sealed and flanking transmission has been effectively eliminated. [9]

In offices, speech privacy sets demands on the sound insulation of partitions – the higher confidentiality is required and the more demanding work task is performed, the more severe are the demands for sound insulation. The requirement for the apparent weighted sound reduction index between office work rooms is usually in the range of 35 – 44 dB. The easiest way to achieve such a level of sound insulation is to use lightweight partitions. When the requirements for confidentiality are higher, $R`_w$ > 52 dB, careful attention has to be paid to eliminate flanking transmission. Furthermore, sealing of structural joints and slits becomes the more important, the higher sound reduction index is striven for. [10]

Although the most severe challenges related to sound insulation arise in spaces with high requirements for acoustical privacy, the problem of inadequate sound insulation is often found even between conventional office work rooms, where the desired sound insulation level is $R`_w \geq 35$ dB. Some of the typical causes for these problems are listed below. [10]

- The sealing of doors in the partition between work room and hallway is inadequate or carelessly executed. Door sill is missing. In such cases $R`_w$ between the room and corridor is typically in the range of 20 – 25 dB.
- The room has a sliding door with inadequate sealing and structural sound reduction index. As a result, $R`_w$ between the room and corridor rarely exceeds 25 dB.
- The junctions of the partition intervening rooms to adjacent structures are not sealed properly. Inadequate sealing is typical especially in the junction to side wall and roof. Due to inadequate sealing, a value of about 30 dB can be measured for $R`_w$ no matter how high is the laboratory value, $R_w$, of the separating partition.
- Lead-ins for cables and pipes penetrating the partition are not airtight. Even small slits and wholes result in a value $R`_w < 30$, dB although the laboratory value $R_w$ exceeded 40 dB.
- The partition is partly or entirely made of glass with an inadequate sound reduction index. As a guideline, the $R_w$-value of the glazed part has to meet about the same requirements as the partition structure. If the wall is comprised entirely of glass, the $R_w$-value of glass has to exceed the value of $R`_w$ between rooms by 3 – 5 dB.
- Sound traverses as flanking transmission via a continuous suspended ceiling plate and/or continuous inner plate layer of partition between rooms and corridor. Flanking transmission can also occur via continuous exterior wall structure.
- The partition structure does not extend to roof slab. As a result, sound traverses via the cavity above the suspended ceiling.
- Sound traverses via an air shaft with lead-ins to both rooms. If the air shaft lacks a proper silencer, flanking transmission via the shaft deteriorates sound insulation to such a degree that a level of $R`_w > 40$ cannot typically be achieved between rooms.

Sometimes it is possible that speech causes distraction, even though the requirements of apparent sound reduction index between rooms were satisfied. The probable reason for this is inadequate background noise level. In such a case, so-called masking sound can be used to “drown” the distracting speech below the ambient noise level. Another possibility is to further improve sound insulation. [10]

Flanking sound transmission in lightweight structures significantly affects sound insulation between adjacent rooms. Figure 4 illustrates the two typical flanking paths in offices: continuous plate layer in a lightweight partition separating work room from adjacent corridor and the face of a suspended ceiling. A lightweight exterior wall structure constitutes another flanking path that is common in office buildings. In order to minimize flanking transmission, a general rule of a thumb is to truncate any plate layers that extend continuously over partition junctions. The apparent weighted sound reduction index between adjacent rooms is typically below 35 dB, if a plate layer extends continuously from room to room. [10]

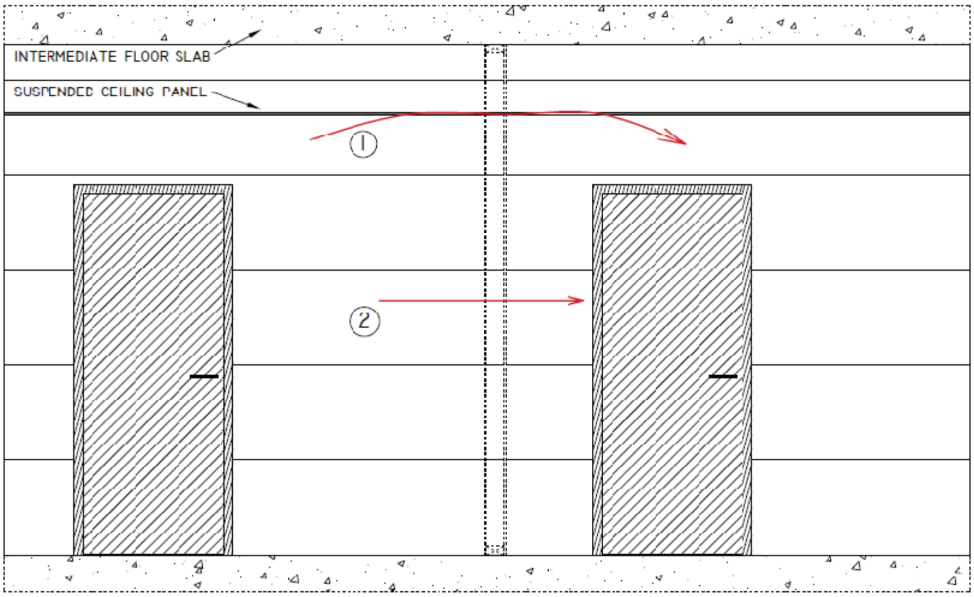


**Figure 4.** Typical flanking paths in offices, adapted from [10]. 1) via continous suspended ceiling panel; 2) via continuous inner plate layer of corridor partition.

It is common that partitions used in offices and public buildings include electrical installations and HVAC lead-ins. Such installations can compromise sound insulation if carelessly executed. As a rule of a thumb, any ducts penetrating a solid partition structure should be carefully sealed and wall sockets should not be installed directly at opposite sides of the partition [21]. In a double-leaf partition it is important that there are no installations in the cavity which might cause coupling between the plates, as this deteriorates sound insulation [21]. The two last-mentioned cases are illustrated in Figure 5.

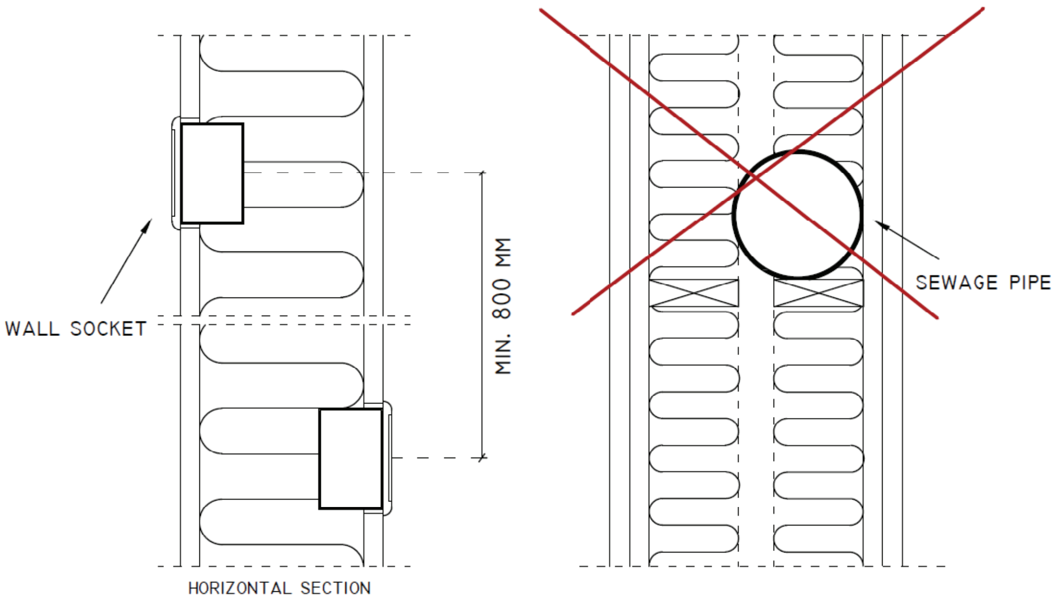


**Figure 5.** Opposite wall sockets should be installed at a sufficient distance from each other. Large pipes etc. should not be installed in the cavity so that the air space between studding is filled. Adapted from [21].

## 3.2 Sound Absorption

### 3.2.1 Significance of sound absorbing wall treatment

A common solution in offices and public buildings is to place the majority, if not all of the sound absorbing material in the ceiling. This is in many ways convenient, since suspended ceilings are generally used. One could then ask, what is the motivation of having partitions with sound absorbing properties – is it not enough to cover the ceiling with sufficient amount of sound absorbent and leave the wall surfaces untreated? Acoustically, such a solution often results in drawbacks: a sound field within a room with smooth, sound reflecting room surfaces and sparse furnishing tends to be unpleasant no matter how effective ceiling absorption is used.

Sound absorbing wall treatments have many room acoustical advantages: they can be used to attenuate unwanted sound reflections and noise level as well as to improve speech acoustical conditions [10] [38]. Insufficient sound absorption in wall surfaces basically means that the attenuation of horizontal sound field is poor, which results in distracting flutter echoes between side walls. In small enclosed spaces, such as office work rooms, such room acoustical defects can be especially problematic. As for larger spaces, such as conference rooms in offices and school classrooms, sound absorbing wall treatments serve a specific room acoustical purpose: they can be used as means to improve speech intelligibility. According to an investigation by Sala and Viljanen [38], absorbing material should be placed on at least one wall surface, along with the conventional ceiling installation, in order to achieve good speech distinction in a classroom.

### 3.2.2 Types of sound absorbers

Sound absorbers can be divided into three main groups depending on their acoustical operational principle and absorption characteristics: porous materials, such as mineral wool, panel or membrane absorbers, consisting of an impervious plate mounted over airspace, and resonators. Perforated panel absorbers constitute an important type of resonators. [39]

The absorption characteristics of sound absorbers can be described by the absorption coefficient, $\alpha$, which indicates the amount of absorbed sound energy according to Equation [9]

$$\alpha = \frac{W_t}{W_i} = \frac{W_i - W_r}{W_i} \tag{4}$$

where $W_t$ is the sound energy transmitted through the absorbing material and $W_i$ and $W_r$ are the energies of incident and reflected sound, respectively. The absorption coefficient has a real number values between 0…1.

Figure 6 illustrates the principled differences in absorption characteristics between the three main absorber types. A characteristic of porous absorbers is effective absorption at high frequencies but compromised low-frequency absorption, while panel absorbers broadly represent the opposite case. Resonators are typically effective only at a narrow frequency range. [13]

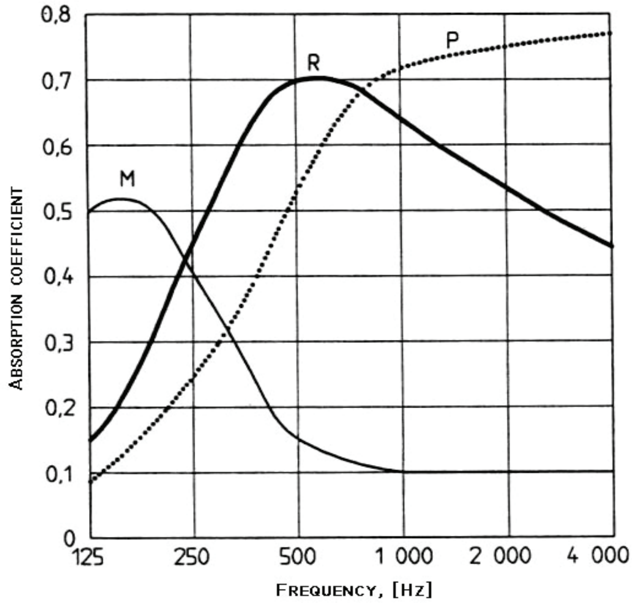


**Figure 6.** Absorption characteristics of common absorber types (principle). P: porous absorber, M: membrane or panel- absorber, R: resonant absorber. Adapted from [13].

The sound absorbing mechanism of porous absorbers – such as mineral wool, glass fiber or open-cell foam – is based on sound energy losses as sound traverses in the cellular structure of the absorbent. Absorption is most efficient at high frequencies, where the losses are mainly due to friction of the movement of the molecules in the absorbent converting sound energy into heat. At low frequencies, absorption is based on isothermal losses and tends to be ineffective. [34]

For porous absorbers to work properly, incident sound waves have to be able to enter the pores of the absorbing material unrestrictedly. Covering the absorbent with thin impervious membrane, for example a plastic sheet or a layer of paint, significantly decreases absorption at high frequencies which is usually highly undesirable. A typical solution is to cover porous material with a perforated facing. This also alters the absorption characteristics of the underlying porous material, mostly depending on the amount of openings in the panel facing, called perforation ratio. As a broad rule, low-frequency absorption improves and high-frequency absorption diminishes as perforation ratio decreases [3].

The aforementioned structure – porous material covered with perforated facing – is called a perforated panel absorber. Such sound absorber consists of a plate, for example a ceiling- or wall tile, with a grid of holes opening to a background airspace that can be totally or partially filled with sound absorbing material. The perforated panel absorber is an application of a Helmholz resonator – a simple resonator structure comprising of an air volume in a cavity within a massive solid, which is connected to air in a room via a small aperture or “neck” [34]. An open bottle is a simple example of a Helmholz resonator.

The Helmholz resonator is essentially a mass-spring system in which the air in the resonator opening acts as a mass and the air within the cavity as a spring. The system absorbs sound effectively at a narrow frequency range around its resonance frequency. The advantage of a perforated panel absorber over a single Helmholz resonator is that, while the absorption of a single Helmholz resonator is effective only at very narrow a frequency band, perforated panels can be designed to yield relatively broad-frequency absorption and also provide mechanical protection for the underlying porous absorbent [34].

Perforated panel absorbers can be used in partitions to control unwanted sound reflections. As pointed out by Cox and D`Antonio [3], flat wooden panels used in surfaces of partitions and ceilings may cause problematic sound reflections compromising speech intelligibility and music quality. Such unwanted reflections can be damped by perforating the panels with a sufficient percentage of open area, which essentially improves sound absorption at high frequencies [3].

### 3.2.3 Effect of sound absorbing treatment on sound insulation

Achieving effective sound absorption requires that sound waves are able to enter the pores of a porous material. If the absorbing material is covered with a plate, such as a building board, this basically requires that the plate is perforated. In a double-leaf partition – with plates installed over studding – there are essentially two ways of implementing such a perforated panel absorber: the absorbing treatment is placed against the partition as a separate structure or one of the plate layers is perforated. These two cases are illustrated in Figure 7. The structure of a conventional double-leaf partition is illustrated on the left for comparison.

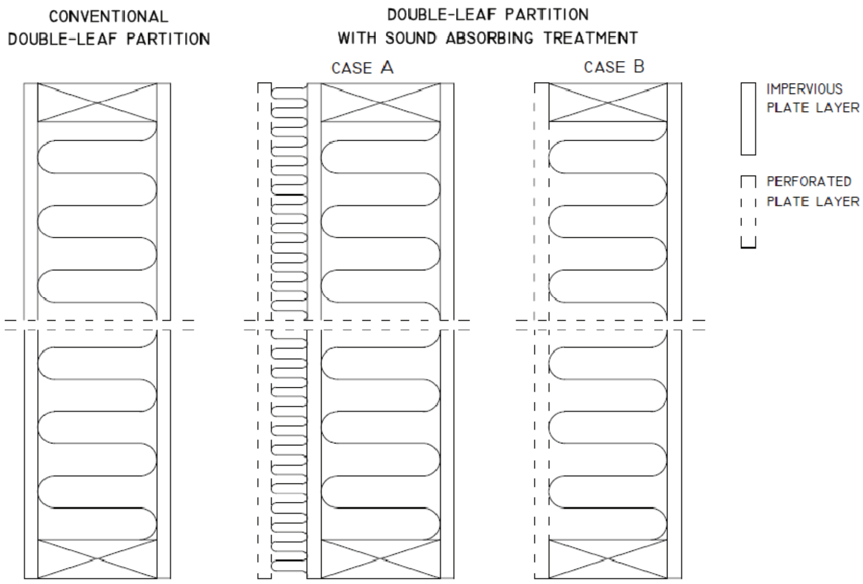


**Figure 7.** Two basic solutions for implementing a sound absorbing treatment into a double-leaf partition using perforated panels.

It is important to distinguish between the acoustical functions of a so-called finishing absorbent and a cavity absorbent. Case A in Figure 7 corresponds to a finishing absorbent, which is placed against an impervious surface and has mainly a room acoustical function. As porous material is enclosed within the cavity of a double-leaf partition, however, its acoustical function and behaviour fundamentally changes. Such a cavity absorbent no longer acts as a room acoustical layer, but its main purpose is to dampen the sound reflections and resonances occurring within the airspace between impervious surface plates [16].

The room acoustical behaviour of structures A and B in Figure 7 is very much similar: in both cases porous material behind the perforated panel surface absorbs the incident sound energy. From a sound insulation point of view, however, there is a significant difference between the two solutions. Whereas the additional layer of absorbing material in case A somewhat improves the overall sound reduction index of the structure, in case B, the sound reduction index deteriorates because the partition no longer contains two, but only one impervious plate layer.

The improvement in sound insulation that can be achieved in case A of Figure 7 can be estimated by considering the sound reduction index of a bare sheet of mineral wool. The sound insulation properties of porous materials can be evaluated in three frequency regions: low-frequency region (A), middle region (B) and high-frequency region (C). In region A, the thickness of the material is considerably smaller than the sound wavelength and the attenuation of sound energy due to friction is insignificant. According to investigations, porous absorbent does not yield any improvement in the sound reduction index when its thickness is less than one tenth of the sound wavelength in the absorbent. At high frequencies, in region C, friction causes sound energy conversion to heat and sound attenuation is most efficient. The improvement in the sound reduction index caused by a porous material layer is also most significant in the high-frequency region. Region B is a transition between the low- and high-frequency regions. As a rule of a thumb, when the thickness of the porous material placed against a structure is below 100 mm, the improvement in sound reduction index is typically limited to frequencies above 200 – 400 Hz. [9] [16]

Hongisto et al. [19] measured the sound reduction indexes of bare mineral wool sheets with different thicknesses, flow resistivities and densities. It was found that the sound reduction index increases with increasing flow resistivity and thickness. As an example of the results, mineral wool sheets with a flow resistivity of 8000 Pa·s/m$^2$ and density of 19 kg/m$^3$ each and thicknesses of 50 mm, 80 mm and 110 mm resulted in weighted sound reduction indexes of $R_w$ = 6 dB, $R_w$ = 10 dB and $R_w$ = 13 dB, respectively. A heavy mineral wool used for fire protection purposes, with a thickness of 50 mm and corresponding material parameters 90000 Pa·s/m$^2$ and 117 kg/m$^3$, had a sound reduction index of $R_w$ = 18 dB. [19]

The overall thickness of a partition is often an essential design consideration. This sets limitations for the thickness of the finishing absorbent as well. If the thickness of the absorbing layer is below 50 mm and a lightweight mineral wool is used, the investigation by Hongisto et al. [19] would indicate that the increase in weighted sound reduction index caused by the finishing absorbent is less than 6 dB. A more notable improvement would require either that the absorbing layer is very thick or that the flow resistivity of the material is substantially higher than with conventionally used mineral wools.

The main acoustical difference between solutions A and B in Figure 7 is that, in case B, sound insulation suffers due to the perforations. It would seem logical to assume that the deterioration in sound insulation depends on the amount of perforated area in the partition. The magnitude of deterioration is, however, difficult to predict. Section 5.6 presents the measurement results that were obtained in this study concerning the effect of perforated panels on sound insulation.

# 4 THEORY AND PREDICTION MODELS

## 4.1 Acoustical Differences Between Partition Types

Lightweight partition walls can be divided into four main categories: single panels, double-leaf partitions, multiple-leaf partitions and sandwich structures [18]. These basic partition types are schematically illustrated in Figure 8.

A double-leaf partition comprises of two impervious plates and an intervening cavity which can be partially or totally filled with a sound absorbing material. The two partition leaves can comprise of several overlapping plates, as long as there is no airspace between them. If there is a physical connection via studs between the two plate layers, the partition is a said to be a coupled structure, whereas in an uncoupled partition the studs are separated from one another by an air space. [9]

The configuration of a multiple-leaf partition is similar to a double-leaf structure, with the exception that the first includes at least three impervious panel layers separated by cavities. A lightweight sandwich structure, on the other hand, comprises of two plates connected to each other via a flexible core material, such as foam or mineral wool, which is attached to both plates with glue [9].

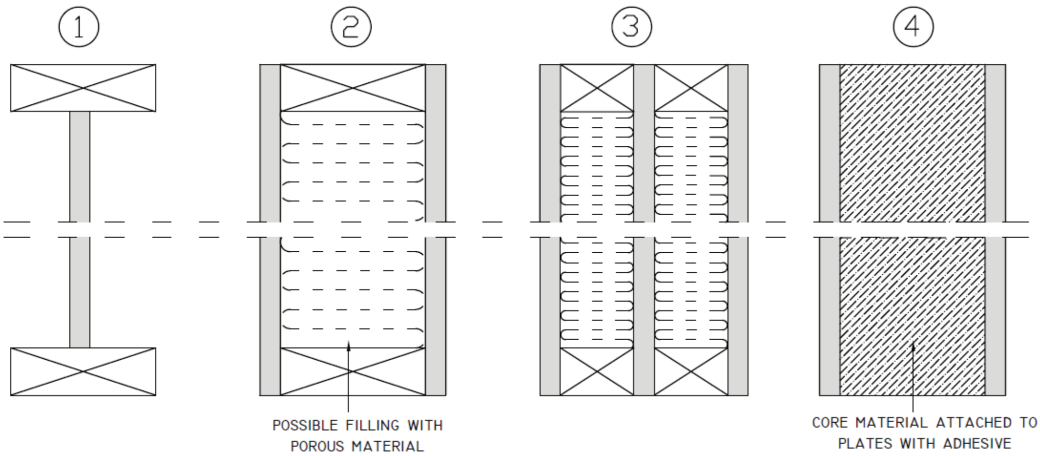


**Figure 8.** The basic types of lightweight partitions. 1) single plate, 2) double-leaf partition, 3) multiple-leaf partition, 4) sandwich structure.

Lightweight sandwich structures are mainly used for production- and fire technical reasons, but their sound insulation capability is considerably weaker than that of an equally thick and heavy double-leaf partition. From the acoustical point of view, the main difference between double-leaf and sandwich structures relates to the core material and its attachment to plates. The core material, such as mineral wool, has a high dynamic stiffness compared to that of air. In a sandwich structure, the core material is also fastened to the plate layers with adhesive. As a result, a strong coupling is caused between the sandwich plates deteriorating sound reduction. [9]

The cause for characteristically poor sound reduction index of sandwich structures is a resonance phenomenon, called dilatation resonance, which is similar to the so-called mass-air-mass resonance associated with double-leaf partitions. The significant difference between the two resonance phenomena is that, whereas the mass-air-mass resonance frequency typically occurs at the lower end of the building acoustical frequency range, dilatation resonance usually falls between 500 and 2000 Hz causing more severe deterioration in sound reduction index. Characteristically of sandwich structures, their sound reduction index does not significantly improve as the thickness of the core material is increased. [9]

Compared to double-leaf partitions, multiple-leaf structures are also problematic due to resonant behaviour. Although it would seem intuitively logical to assume that the sound reduction index improves as the number of individual panel layers increases, this is not the case in reality. In fact, the SRI of a triple-leaf structure – a schematic illustration of which is given in case 3 of Figure 8 – can be considerably lower than that of a conventional double-leaf partition with equal thickness. This was demonstrated in a study by Uris et al. [43]: the sound reduction index of a double-leaf, gypsum board partition decreased by 7 – 8 dB when a third impervious panel layer was inserted in the cavity.

The reason for ineffective sound insulation of multiple-leaf structures is the number of mass-air-mass resonance frequencies, which increases as impervious panel layers are added to the system. In a triple-leaf, plate-cavity-plate-cavity-plate –system there are two such resonance frequencies compared to the single mass-air-mass resonance associated with a double-leaf structure [20]. The additional resonances deteriorate the sound reduction index at low frequencies [32]. It could be said as a broad rule that, although the overall weight of a partition increases as panel layers are added, the improvement in sound reduction index thus gained is typically annulled by the deteriorating effect of additional low-frequency resonances.

The sound insulation theory presented in subsequent chapters concentrates on thin, single plates and double-leaf partitions. Sandwich structures and multiple-leaf partitions will not be discussed further, since double-leaf partitions generally offer a better starting point for achieving effective sound insulation.

## 4.2 Material Properties of Wood and Wood-based Building Boards

Wood is a substance composed primarily of cellulose, hemicelluloses and lignin [42]. The most common wood species in Finland are pine, spruce, birch, aspen, alder and oak, pine and spruce being the most significant raw materials of the domestic building- and carpenter industry [41]. Because wood is a natural material and trees are constantly influenced by changing environmental conditions, there is considerable variation in the physical and mechanical properties between different wood species [42]. As a result, the properties of wood-based building boards used in lightweight partitions also vary. From a sound insulation point of view, the two most important material properties of wood-based building boards are density, $\rho$ [kg/m$^3$], and modulus of elasticity, $E$ [Pa]. Other properties which affect sound insulation include Poisson`s ratio, $\mu$, and loss factor, $\eta$.

Table 3 presents the average density and the modulus of elasticity of common Finnish wood species. Density values are given in a moisture content of 15 % and the elastic moduli correspond to the direction along the wood grain. As a broad rule, wood density ranges from about 150 kg/m$^3$ for beech to 1230 kg/m$^3$ for ebenholz, while the corresponding range for Finnish pine and spruce is 450…500 kg/m$^3$ [41]. The density of wood is characteristically low compared to, for example, masonry building materials and steel.

From the sound insulation viewpoint density is an important material parameter since, together with thickness, it determines the mass per unit area or surface density, $m`$ [kg/m$^2$], of a plate. Surface density largely determines sound insulation at low frequencies according to the so-called mass law; see Section 4.4.1. Mass law states that the sound reduction index increases by 6 dB with a doubling of surface density or frequency. Large surface density alone does not, however, guarantee effective sound insulation, since mass law applies only to a part of the building acoustical frequency range.

**Table 3.** Density and modulus of elasticity of common Finnish wood species. [41]

| Wood species | Density, $\rho$ [kg/m$^3$] | Modulus of elasticity, $E$ [GPa] |
|---|---|---|
| Spruce (*Picea abies*) | 440 | 10.5 |
| Pine (*Pinus Silvestris*) | 480 | 11.8 |
| Aspen (*Populus tremula*) | 490 | 10.5 |
| Alder (*Alnus glutinosa*) | 530 | 10.0 |
| Birch (*Betula sp.*) | 600 | 16.2 |
| Oak (*Guercus sp.*) | 690 | 11.5 |

Modulus of elasticity describes the stiffness of a wood material along its axes and is usually obtained from compression tests [42]. The elastic modulus is acoustically an important material parameter, since it affects the value of the lowest coincidence frequency, also called the critical frequency, around which the sound reduction index steeply deteriorates and falls below the value predicted by mass law. As a rule of a thumb, the critical frequency of a building board should be as high as possible to avoid a decrease in sound reduction index. The critical frequency of a plate is the lower, the higher is the modulus of elasticity and plate thickness and the lower is the surface density [31].

While the values of elastic modulus and density for different wood products used in the building industry are generally well-documented, Poisson`s ratio, $\mu$, and loss factor, $\eta$, are parameters of which there is less material-specific data available in the literature. Poisson`s ratio is defined as the ratio of the transverse to axial strain [42]. There is some ambiguity in the literature relating to what values should be used for Poisson`s ratio. A value of $\mu \approx 0{,}20$ is sometimes applied to building boards [15], while Hongisto and Kylliäinen [9] suggest a corresponding value of $\mu = 0{,}25$. Hopkins [20], on the other hand, gives an estimation of $\mu = 0{,}30$ for different types of building boards.

The total loss factor, $\eta$, comprises of internal losses caused within a building board, coupling losses occurring at the edges of a board as well as radiation losses [33]. A parameter called the internal loss factor, $\eta_{int}$, describes the internal losses. The total loss factor is frequency-dependent but it only has significance above the coincidence frequency [9]. The value of $\eta$ has been found to decrease steadily from 0,10 to 0,01 in the frequency range of 50 – 5000 Hz [16]. Larm et al. [32] have measured an average total loss factor of 0,02 – 0,03 in a frequency range of 100 – 10000 Hz for chipboard, plywood and medium density fiberboard. According to Hongisto and Kylliäinen [9], a constant value of $\eta$ = 0,02 can be used above the critical frequency for building boards attached with screws from the edges.

Table 4 presents a comparison of density, modulus of elasticity, Poisson`s ratio and the internal loss factor of common wood-based building boards and other materials. All the values listed in the table are average values, since there is always some variation in the material-specific properties of building products depending on, for example, the type of the material and manufacturer. Some variation in the properties of wood-based materials is also caused by the orthotropic nature of wood, due to which the values of elastic modulus and Poisson`s ratio differ depending on the direction along the wood axis [42].

**Table 4.** Comparison of the properties of wood-based building boards and other building materials. [11,20,32,46]

| Material | $\rho$ [kg/m$^3$] | $E$ [Gpa] | $\mu$ | $\eta_{int}$ |
|---|---|---|---|---|
| *Wood-based building boards:* | | | | |
| Chipboard | 600 – 800 $^{3)}$ | 2.5 – 3.5 $^{3)}$ | 0.3 $^{2)}$ | 0.01 $^{3)}$ |
| Plywood (birch) | 690 $^{1)}$ | 10.1 – 13.2$^{1)}$ | 0.3 $^{2)}$ | 0.016 $^{3)}$ |
| Plywood (spruce) | 530 $^{1)}$ | 6.5 – 9.6 $^{1)}$ | - | - |
| Structural insulating board | 160 – 480 $^{4)}$ | 0.2 – 0.9 $^{4)}$ | - | - |
| MDF (medium dens. fiberboard) | 530 – 800 $^{4)}$ | 2.2 – 4.8 $^{4)}$ | 0.3 $^{2)}$ | 0.01 $^{3)}$ |
| High density hardboard | 800 – 1280 $^{4)}$ | 2.8 – 5.5 $^{4)}$ | - | - |
| Tempered hardboard | 960 – 1280 $^{4)}$ | 4,5 – 7.6 $^{4)}$ | - | - |
| *Other materials* [32]: | | | | |
| Concrete (heavy) | 2400 – 2500 | 20 – 40 | 0 – 0.2 | 0,005 – 0.02 |
| Gypsum board, normal, GN13 | 700 | 2 – 3 | 0.28 | 0,006 – 0.022 |
| Gypsum board, high dens., EK13 | 880 | 3.2 | 0.28 | - |
| Steel | 7850 | 210 | 0.3 | 0,0001 – 0.0006 |
| Glass | 2500 – 3000 | 70 – 75 | 0.24 | 0,003 – 0.006 |

$^{1)}$ [45] $^{2)}$ [20] $^{3)}$ [32] $^{4)}$ [11]

Larm et al. [33] conducted a survey of Finnish building boards and other plate materials that are conventionally used in partitions. Table 5 lists the material parameters that were measured for wood-based building boards.

**Table 5.** Material parameters of Finnish wood-based building boards according to measurements by Larm et al. [33].

| Building board | Thickness, [mm] | $m$` [kg/m$^2$] | $E$ [Gpa] |
|---|---|---|---|
| Chipboard | 11 | 7.0 | 2,9 |
| Chipboard | 22 | 13.9 | 3,4 |
| Medium density fiberboard | 12 | 9.2 | 6,3 |
| Medium density fiberboard | 19 | 13.8 | 4,8 |
| Plywood | 15 | 10.4 | 11 |
| Plywood | 21 | 15.0 | 11 |

## 4.3 Acoustical Behaviour of Thin Single Plates

### 4.3.1 Wave types

Single plates can be divided into four categories: thin, thick, stiffened, corrugated and poroelastic panels [18]. The following concentrates on the properties of thin plates, of which wood-based building boards are a typical example.

A lightweight partition can be conceived as a structural system constituting of plates and intervening beams, corresponding to studs. The sound insulation characteristics – sound radiation and structure-borne sound transmission – of a partition are largely determined by plates. The studs have a significant effect on structure-borne sound transmission, but their effect on airborne sound radiation is insignificant. [20]

In air and other gases sound propagates as longitudinal waves. In solid plates, however, there are four wave types that contribute to sound propagation: bending waves, transverse shear waves, quasi-longitudinal waves and Rayleigh waves [16]. Bending waves and shear waves are the most important wave types and largely determine the sound reduction properties of partitions [15]. From the practical sound insulation point of view, Rayleigh waves are mostly negligible since they only exist at the surface of very thick plates [15]. Furthermore, sound radiation caused by quasi-longitudinal waves is usually insignificant compared to bending waves [20]. This is because the strains associated with quasi-longitudinal waves are so small that only very little interaction between the vibrating structure and adjacent air molecules is achieved [20]. Thus, quasi-longitudinal waves primarily transmit structure-borne sound and their contribution to airborne sound radiation is insignificant [20].

The phase velocities of bending waves and transverse shear waves, $c_B$ and $c_s$, are given in Equations (5) and (6), respectively [20]:

$$c_B = \sqrt[4]{\frac{\omega^2 B}{m`}} = \sqrt[4]{\frac{4\pi^2 f^2 h^2 E}{12\rho(1-\mu^2)}} \tag{5}$$

$$c_s = \sqrt{\frac{G}{\rho}} = \sqrt{\frac{E}{2\rho(1+\mu)}} \tag{6}$$

where $\omega$ is the angular frequency [Hz] ($\omega = 2\pi f$), $B$ is the bending stiffness per unit width of plate [Nm], $h$ is the plate thickness [m] and $G$ is the modulus of rigidity [Pa]. Bending stiffness of a plate is expressed as [20]

$$B = \frac{Eh^3}{12(1-\mu^2)} \tag{7}$$

For comparison to Equations (5) and (6), the phase velocity of longitudinal sound waves in air is given by an approximate equation [20]

$$c_0 = 331 + 0{,}6T \tag{8}$$

where $T$ is temperature in Celsius [°C]. In a temperature of 20 °C, $c_0$ = 343 m/s.

### 4.3.2 Transition frequencies

Contrary to the other three wave types, bending waves are dispersive, that is, the phase velocity of bending waves is a function of frequency. The frequency at which bending wave phase velocity in a plate equals the phase velocity of longitudinal waves in air, $c_B = c_0$, is called critical frequency, which is determined by the equation [20]

$$f_c = \frac{c_0^2}{2\pi}\sqrt{\frac{m`}{B}} = \frac{c_0^2}{2\pi}\sqrt{\frac{12(1-\mu^2)m`}{Eh^3}} \tag{9}$$

Equation (9) yields the lowest coincidence frequency of a plate, thus it describes the lowest frequency at which the so-called coincidence phenomenon occurs. The critical frequency is achieved when the incidence angle of sound waves impinging on a plate is θ = 90°. [20]

Coincidence phenomenon occurs when the wavelengths of longitudinal sound waves in air and bending waves in a plate are equal. At the lowest coincidence frequency, or critical frequency, a plate constitutes virtually no obstacle for airborne sound hitting its surface and sound reduction is minimal [9]. Below the critical frequency sound radiation from the plate is ineffective and sound insulation is largely determined by surface density [16]. Although coincidence is a narrow-band phenomenon, it is detrimental to the sound reduction index if critical frequency occurs within the building acoustical frequency range.

Figure 9 presents the critical frequency of commonly used building boards as a function of plate thickness. The values were calculated using Equation (9) and the material parameters listed in Table 4. As a broad rule, in order to avoid severe decrement in the sound reduction index caused by the coincidence phenomenon, the critical frequency of building boards used in sound insulating partitions should lie above about 2000 Hz [32]. This limiting frequency is denoted in Figure 9 by a horizontal line.

The critical frequency decreases with increasing plate thickness. When the thickness exceeds a certain point, critical frequency falls in the building acoustical frequency region and sound insulation suffers. The coincidence phenomenon is essentially the reason why, for example, the maximum thickness of gypsum boards used in the building industry is limited to about 15 mm [32]. When comparing the coincidence behaviour of wood-based building boards presented in Figure 9, some broad guidelines can be drawn. In order to minimize the coincidence effect, the thickness of a normal plywood board should not exceed about 7 – 8 mm, whereas the thickness of medium density fiberboards should be limited to about 11 – 12 mm and chipboards to 12 – 13 mm.

Another important resonance frequency which affects the sound insulation properties of plates is called natural frequency. Natural frequencies depend on plate dimensions as well as the critical frequency according to equation

$$f_{mn} = \frac{c_0^2}{4 f_c}\left[\left(\frac{m}{L_x}\right)^2 + \left(\frac{n}{L_y}\right)^2\right] \tag{10}$$

where $L_x$ is the width and $L_y$ the length of the plate [m], *m,n* are integers 0,1,2,… and the critical frequency, $f_c$, is determined by Equation (9). From the sound insulation point of view, the most important natural frequency is the lowest natural frequency, $f_{11}$, at which the plate resonates totally between its joints [15]. The sound reduction index has a minimum at $f_{11}$.

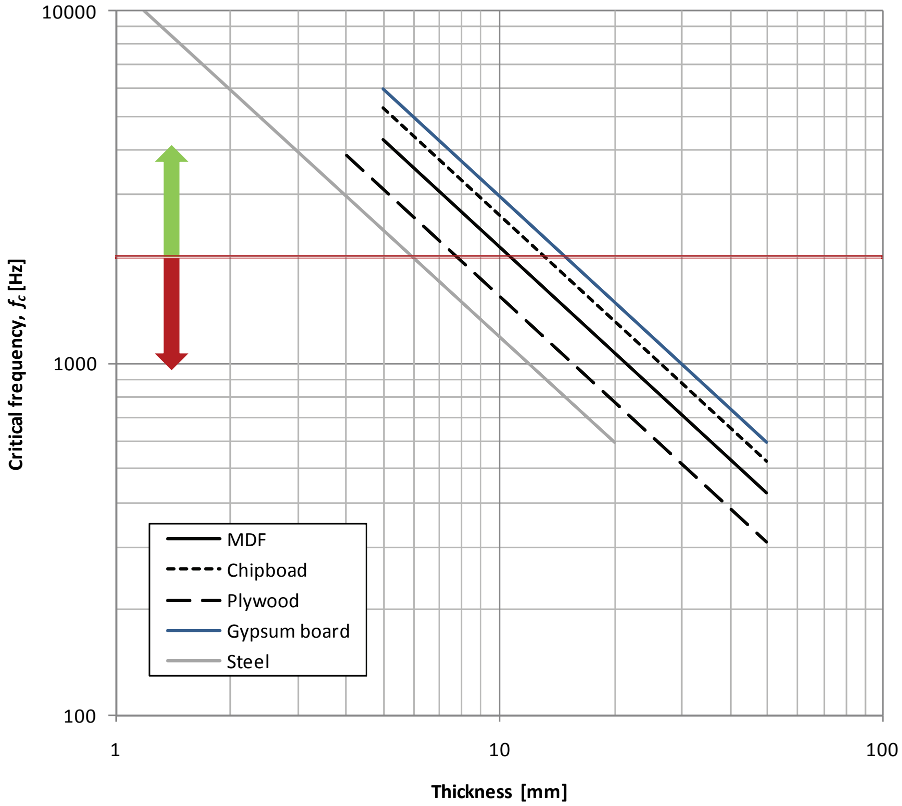


**Figure 9.** The critical frequency of common building boards as a function of thickness. Calculated with Equation (9).

The third important transition frequency, at which the acoustical behaviour of a plate changes typically occurs at the high-frequency range. In thin plates the bending waves determine sound radiation, but as the thickness of a plate increases above a certain point, shear waves begin to dominate [15]. A transition frequency can be discerned, above which shear waves begin to significantly affect sound reduction. This frequency, denoted as $f_h$, depends on the thickness and critical frequency of a plate [29]:

$$f_h = \frac{1}{f_c}\left(\frac{c_0}{6h}\right)^2 . \tag{11}$$

In plates with thickness below 30 mm or surface density below 100 kg/m$^2$, bending waves dominate up to 5000 Hz [15], which covers the frequency range used in building acoustical measurements, 100 – 3150 Hz or 50 – 5000 Hz. This indicates that the sound reduction index of thin plates can be estimated to a good accuracy even if the effect of shear waves is neglected [15].

## 4.4 Prediction Models of Sound Reduction Index

### 4.4.1 Thin single plates

The sound reduction index of a thin single plate, such as a typical building board, is determined above the lowest natural frequency by the so-called mass law [32]. The value of the SRI indicated by the mass law depends on the incident angle, θ, of sound impinging on a plate. The mass law for normal incidence, θ = 0°, denoted as $R_0$ [dB], is given by the equation [29]

$$R_0 = 20\log_{10}\left(\frac{\pi f m`}{\rho_0 c_0}\right) \cong 20\log_{10}(m`f) - 42 \tag{12}$$

where $m`$ is the surface density of the panel [kg/m$^2$]. For field incidence, θ = 0…78°, the corresponding quantity is denoted as $R_f$ [dB] and given by the equation [16]

$$R_f \cong 20\log_{10}(m`f) - 47 \tag{13}$$

The mass law defined in Equations (12) and (13) indicates an increase in the sound reduction index by 6 dB with a doubling of surface density or frequency. A correction, depending on the area of the plate, S = $l_x$ x $l_y$ [m$^2$], and frequency, can be applied to the conventional mass law equation. The correction term, proposed by Sewel, improves calculation accuracy at low frequencies by taking into account that the amount sound energy per unit area incident on a surface decreases towards low frequencies [32]. Field incidence mass law with the so-called Sewel-correction is given by [16]

$$R_0 = 20\log_{10}(m`f) - 42 - 10\log_{10}\left(\ln\left(\frac{2\pi f}{c}\sqrt{S}\right)\right) \tag{14}$$

According to Kristensen and Rindel [29], the sound reduction index of thin plates can be estimated below and above the critical frequency by the equation pair

$$R \cong \begin{cases} R_0 - 10\log_{10}(2\sigma_d) + 20\log_{10}\left(1 - \left(\dfrac{f}{f_c}\right)^2\right), f < f_c \\[2ex] R_0 + 10\log_{10}\eta + 10\log_{10}\dfrac{f}{f_c} - \Delta R_h - 2, f \geq f_c \end{cases} \tag{15}$$

where $R_0$ is the normal incidence mass law, $\sigma_d$ is the radiation factor for diffuse sound incidence [m/s], $\eta$ is the total loss factor and $\Delta R_h$ [dB] is a correction term. The radiation factor is given by an approximate equation [29]

$$\sigma_d \cong \frac{1}{2}\left(0{,}2 + \ln\left(\frac{2\pi}{c_0} f\sqrt{S}\right)\right) \tag{16}$$

where $S$ is the area of the plate [m$^2$]. Equation (16) applies when $S \geq 10$ m$^2$ [k&r]. When the plate area and frequency are small ( $f\sqrt{S}$ < 55 Hz·m), $\sigma_d$ is given by

$$\sigma_d \cong \frac{8Sf^2}{c_0^2\left(\frac{l_x}{l_y}+\frac{l_y}{l_x}\right)} \tag{17}$$

The correction term $\Delta R_h$ in Equation (15) depends on frequency and transition frequency $f_h$ as follows [29]

$$\Delta R_h = 10\log_{10}\left[\frac{f}{5f_h}+\sqrt{\left(\frac{f}{5f_h}\right)^2+1}\right] \tag{18}$$

The correction term can be approximated as $\Delta R_h \approx 0$ dB when $f < f_h$ [29]. This indicates that the sound reduction index of thin plates can be estimated in three frequency regions: below the critical frequency ($f < f_c$), above the critical frequency ($f \geq f_c$) and above the transition frequency ($f > f_h$). The corresponding three-part equation system can be deduced by inserting expression (18) into the latter equation of (15):

$$R \cong \begin{cases} R_0 - 10\log_{10}(2\sigma_d) + 20\log_{10}\left(1-\left(\frac{f}{f_c}\right)^2\right), f < f_c \\ R_0 + 10\log_{10}\eta + 10\log_{10}\frac{f}{f_c} - 2, f \geq f_c \\ R_0 + 10\log_{10}\left(\eta\frac{f}{f_c}\right) - 10\log_{10}\left(\frac{f}{5f_h}+\sqrt{\left(\frac{f}{5f_h}\right)^2+1}\right) - 2, f > f_h \end{cases} \tag{19}$$

Kristensen and Rindel [29] also provide a formula for estimating the sound reduction index of thin plates below the lowest natural frequency $f_{11}$:

$$R \cong R_0 - 10\log_{10}(2\sigma_d) + 40\log_{10}\left(\frac{f_{11}}{f}\right), f < f_{11} \tag{20}$$

As pointed out by Kylliäinen [32], however, extending the calculation of SRI below $f_{11}$ is in most cases unnecessary, since the lowest natural frequency of building boards typically lies below the lower limit of the building acoustical frequency range.

The total loss factor, $\eta$, in Equations (15) and (19) describes the energy losses occurring within a plate due to its couplings to adjacent structures. When the surface density is below 800 kg/m$^2$, the total loss factor can be estimated by the equation [5]

$$\eta = \eta_{\text{int}} + \frac{m`}{485\sqrt{f}} \tag{21}$$

where $\eta_{int}$ is the internal loss factor.

Figure 10 illustrates the sound reduction index of a chipboard panel, with a thickness of 22 mm, calculated with Equations (19) and (20). The three transition frequencies are indicated by arrows. The two vertical dashed lines indicate the frequency range of 100 – 3150 Hz, which is typically used in building acoustical measurements and from the basis of which the weighted sound reduction index is determined according to standard *ISO 717-1* [27]. In order to distinguish the two transition frequencies, $f_{11}$ and $f_h$, which typically lie outside this frequency range, the sound reduction index in Figure 10 is presented from 20 to 10000 Hz.

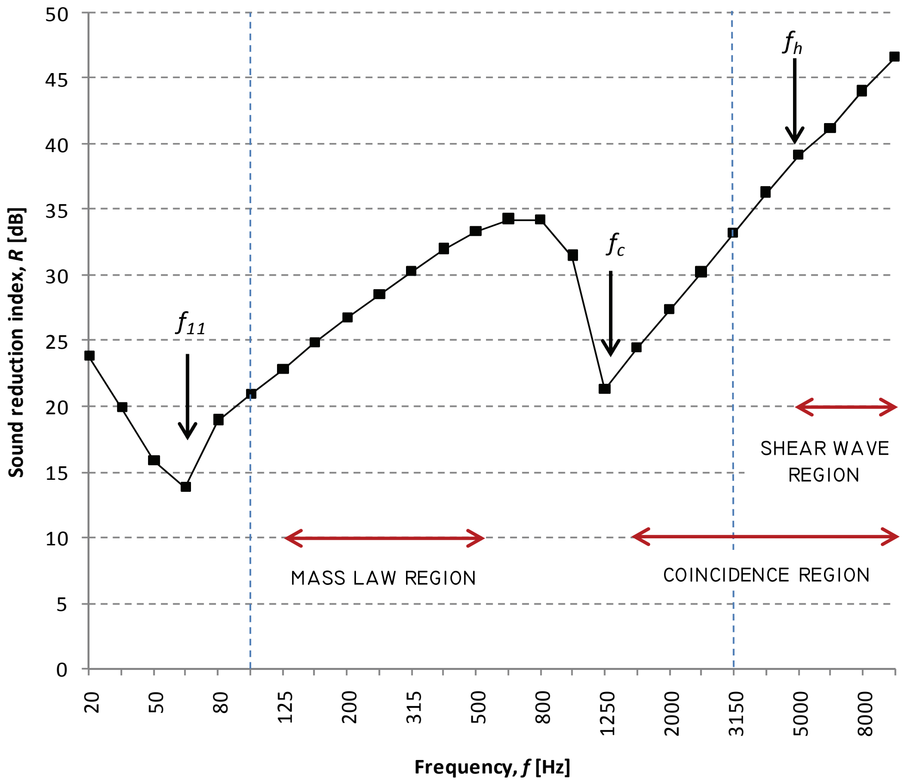


**Figure 10.** The sound reduction index of chipboard (22 mm) calculated with prediction model. Regions of sound insulation behaviour according to [32].

The lowest natural frequency, $f_{11}$, of partition structures lies typically below 100 Hz [1], as is the case in Figure 10 also. The mass law governs frequencies up to about half the critical frequency, $f_c$, above which the sound reduction index begins to deteriorate due to the coincidence phenomenon reaching a minimum at $f_c$ [32]. Above the critical frequency the SRI begins to increase again, typically about 10 dB/octave [1]. Bending waves largely determine the sound reduction properties of thin plates up to transition frequency $f_h$, above which the effect of shear waves becomes significant. In the case of thin plates, $f_h$ typically lies above the upper limit of the building acoustical frequency range, thus it has little impact on the sound reduction index.

In double-leaf partitions, two or several building boards can be attached together. Compared to single plates, this yields improvement in sound insulation. The total sound reduction index of $n$ building boards, attached together loosely with screws or nails, can be calculated from the equation [16]

$$R_{sum} = 20\log_{10}\left(\sum_{i=1}^{n} 10^{R_i/20}\right) \tag{22}$$

Equation (22) can be applied only if the attachment between plates is done with screws or nails. In such a case the plates can be considered acoustically independent, that is, the bending stiffnesses and critical frequencies of individual plates do not change significantly. If the plates are glued together, the acoustical behaviour of the combination changes and Equation (22) cannot be used reliably. [16]

### 4.4.2 Double-leaf partitions

A double-leaf partition consists of impervious plates and an intervening cavity which may contain sound absorbing material. Sound traverses through double-leaf partitions essentially via two routes: as airborne sound through the cavity space and as structure-borne sound through the studding and frames to which the plates are attached [9]. Considering only the airborne route, the sound reduction index of a double-leaf partition can be estimated by the following equation system [29]:

$$R \cong \begin{cases} 20\log_{10}\left(10^{R_1/20} + 10^{R_2/20}\right), f < f_{mam} \\ R_1 + R_2 + 20\log_{10}\left(2n\dfrac{f}{f_d}\right), f_{mam} < f \leq f_d \\ R_1 + R_2 + 20\log_{10}(2n), f > f_d \end{cases} \tag{23}$$

where $R_1$ and $R_2$ are the sound reduction indexes of the two plate layers [dB], $n$ is the relative impedance between air and material in the cavity, $f_{mam}$ is the mass-air-mass resonance frequency given in equation (27) and $f_d$ is the resonance frequency corresponding to the thickness of the cavity, $d$ [m] [29]:

$$f_d = \frac{c_d}{2\pi d} \tag{24}$$

where $c_d$ is sound velocity in the cavity material [m/s]. The relative impedance $n$ is given by [29]

$$n = \frac{\rho_0 c_0}{\rho_d c_d} \tag{25}$$

where $\rho_0$, $\rho_d$ are the densities of air and cavity material [kg/m$^3$] and $c_0$, $c_d$ are the sound velocities in air and cavity material [m/s], respectively. When the cavity is filled with air, the relative impedance equals unity [29]. Inserting $n$ = 1 and expression (24) into (23) yields the following, simplified equation system:

$$R \cong \begin{cases} 20\log_{10}\left(10^{R_1/20} + 10^{R_2/20}\right), f < f_{mam} \\ R_1 + R_2 + 20\log_{10} fd - 29, f_{mam} < f \le f_d \\ R_1 + R_2 + 6, f > f_d \end{cases} \tag{26}$$

Transition frequency $f_{mam}$ in equations (23) and (26) is called the mass-air-mass resonance frequency and corresponds to a mass-spring-mass system where the plates act as masses and intervening air in the cavity acts as a spring [32]. The mass-air-mass resonance frequency of a double-leaf partition is given by the equation [16]

$$f_{mam} = \frac{1}{2\pi}\sqrt{\frac{1{,}8\rho_0 c_0^2 (m_1^` + m_2^`)}{d m_1^` m_2^`}} \cong 80\sqrt{\frac{m_1^` + m_2^`}{d m_1^` m_2^`}} \tag{27}$$

where $m`_1$ and $m`_2$ are the surface densities of the plates [kg/m$^2$]. The latter, simplified expression is found by using a value of 1,20 kg/m$^3$ for air density, corresponding to dry indoor air at a temperature of 20 °C.

Equations (23) and (26) take account only of the airborne sound route, presupposing that there is no physical connection between the plates via studding. The corresponding sound reduction index can be defined as an ideal sound reduction index, denoted as $R_{ideal}$, which yields the maximum SRI that can theoretically be achieved with a double-leaf structure [16]. An ideal double-leaf partition is uncoupled and has a totally sound absorbing cavity [16].

According to a model proposed by Hongisto [16], the sound reduction index of a double-leaf partition can be estimated in consecutive steps. The procedure is illustrated schematically in Figure 11. The starting point in the model is to predict the SRI of an ideal, uncoupled partition with a perfectly absorbing cavity. This stage yields the ideal sound reduction index, $R_{ideal}$. The second step is to take into account imperfectness of cavity absorption, which is due to the fact that absorption coefficient of porous material placed in the cavity is, in practice, always below unity. In practical partitions the cavity may also be only partially filled, which further diminishes cavity absorption. The second stage results in a sound reduction index denoted as $R_{real}$. The last stage models the deterioration in SRI caused by sound traversing via stiff studs, yielding a value denoted as $R_{br}$. [16]

The fourth stage in the modeling of the sound reduction index would be to take into account the flexibility of studs. Such a model can be applied to partitions with steel studs. Compared to flexible steel studs, wooden studs are characteristically stiff, that is, their dynamic stiffness is high. As a result of high dynamic stiffness, structural coupling between the leaves in a wooden double-leaf partition is more effective than when flexible steel studs are used. This causes a decrease in the sound reduction index. [16]

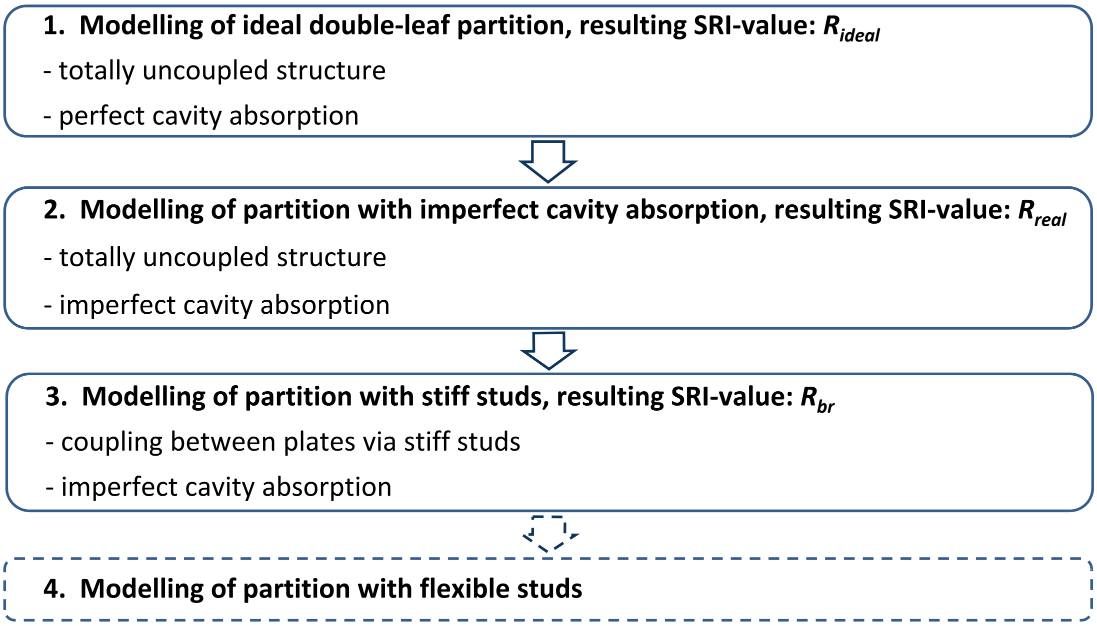


**Figure 11.** Procedure for predicting the sound reduction index of a double-leaf partition; adapted from [15].

### Modelling of absorbing cavity

In practical partitions the airspace between plates is not totally sound absorbing but, due to less than ideal material properties and partial filling, cavity absorption is virtually always imperfect. Imperfect cavity absorption and filling percentage are taken into account in a factor denoted as $R_{real}$ [dB], which is given by the equation [16]

$$R_{real} = \begin{cases} R_{ideal}, f < f_{c1} \\ R_{ideal} + \Delta R_{abs}, f \geq f_{c1} \end{cases} \tag{28}$$

where $\Delta R_{abs}$ [dB] is the deterioration of the ideal sound reduction index, $R_{ideal}$, caused by imperfect cavity absorption and $f_{c1}$ is the lowest resonance frequency of the cavity [Hz], defined in Equation (32). $\Delta R_{abs}$ is expressed as [15]

$$\Delta R_{abs} = 10 \log_{10} \alpha_{eff} \tag{29}$$

where $\alpha_{eff}$ is the effective absorption coefficient of the cavity, which depends on the absorption coefficient of the material, $\alpha_c$, and filling ratio of the cavity, $FR$ [16]:

$$\alpha_{eff} = \alpha_c \cdot FR \tag{30}$$

The filling ratio is given by [16]

$$FR = \frac{V_a}{V_c} \approx \frac{d_a}{d_c} \tag{31}$$

where $V_a$ [m$^3$] is the volume of air in the cavity, $V_c$ [m$^3$] is the total volume of the cavity and $d_a$ [m] and $d_c$ are the widths [m] of the cavity and sound absorbing material, respectively. The latter expression applies if the absorbing material is laminar and has a fixed width, such as a typical sheet of mineral wool [16].

The decrease in the sound reduction index caused by imperfect cavity absorption is due to reverberation and resonances in the cavity. Absorbing material in the cavity does not, in essence, improve the sound reduction index but rather prevents it from deteriorating by damping the cavity resonances [9] [16]. This damping is effective only at frequencies above the lowest cavity resonance, $f_{c1}$, given in Equation (32). Below $f_{c1}$ half of the sound wavelength is greater than the maximum dimension of the cavity, thus sound waves cannot "fit" inside the cavity and no resonances occur [16]. The lowest cavity resonance is given by [16]

$$f_{c1} = \frac{c_0}{2 \cdot \max\left[L_{x,c}; L_{y,c}\right]} \tag{32}$$

where $L_{x,c}$ is the width and $L_{y,c}$ the height of the cavity [m]. The cavity dimensions are limited in practice by the centres distance of studs and room height.

### Modelling of stiff studs

The next step in the calculation of the sound reduction index is to take into account the deterioration caused by sound traversing through the studding. The idea is to first calculate sound reduction index using the upper part of Equation (26), denoted here as $R_{sum}$ [dB] [32]:

$$R_{sum} = 20\log_{10}\left(10^{R_1/20} + 10^{R_2/20}\right) \tag{33}$$

where $R_1$ and $R_2$ are the sound reduction indexes of plate layers 1 and 2, respectively. Then a factor, denoted as $\Delta R_M$ [dB] is added to $R_{sum}$. The maximum sound reduction index that can be achieved with stiff studs above a so-called bridge frequency, $f_{br}$, is determined by the equation [15]

$$R_{br} = \min\left[R_{real}; R_{sum} + \Delta R_M\right], f > f_{br} \tag{34}$$

The deteriorating effect of studs is limited to frequencies above the bridge frequency. Below $f_{br}$ the sound reduction index is determined by the factor $R_{real}$. As a rule of a thumb, studding does not significantly decrease the sound reduction index at low frequencies, since low-frequency sound insulation mostly depends on the total mass of the structure. The deterioration is typically most significant at mid- and high frequencies, above the bridge frequency, which is typically around 100 – 200 Hz. [15]

The bridge frequency depends on the centres distance of studs as well as the fastening of plates to studs. As the number of attachment points between plates and studs – screws or nails – increases above a certain limit, the studs begin to act acoustically as line couplings rather than point couplings. In the case of line couplings, the screws or nails are assumed to lie so close to one another that they form a continuous line from which sound radiation occurs. Point couplings, on the other hand, are considered to act independently, serving as point sources for sound radiation. [16]

With line couplings, factor $\Delta R_M$ and bridge frequency are given by equations [16]

$$\Delta R_M = 10\log_{10}(bf_c) + 20\log_{10}\left(\frac{m_1^`}{m_1^` + m_2^`}\right) - 18 \tag{35}$$

$$f_{br} = f_{mam}\left(\frac{\pi b f_c}{2c_0}\left(\frac{m_1^`}{m_1^` + m_2^`}\right)^2\right)^{1/4} \tag{36}$$

where $b$ is the centres distance of studs [m] and $f_c$ is the critical frequency of the plate with lower surface density. If screw spacing is sufficiently sparse, studs act as point couplings yielding the following equations for $\Delta R_M$ and $f_{br}$ [16]:

$$\Delta R_M = 20\log_{10}\left(\sqrt{\frac{1}{n}}f_c\right) + 20\log_{10}\left(\frac{m_1^`}{m_1^` + m_2^`}\right) - 45 \tag{37}$$

$$f_{br} = f_{mam}\left(\frac{1}{n}\frac{\pi^3 f_c^2}{8c_0^2}\left(\frac{m_1^`}{m_1^` + m_2^`}\right)^2\right)^{1/4} \tag{38}$$

where $n$ is the number of the point couplings, that is, screws or nails per unit area [1/m$^2$]. The attachments between plates and studs can be considered as line couplings with reasonable accuracy, when half the bending wavelength fits between the screws or nails [16]. The bending wavelength can be calculated by the equation [16]

$$\lambda_B = 2\pi\left(\frac{B}{2\pi m`f}\right)^{1/4} = 2\pi\left(\frac{Eh^3}{24\pi m`f(1-\mu^2)}\right)^{1/4} \tag{39}$$

As an example, the half bending wavelength in a chipboard panel with material parameters $h$ = 11 mm, $m$` = 7.0 kg/m$^2$, $E$ = 2900 Mpa and $\mu$ = 0.30 calculated with Equation (39), decreases from a value of about 2.0 m to 0.5 m in a frequency range of 50 – 10000 Hz, having a value of 0.6 m at 5000 Hz. Thus, a screw spacing of 600 mm, for example, would mean that the transition from line- to point couplings occurs at 5000 Hz.

In addition to studs, structural connection between the plates of a double-leaf partition occurs at the perimeters, or gables, of the structure. Kristensen and Rindel [29] provide a formula for calculating the sound reduction index of a partition with such couplings. The value of $\Delta R_M$ for perimeter couplings is given by [29]

$$\Delta R_M \cong 10\log_{10}\left[b_g\left(\frac{m_1^`\sqrt{f_{c2}} + m_2^`\sqrt{f_{c1}}}{m_1^` + m_2^`}\right)^2\right] - 20 \tag{40}$$

where $b_g$ is used here to denote the centers distance of partition gables [m] and $f_{c1}$ and $f_{c2}$ are the critical frequencies of plates 1 and 2 [Hz], respectively.

Figure 12 presents an example of the sound reduction index calculated with the prediction model. The structure is a double-leaf partition comprising of single medium density fiberboards, thickness 12 mm, attached to wooden studs with a centres distance of 600 mm. The cavity has a depth of 100 mm and is totally filled with sound absorbing material. The attachments between plates and studs are assumed to act as line couplings. The critical frequency of MDF-plates, about 1800 Hz, and the mass-air-mass resonance frequency of the structure, about 119 Hz, are indicated with arrows in the figure. The two vertical dashed lines denote the frequency range of 100 – 3150 Hz, from the basis of which the weighted sound reduction index is calculated.

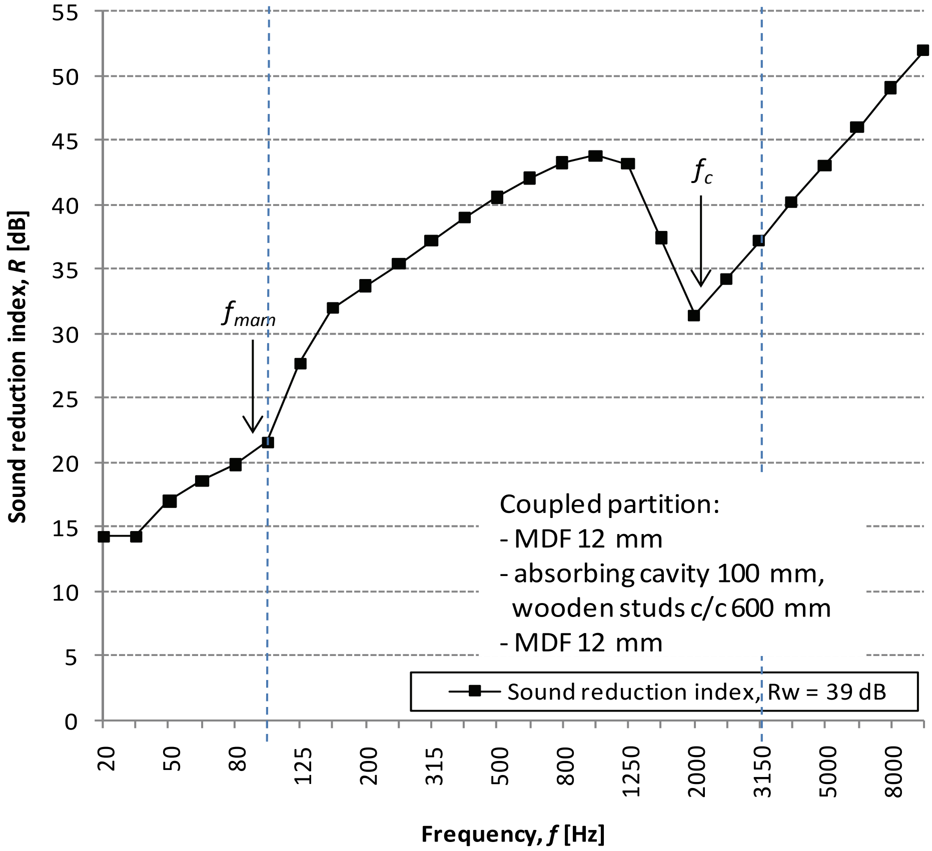


**Figure 12.** The sound reduction index of a double-leaf partition calculated with the prediction model. The structure has single 12 mm MDF-plates attached to wooden studs with a centres distance of 600 mm. Absorbing cavity has a depth of 100 mm. The area of the structure is 10 m$^2$. Connections between plates and studs are assumed to act as line couplings. Material parameters of MDF according to Tables 4 and 5, Section 4.2.

## 4.5 Sound Insulation of Combined Structures and Slits

A structure often comprises of components with different sound reduction properties. A partition wall, for example, may contain windows, doors, footings, HVAC lead-ins and other elements whose sound reduction index differs from that of the partition. A combined sound reduction index of such structures, denoted here as $R_{total}$ [dB], is given by the equation [9]

$$R_{total} = 10\log_{10}\left(\frac{\sum_{i=1}^{N} S_i}{\sum_{i=1}^{N} S_i 10^{-R_i/10}}\right) \tag{41}$$

where $S_i$ is the area [m$^2$] and $R_i$ the sound reduction index [dB] of an element $i$ in the structure.

Equation (41) can also be used to estimate the sound reduction index of a structure with slits, provided that the SRI of the slits is known. In such a case, Equation (41) becomes [17]

$$R_{total} = 10\log_{10}\left(\frac{S_{struct} + S_{slit}}{S_{struct}10^{-R_{struct}/10} + S_{slit}10^{-R_{slit}/10}}\right) \tag{42}$$

where $S_{struct}$, $S_{slit}$, $R_{struct}$ and $R_{slit}$ are the areas [m$^2$] and the sound reduction indexes [dB] of the solid part of the structure and slits, respectively.

In a simplified evaluation, the effect of slits to the overall sound reduction index can be demonstrated by setting the SRI of the slit to 0 dB [9]. This requires that the inside surfaces of the slit are hard and sound reflective, which basically means that the slit is not sealed. If a partition contains a non-sealed slit with a sound reduction index of $R_{slit}$ = 0 dB and a size more than 0,1 % of the partition area, the slit –term in the denominator of Equation (42) dominates and the SRI of the solid partition, $R_{struct}$, has very little effect on total sound reduction index [32].

In reality, the sound reduction index of a slit depends on frequency [9]. The frequency-dependent SRI of a slit-shaped, non-sealed aperture, $R_{slit}$ [dB], can be estimated by the equation [17]

$$R_{slit} = 10\log_{10}\left(\frac{2n^2\left\{\begin{array}{l}\sin^2(K(L+2E))/\cos^2(KE)+\\ (K^2/2n^2)[1+\cos(K(L+2E))\cos(KL)]\end{array}\right\}}{mK\cos^2(KE)}\right) \tag{43}$$

where $m$ and $n$ are constants depending on the position of the slit in the structure and the nature of incident sound field, $K = 2\pi fW/c_0$, $W$ is the width of the slit [m], $L = D/W$ and $D$ is the depth of the slit [m]. Factor $E$ is a correction term given by [17]

$$E \cong \frac{1}{\pi}\left[\ln\left(\frac{4c_0}{\pi fW}\right) - 0{,}5772\right] \tag{44}$$

Equation (43) can be applied only if all the inner surfaces of the slit are hard and sound reflecting.

The sound reduction index of a slit has values above zero, typically 5…10 dB, for the majority of the building acoustical frequency range [9]. At the resonance frequencies of the slit SRI falls below zero, having typically values between -5 and -10 dB [9].

Figure 13 presents the sound reduction index of a non-sealed slit with a width of 2 mm and depth of 100 mm calculated with equation (43). Values of $m$ = 8 and $n$ = 1 were used for the constants, in accordance with [17]. A similar slit to the one considered in Figure 13 could be found, for example, in the junction of a lightweight partition and side wall. The effect of slit resonances can be seen at high frequencies. At the resonance frequencies slit "absorbs" sound from an area effectively larger than its cross-sectional dimensions, which results in strong sound radiation and a poor sound reduction index [9].

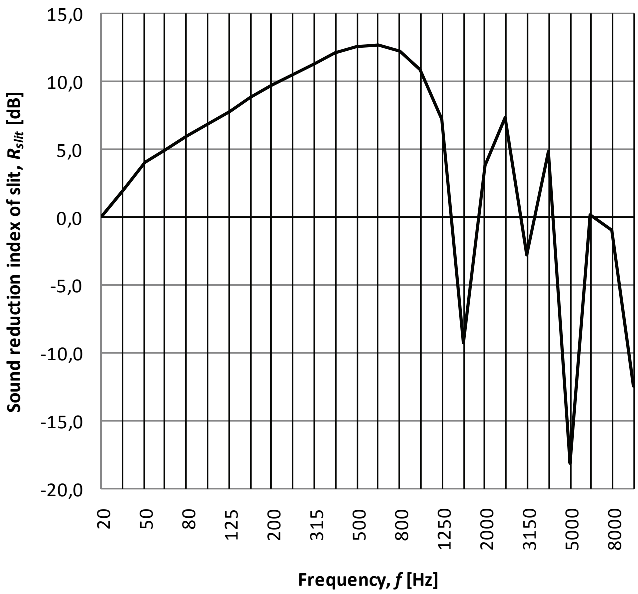


**Figure 13.** The sound reduction index of a non-sealed slit. Calculated with Equation (43); W = 2 mm, D = 100 mm.

Careless workmanship and deficiencies in site supervision are common causes for slits and holes in structures [9]. It is also possible that sealing details have not been planned properly. In lightweight partitions, slits are often found at the perimeters of the partition, at the junctions to adjacent structures: side walls, floor and roof. A study by Uris et al. [44] showed that slits between the perimeters of a lightweight partition and tangential structures significantly decrease sound reduction index. The decrease was found to be most severe around the resonance frequencies of the slits. A single slit with a width of 1,5 mm between the partition and ceiling was found to cause a decrease of 22 dB in weighted sound reduction index [44].

## 4.6 Structural Flanking Transmission

### 4.6.1 Effect of structural junctions on flanking transmission

Flanking sound transmission is a phenomenon in which sound traverses between rooms via other paths than directly through the separating partition. The structural flanking path involves at least one structure tangential to the rooms. In addition to structural flanking transmission flanking can also occur, for example, via HVAC installations. The amount of deterioration in the sound reduction index caused by structural flanking transmission depends on the properties of the structures involved in the flanking path as well as their junctions to each other. [9]

The amount of flanking transmission occurring between two rooms is significantly affected by details of the structural junctions. An important parameter of a junction is the vibration reduction index, $K_{ij}$ [dB], which describes the vibrational power transmitted over a junction between structural elements *i* and *j* [5]. The amount of vibration reduction achieved in a structural junction depends on the surface densities, $m`$ [kg/m$^2$], of the structures involved as well as the stiffness of the connection [32]. The vibration reduction index is a frequency-dependent quantity. According to standard *ISO 12354-1* [5], transmission over a junction is slightly dependent on frequency in the range of 125 – 2000 Hz, but outside this range the effect of frequency can be more significant.

Homb et al. [14] give values for the vibration reduction index as a function of two different junction types: T- and cross junction. Some of the values are listed in Table 6. The vibration reduction index depends on the relative difference of surface densities, $m`_1$ and $m`_2$ [kg/m$^2$], of the connected structures as well as the type of connection.

**Table 6.** Values of the vibration reduction index given by Homb et al. [14].

| **Surface density difference** | **Vibration reduction index, $K_{ij}$ [dB]** | |
|---|---|---|
| $m`_2$ / $m`_1$ | T-junction | Cross junction |
| ≤ 0.25 | 2 | 2 |
| 0.40 | 3 | 4 |
| 0.60 | 4 | 7 |
| 0.80 | 7 | 10 |
| 1.00 | 9 | 12 |
| 2.00 | 13 | 18 |
| 4.00 | 19 | 24 |

From the viewpoint of this study, the most important type of structural junction is the one between two lightweight structures. Such a case may occur, for example, in offices when a lightweight partition between adjacent work rooms connects to a partition between the work rooms and the corridor. The most effective means for minimizing flanking transmission in a junction of two lightweight partitions is to truncate the inner leaf of the flanking structure at the junction [32]. An example of such truncation is presented in Figure 14.

In Figure 14, the partition denoted as E is a coupled structure with building boards attached to common studding, while partition C has separate studs. In the left-hand side of the figure truncation is missing resulting in a poor vibration reduction index, $K_{ij}$ = 0 dB, while the structural junction on the right has a truncated inner building board and the corresponding value is $K_{ij}$ = 15 dB [14]. According to Homb et al. [14], $K_{ij}$ = 15 dB is an estimated value.

Figure 15 illustrates how flanking transmission can be minimized in the junction of lightweight partition and suspended ceiling panel in roof or intermediate floor. Flanking transmission significantly deteriorates sound insulation if the building board layer of the ceiling panel extends continuously from room to room over the partition junction. Sound insulation diminishes further if the partition structure does not extend to the load-bearing slab of the roof / intermediate floor. The vibration reduction index presented on the right-hand side of the figure, $K_{ij}$ = 25 dB, is an estimated value. [14]

Similarly as with suspended ceilings, any lightweight building board coverings on side walls should also be truncated to minimize flanking. This is illustrated in Figure 16. Sound insulation is compromised if the plate structure extends continuously from room to room.

In addition to side walls and roof, flanking transmission between two rooms also occurs via the floor structure. For optimal elimination of flanking transmission, continuous floor structures should also be truncated at the partition junction. Figure 17 illustrates how a floating floor structure can be truncated to avoid flanking. The vibration reduction index of the T-junction presented on the left-hand side of the figure was estimated from Table 6.

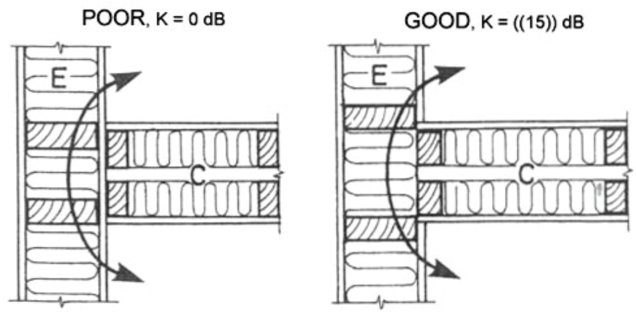


**Figure 14.** Minimizing flanking transmission in the junction of two lightweight partitions; adapted from Homb et al. [14]. On the left, truncation of the inner plate layer is missing, causing deterioration in the apparent sound reduction index between adjacent rooms. Structure E: lightweight coupled double-leaf partition, C: lightweight uncoupled double-leaf partition.

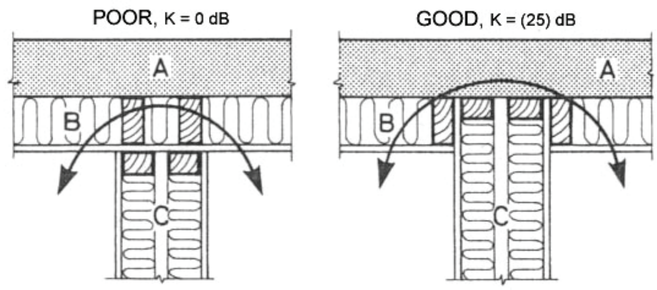


**Figure 15.** Minimizing flanking transmission in the junction to lightweight panel facing in the roof; adapted from Homb et al. [14]. Structure A: concrete ≥ 120 mm or lightweight concrete ≥ 150 mm, B: panel facing with mineral wool filling.

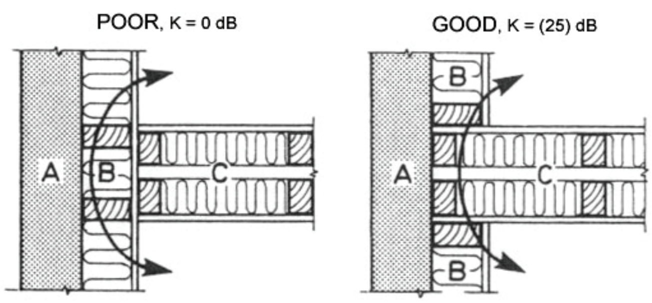


**Figure 16.** Truncation of the inner leaf of a lightweight panel facing. Adapted from Homb et al. [14]. Structures A and B as in Figure 15.

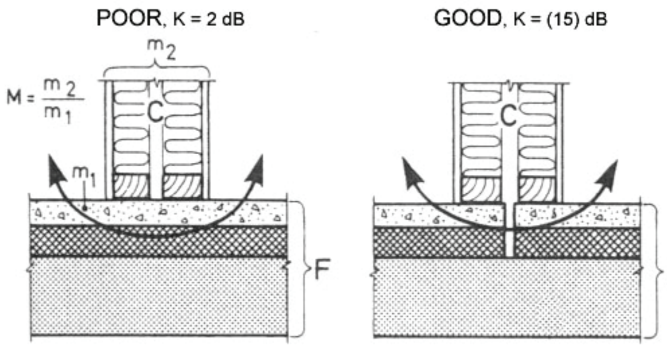


**Figure 17.** Truncation of a floating floor structure to minimize flanking transmission. Adapted from Homb et al. [14]. Structure C as in Figure 14. Structure F: concrete 50 – 120 mm on expanded polystyrene 50 mm on massive floor structure.

The intermediate floor structures normally used in office buildings are hollow core slabs, cast-in-situ concrete slabs or composite slabs [10]. The thickness of hollow core slabs is typically 265 mm or more. Because of the massiveness of the structures involved, truncation of a concrete floor or roof slab can be very difficult to implement in practice. Flanking transmission via concrete structures is, however, usually not an issue in office buildings because the requirements for the apparent sound reduction index between adjacent rooms are mostly below 50 dB [10]. Nevertheless, if the sound insulation requirements are of the magnitude $R`_w \geq 50$ dB, flanking transmission via masonry structures has to be taken into consideration.

In offices, the inner concrete envelope of an exterior wall constitutes a typical path for flanking transmission. The inner structural layer of an exterior wall can also consist of a lightweight building board. If the building board layer extends continuously between adjacent rooms, the apparent sound reduction index between the rooms is typically below 35 dB. To avoid deterioration of sound insulation, the building board should be truncated at the partition junction. [10]

### 4.6.2 Prediction model for flanking in lightweight constructions

Standard *EN 12354-1* [5] provides a model for predicting the effect of flanking transmission on sound reduction index. However, the standardized model has a limitation: it is primarily intended to be applied to massive, homogenous structures. The model does not yield reliable results if all the structures involved in flanking transmission are lightweight [9]. According to Kylliäinen [32], the *EN 12354-1* model is suitable for calculating sound reduction indexes only, when the structures involved in the flanking path are massive masonry structures or a lightweight structure connects to the latter.

Nightingale [37] has investigated the applicability of the *EN 12354-1* method to lightweight structures. According to Nightingale, flanking is a combination of two sound transmission types: resonant transmission, which occurs above the critical frequency, $f > f_c$, and non-resonant transmission dominating sound transmission at frequencies below the critical frequency, $f < f_c$. Flanking transmission via structure-borne paths is theoretically determined solely by resonant transmission. From the viewpoint of lightweight structures this is problematic, because the critical frequency of building boards typically occurs within the building acoustical frequency range;

thus, the sound reduction index is mostly determined by non-resonant transmission. If standard SRI-values are used as input parameters in the *EN 12354-1* model, the resulting apparent sound reduction index tends to be underestimated below the critical frequency. A correction can be applied to the *EN 12354-1* which can, in some cases, notably improve the prediction accuracy of flanking in lightweight constructions. However, the method requires knowledge of surface velocities and other parameters that are impractical to measure. [37]

Homb et al. [14] provide a prediction model for estimating the sound reduction index between two rooms in field conditions. According to the authors, the model is not exact but yields good estimates of the apparent sound reduction between rooms. The model takes account of four first-order flanking paths: two side walls, intermediate- / base floor and roof. An illustration of the flanking paths 1 – 4 is given in Figure 18. The direct route through the separating partition is indicated with the straight arrow.

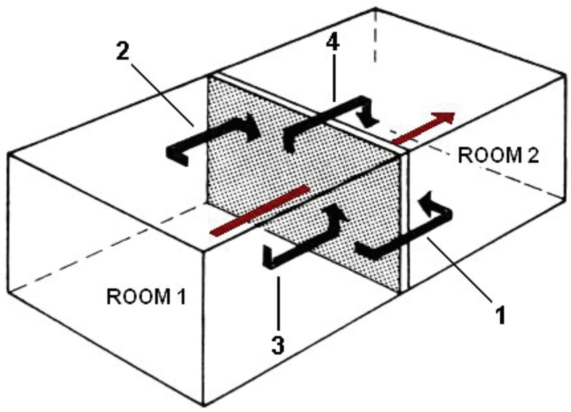


**Figure 18.** Flanking paths in a prediction model of the apparent sound reduction index; adapted from Homb et al. [14].

In the model, the apparent weighted sound reduction index, $R`_w$ [dB], is calculated by the equation [14]

$$R_w^` = R_w - 10\log_{10}\left[1 + \left(\frac{1}{S}\right)\sum_{n=1}^{4}\left(S_{sn} \cdot 10^{(R_w - F_n)/10}\right)\right] \tag{45}$$

where $R_w$ is the weighted sound reduction index of the separating partition [dB], $S$ is the area of the separating partition [m$^2$], $S_{sn}$ are the areas of flanking structures 1 – 4 in the source room [m$^2$] and $F_n$ is the characteristic sound radiation via flanking structures [dB].

The characteristic flanking sound radiation, $F_n$, is given by [14]

$$F_n = R_{fn} + K_{ij} + 10\log_{10}\left(\frac{S_{sn}}{S_{rn}}\right) \tag{46}$$

where $R_{fn}$ is the sound reduction index of flanking structure $n$ [dB] with corrections given by Homb et al. [14], $K_{ij}$ is the vibration reduction index [dB] of the junction between separating partition $i$ and flanking element $j$ and $S_{rn}$ are the areas of flanking structures 1 – 4 in the receiving room [m$^2$].

# 5 Development of Partitions

## 5.1 Definition of Target Values

Table 7 presents the target values that were set for the new partitions. The target values of the apparent weighted sound reduction index were defined on the basis of standard *SFS 5907 Acoustical Classification of Buildings* [40], which gives acoustical guidelines for offices and other public buildings. Table 8 presents a summary of some of the values concerning sound insulation between office spaces. The standard classifies buildings acoustically in classes A – D. Class C corresponds to the minimum level which should be achieved in new buildings, while class D can be applied to older buildings when needed [9]. Classes A and B enable better acoustical quality than required in the building codes [9].

The target value of $R`_w$ set for the new partitions in class 3 corresponds to class C in standard *SFS 5907*, concerning sound insulation between single person office rooms. The class 2 target value, on the other hand, is roughly analogous to the class A guideline value between work rooms. The target value in class 1, $R`_w \geq 55$ dB, corresponds to class B in *SFS 5907* regarding spaces with high requirements for confidentiality.

It was set as a goal that the weighted sound reduction index, $R_w$, of the partition separating adjacent rooms should exceed the desired apparent weighted sound reduction index, $R`_w$, by at least 5 dB in each target class. The intention was that this would leave a margin for flanking transmission and possible sound leaks, which virtually always deteriorate sound insulation under field conditions.

**Table 7.** Target values for the apparent weighted sound reduction index between adjacent rooms and the weighted sound reduction index of the separating partition.

| Class | Apparent weighted SRI between adjacent rooms, $R`_w$ [dB] | Weighted SRI of the separating partition, $R_w$ [dB] |
|---|---|---|
| 1 | ≥ 55 | ≥ 60 |
| 2 | ≥ 45 | ≥ 50 |
| 3 | ≥ 35 | ≥ 40 |

**Table 8.** Minimum values of the apparent weighted sound reduction index, $R`_w$ [dB], in offices according to standard SFS 5907. [40]

| Space | Class | | | |
|---|---|---|---|---|
| | A | B | C | D |
| Between single person office rooms | 44 | 40 | 35 | 35 |
| - from the above to corridor | 34 | 30 | 25 | 25 |
| Customer-, conference- and management rooms | 48 | 44 | 40 | 40 |
| Spaces which require absolute confidentiality | 60 | 55 | 52 | 48 |

## 5.2 Starting point: Measurements of Typical Partitions

### 5.2.1 Description of measured structures

The sound insulation properties of the typical partition system were investigated with measurements of the apparent sound reduction index. The measurements were carried out according to standard *ISO 140-4* [25]. A plan of the measurement space is given in Figure 19. The spatial layout resembled an office space with individual work rooms, denoted as room 1 and room 2, separated from each other and the corridor by floor to ceiling height partitions. Altogether three measurements were carried out in the directions indicated by arrows. The lightweight partition structures separating the rooms from each other and the corridor are indicated in Figure 19 as partitions P1, P2, and P3. The flanking wall structures are denoted as F1, F2 and F3.

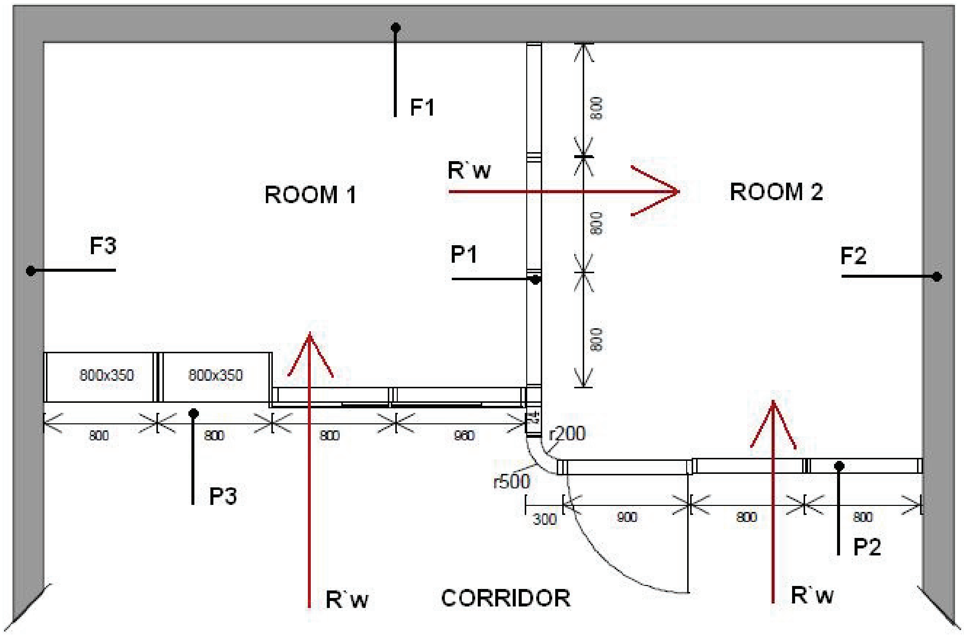


**Figure 19.** Plan of the office space in which the typical partition system was measured. Measurement directions are indicated by arrows.

Partition P1 intervening rooms 1 and 2 consisted of veneered medium density fiberboard panels attached to wooden studs. A principle of the section as well as the connection to roof and intermediate floor is given in Figure 20. The basic structure of partition P1 was the following:

1. Medium density fiberboard 12 mm + veneer 0,5 mm on both sides, size of the panels 600 x 600 mm, 11 % of the wall surface perforated panel with a perforation ratio of 6,7 %
2. Glued laminated timber studs 30 x 92 mm, cavity totally filled with mineral wool
3. Medium density fiberboard 12 mm + veneer 0,5 mm on both sides, size of the panels 600 x 1200 mm, solid wall surface

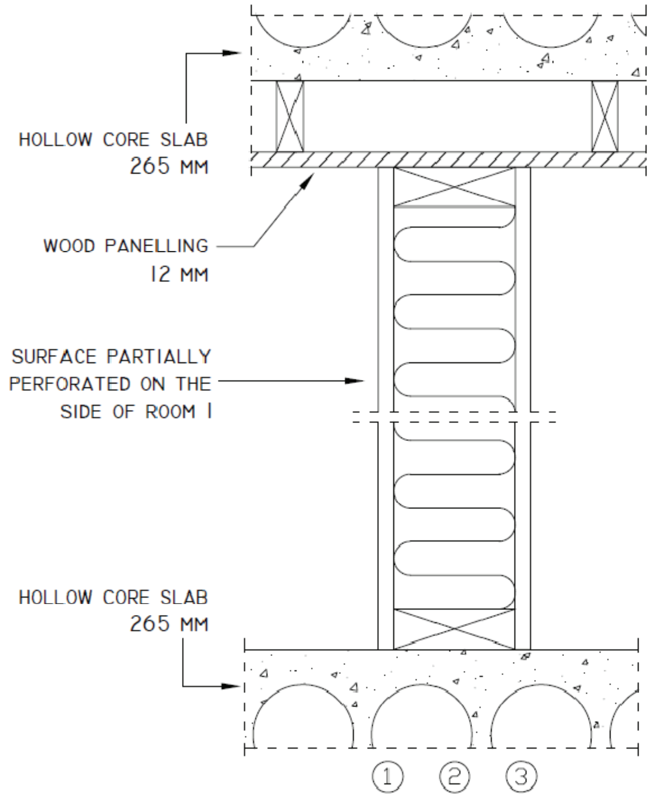


**Figure 20.** Section of partition P1 and connection to intermediate floor and roof (principle).

The MDF-panels were attached to studding with aluminum rails. A detail of the connection is given in Figure 21. The rails were attached to the studs with screws. Screw spacing was 800 mm in the horizontal and 600 mm in the vertical direction. There was no mechanical fastening between the MDF-panels and rails.

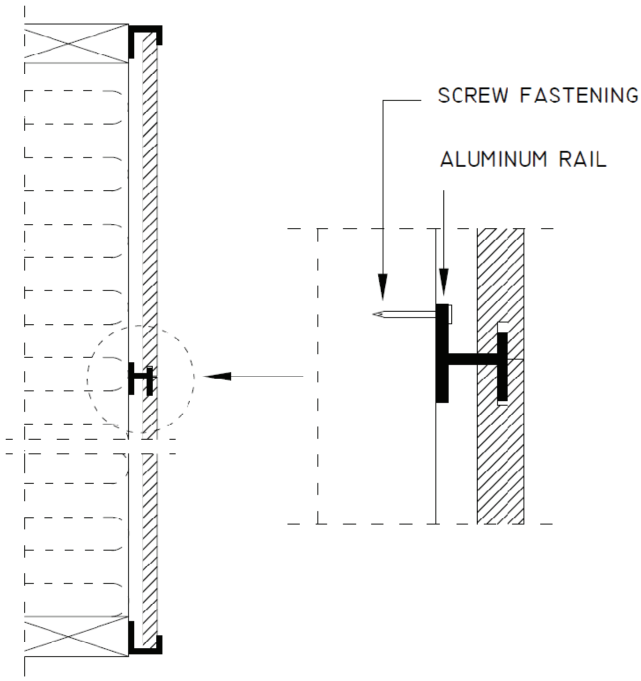


**Figure 21.** Detail of the panel connection in partition P1.

Partitions P2 and P3 intervening the rooms and corridor were single plate structures: the first consisted of various-sized laminated glass sheets with a thickness of 6 mm and the latter of similar MDF-panels that were used in partition P1. In both partitions the plates were attached to wooden studs. There was a curved part between the two partitions, comprising of two slotted MDF-panels with a thicknesses of 13 mm, attached to wooden studding. The intervening cavity was empty and had a thickness of 58 mm.

Partition P2 included a conventional door, manufactured by Fiskars Oy, with a honeycomb structure and a size of 900 x 2100 mm. The door structure had no decibel rating. The door frame was sealed throughout, but the sealing was rather loose leaving notable slits especially between the base of the door and sill. In partition P3, there was an opening with a size of 830 x 2100 mm with no door. During the measurements, the opening was covered with a 15 mm plywood panel, which was sealed from the edges with foamed plastic and pressed tightly against the frames of the opening.

The flanking walls denoted as F1 and F2 in Figure 19 were lightweight partitions with 13 mm chipboard panels attached to wooden studs. The inner building board layer in both structures extended continuously over the partition junction. The exterior wall structure F3 was hardened aerated concrete, or Siporex, with a total thickness of 375 mm, and the load-bearing structure of both intermediate floor and roof was a 265 mm hollow core slab. A wooden panelling was installed in the ceiling. The panel structure extended continuously from room 1 to room 2. None of the partition structures P1 – P3 extended above the ceiling panelling.

### 5.2.2 Measurement equipment and arrangements

The equipment that was used for the measurements of the apparent sound reduction index is listed in the following. The same equipment was used for all the measurements conducted in this study.

- Sound level meter: Norsonic type 118
- Microphone: Norsonic type 1206/27620
- Microphone calibrator unit: type 1251, with adapter type 1443
- Loudspeaker: Yorkville 50B Bass Amp
- Audio generator: NTI Minirator MR1

Reverberation time of rooms 1 and 2 was measured according to *ISO 354* [26] using two discrete positions of the sound source. Two measurements at four different points were conducted with both loudspeaker positions, constituting altogether 16 reverberation time measurements per room. The measurement results were averaged in each third-octave frequency band.

In the measurements of the apparent sound reduction index, two discrete loudspeaker positions were used in the source room. The sound pressure level in the source and receiving rooms was measured at five different points with both loudspeaker positions. Thus, altogether ten sound pressure levels were registered in both rooms. An averaging time of 10 seconds was used in all the measurements. To avoid direct sound radiation, the loudspeaker in the source room was positioned at a distance from the separating partition, the speaker enclosure facing away from the partition. In all the measurements, microphone positions were scattered throughout the measurement room at different heights and the room with larger volume was used as the source room.

The measurements were conducted in third-octave bands, in a frequency range of 50 – 5000 Hz, using a single sound source and fixed microphone positions. The microphone was calibrated before measurements. The sound signal driven through the loudspeaker was pink noise generated by the NTI Minirator MR1 audio generator.

### 5.2.3 Measurement results

The measured apparent sound reduction index from room 1 to room 2, corridor to room 1 and corridor to room 2 are illustrated in Figures 23 – 25, respectively. A more detailed presentation of the results is given in Appendix A. The apparent weighted sound reduction index was determined according to standard *ISO 717-1* [27]; the calculated values for each measurement are shown above the legend. The reference curve given in *ISO 717-1* is indicated in the figures by a dotted line.

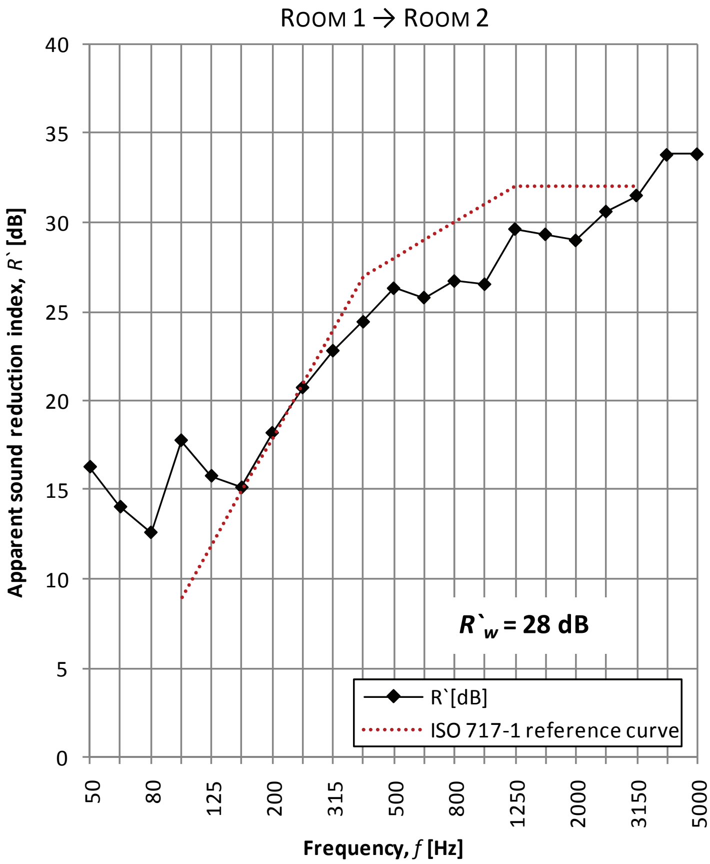


**Figure 22.** The apparent sound reduction index from room 1 to room 2. Typical partition structure.

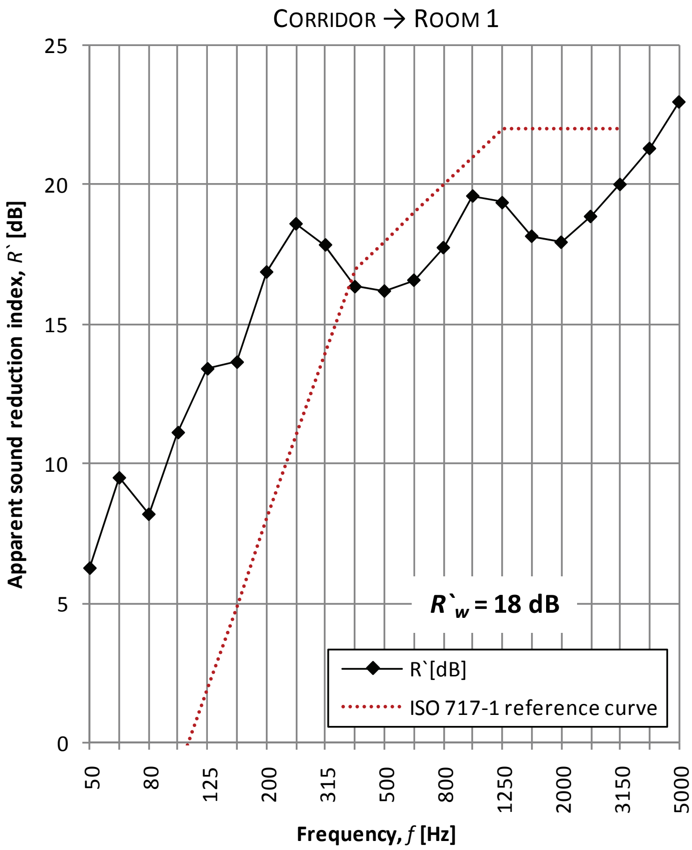


**Figure 23.** The apparent sound reduction index from corridor to room 1. Typical partition structure

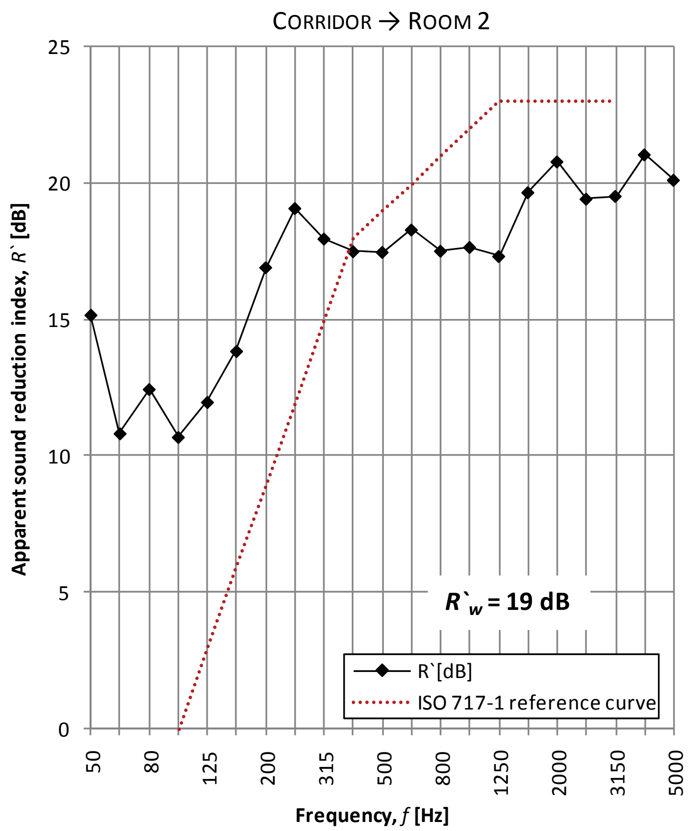


**Figure 24.** The apparent sound reduction index from corridor to room 2. Typical partition structure.

### 5.2.4 Discussion and comparison to target values

Table 9 presents the difference between the measured apparent sound reduction index from room 1 to room 2, $R`_w$ = 28 dB, and the corresponding target values set in the three classes. The measurement results indicated that a substantial improvement in sound insulation would be required in order to achieve the target values: the sound reduction indexes of the two partitions would have to be increased, flanking transmission diminished and sealing of structural junctions improved.

**Table 9.** Difference between the measured apparent weighted sound reduction index between adjacent rooms, $R`_w$ = 28 dB, and target values.

| Class | Target value of the apparent SRI between adjacent rooms, $R`_w$ [dB] | Difference of the measured apparent SRI to target value, [dB] |
|---|---|---|
| 1 | ≥ 55 | 27 |
| 2 | ≥ 45 | 17 |
| 3 | ≥ 35 | 7 |

The deficiencies associated with the typical partitions were found to be largely similar to the ones commonly found in office buildings relating to, for example, inadequate sealing and flanking transmission via continuous plate structures; see Section 3.1.3. Visual inspection of the typical partitions revealed slits between the perimeters of the partitions and tangential structures as well as inadequate or careless sealing of structural joints. In the partition separating adjacent rooms there was also a lead-in for electrical wires that penetrated the partition structure. All the lightweight plate structures tangential to the adjacent measurement rooms were non-truncated, extending continuously from room to room and constituting notable paths for flanking sound transmission.

## 5.3 Means for Improving Sound Insulation

### 5.3.1 Connection type between partition leaves

One of the most important parameters that affects the sound reduction index of a double-leaf partition is the connection type between the two partition leaves. Thus, this was an essential consideration when improving sound insulation compared to the typical partition. Figure 25 illustrates the four basic connection types.

A clear distinction can be made between two partition types: uncoupled and coupled partitions. In an uncoupled structure the studding is separated by an airspace and there is no direct structure-borne sound transmission path between the plates. This corresponds to cases 1 and 2 in Figure 25. The difference between the two cases is that, in the first, the tangential structure has been truncated to avoid flanking transmission. From a sound insulation point of view, case 1 represents the most efficient solution. [9]

Case 4 in Figure 25 corresponds to the measured, typical partition structure – a totally coupled partition with two plate layers are attached to common studs. In case 4, the structure is also coupled via the perimeters of the partition. Whereas in an uncoupled partition there is no direct structure-borne path between the plates, in a coupled partition the structure-borne route via studding and perimeters constitutes a significant sound transmission path. Sound transmission from one plate layer to the other can be decreased if there is no physical connection via the studs. This could be achieved by a staggered studding, illustrated in case 3 of Figure 25.

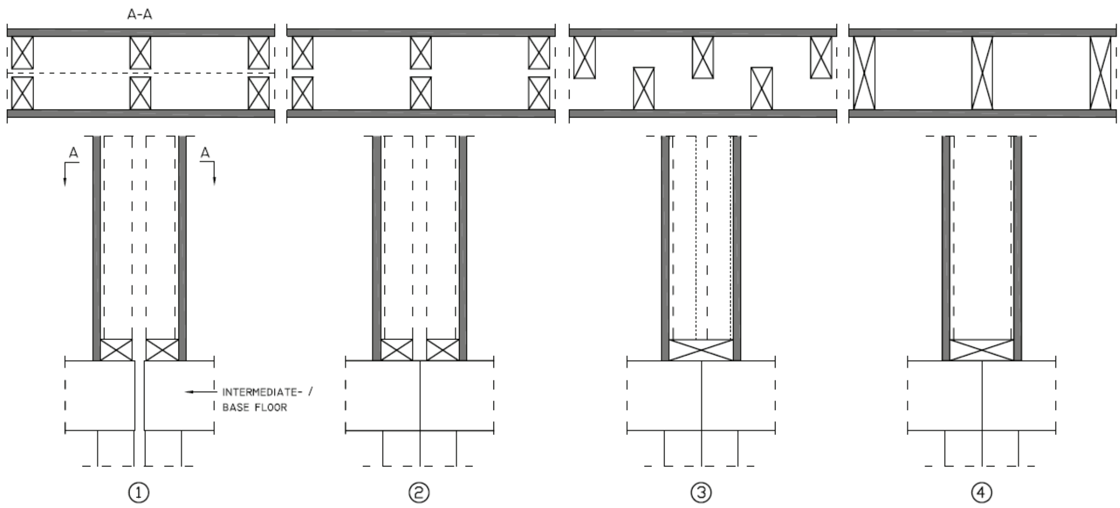


**Figure 25.** The basic types of double-leaf partitions; adapted from [9].

Figure 26 presents the calculated sound reduction indexes of an uncoupled, partially coupled and totally coupled double-leaf partition. The structure consists of two medium density fiberboards with a thickness of 12 mm attached to wooden studding. The cavity is totally filled with mineral wool. The three partition types correspond to cases 2 – 4 in Figure 25.

The lowest curve in Figure 26 corresponds to the typical partition, which was a totally coupled structure. As the amount of connections between plates reduces, the sound reduction index increases. The second-highest curve corresponds to case 3 partition in Figure 25 with staggered studding and coupling only via the perimeters and the highest curve to case 2, where the studs are separated by an air space.

The calculation results indicated that it would be possible to implement the partition in the lowest target class as a totally coupled structure. In order to achieve the target values in classes 1 and 2, however, it seemed that the connection type should be altered, either to a totally coupled or partially coupled structure. Furthermore, the calculated weighted sound reduction index of the uncoupled partition, $R_w$ = 49 dB, indicated that changing the connection type would not alone guarantee sufficient improvement in the sound reduction index, but other means would have to be considered as well.

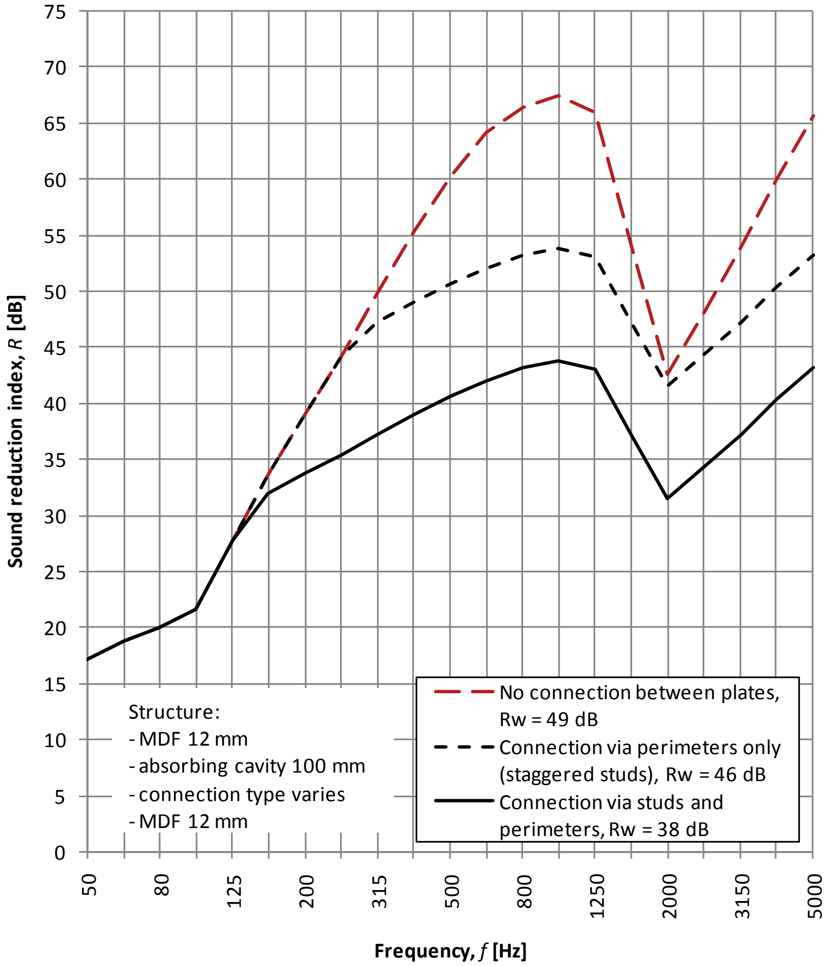


**Figure 26.** The effect of connection type on the sound reduction index. Centres distance of studs is 600 mm and area of the structure is 10 $m^2$. Calculated with prediction model; see Section 4.4.2.

### 5.3.2 Type and amount of building boards

From a sound insulation perspective, coincidence phenomenon is one of the most significant factors that should be taken account of when determining what types of building boards should be used in partitions [32]. Figure 27 presents the calculated SRI of common wood-based building boards – chipboard, medium density fiberboard and birch plywood – with different thicknesses. Coincidence occurs at the critical frequency of a plate and causes a notable dip in the SRI-curve.

Table 10 presents the aforementioned building boards arranged in ascending order according to surface density. The surface densities listed on the right-hand side of the dashed line are measured values reported by Larm et al. [33]. The two columns on the left consist of calculated values. The critical frequencies were calculated with Equation (9), Section 4.3.2.

The calculation and measurement results suggested that a thin chipboard panel would be a good choice for the new partitions. Compared to other conventionally used building boards, a 11 mm chipboard panel has a high critical frequency, thanks to which coincidence phenomenon does not seem to significantly deteriorate the sound reduction index. Furthermore, the thinner chipboard seems to have good sound insulation properties compared to a relatively low surface density. In this respect the thickest plywood represents the opposite case.

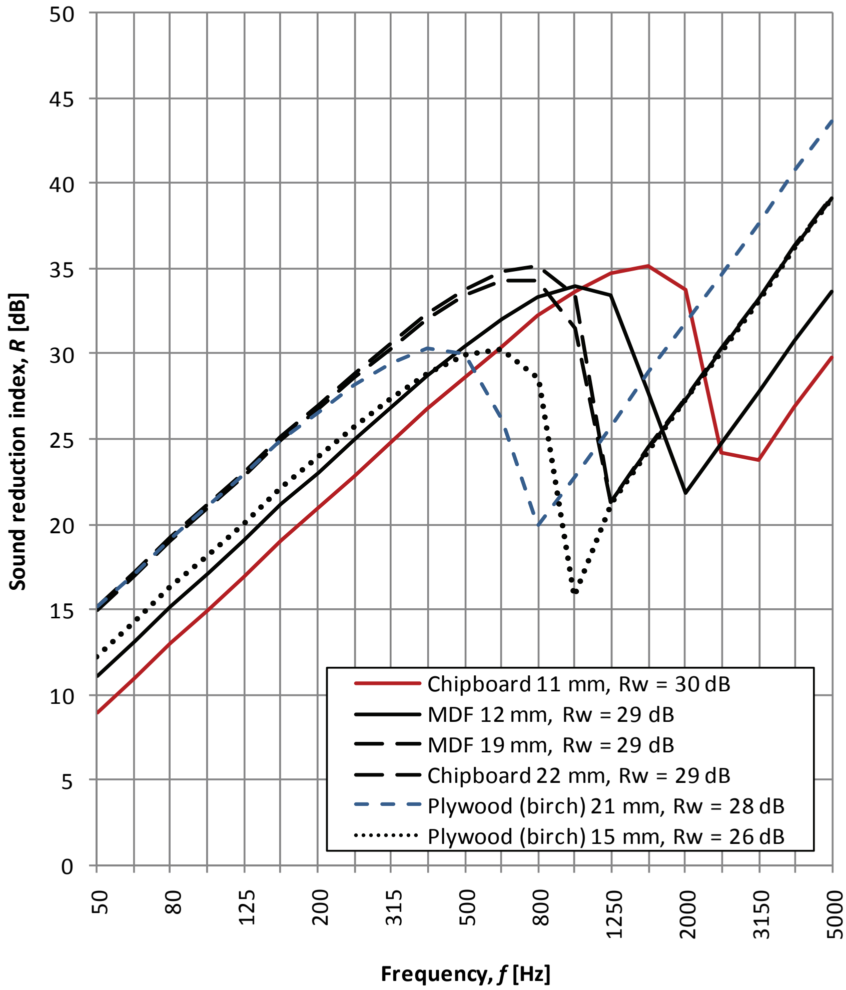


**Figure 27.** The sound reduction index of common wood-based building boards. Calculated with prediction model; see Section 4.4.1. Material parameters according to Tables 4 and 5, Section 4.2.

**Table 10.** Common wood-based building boards arranged in ascending order according to surface density. The critical frequency calculated with Equation (9) and the weighted sound reduction index with prediction model; see Section 4.4.1. Material parameters according to Tables 4 and 5, Section 4.2.

| Building board / thickness | Critical frequency, $f_c$ [Hz] | Weighted SRI, $R_w$ [dB] | Surface density, $m`$ [kg/m$^2$] [1)] |
|---|---|---|---|
| Chipboard 11 mm | 2660 | 30 | 7,0 |
| MDF 12 mm | 1800 | 29 | 9,2 |
| Plywood 15 mm | 1040 | 26 | 10,4 |
| MDF 19 mm | 1300 | 29 | 13,8 |
| Chipboard 22 mm | 1230 | 29 | 13,9 |
| Plywood 21 mm | 740 | 28 | 15,0 |

[1)] Measured values according to Larm. et al [33]

The calculated sound reduction indexes of building boards presented in Table 10 are within 4 dB, thus the difference in sound insulation between single plates seems to be rather small. Nevertheless, it has been found that optimizing the properties of single building boards becomes of great significance in double-leaf partitions, since such structures often consists of several plate layers [33].

A general guideline is that a sound insulating partition should only contain plates with sufficiently high critical frequency. Nevertheless, calculations with the prediction model seemed to indicate that, in some cases, also thick building boards could be used to achieve efficient sound insulation. A possible solution would be to use a combination of a light, thin building board with high critical frequency and a slightly thicker board with a higher surface density and lower critical frequency. In such a combination, the thinner plate would serve to minimize the decrease in sound reduction index caused by the coincidence phenomenon, while the thicker plate would provide sufficient mass for the structure.

Figure 28 illustrates how the sound reduction index is affected when a thin building board with a low surface density and a thicker board are combined. The structure on the left-hand side of the figure is an uncoupled partition and a coupled partition on the right. One of the plates is a chipboard panel with a thickness of 11 mm and the other plate varies.

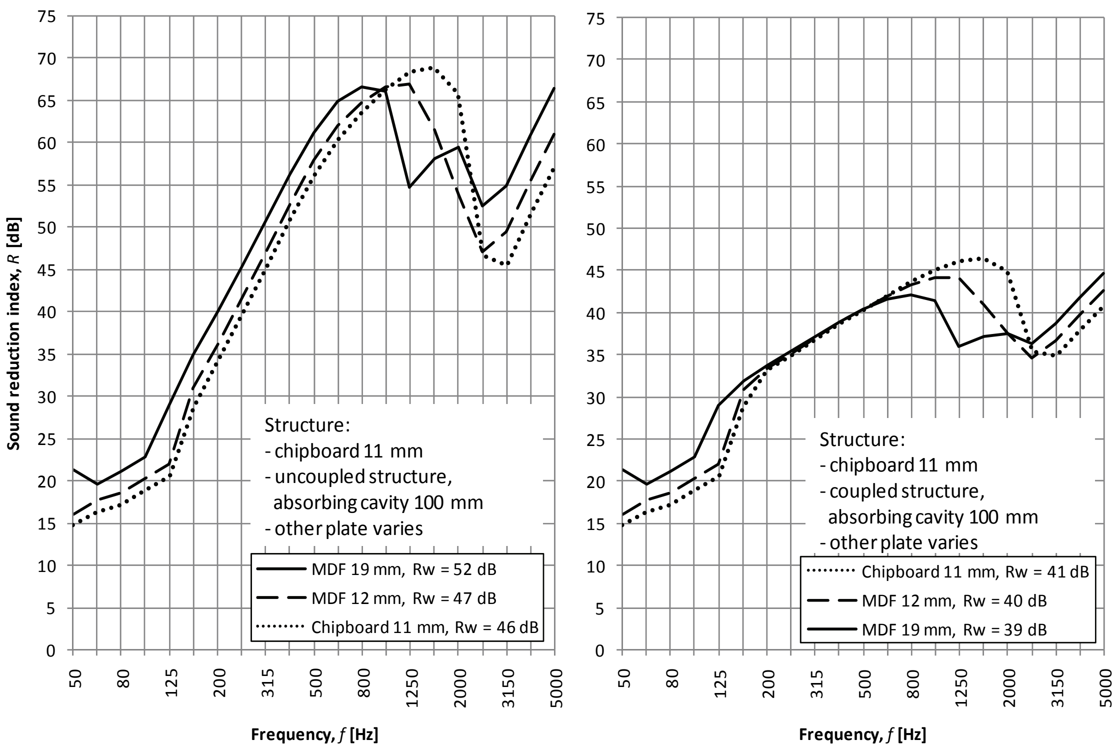


**Figure 28.** The sound reduction index of a partition with thin, lightweight building board on one side and a thicker building board on the other. Calculated with prediction model; see Section 4.4.2.

The calculation results indicated that a thick plate with a high surface density could be used to improve the sound reduction index of an uncoupled structure. The prediction model suggested, however, that the sound reduction index does not improve correspondingly if the partition is coupled. Judging by the calculation results, it seemed that a combination of 11 mm chipboard and 19 mm MDF could be used to achieve the target value set for the class 2 partition.

Increasing the total mass of a partition structure is generally an efficient means for improving the sound reduction index [9]; the improvement in the SRI seen in the left-hand side of Figure 29 is also based on increased mass. An efficient means of increasing the overall mass of a partition is to attach several building boards together. The advantage of this, compared to increasing the thickness of a single building board, is that if the attachment is done with screws or nails, the critical frequencies of the individual plates do not significantly change [16] and the coincidence phenomenon can be avoided.

Figure 29 illustrates how the sound reduction index improves as the number of overlapping building boards increases. It is assumed that the attachment is done with screws or nails. The structure on the left-hand side is uncoupled and coupled on the right. According to the prediction model, the improving effect on sound insulation seems to be even more considerable in an uncoupled partition.

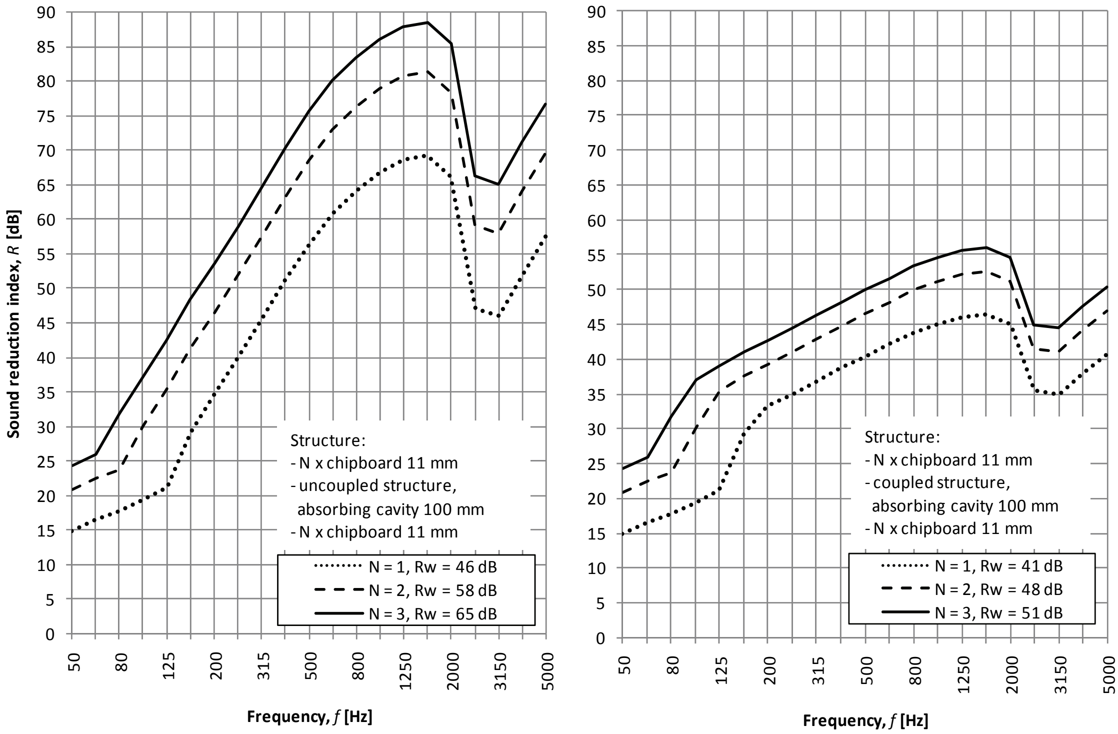


**Figure 29.** Calculated improvement in the sound reduction index as the number of overlapping building boards increases; see Equation (22), Section 4.4.1. It is assumed that the plates are attached loosely with screws or nails. If the plates are glued together, similar improvement in the SRI is not achieved.

The calculation results suggested that, while the target value in class 2 could be achieved with a coupled structure, this would basically require using at least three building boards per partition side. While such a structure would have a sufficiently high sound reduction index, it would be rather impractical to implement. Furthermore, the calculations indicated that an uncoupled structure would ultimately be the only viable solution for the separating partition in class 1. Even with an uncoupled partition, at least two overlapping building boards per partition side would have to be used to achieve a sound reduction index level of $R_w \geq 60$ dB.

## 5.3.3 Depth and filling ratio of the cavity

Figure 30 illustrates the effect of cavity depth on the sound reduction index, when the cavity is totally filled with sound absorbing material. On the left-hand side of the figure the studding is totally separate and, on the right, the partition leaves are coupled. Calculation results seem to indicate that the cavity depth plays a considerable role in an uncoupled partition, whereas in a totally coupled partition it has little significance. Laboratory measurements conducted with double-leaf partitions support this observation: it has been found that increasing cavity depth significantly improves the SRI of an uncoupled partition, whether the cavity is empty or filled with absorbing material [19]. When the plates are coupled via common studs, however, increasing cavity depth has only little effect on the sound reduction index [19].

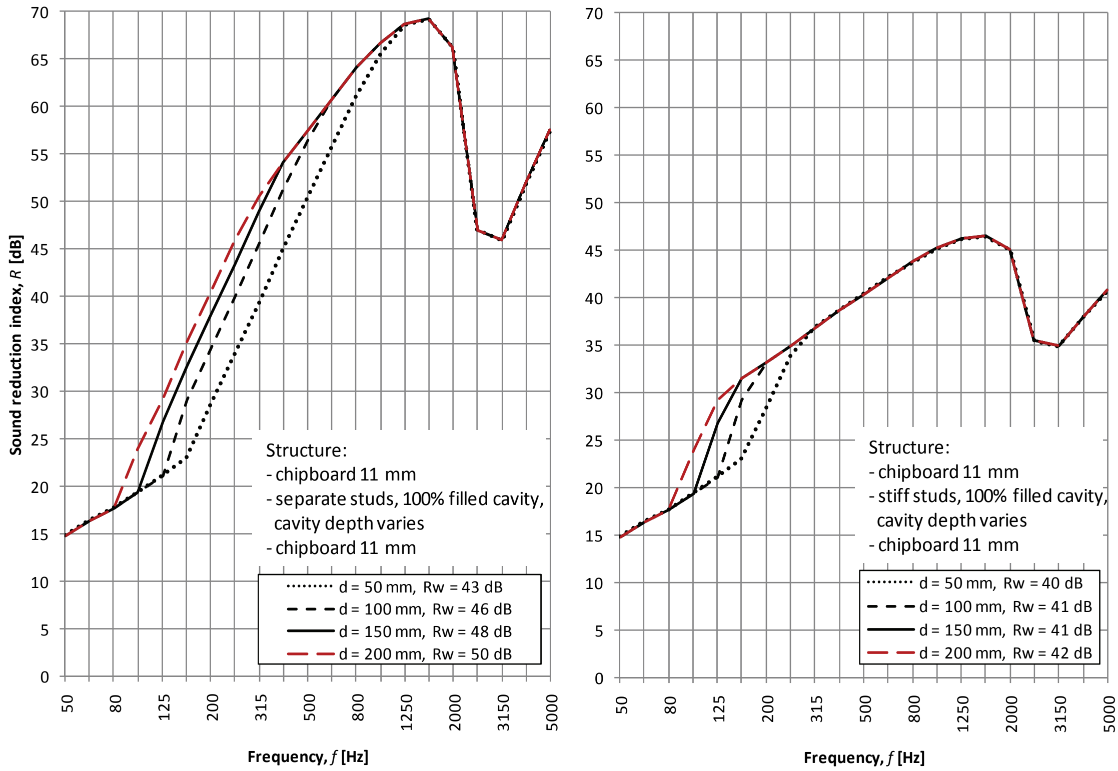


**Figure 30.** The effect of cavity depth on the sound reduction index. Cavity is totally filled (FR = 100%) with mineral wool, $\alpha_c$ = 0,90. Calculated with prediction model; see Section 4.4.2.

The calculations concerning cavity depth indicated that the partition in the lowest target class could be implemented as a coupled partition with a cavity depth of about 100 mm. The calculation results indicated, however, that it would not seem reasonable to increase cavity depth further, since this does not yield significant improvement in the sound reduction index. The calculation results of the uncoupled structure suggested that increasing the depth of the cavity would not be a sufficient means alone for achieving the target value in class 1; see the left-hand side of Figure 30.

Calculations with the prediction model indicated that achieving a sound reduction index of the magnitude $R_w \geq 50$ dB, corresponding to the target value in class 2, would require a rather high cavity depth, about 200 mm. From the practical viewpoint it seemed a better alternative to limit the cavity depth of the class 2 partition to a moderate level, below 150 mm, and select the plates so that the desired level of sound reduction index could be achieved. This way the overall thickness of the partition could also be kept within the boundary conditions set in the study.

Figure 31 illustrates how the amount of absorbing material in the cavity, filling ratio, affects the sound reduction index. The partition on the left-hand side of the figure is uncoupled. Filling ratio has been found to be a parameter that, along with cavity depth, has the most significant effect on the SRI of uncoupled double-leaf partitions [19]. The improving effect of cavity filling material is relatively greatest when comparing an empty cavity with a filling ratio of about 20 % [19]. The sound reduction index improves when the amount of absorbing material is increased further, but the relative improvement is not as significant.

Acoustically, the primary purpose of filling material is to dampen the cavity resonances which have a deteriorating effect on the sound reduction index. It has been found that even a small amount of absorbing material is effective in damping the resonances. While filling ratio is an important factor, measurement results have indicated that the material properties of the cavity filling material – density and flow resistivity – are mostly insignificant from a sound insulation point of view in both coupled and uncoupled double-leaf partitions. [19]

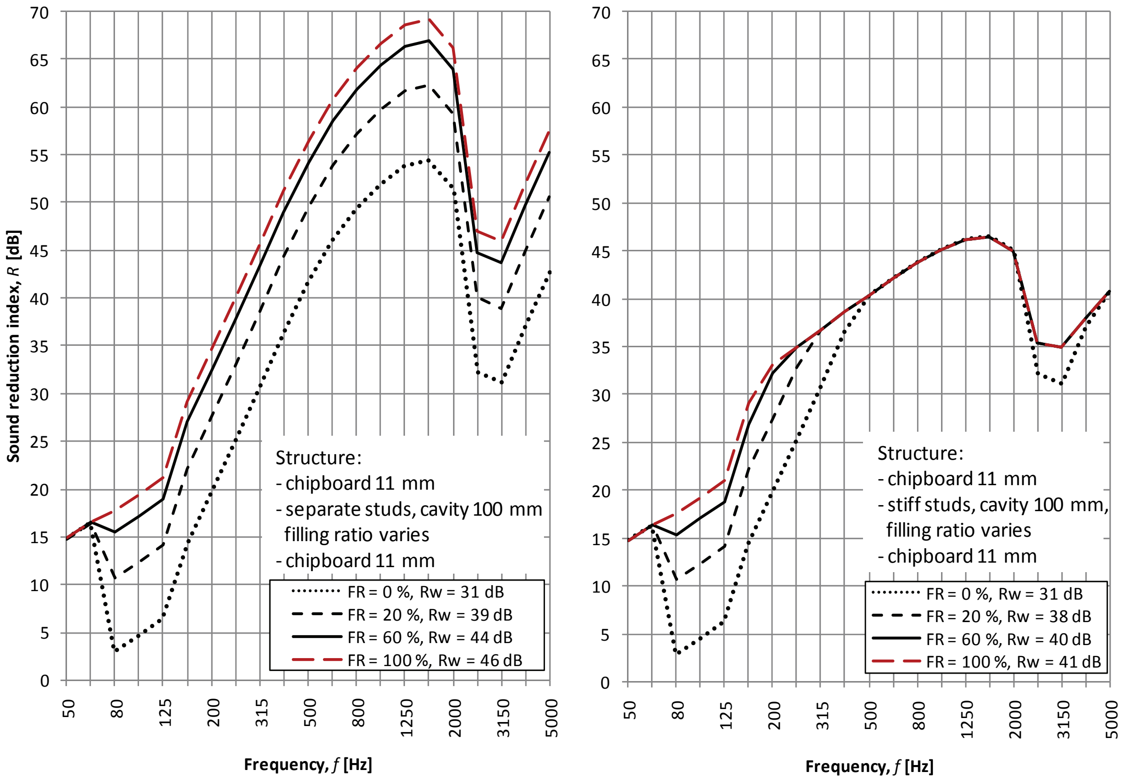


**Figure 31.** The effect of cavity filling ratio on the sound reduction index. Calculated with prediction model; see Chapter 4.4.2.

The overall conclusion drawn based on the calculations concerning the filling ratio was that at least half of the cavities of the new partitions should be filled with mineral wool. Even total filling would not be exaggerated as it could yield some, although little, additional improvement in sound insulation. Most importantly, however, it was concluded that the cavity should not be left empty of absorbing material since this seems to considerably deteriorate the sound reduction index of both coupled and uncoupled partitions.

### 5.3.4 Screw spacing and centers distance of studs

Figure 32 illustrates the effects of screw and stud spacing on the sound reduction index. Both structures are coupled via common studding. According to the prediction model, it seems that increasing screw spacing improves the SRI above a limiting frequency, which is around 200 Hz with this particular structure. At mid- and high frequencies, above the limiting frequency, the difference in the SRI between dense, 200 mm, and sparse, 1000 mm, screw spacing is at least 10 dB. The right-hand side of the figure illustrates how the centres distance of studs affects the sound reduction index. Improvement in the SRI seems to be most notable when stud spacing increases from 300 mm to 600 mm. However, increasing the spacing above a typically used centres distance of 600 mm does not seem to yield much practical improvement.

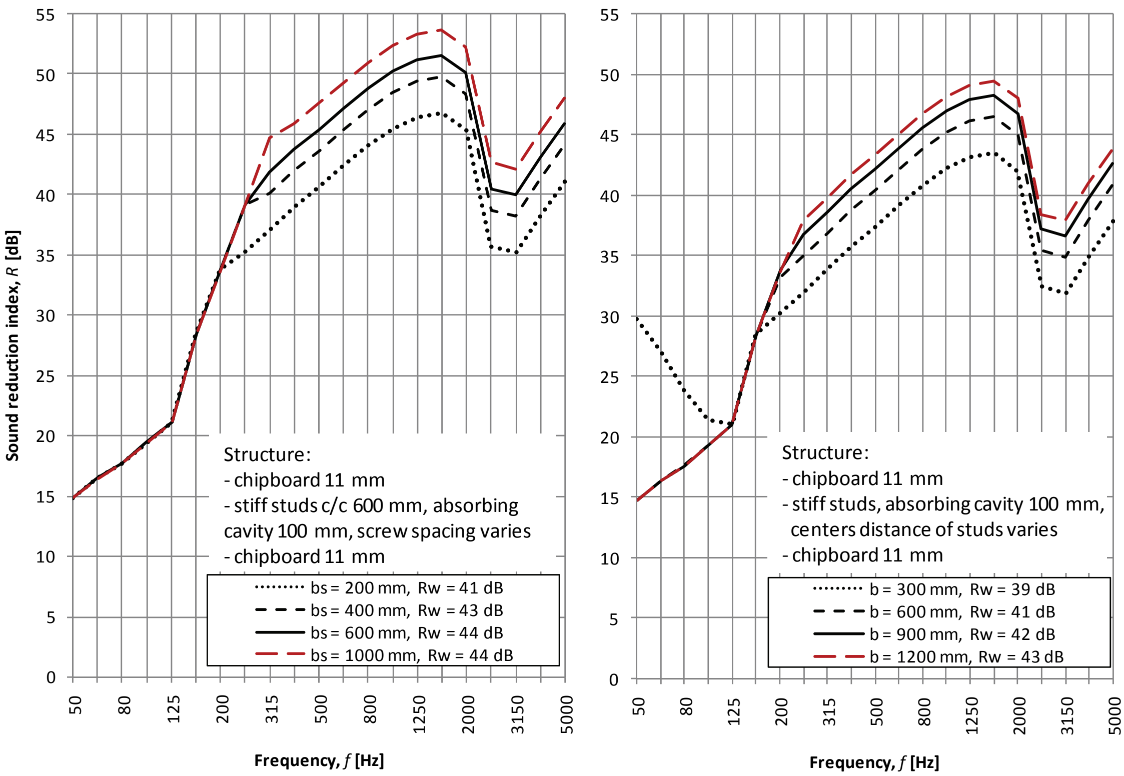


**Figure 32.** The effects of screw spacing (left) and centres distance of studs (right) on the sound reduction index. Calculated with prediction model; see Section 4.2.2.

Of the two parameters presented in Figure 32, screw spacing is the factor that has been found to have most significance with coupled double-leaf partitions. According to laboratory measurements, the improvement in sound insulation gained by sparse screw spacing is slightly more significant than suggested by the calculation results in Figure 32. The centres distance of studs, on the other hand, has been found to have very little practical effect on the sound reduction index of a double-leaf partition. According to investigations, increasing the centers distance of studs improves sound insulation only by a little amount above 200 Hz. [19]

Although screw spacing has been shown to affect sound insulation, it is a parameter subjected to practical constraints. Such a sparse screw spacing that would yield a significant improvement in sound insulation could be difficult to achieve since, in practice, the maximum distance between screws or nails is often determined by strength requirements. The distance between adjacent points of attachment between plate and studding can be increased only up to a certain point, above which mechanical strength begins to severely deteriorate.

Laboratory measurement results [19] and calculations indicated that a rule of a thumb would be to use as sparse screw spacing in the new partitions as practical constraints allow. From a product development point of view, however, increasing the screw spacing did not seem to be rather impractical means for improving sound insulation. Judging by the results of prior investigations [19] and calculations with the prediction model, it seemed that the target values of the sound reduction index could be achieved if a conventional centres distance of studs, 600 mm, was used in all the new partitions.

### 5.3.5 Vibration reduction index of partition junction

The partitions intervening rooms and corridor in the typical partition system were single plate structures, one consisting of single MDF-panels and the other of laminated glass sheets; see Section 5.2.1. There was a structural flanking path from room 1 to room 2 via the continuous plate structures. A principle of the flanking path is illustrated in Figure 33.

Compared to the solution presented in Figure 33, it seemed that flanking transmission via the corridor partition could be considerably diminished if the junction of the two partitions was implemented as a truncated T-junction. As a result, the apparent sound reduction index between the adjacent rooms would improve compared to the typical partition structure. Figure 34 presents the two possible solutions of a truncated T-junction that were considered. A non-truncated junction is illustrated for comparison.

The vibration reduction index for the continuous plate structure in Figure 34, case A, is $K_{ij}$ = 0 dB [14]. This roughly corresponds to the vibration reduction index of the junction between the typical partitions. In case B, the inner plate layer is truncated. Homb et al. [14] give an estimated vibration reduction index of $K_{ij}$ = 15 dB for such a junction. In case C of the figure, both continuous plate layers are truncated. It was estimated that the vibration reduction index of such a junction could be even considerably higher than the corresponding value achieved with a single truncated plate; possibly in the range of $K_{ij}$ = 15…30 dB.

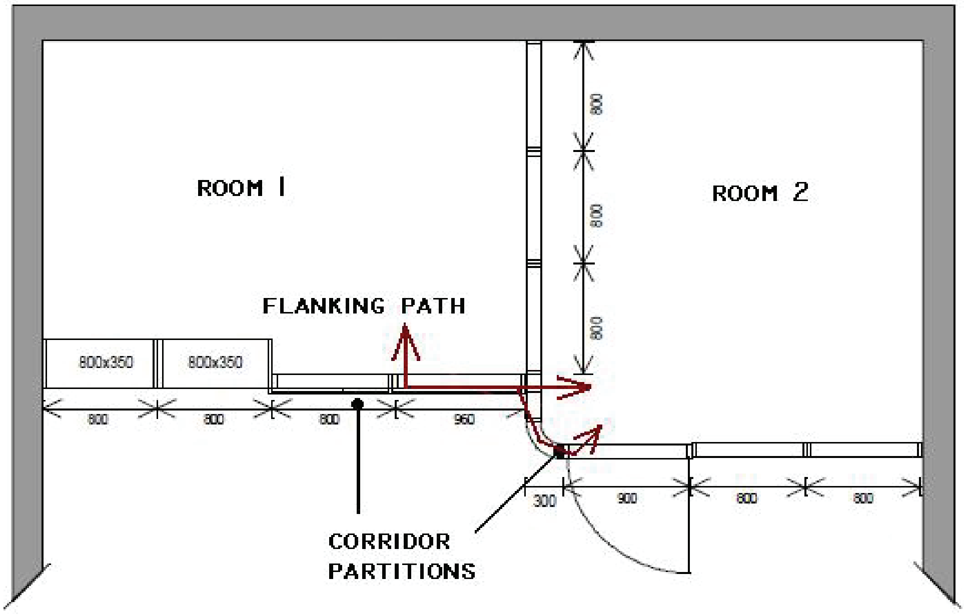


**Figure 33.** In the typical partition structure the continuous plate structure of the corridor partition constituted a notable flanking transmission path.

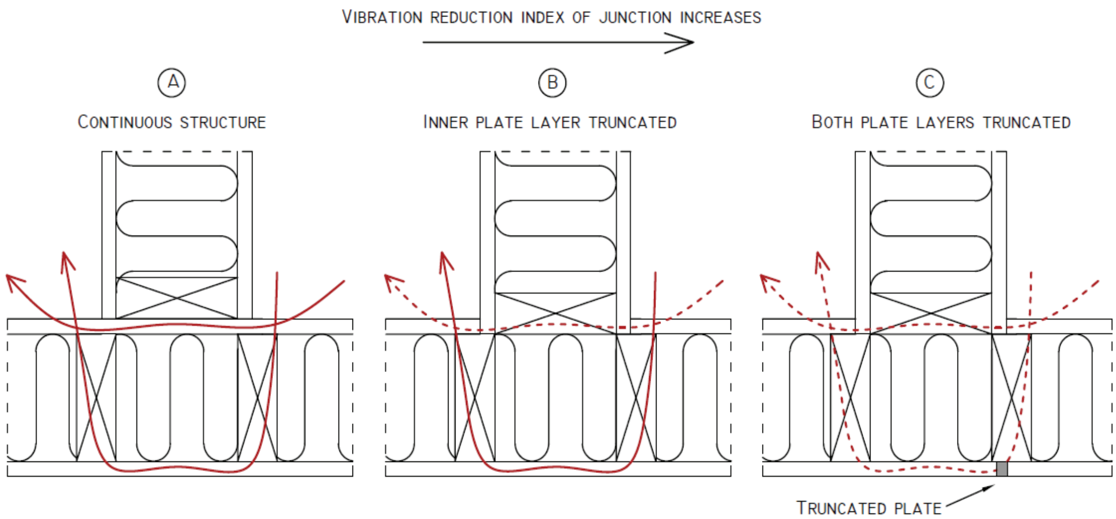


**Figure 34.** Practical approach for improving the vibration reduction index of the junction between two double-leaf partitions. Flanking transmission paths illustrated by arrows.

## 5.4 Solutions for New Partitions and Modelling Results

### 5.4.1 Modelling parameters

The sound reduction index of different partition structures was calculated with the prediction model; see Section 4.4. Alternative structural solutions were compared by changing the material and number of plates, cavity thickness and filling ratio as well as the type of connection between the partition leaves. Table 11 lists the parameters that were included in the calculations.

In addition to the aforementioned parameters, the centres distance of studs and the spacing of screws or nails were also included in the model, but these factors were not used as a means of improving sound insulation. All the calculations were made using a constant centres distance of studs, 600 mm. Screw spacing was assumed to be so dense that the connections between building boards and studs act as line couplings.

**Table 11.** Parameters in the prediction model of the sound reduction index.

| Parameter | Symbol |
|---|---|
| **Plates** | |
| Number of overlapping plates (attachment with screws or nails) | $N$ |
| Thickness | $h$ |
| Density | $\rho$ |
| Poisson`s ratio | $\mu$ |
| Modulus of elasticity | $E$ |
| Internal loss factor | $\eta_{int}$ |
| **Cavity / absorbing material** | |
| Cavity depth | $d$ |
| Cavity, x-dimension | $L_{x,c}$ |
| Cavity, y-dimension | $L_{y,c}$ |
| Filling ratio | $FR$ |
| Absorption coefficient | $\alpha_c$ |
| **Studs / attachment of plates to studs** | |
| Centers distance of studs | $b$ |

## 5.4.2 Class 1 partitions

Figure 35 presents the section of the class 1 partition between adjacent rooms. A value of $R_w$ = 61 dB was calculated for the weighted sound reduction index of the structure using the prediction model. The sound reduction index is presented in Figure 36. Table 12 lists the parameters that were used in the calculations.

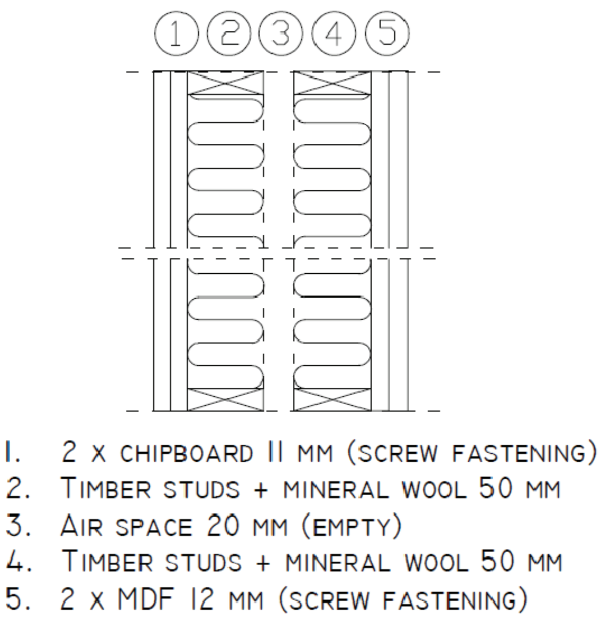


**Figure 35.** Section of the partition separating adjacent rooms in class 1.

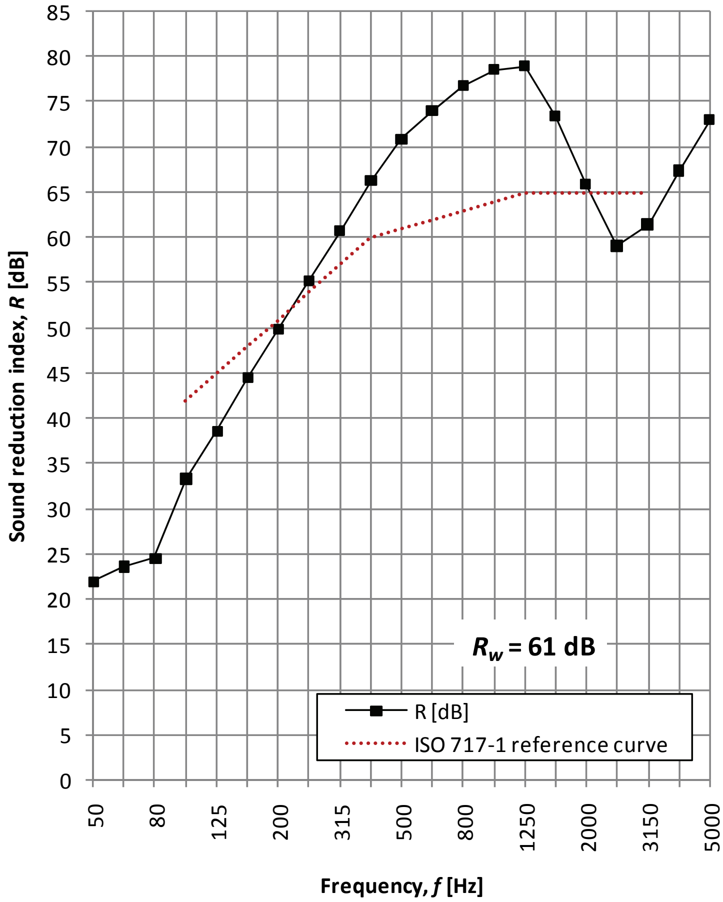


**Figure 36.** The calculated sound reduction index of the partition separating adjacent rooms in class 1.

**Table 12.** Parameters used in the calculation of the sound reduction index; class 1 partition.

| Parameter | Symbol | Value |
|---|---|---|
| **Plate layer 1: 2 x chipboard 11 mm** | | |
| Thickness | $h$ | 0.011 m |
| Density | $\rho$ | 640 kg/m$^3$ |
| Poisson`s ratio | $\mu$ | 0.30 |
| Modulus of elasticity | $E$ | 2900 Mpa |
| Internal loss factor | $\eta$ | 0.01 |
| **Plate layer 2: 2 x MDF 12 mm** | | |
| Thickness | $h$ | 0.012 m |
| Density | $\rho$ | 760 kg/m$^3$ |
| Poisson`s ratio | $\mu$ | 0.30 |
| Modulus of elasticity | $E$ | 6300 Mpa |
| Internal loss factor | $\eta$ | 0.01 |
| **Cavity / absorbing material** | | |
| Cavity thickness | $d$ | 0.120 m |
| Cavity, x-dimension | $L_{x,c}$ | 0.580 m |
| Cavity, y-dimension | $L_{y,c}$ | 2.400 m |
| Filling ratio | $FR$ | 0.90 |
| Absorption coefficient | $\alpha_c$ | 0.90 |
| **Studs** | | |
| Centres distance of studs | $b$ | 0.600 m |

Figure 37 presents the section of the corridor partition in class 1. Using the prediction model, the structure was estimated to have a weighted sound reduction index of $R_w$ = 46 dB; see Figure 38. The same calculation parameters were used as listed in Table 12. Figure 39 presents a detail of the T-junction for the two class 1 partitions.

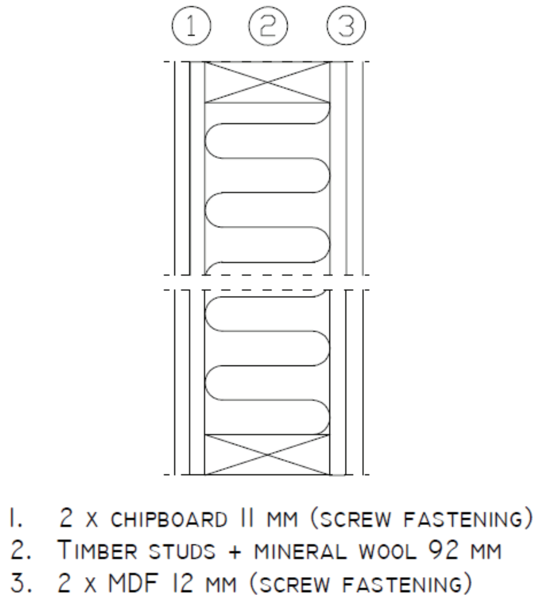


**Figure 37.** Section of the corridor partition in class 1.

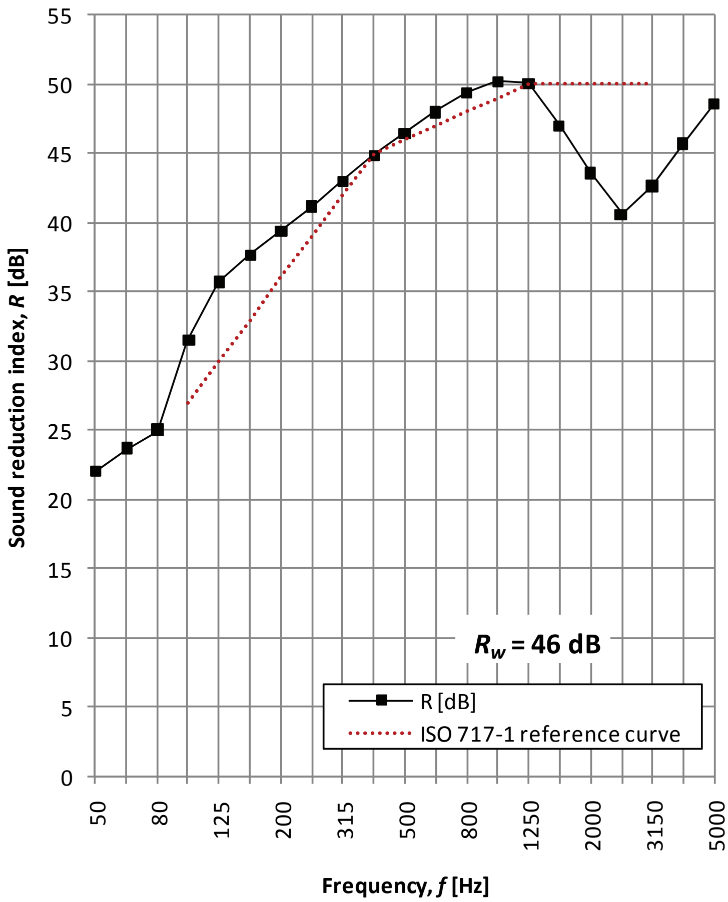


**Figure 38.** Predicted sound reduction index of the corridor partition in class 1.

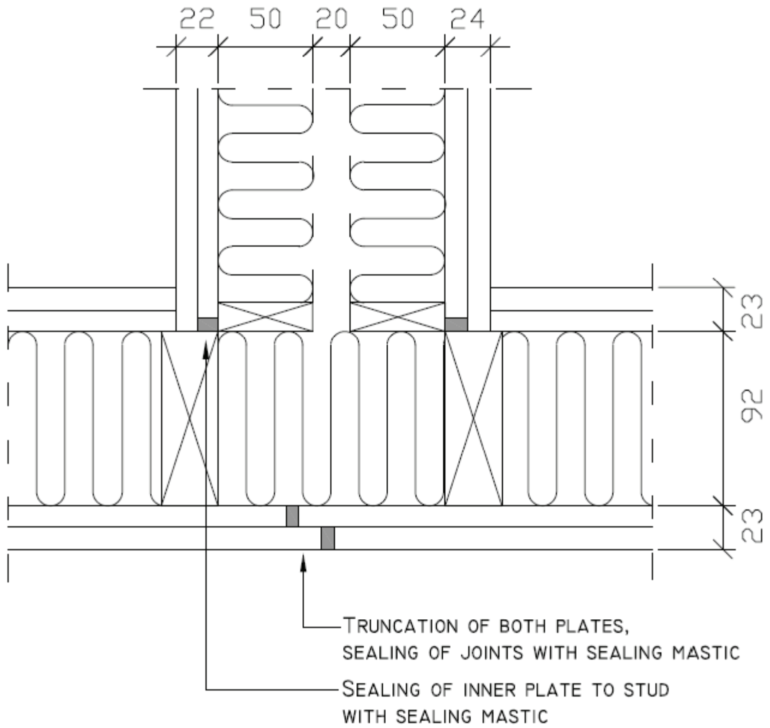


**Figure 39.** Detail of the T-junction between class 1 partitions.

### 5.4.3 Class 2 partitions

The section of the partition separating adjacent rooms in class 2 is presented in Figure 40. It was calculated that the structure has a weighted sound reduction index of $R_w$ = 53 dB. The sound reduction index is presented in Figure 41 and parameter values are listed in Table 13. Figure 42 presents the T-junction between the partition intervening rooms and the corridor partition in class 2.

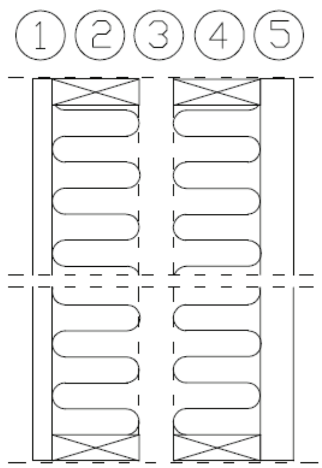


**Figure 40.** Section of the partition between adjacent rooms in class 2.

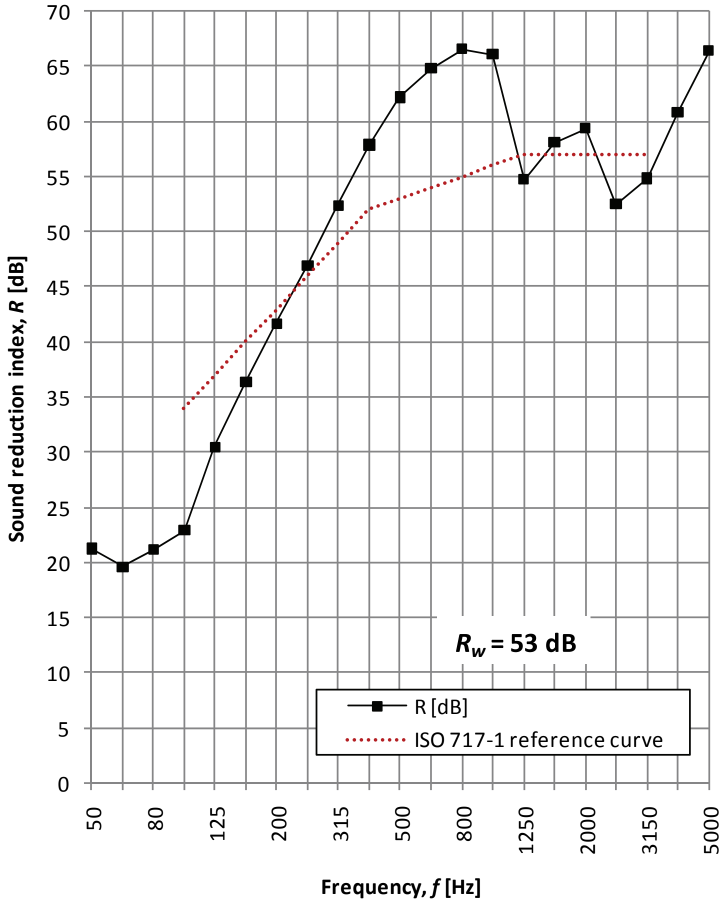


**Figure 41.** The calculated sound reduction index of partition separating adjacent rooms in class 2.

**Table 13.** Parameters used in the calculation of the sound reduction index; class 2 partition.

| Parameter | Symbol | Value |
|---|---|---|
| **Plate 1: chipboard 11 mm** | | |
| Thickness | $h$ | 0.011 m |
| Density | $\rho$ | 640 kg/m$^3$ |
| Poisson`s ratio | $\mu$ | 0.30 |
| Modulus of elasticity | $E$ | 2900 Mpa |
| Internal loss factor | $\eta$ | 0.01 |
| **Plate 2: MDF 19 mm** | | |
| Thickness | $h$ | 0.019 m |
| Density | $\rho$ | 760 kg/m$^3$ |
| Poisson`s ratio | $\mu$ | 0.30 |
| Modulus of elasticity | $E$ | 4800 Mpa |
| Internal loss factor | $\eta$ | 0.01 |
| **Cavity / absorbing material** | | |
| Cavity thickness | $d$ | 0.120 m |
| Cavity, x-dimension | $L_{x,c}$ | 0.580 m |
| Cavity, y-dimension | $L_{y,c}$ | 2.400 m |
| Filling ratio | $FR$ | 0.90 |
| Absorption coefficient | $\alpha_c$ | 0.90 |
| **Studs** | | |
| Centres distance of studs | $b$ | 0.600 m |

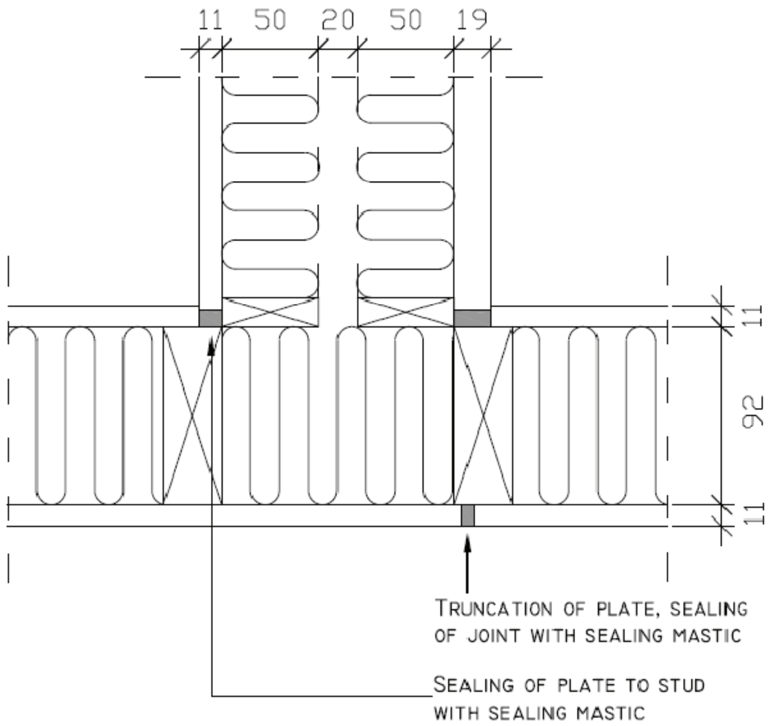


**Figure 42.** Detail of the T-junction in class 2.

### 5.4.4 Class 3 partitions

Figure 43 presents the section of the partitions in class 3. The same structure is the same as the corridor partition in class 2; see Figure 42. Calculations with the prediction model yielded a value of $R_w$ = 41 dB for the weighted sound reduction index of the class 3 structure. The calculated sound reduction index is presented in Figure 44. Table 14 lists the calculation parameters and Figure 45 presents the T-junction between the class 3 partitions.

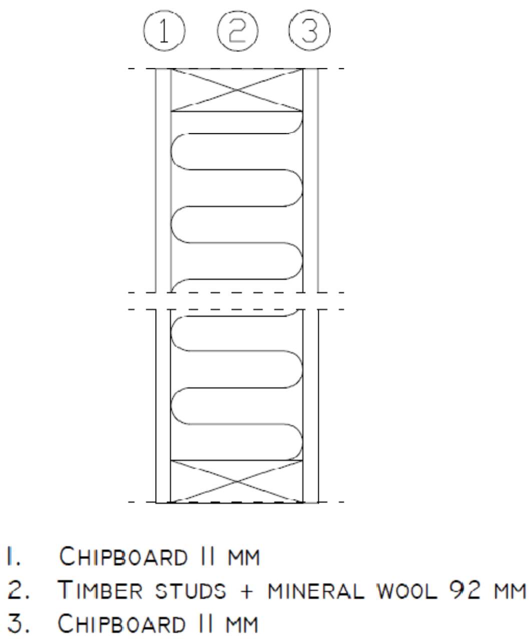


**Figure 43.** Section of partitions in class 3.

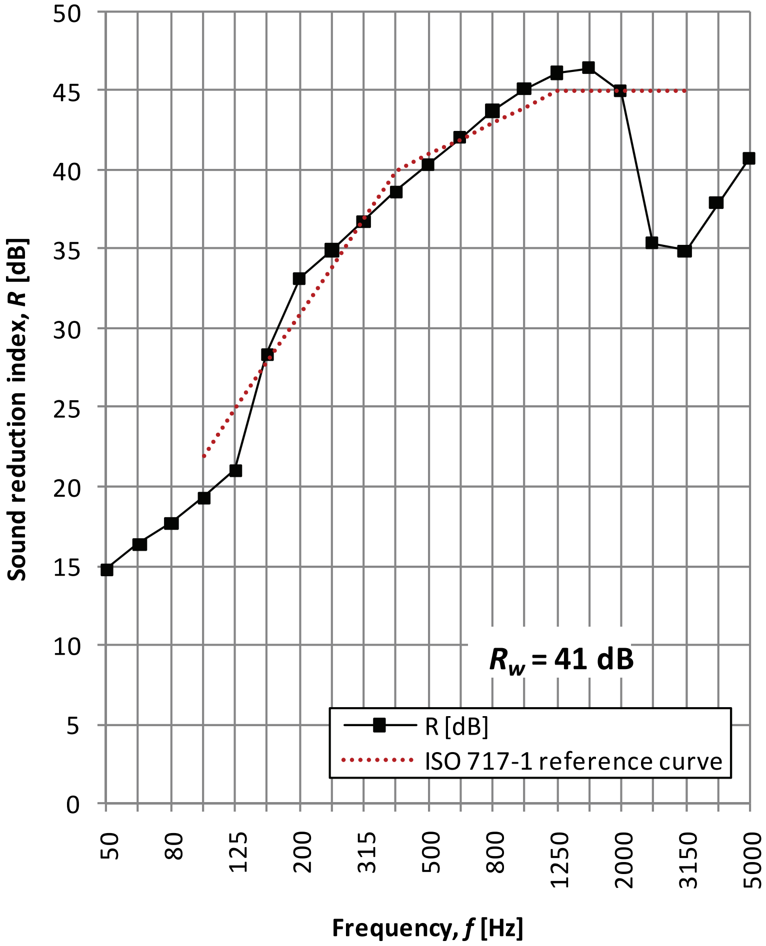


**Figure 44.** The calculated sound reduction index of partitions in class 3.

**Table 14.** Parameters used in the calculation of the sound reduction index; class 3 partitions.

| Parameter | Symbol | Value |
|---|---|---|
| **Plates 1 and 2: chipboard 11 mm** | | |
| Thickness | $h$ | 0.011 m |
| Density | $\rho$ | 640 kg/m$^3$ |
| Poisson`s ratio | $\mu$ | 0.30 |
| Modulus of elasticity | $E$ | 2900 Mpa |
| Internal loss factor | $\eta$ | 0.01 |
| **Cavity / absorbing material** | | |
| Cavity thickness | $d$ | 0.092 m |
| Cavity, x-dimension | $L_{x,c}$ | 0.580 m |
| Cavity, y-dimension | $L_{y,c}$ | 2.400 m |
| Filling ratio | $FR$ | 1.00 |
| Absorption coefficient | $\alpha_c$ | 0.90 |
| **Studs / attachment to plates** | | |
| Centres distance of studs | $b$ | 0.600 m |

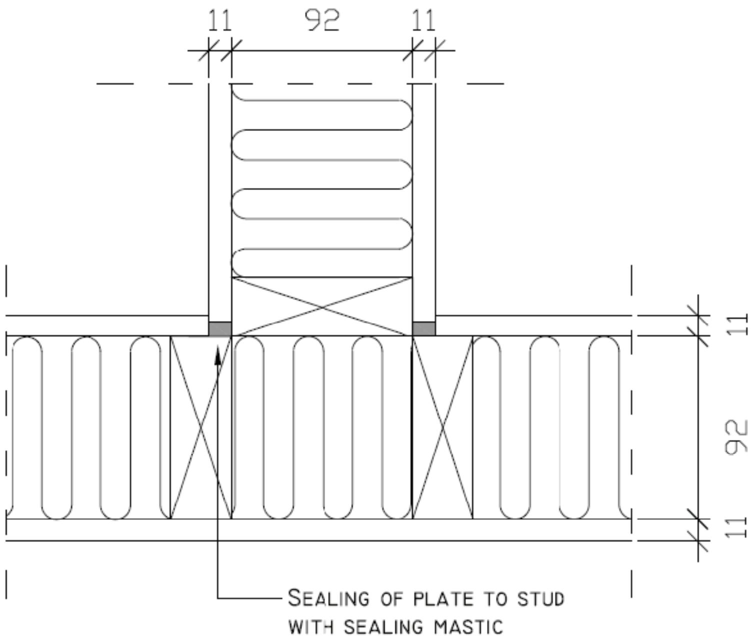


**Figure 45.** Detail of the T-junction in class 3.

### 5.4.5 Sealing details

Figure 47 illustrates the sealing detail of base floor junction for the class 1 partition. Effective sealing is achieved by using an EPDM-rubber band between the studding and tangential structure and by sealing all visible joints with mastic. Sealing details for each partition type are presented in Appendix F.

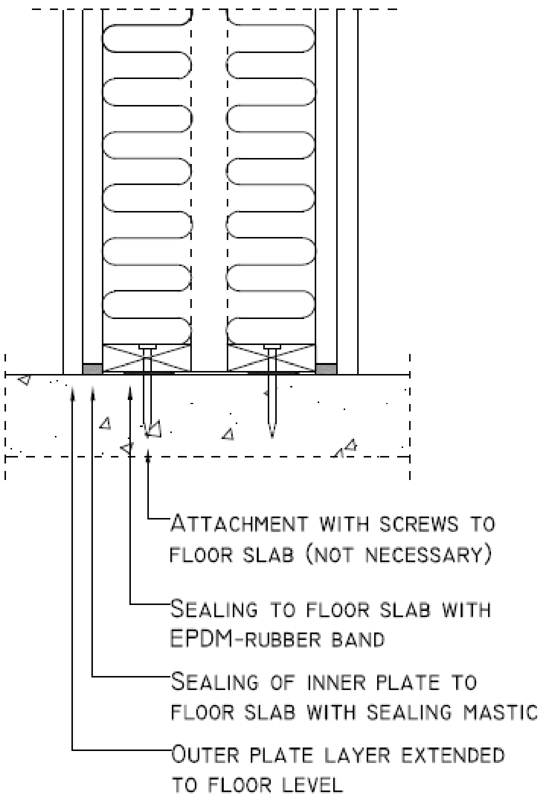


**Figure 46.** Sealing detail of the junction between class 1 partition and base floor; principle adapted from [35].

### 5.4.6 Estimation of apparent sound reduction index in test room

Flanking transmission in the test room was evaluated using the prediction model; see Section 4.6.2. The calculations yielded estimate values of apparent weighted sound reduction index that could be achieved in the test room, with the particular tangential structures. Figure 47 presents a plan of the test room. The placement of the new partitions is denoted by dashed lines.

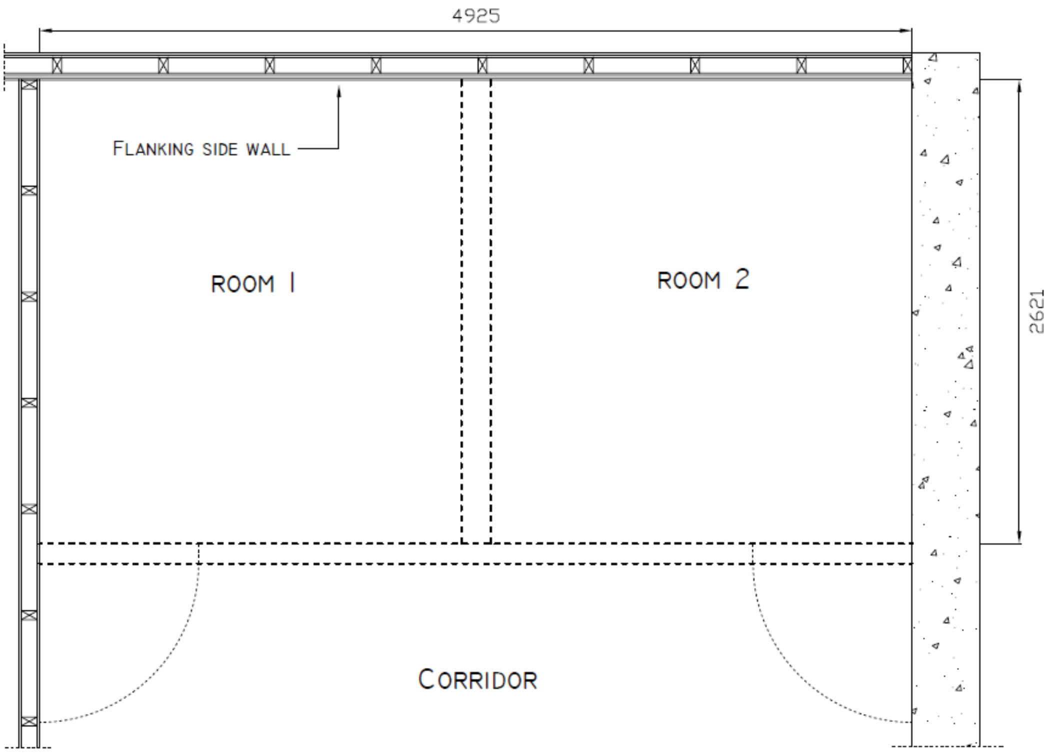


**Figure 47.** Plan of the test room. The new partitions are indicated with a dashed line.

The four flanking paths in the test room that were used in the calculations are illustrated in Figure 48. These flanking paths were:

- Flanking path 1: corridor partition according to class 1, 2 or 3
- Flanking path 2: side wall, structure explained below
- Flanking path 3: base floor, concrete slab 150 mm
- Flanking path 4: intermediate floor, hollow core slab 265 mm

The structure of the flanking side wall was the following

1. Chipboard 12 mm + gypsum board 15 mm, screw fastening
2. MDF 12 mm, attached with glue to the previous plate layer
3. Studding + mineral wool 90 mm
4. Chipboard 12 mm + perforated MDF 12 mm, screw fastening

Based on the prediction model, it could be estimated that the weighted sound reduction index of the flanking side wall structure is $R_w$ = 54 dB.

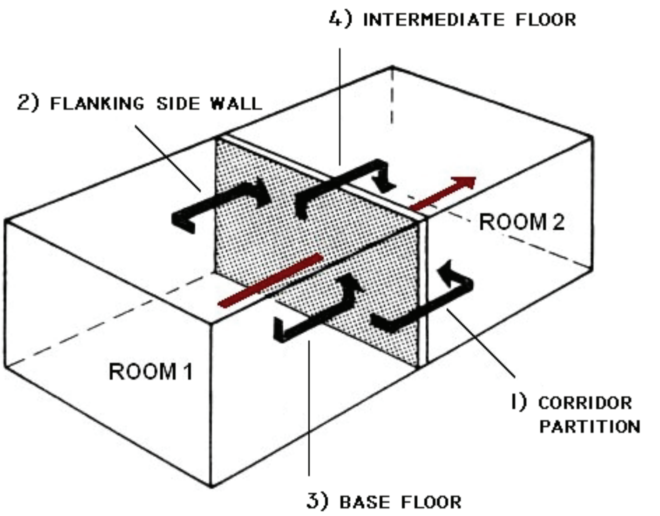


**Figure 48.** The four flanking structures in the test room. Direct sound transmission path through the separating partition is indicated with straight arrow.

Table 15 lists the values of the apparent weighted sound reduction index that were calculated using the flanking transmission prediction model. The values of the weighted sound reduction index and the vibration reduction index that were used in the calculations are presented in Table 16. Detailed calculation steps for each partition class are shown in Appendix D.

**Table 15.** The apparent sound reduction index from room 1 to room 2 in the test room. Calculated with prediction model; see Section 4.6.2.

| Class | Apparent sound reduction index from room 1 to room 2, $R`_w$ [dB] |
|---|---|
| 1 | 48 |
| 2 | 47 |
| 3 | 40 |

**Table 16.** The values of the weighted sound reduction index and the vibration reduction index used for evaluating the apparent weighted sound reduction index in the test room.

| Parameter description | Symbol | Value used in class 1 / 2 / 3 [dB] |
|---|---|---|
| **Partition separating rooms 1 and 2** | | |
| Weighted SRI of the partition | $R_w$ | 60/53/41 |
| **Flanking path 1: corridor partition** | | |
| Weighted SRI of flanking structure 1 | $R_{w1}$ | 46/41/41 |
| Vibration reduction index of the T- | $K_{ij,1}$ | 25/25/25 |
| **Flanking path 2: side wall F1** | | |
| Weighted SRI of flanking structure 2 | $R_{w2}$ | 54/54/54 |
| Vibration reduction index of junction | $K_{ij,2}$ | 0/0/0 |
| **Flanking path 3: base floor** | | |
| Weighted SRI of flanking structure 4 | $R_{w3}$ | 58/58/58 [1)] |
| Vibration reduction index of junction | $K_{ij,3}$ | 0/0/0 |
| **Flanking path 4: intermediate floor** | | |
| Weighted SRI of flanking structure 3 | $R_{w4}$ | 61/61/61 [2)] |
| Vibration reduction index of junction | $K_{ij,4}$ | 0/0/0 |

[1)] concrete slab 150 mm, $R_w$ = 58 dB [2]
[2)] hollow core slab 265 mm, $R_w$ = 61 dB [2]

## 5.5 Measurements of New Partitions

### 5.5.1 Description of structures and measurement arrangements

The apparent sound reduction index was measured in the test space using the partitions in classes 1, 2 and 3 as the separating walls between adjacent rooms and corridor. The partitions between adjacent rooms were implemented using large building boards: the 11 mm chipboard layers consisted of three panels, while the number of MDF-panels with thicknesses of 12 mm and 19 mm were three and two, respectively. The panels used in the corridor partitions had varying sizes.

All the attachments between overlapping panels as well as between the panels and studs were done with screws. Panels were screwed to studs directly. Screw spacing varied mostly in a range of 600 – 1100 mm, and the centres distance of studs was 590 mm. Visible joints in all partitions were sealed with sealing mastic.

The partition intervening adjacent rooms in class 3 was implemented so that two studs, with thicknesses of 50 mm, were attached together with screws. The structure of the partition was otherwise the same as presented in the sectional drawing; see Section 5.4.4.

### 5.5.2 Measurement results

Figures 49 – 51 present the measured apparent sound reduction indexes from room 1 to room 2 for partition classes 1, 2 and 3, respectively. A more detailed listing of the results is presented in Appendix A.

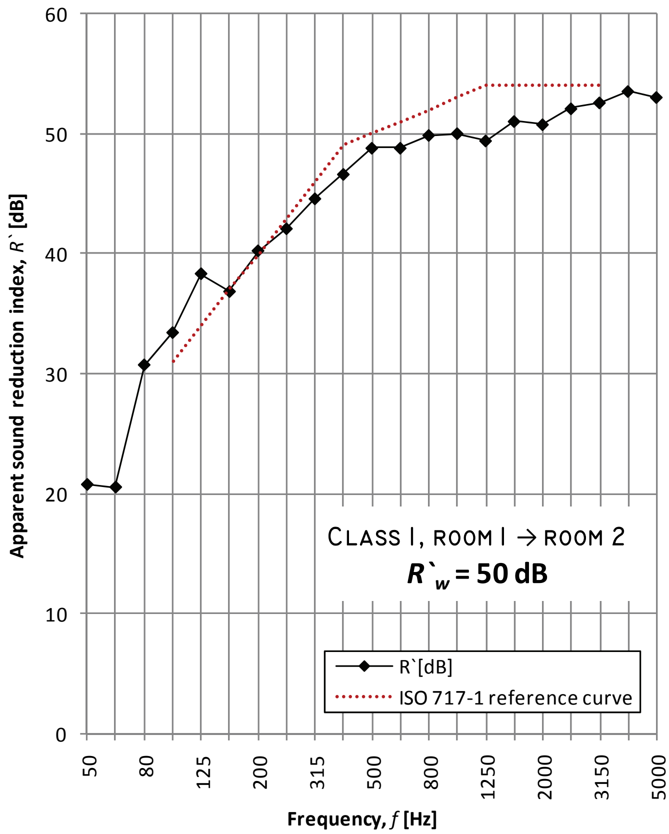


**Figure 49.** The apparent sound reduction index between adjacent test rooms, class 1 partitions.

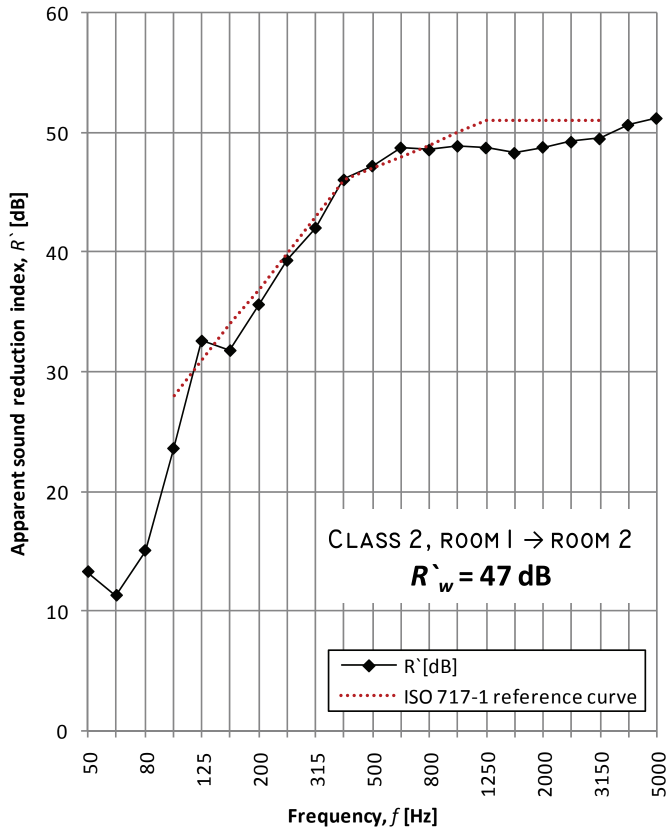


**Figure 50.** The apparent sound reduction index between adjacent test rooms, class 2 partitions.

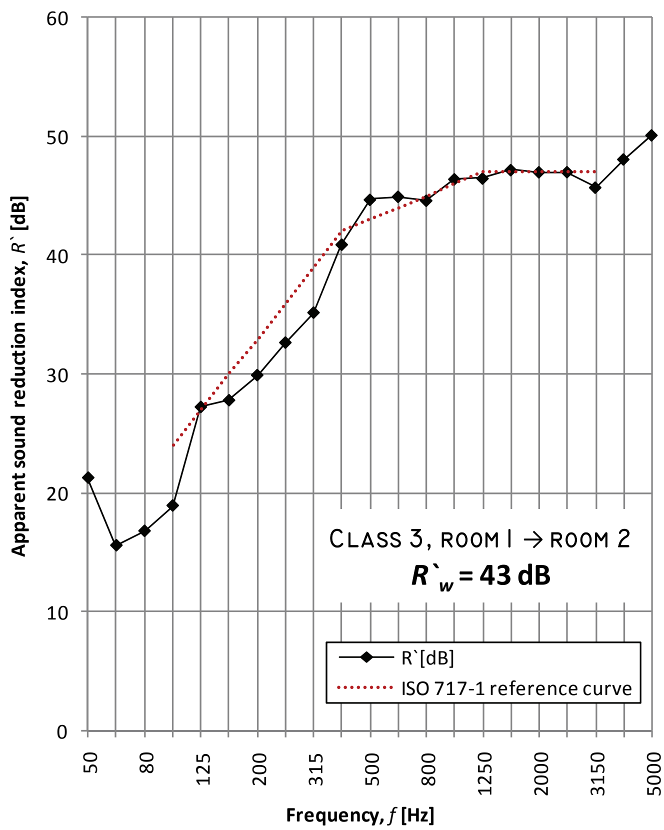


**Figure 51.** The apparent sound reduction index between adjacent test rooms, class 3 partitions.

## 5.6 Measurements of Partition with Perforated Panels

### 5.6.1 Description of structures and measurement arrangements

The effect of panel perforation on the sound reduction index was investigated in the test room; see Figure 47. The apparent sound reduction index from room 2 to room 1 was measured with different areas of perforated panel on the room 2 side of the separating partition.

The structure of the separating partition was the same as the class 3 partition, except that the chipboard layer on the side of room 2 was replaced with a panelling consisting of five medium density fiberboards. A solid chipboard block was used to seal the structure from one side. The wall surface is illustrated in Figure 52.

The MDF-panels were attached to studs via aluminum rails similarly as in the typical partition structure; see Section 5.2.1. Both impervious and perforated MDF-panels were used in order to compare different perforated panel areas. The perforation ratio was 17.1 %. All the panels had a nominal thickness of 12 mm and the perforated panels had an additional 0.5 mm veneer layer on both sides.

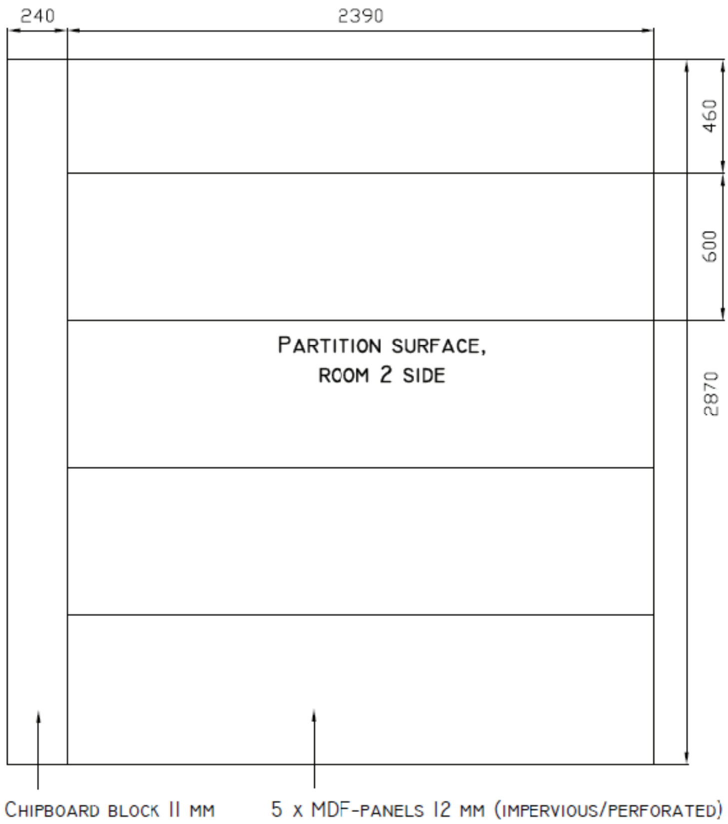


**Figure 52.** Wall surface on the side of room 2 in the measurements of perforated panels.

The chipboard panels on the side of room 1 were sealed to base- and intermediate floor and side walls with sealing mastic and EPDM-rubber battens. Sealing mastic was not used on the room 2 side of the partition.

Fives cases were compared with varying amounts of perforated panel area on the room 2 side of the separating partition. Table 17 lists the surface areas of imprevious and perforated panels in the measurements.

**Table 17.** The five cases of measurements for investigating the effect of perforated panels on sound insulation. The number of impervious and perforated panels is indicated in the left column.

| No. of impervious / perforated panels | Area of impervious surface [m$^2$] | Area of perforated panel surface [m$^2$] | Percentage of perforated area |
|---|---|---|---|
| 0/5 | 0.69 | 6.86 | 90 % |
| 2/5 | 2.43 | 5.12 | 57 % |
| 3/5 | 3.86 | 3.69 | 38 % |
| 4/5 | 5.39 | 2.16 | 19 % |
| 5/0 | 7.55 | 0 | 0 % |

## 5.6.2 Measurement results

Figure 53 presents a summary of the measurement results. Separate sound reduction index curves for each measurement are given in Appendix B. The values of $R`_w$ for each measurement are given in the legend.

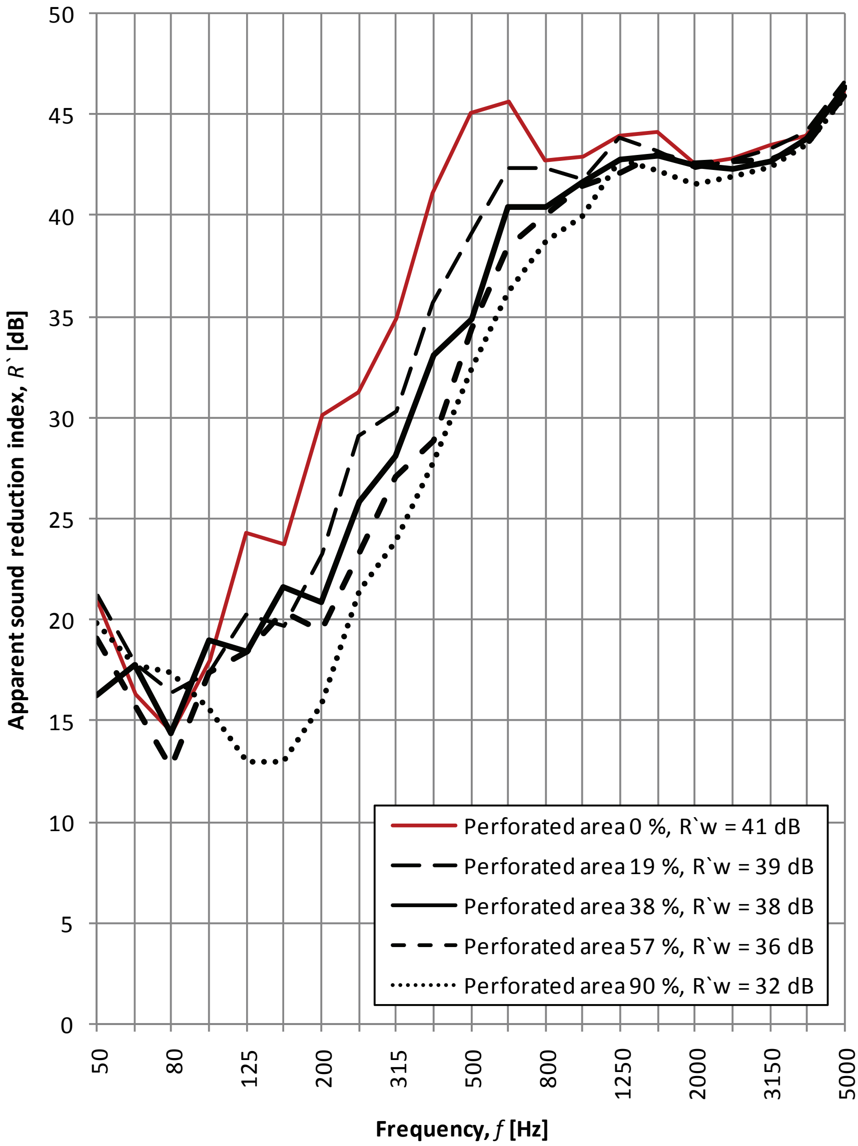


**Figure 53.** The apparent sound reduction index from room 2 to room 1 in the test room. The total surface area of perforated panels on the side of room 2 and the corresponding weighted sound reduction index are shown in the legend.

# 6 EVALUATION OF RESULTS

## 6.1 Reliability of Measurement Results

All the measurements of the apparent sound reduction index in this study were conducted according to standard *ISO 140-4* [25], following the standardized measurement guidelines and procedures. The equipment that was used in the measurements satisfies the accuracy requirements stated in *ISO 140-4*.

According to standard *ISO 140-2* [24], the repeatability of sound insulation measurements conducted in field conditions according to *ISO 140-4* is essentially similar to laboratory measurements, provided that appropriate testing procedures and equipment are used. The repeatibility of laboratory tests is within 1.5 – 4.5 dB in the frequency range of 100 – 3150 Hz. Measurement uncertainty is highest at low frequencies. [24]

Standard *ISO 140-4* states that measurement accuracy in small rooms, with a volume of the magnitude 50 m$^3$ or less, may be compromised at low frequencies – especially below 100 Hz. This is because sufficiently diffuse a sound field cannot typically be created in small spaces due to standing waves. A limiting frequency, below which sound field within a room is not diffuse can be estimated from the equation [32]

$$f_s = 2000\sqrt{\frac{T}{V}} \tag{47}$$

where $f_s$ is the limiting frequency, called the Schroeder frequency [Hz], $T$ is the reverberation time [s] and $V$ the volume of the room [m$^3$].

The volumes of the test rooms used for the measurements of the apparent sound reduction index were 17.8 m$^3$ and 18.0 m$^3$ and the corresponding measured reverberation times, averaged over third-octave bands 100 – 5000 Hz, were 0.51 s and 0.64 s. With these values, the Schroeder frequencies in the measurement rooms are 339 Hz and 377 Hz.

Judging by the calculated Schroeder frequencies, it can be concluded that the sound field within the test rooms was not diffuse at low frequencies. This probably caused some measurement error in the apparent sound reduction index at the lowest frequency bands. Nevertheless, as the size of single person office rooms is typically below the limit of 50 m$^3$ given in standard *ISO 140-4*, the problems with measurement accuracy in such rooms are general rather than specifically associated with the measurements conducted in this study.

According to *ISO 140-4*, achieving reliable measurement results requires that sound pressure level in the receiving room is at least 10 dB higher than the background noise level in all frequency bands. In order to ensure an adequate signal-to-noise ratio, background noise level was registered during all of the measurements. The measured noise levels in third-octave bands are presented in Appendix C along with other measurement data. Background noise level in all measurements was clearly below the limit stated in *ISO 140-4*.

## 6.2 Modelling Accuracy

### 6.2.1 Prediction model of single plates

The prediction model for calculating the sound reduction index of thin single plates was based on theory presented by Kristensen and Rindel [29]; see Section 4.4.1. It was found that the values of $R_w$ calculated with the model are largely dependent on the material parameters.

Table 18 presents the variance in the calculated sound reduction index of a single plate that was caused by changing the four main material parameters: plate density, elastic modulus, Poisson`s ratio and the internal loss factor. On each row of Table 18, one of the parameters is altered while others are kept constant in order to demonstrate the relative effect of a single parameter.

**Table 18.** Relative effects of modelling parameters on the sound reduction index of a thin single plate. Calculated with the prediction model; see Section 4.4.1. Plate area in all the calculations is 10 $m^2$.

| Density [$kg/m^3$] | Elastic modulus [Mpa] | Poisson`s ratio [-] | Internal loss factor [-] | Calculated $R_w$ [dB] | Difference in $R_w$ [dB] |
|---|---|---|---|---|---|
| **Chipboard 11 mm** | | | | | |
| 600 – 800 | 2900 | 0.3 | 0.01 | 29 – 33 | 4 |
| 640 | 2500 – 3500 | 0.3 | 0.01 | 30 – 31 | 1 |
| 640 | 2900 | 0.1 – 0.3 | 0.01 | 30 – 31 | 1 |
| 640 | 2900 | 0.3 | 0.01 – 0.03 | 30 – 31 | 1 |
| **MDF 12 mm** | | | | | |
| 530 – 800 | 6300 | 0.3 | 0.01 | 24 – 30 | 6 |
| 760 | 2200 – 6300 | 0.3 | 0.01 | 29 – 33 | 4 |
| 760 | 6300 | 0.1 – 0.3 | 0.01 | 29 | 0 |
| 760 | 6300 | 0.3 | 0.01 – 0.03 | 29 – 31 | 2 |

The calculation results suggested that plate density has the most notable effect on the calculated sound reduction index. Modulus of elasticity seemed to be less critical material parameter, although the variation in the calculated sound reduction index with medium density fiberboard was greater than with chipboard. It seemed that variance in Poisson`s ratio or the internal loss factor does not affect the calculation result very significantly.

Table 19 presents the difference between measured and calculated values of the sound reduction index. The measured values listed in the table are according to a study by Larm et al. [33]. Surface density and elastic modulus of wood-based building boards were chosen according to Table 5, Section 4.2, while values of 3000 Mpa and 8.8 $kg/m^2$ were used for the normal-density and 4500 Mpa and 11.7 $kg/m^2$ for high-density gypsum board. In all the calculations, values of $\mu$ = 0.3 and $\eta$ = 0.01 were used for Poisson`s ratio and the internal loss factor.

Comparison to laboratory values suggested that the prediction model yields rather accurate estimations of the sound reduction index – at least with common wood-based building boards – the difference between measured and calculated values being within 1 dB. A slightly greater variation, 3 dB, was found with normal density gypsum board. It is possible that the values of the internal loss factor or Poisson`s ratio used in the calculations were somewhat inaccurate, which could – at least to some extent – explain the differences between measured and calculated $R_w$-values.

**Table 19.** Comparison of calculated and measured values of the weighted sound reduction index. Calculated with the prediction model; see Section 4.4.1. Measured values according to Larm. et al [33]. Plate area in all calculations is 10 m$^2$.

| Building board /thickness | Weighted sound reduction index, $R_w$ [dB] | |
|---|---|---|
| | Calculated value | Measured value [1)] |
| Chipboard 11 mm | 30 | 29 |
| Chipboard 22 mm | 29 | 29 |
| MDF 12 mm | 29 | 29 |
| MDF 19 mm | 27 | 28 |
| Plywood 15 mm | 26 | 26 |
| Plywood 21 mm | 28 | 28 |
| Gypsum board 13 mm, normal density | 31 | 28 |
| Gypsum board 15 mm, high density | 30 | 29 |

[1)] Measured values according to Larm. et al [33]

One possible source of inaccuracy related to the modelling of the sound reduction index below the lowest natural frequency of a plate. Figure 54 presents a comparison of the sound reduction index calculated with the prediction model and the corresponding result of a laboratory measurement [16]. The plate in the comparison is a chipboard with a thickness of 25 mm and size 1.25 x 2.25 m. Material parameters used in the calculation were $m`$ = 17.5 kg/m$^2$, $E$ = 3500 Mpa, $\mu$ = 0.28 and $\eta$ = 0.01.

The frequency range below the lowest natural frequency, $f_{11}$, was estimated using the model given by Kristensen and Rindel [29]; see Equation (20), Section 4.4.1. The model seemed to predict a steeper increase in the sound reduction index towards the lowest frequencies compared to measurement result. For some reason, the calculated and measured values of the lowest natural frequency were also found to differ slightly. Whether the shape and steepness of the calculated sound reduction curve in Figure 54 is plausible or not would be a subject for further research.

Although there are issues relating to calculation accuracy below the lowest natural frequency, these do not usually affect the value of weighted sound reduction index since $R_w$ is determined from 100 Hz upwards [32]. For the wood-based building boards presented in Table 19, the lowest natural frequencies are in a range of $f_{11}$ = 21…106 Hz when plate dimensios $l_x$ and $l_y$ are 4 m and 2.5 m, respectively. For these common wood-based building boards it would, thus, seem that frequencies below $f_{11}$ are mostly insignificant as the value of the weighted sound reduction index is concerned. Nevertheless, depending on the plate dimensions and critical frequency, the lowest natural frequency can also exceed 100 Hz, in which case the effect on the sound reduction index could be notable.

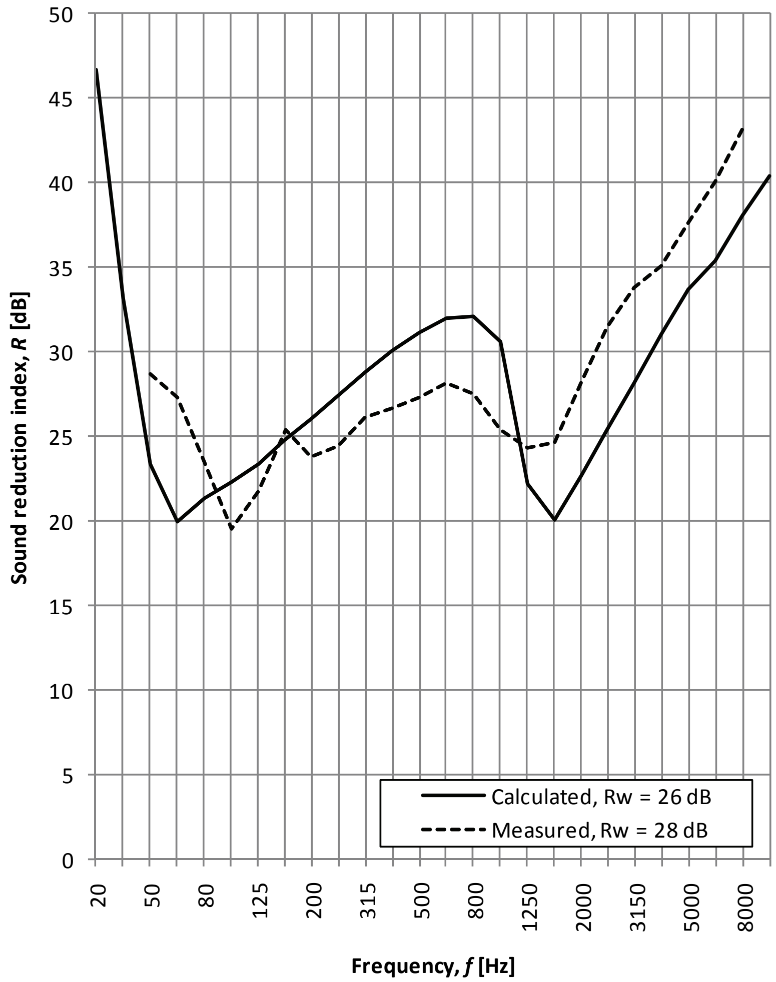


**Figure 54.** Comparison of the sound reduction index calculated with prediction model and laboratory measurement result. Measurement curve is according to Hongisto [16]. Calculations were done with the prediction model presented in Section 4.4.1, using Equation (20) for frequencies below the lowest natural frequency. The structure is chipboard 25 mm with the following material parameters: $m`$ = 17.5 kg/m$^2$, $E$ = 3500 Mpa, $\mu$ = 0.28 and $\eta$ = 0.01. Plate dimensions are 1.25 x 2.25 m.

### 6.2.2 Prediction model of double-leaf partitions

The prediction model for double-leaf partitions used in the study was a combination of different models. The theoretical basis was formed by a model proposed by Kristensen and Rindel [29], which was used to calculate the sound reduction index of an uncoupled double-leaf partition with totally absorbing cavity. The effects of imperfect cavity absorption and coupling via stiff studs were evaluated using models presented by Hongisto [16]. According to Hongisto, the values of $R_w$ calculated with the prediction model fall within ± 1…3 dB of a laboratory measurement result with 68% probability.

Although the calculation accuracy of the prediction model for double-leaf partitions has been found satisfactory from the practical product development point of view [16], the calculation results were found to be highly dependent on the material properties of plates used in the partition structure. As with single plates, plate density was found to have the most significant effect on the calculated value of $R_w$.

Table 20 illustrates how the calculated sound reduction index varied when different density values were used in the prediction model. The density of conventional chipboard given in literature sources varies between about 600…800 kg/m$^2$ and that of medium density fiberboard between 530…800 kg/m$^2$; see Table 4, Section 4.2. Elastic modulus for both chipboard and MDF in Table 20 were kept constant: 2900 Mpa for 11 mm chipboard, 4800 Mpa for 19 mm MDF and 6300 Mpa for 12 mm MDF. Values of Poisson`s ratio and the internal loss factor were chosen according to Table 5, Section 4.2.

**Table 20.** The weighted sound reduction index of partitions in classes 1, 2 and 3 calculated with different density values. Elastic modulus is constant; 2900 Mpa for chipboard (11 mm), 4800 Mpa for MDF (19 mm) and 6300 Mpa for MDF (12 mm).

| Chipboard, density [kg/m$^3$] | Medium density fiberboard, density [kg/m$^3$] | Weighted SRI, calculated, $R_w$ [dB] |
|---|---|---|
| **Class 1 partition** | | |
| 600 | 530 | 57 |
| 700 | 670 | 61 |
| 800 | 800 | 64 |
| **Class 1 corridor partition** | | |
| 600 | 530 | 42 |
| 700 | 670 | 47 |
| 800 | 800 | 49 |
| **Class 2 partition** | | |
| 600 | 530 | 49 |
| 700 | 670 | 53 |
| 800 | 800 | 57 |
| **Class 3 partition, Class 2/3 corridor partition** | | |
| 600 | - | 39 |
| 700 | - | 42 |
| 800 | - | 44 |

The calculation results indicated that the lowest sound reduction index with the new partitions is achieved with lowest values of plate density, while the highest predicted SRIs correspond to the highest density values. The variance in the predicted weighted sound reduction index was found to be 5…8 dB depending on the partition structure: 7 dB for class 1 partitions, 8 dB for class 2 partitions and 5 dB for class 3 partition.

Figure 55 illustrates the effect of varying modulus of elasticity on the sound reduction index of class 3 partition and class 1 corridor partition. Elastic modulus of 11 mm chipboard has values between 2500…3500 Mpa and 12 mm MDF between 2200…6300 Mpa in accordance with Table 5, Section 4.2. The variance in the weighted sound reduction index was found to be 2 dB for the class 3 partition and 5 dB for the class 1 corridor partition. Corresponding values of 2 dB and 1 dB were calculated for the class 1 separating partition and class 2 partition, respectively. The calculation results suggested that the magnitude of deterioration in $R_w$ depends on how the critical frequencies of the individual plates overlap.

As in the case of single plates, the effect of Poisson`s ratio and the internal loss factor on the sound reduction index seemed to be rather small. With the class 1 – 3 partition structures, a variance of $\mu$ = 0.1 – 0.3 or $\eta$ = 0.01 – 0.03 was found to cause a difference of ± 1 – 2 dB in the calculated weighted sound reduction index.

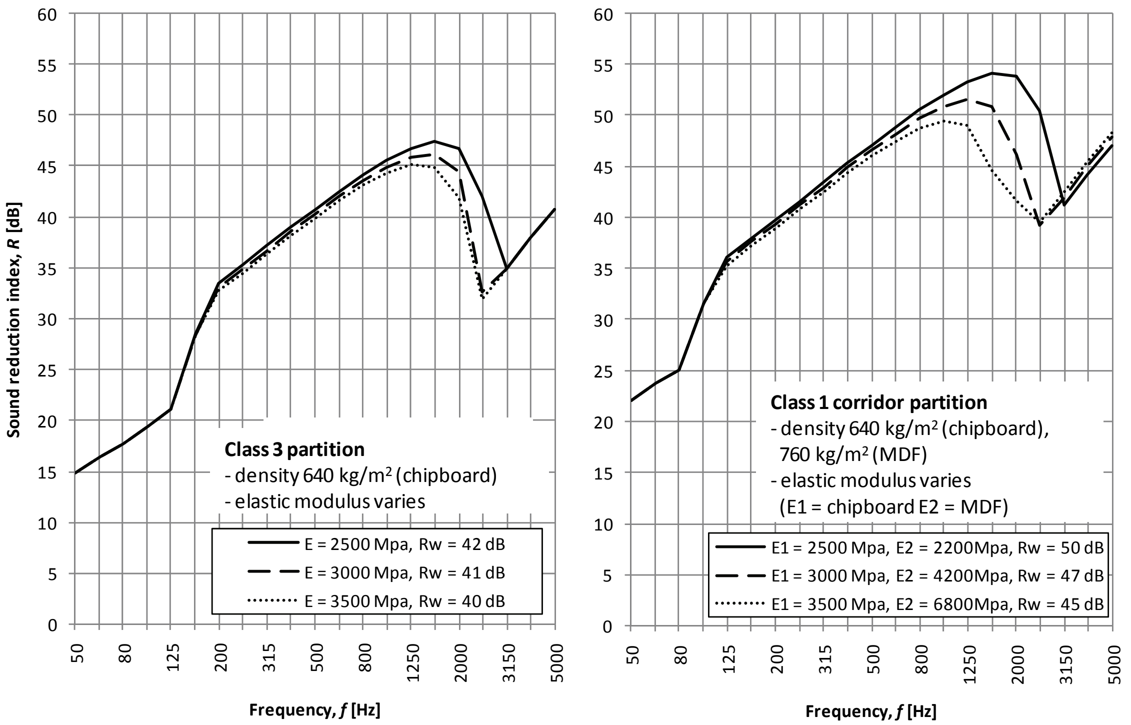


**Figure 55.** The effect of varying elastic modulus on the calculated sound reduction index. Class 3 partition (left), class 1 corridor partition (right).

### 6.2.3 Prediction model of flanking transmission

The calculation accuracy of the flanking transmission prediction model used in the study is, according to the authors, ± 4 dB [14]. The apparent weighted sound reduction index calculated with the model essentially depends on the weighted sound reduction indexes, $R_w$, of the separation partition and flanking structures as well as the vibration reduction indexes, $K_{ij}$, of the structural junctions. Table 21 presents how these parameters were found to affect the apparent sound reduction index in the test room. The weighted sound reduction indexes of the separating and corridor partitions are the same as in Table 20.

The weighted sound reduction index of the existing flanking side wall in Table 21 has values between 50 – 54 dB. The value of $R_w$ = 54 dB was estimated to be the theoretical maximum that could be achieved with the flanking side wall structure; see Section 5.4.6. An exact value could not be determined because the structure contained panels which were attached with glue as well as a perforated panel layer. While it is known that gluing and panel perforations deteriorate sound insulation compared to screw fastening and solid plates, the resulting sound reduction index cannot be determined with the prediction models presented in this study.

The vibration reduction index in Table 21 is given values in a range of $K_{ij}$ = 15 – 30 dB. The minimum value, $K_{ij}$ = 15 dB, is in accordance with the estimation given by Homb et al. [14] for a T-junction with the inner plate layer truncated. It was estimated that the vibration reduction index is higher for a T-junction with both plates truncated; see Section 5.3.5. An estimated maximum value of $K_{ij}$ = 30 dB is used in Table 21.

**Table 21.** The apparent weighted sound reduction index from room 1 to room 2 in the test room. Calculated with the prediction model using different values of weighted sound reduction index for the separating partition, corridor partition and the side wall.

| **Weighted SRI (calculated), $R_w$ [dB]** | | | **Vibration reduction index of the T-junction, $K_{ij}$ [dB]** | **Apparent SRI from room 1 to room 2, calculated, $R`_w$ [dB]** |
|---|---|---|---|---|
| Separating partition | Corridor partition | Flanking side wall | | |
| **Class 1** | | | | |
| 57 | 42 | 50 | 15 | 44 |
| 61 | 47 | 52 | 25 | 47 |
| 64 | 49 | 54 | 30 | 49 |
| **Class 2** | | | | |
| 49 | 39 | 50 | 15 | 43 |
| 53 | 42 | 52 | 25 | 46 |
| 57 | 44 | 54 | 30 | 48 |
| **Class 3** | | | | |
| 39 | 39 | 50 | 15 | 38 |
| 42 | 42 | 52 | 25 | 41 |
| 44 | 44 | 54 | 30 | 43 |

The calculated values of the apparent weighted sound reduction index were found to vary in a range of 44 – 49 dB in the case of class 1 partitions and, correspondingly, 43 – 48 dB for class 2 and 38 – 43 dB for class 3 partitions. The measured values of the apparent sound reduction index in classes 2 and 3, $R`_w$ = 47 dB and $R`_w$ = 43 dB, fall within these ranges. Compared to the measurement result for class 1 partitions, $R`_w$ = 50 dB, the prediction model seemed to slightly underestimate the apparent weighted sound reduction index.

The authors of the flanking transmission prediction model state that the model is a simplification [14]. One limitation seems to be that the model does not take account of the frequency dependency of the $K_{ij}$ –values, another that it omits higher order flanking paths in which sound traverses via two or several structural junctions. According to an investigation by Craik [4], concerning flanking transmission in masonry structures, the omission of higher-order flanking paths can lead to a prediction error of the magnitude 5 dB in the apparent sound reduction index. While the same inaccuracy probably cannot directly be applied to the model used in this study, the research result could give an indication of the magnitude of calculation error possibly involved.

It would seem that one of the notable sources of inaccuracy in the prediction model by Homb et al. [14] relates to a lack of reliable input data. Some of the values of the vibration reduction index given by the authors – especially those concerning the junction between two lightweight structures – are categorized as “unreliable” or “very unreliable” [14]. This probably somewhat limits the calculation accuracy of the model when applied to lightweight constructions.

## 6.3 Effect of Perforated Panels on Sound Insulation

The measurements of the double-leaf partition with perforated panels confirmed the intuitive assumption that sound insulation deteriorates when the amount of perforated panel area increases; see Section 5.6.2. The measurement results indicated, however, that the decrease in the sound reduction index is not constant over the building acoustical frequency range. For the measured partition, the decrease was most notable in a frequency range of about 100 – 1000 Hz. In this frequency region, the difference in the SRI between a solid double-leaf partition and a partition with one surface almost totally perforated, was up to 15 dB. At low frequencies, approximately below the mass-air-mass resonance frequency, and above the critical frequency the decrease in the sound reduction index was small.

Figure 56 illustrates the measured values of the apparent weighted sound reduction index as a function of the perforated panel area. The apparent sound reduction index was found to decrease almost linearly as the perforated panel area on one side of the partition was increased. The decrease in $R`_w$ was 3…4 dB when the perforated panel area was increased from about 0 to 20 %, 20 to 60 % or 60 to 90 %. For some reason, a smaller decrease was measured for an increase in perforated area from 20 to 40 %.

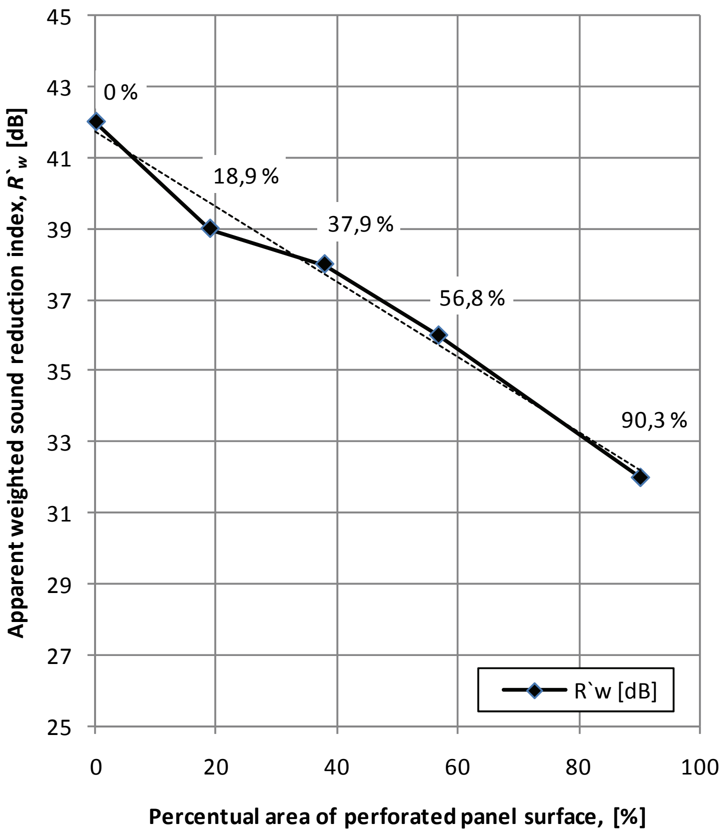


**Figure 56.** The apparent weighted sound reduction index as a function of percentual perforated panel area on one side of a coupled double-leaf partition. Percentual perforated areas are shown above the data points. The other plate layer of the partition was solid in all the measurements.

The measurement results indicated that a sound insulation level of $R`_w \geq 35$ dB could be achieved between adjacent rooms even if up to 60 % of the surface on one side of the separating double-leaf partition is perforated. Thus, it seemed that part of the class 3 partition structure could be perforated for room acoustical purposes, while retaining a reasonable level of sound insulation.

The measurements were conducted using a solid and carefully sealed plate layer on the other side of the partition. It is likely that the deterioration in the sound reduction index would have been more severe if the both sides of the partition had been perforated or sealing had been inadequate. In such a case, the maximum perforated panel area that could be used – while retaining a sound insulation level of $R`_w \geq 35$ dB – would probably be significantly less than 60 %, perhaps around 20 % per plate layer.

The perforation ratio of the perforated MDF-panels used in the measurements was 17.1 %. Although other perforation ratios were not investigated, it would seem likely that if a lower perforation ratio was used, the perforated panel area in the partition could be larger.

## 6.4 Applicability of New Partitions to Typical Office Building

The measurement results of the class 1 partitions in the test room indicated that it is not possible to achieve a sound insulation level of $R`_w \geq 55$ dB, unless flanking transmission via tangential structures is effectively minimized. Modelling results suggested that achieving the target values would essentially require considering the junction of the partition to side wall, which in a typical office building is an exterior wall; see Figure 57.

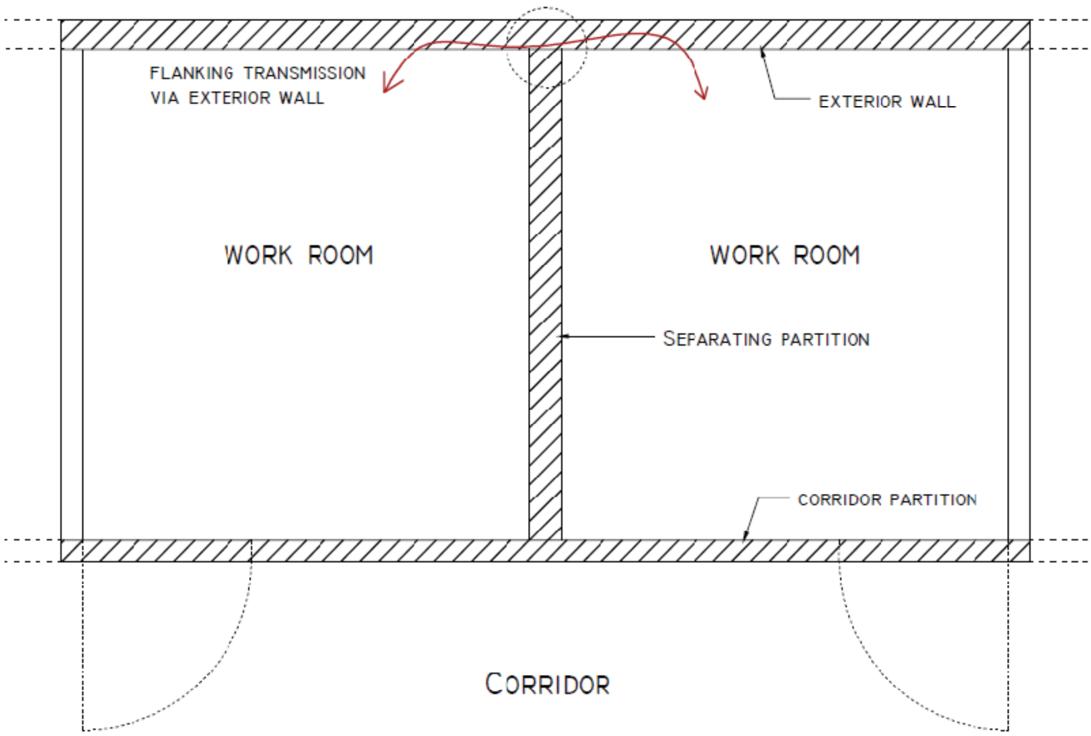


**Figure 57.** Schematic plan of an office space with adjacent work rooms. Achieving the target values of the apparent sound reduction index with the new partitions would require minimizing flanking transmission via the exterior wall junction.

Figures 58 – 61 illustrate how the junction between the partition – in either class 1, 2 or 3 – and exterior wall should be implemented to minimize flanking transmission. Two typical cases of exterior wall structures are considered: a structure with a lightweight building board layer facing the interior and one with a concrete inner envelope. The exterior wall in each figure is presented in a simplified manner, showing only the part of the structure that is crucial to flanking transmission.

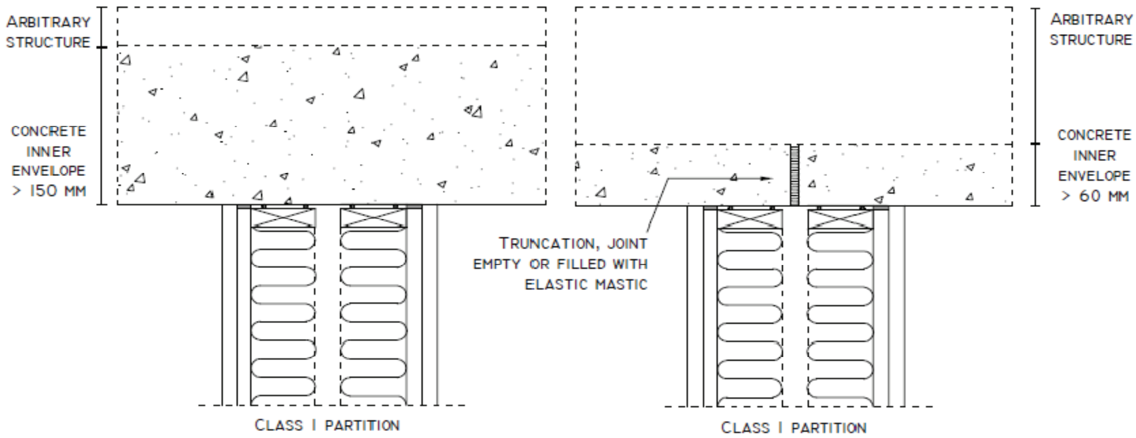


**Figure 58.** Junction between class 1 partition and exterior wall structure with either continuous (left) or truncated (right) concrete inner envelope.

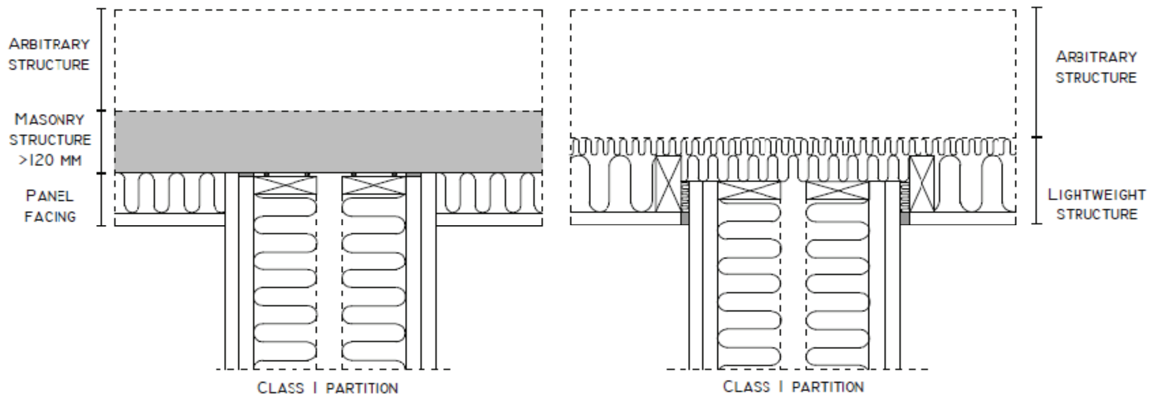


**Figure 59.** Junction between class 1 partition and exterior wall with panel facing installed over masonry structure (left) or lightweight exterior wall structure (right).

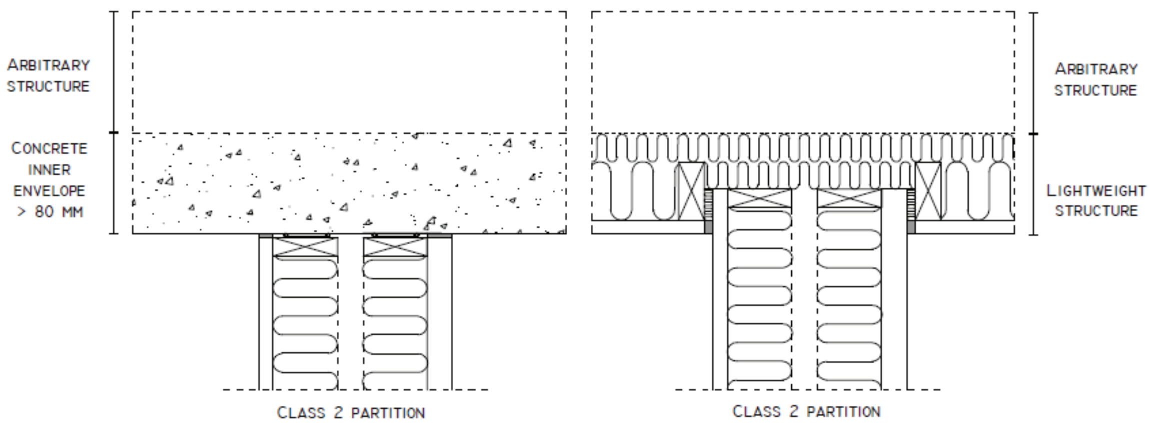


**Figure 60.** Junction between class 2 partition and exterior wall; continuous concrete inner envelope (left), lightweight structure (right).

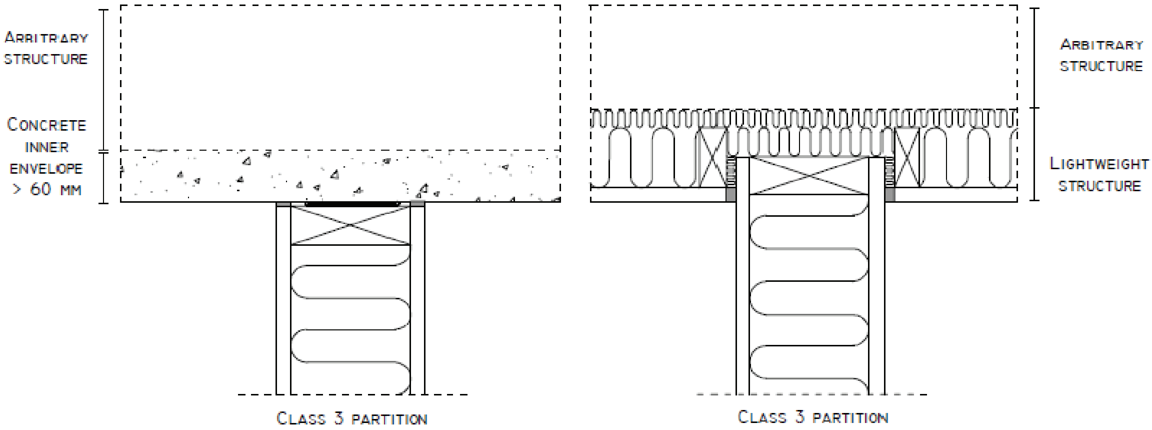


**Figure 61.** Junction between class 3 partition and exterior wall; continuous concrete inner envelope (left), lightweight structure (right).

The minimum thicknesses of concrete structures given in Figures 59 – 62 were estimated based on the weighted sound reduction indexes calculated with the flanking transmission prediction model. Table 22 lists the calculated minimum values for the weighted sound reduction index of different exterior wall structures. The values in bold correspond to Figures 58 – 61, which would probably be the most viable structural solutions from the practical point of view. Detailed calculation steps and parameters relating to these exterior wall junctions are presented in Appendix E.

**Table 22.** Minimum requirements for the weighted sound reduction index of a continuous or truncated exterior wall structure. Estimated with the flanking transmission prediction model. Partitions separating rooms and corridor according to class 1, 2 or 3. Intermediate floors are assumed to be 265 mm hollow core slabs, $R_w$ = 61 dB.

| Target value in class 1/2/3, $R`_w$ [dB] | Exterior wall, minimum value of the weighted SRI, $R_w$ [dB] | | | |
|---|---|---|---|---|
| | **Concrete inner envelope** | | **Lightweight plate structure** | |
| | continuous | truncated | continuous | truncated |
| ≥ 55 | **59** | **44** | 64 | **49** |
| ≥ 45 | **46** | 31 | 51 | **36** |
| ≥ 35 | **36** | 21 | 41 | **26** |

In all the calculations relating to Table 22 it was assumed that both intermediate floor structures, or base floor and roof, are continuous with a weighted sound reduction index of $R_w$ = 61 dB. This value corresponds to a hollow core slab with a thickness of 265 mm and surface density 380 kg/m$^2$ [2], which is a typical structure in office buildings [10].

The minimum thickness of concrete structures typically used in exterior walls in office buildings is 60 mm [8]. Such a concrete slab has a sound reduction index of $R_w$ = 43 dB [14]. Judging by this value and the calculation results in Table 22, it seems evident that the target values of $R`_w$ in classes 2 and 3 could be achieved with a continuous concrete exterior wall structure. The thickness of the slab should be at least 80 mm to achieve the target value in class 2 and, correspondingly, 60 mm in class 3.

The weighted sound reduction index of a concrete slab with a thickness of 150 mm is $R_w$ = 58 dB [2]. Although the calculated minimum requirement for $R_w$ stated in Table

22 exceeds this value by 1 dB, it is likely that the target value in class 1 could also be achieved with a continuous concrete inner envelope, provided that its thickness is sufficiently high. Practical measurements have indicated that it is possible to achieve a sound insulation level of $R`_w \geq 55$ dB between adjacent rooms, if one of the flanking side walls has a continuous concrete inner envelope with a thickness of 150 mm [8].

Judging by the calculation results in Table 22, a lightweight exterior wall structure should be truncated regardless of partition class. The estimated requirement for the sound reduction index of a non-truncated lightweight exterior wall in class 1, $R_w \geq 64$ dB, is unreasonably high to be achieved with any practical structure. In class 2 the required minimum sound reduction index, $R_w \geq 51$ dB, also seems rather high to be achieveable in practice. In the lowest target class, lightweight exterior wall could possibly be implemented as a non-truncated structure as well. The calculation results in Table 22 indicate that this would require a sound reduction index of the magnitude $R_w \geq 41$ dB.

## 6.5 Estimated Improvement in Speech Privacy

The measured value of apparent weighted sound reduction index with the typical partition structure was $R`_w = 28$ dB, and the corresponding values for new partitions in classes 1 – 3 measured in the test room were 50, 47 and 43 dB, respectively. Thus, the improvement in $R`_w$ was in a range of 15...22 dB.

From the subjective perspective, the magnitude of improvement in the apparent sound reduction index that was achieved with the new partitions is very significant. A value of $R`_w$ below 30 dB corresponds to a subjective impression that speech can be effortlessly distinguished between rooms, whereas a value of $R`_w > 45$ dB indicates that normal speaking voice in the neighbouring room is not audible; see Table 1, Section 2.2. In an office setting, an apparent sound reduction index of the magnitude $R`_w < 30$ dB between adjacent work rooms would mean that there is hardly any speech privacy between the rooms, causing reduced work comfort and efficiency. Such a low sound insulation level would also severely compromise confidentiality.

Although speech transmission index measurements were not conducted within the scope of this study, it was possible to draw some rough estimates of speech intelligibility based on the graph presented in Figure 2, Section 2.2. Figure 62 illustrates the difference between two of the measurement results in terms of speech intelligibility. The upper arrow corresponds to the measurement result of the typical partition, $R`_w = 28$ dB, and the lower arrow that of the class 3 partition, $R`_w = 43$ dB.

Figure 62 indicates that the measurement result of the typical partition structure corresponds to a speech transmission index of STI ≈ 0,48, while the measurement result of the class 3 partititon corresponds to a value of STI ≈ 0,05. From the subjective perspective, a speech transmission index of STI = 0,40…0,55 means that speech privacy between adjacent rooms is “reasonable”, whereas a value of STI < 0,05 is equivalent to “complete” speech privacy; see Table 2, Section 2.2.

It is assumed in Figure 62 that the background noise level is $L_{A,eq}$ = 35 dB, which is a typical value in offices [10]. For comparison, the guideline value for maximum HVAC-noise level in office work rooms given in the Finnish building regulations section D2 (2003) is $L_{A,eq}$ = 33 dB [36]. As speech intelligibility also depends on background noise level, additional masking noise could be used to further improve speech privacy.

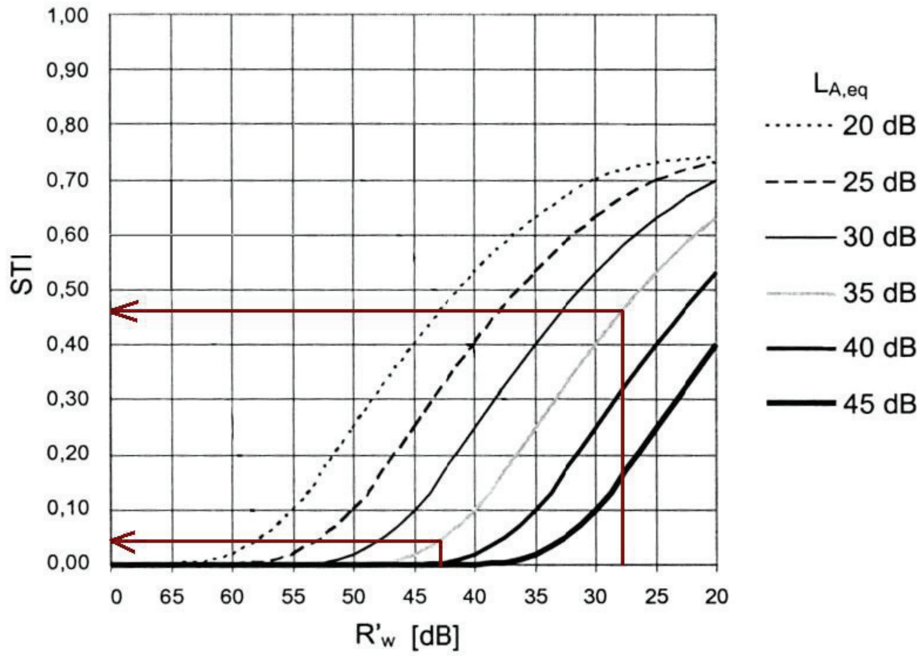


**Figure 62.** Connection between two measured values of apparent sound reduction index and the speech transmission index. Upper arrow: measurement result of typical partition, $R`_w$ = 28 dB. Lower arrow: measurement result of class 3 partition, $R`_w$ = 43 dB. Background noise level is assumed to be $L_{A,eq}$ = 35 dB.

# 7 CONCLUSIONS

This study dealt with the sound insulation of wooden double-leaf partitions which can be used, for example, in office buildings for providing acoustical privacy between work rooms. The main goal was to develop solutions for partition structures that would be suitable for different end uses based on their sound insulation properties. Three classes of target values were set for a desired sound insulation level that should be achieved with the new partitions between adjacent office rooms. The secondary goal was to investigate empirically, how perforated panels affect the sound reduction index of a double-leaf partition.

The research method consisted of theoretical modelling and field measurements of the sound reduction index. Modelling was conducted using two Microsoft Excel – based prediction models: one for calculating the sound reduction index of a double-leaf partition and one for estimating the effect of flanking transmission on sound insulation. The models were drafted utilizing literature sources. Field measurements were conducted according to standard *ISO 140-4* [25].

A typical lightweight partition system served as a starting point for product development. Its sound insulation properties were charted with measurements of the apparent sound reduction index. The purpose of the measurements was to find out the level of improvement in sound insulation that would be required to achieve the target values set for the new partitions. The two prediction models were then used as a tool for evaluating how sound insulation could be improved. The new partitions were built in a test room and measurements of the apparent sound reduction index were conducted for each partition structure. The effect of perforated panels on sound insulation was also investigated with measurements of the apparent sound reduction index.

The measured and calculated values of the apparent sound reduction index corresponding to the new partitions are listed in the following. Measurement result of the typical partition structure is given for comparison.

- Typical partitions: measurement result $R`_w$ = 28 dB
- Class 1 partitions:

  measurement $R`_w$ = 50 dB, modelling $R`_w$ = 48 dB, target value $R`_w \geq$ 55 dB
- Class 2 partitions:

  measurement $R`_w$ = 47 dB, modelling $R`_w$ = 47 dB, target value $R`_w \geq$ 45 dB
- Class 3 partitions:

  measurement $R`_w$ = 43 dB, modelling $R`_w$ = 40 dB, target value $R`_w \geq$ 35 dB

The new partitions in classes 2 and 3 satisfied the target values. The highest target value, $R`_w \geq$ 55 dB, could not be achieved in the test room. According to modelling results, the most probable cause for this was strong flanking transmission via a continuous plate structure of the test room side wall, which could have been avoided if the side wall structure had been properly truncated. Thus, the modelling results indicated that a sound insulation level of $R`_w \geq$ 55 dB would be possible to achieve with the proposed class 1 partitions. In a typical office building this would require diminishing flanking transmission via the exterior wall. Principled solutions for possible exterior wall junctions were presented.

The measurement results of perforated panels indicated that the sound reduction index of a coupled double-leaf partition decreases significantly when the surface area of perforated panels on one side of the partition increases. The results suggested, however, that a sound insulation level corresponding to the class 3 target value, $R`_w \geq 35$ dB, could be achieved, even if over half of one of the partition surfaces consisted of perforated panels. An apparent sound reduction index of $R`_w =$ 36 dB was measured between rooms when the relative surface area of perforated panels on one side of the intervening partition was 57 %.

The accuracy of the prediction model for double-leaf partitions that was used in the study has been found satisfactory from practical product development point of view [16]. The calculation results of the new partitions supported this finding. Nevertheless, it was found that material parameters used in the model can significantly affect the calculated sound reduction index. This should be taken into consideration, since the variation in material values given in literature sources can be notable. In order to achieve optimal calculation accuracy, the required material properties should be measured. If such measurements are not possible, it would be advisable to use average or near-average values in the calculations to avoid overestimation of sound reduction index.

The flanking transmission model used in the study requires knowledge of the vibration reduction indexes of the structural junctions involved in the flanking path. The authors of the model present values of the vibration reduction index for different junction types, but many of the values concerning junctions between lightweight double-leaf partitions are reported as unreliable [14]. The lack of reliable input data somewhat limited the accuracy of the calculations conducted in this study. Nevertheless, the model was found to give rather good estimates of the apparent sound reduction index between two rooms.

The prediction models were found to be very useful, since they enabled investigating the effects of different material parameters and structural configurations on sound insulation before any structures were actually built. The results achieved in the study also indicated that the sound insulation level that can be achieved with partitions can be modelled to rather good accuracy: the measured and calculated values of the apparent weighted sound reduction index for the new partitions were within 3 dB. Although the amount of cases, or partitions, that were investigated within the scope of this study was somewhat concise, the small difference between the modelling and measurement results suggested that the prediction models would be suitable tools for practical design work.

The partitions developed in this study were either totally coupled or uncoupled structures, having common or separate wooden studding. It would, however, be useful to have a “middle ground” between these two solutions. Consequently, future acoustical research of wooden partitions should consider how the structure of a coupled double-leaf partition could be modified so as to diminish the coupling between the partition leaves or by making the coupling more flexible. This would essentially require developing an alternative solution for wooden studs. Such a solution could possibly be used in sound insulating partitions as a competing product for flexible steel studs, which – compared to stiff wooden studs – have better sound insulation properties [16].

Developing the properties of wood-based building boards would constitute another subject for future research. Although the sound reduction index that can be achieved with some of the typical wood-based building boards is comparable to, for example, gypsum boards, it would be beneficial if there was a larger variety of building boards available with a high critical frequency and sound reduction index. Other building physical factors and aesthetics should be considered alongside with acoustical properties.

The functionality of sound insulating partitions would improve if alternative sealing solutions could be developed so as to avoid the use of sealing mastic in structural joints. In this study, elastic mastic was used in all the joints and visible slits of the new partitions to ensure optimal airtightness. While acoustically a beneficial solution, the use of sealing mastic may impair easiness of assembly and structural flexibility.

The results of the perforated panel measurements suggested that perforated panels can be used in a double-leaf partition for room acoustical purposes, while retaining a reasonable level of sound insulation, thus indicating that the two important acoustical factors could be satisfied with the same structure. The scope of the measurements was, however, somewhat limited as different perforation ratios were not investigated and the partition was perforated only on one side. Since perforated panels are a common feature in lightweight partitions, their effect on sound insulation should be investigated more extensively. Future research should include a comprehensive series of measurements with different types of perforated panels and structural configurations. It would also be useful if a prediction model could be drafted with which to evaluate the effect of perforated panels on sound insulation.

# BIBLIOGRAPHY


[1] Andersson, J. Akustik & buller. Stockholm, Sweden: AB Svensk Byggtjänst, 1998. 328 pp. ISBN 91-7332-727-1.

[2] Betonirakenteiden äänitekniikka. Helsinki, Finland: Rakennustuoteteollisuus RTT ry, 2000. 79 pp. ISBN 952-5075-31-1.

[3] Cox, T. J., D'Antonio, P. Acoustic absorbers and diffusers – Theory, Design and Application. London, UK: Spon Press, 2004. 405 pp. ISBN 0-415-29649-8.

[4] Craik, R. M. J. The contribution of long flanking paths to sound transmission in buildings. Applied Acoustics, 2001. Vol 62. pp. 29-46.

[5] EN 12354-1:2000. Building acoustics – Estimation of acoustic performance of buildings from the performance of elements – Part 1: Airborne sound insulation between rooms. Brussels, Belgium: European Committee for Standardization, 2000.

[6] Haapakangas, A., Helenius, R., Keskinen, E., Hongisto, V. Toimistojen koetut ääniolosuhteet – kyselytutkimusten yhteenveto. Akustiikkapäivät 2007, Espoo 27-28.9.2007, pp. 160-165, Akustinen Seura ry, 2007.

[7] Helenius, R., Kaarlela, A., Hongisto, V. Avo- ja koppikonttorin ääniympäristö – miten ne eroavat toisistaan? Sisäilmastoseminaari 2004, Espoo 17-18.3.2004, Ed. Jorma Säteri, Helka Backman, Sisäilmayhdistys ry, report 22, pp. 35-40, 2007.

[8] Helimäki, H., M. Sc. (Eng.) Helimäki Acoustics Ltd. Temppelikatu 6 B, 00100 Helsinki. Interview 24.6.2009.

[9] Hirvonen M. (ed.), Hongisto, V., Kylliäinen, M. RIL 243-1-2007 Rakennusten akustinen suunnittelu – Akustiikan perusteet. Helsinki, Finland: Finnish Association of Civil Engineers, 2007. 224 pp. ISBN 978-951-758-477-7.

[10] Hirvonen M. (ed.), Hongisto, V., Kylliäinen, M. RIL 243-3-2008 Rakennusten akustinen suunnittelu – Toimistot. Helsinki, Finland: Finnish Association of Civil Engineers, 2008. 95 pp. ISBN 978-951-758-486-9.

[11] Hoadley, B. R. Understanding wood – A craftman`s guide to wood technology. 1st edition. Newtown, CT, USA: The Taunton Press, 2000. 280 pp. ISBN 978-1-56158-358-4.

[12] Hockey, G. R. J. Effects of noise on human work efficiency. In the book: Ed. Daryl N. M. Handbook of noise assessment. New York, USA: Van Nostrand Reinhold Company, 1978. pp. 335-368. ISBN 0-442-25197-1.

[13] Homb, A. Lydabsorberende egenskaper til materialer og konstruksjoner. Oslo, Norway: Norges byggforskningsinstitut, 1996. (Byggforskserien, Byggdetaljer 543.414, Sendning 2-1996).

[14] Homb, A., Hveem, S., Strøm, S. Lydisolerenede konstruksjoner – Datasamling og beregningsmetode. Oslo, Norway: Norges byggforskninginstitut, 1983. (Anvisning 28). ISBN 82-536-0187-5.

[15] Hongisto, V. Meluntorjunta – Oppikirja kurssille S-89.3470, 4.11.2008. Helsinki University of Technology, Laboratory of Acoustics and Audio Signal Processing, 2008. 227 pp.

[16] Hongisto, V. Monikerroksisen seinärakenteen ääneneristävyyden laskentamalli. Helsinki, Finland: Työterveyslaitos, 2003. (Työympäristötutkimuksen raporttisarja 2). 216 pp. ISBN 951-802-524-X.

[17] Hongisto, V. Sound insulation of doors - Part 1: Prediction models for structural and leak transmission. Journal of Sound and Vibration, 2000. Vol 230:1. pp. 133-148. Available online: http://www.idealibrary.com. DOI: 10.1006/jsvi.1999.2609.

[18] Hongisto, V. Airborne sound insulation of wall structures - measurement and prediction methods. Doctoral dissertation. Helsinki University of Technology, Laboratory of Acoustics and Audio Signal Processing. (Report 56). Espoo. 2000. 69 pp.

[19] Hongisto, V., Lindgren, M., Helenius, R. Kaksinkertaisen seinärakenteen ääneneristävyys – laboratoriotutkimus. Helsinki, Finland: Tyäterveyslaitos, 2002. (Työympäristötutkimuksen raporttisarja 1). 53pp. ISBN 951-802-520-7.

[20] Hopkins, C. Sound Insulation. 1st edition. Oxford, UK: Butterworth-Heineman, 2007. 622 pp. ISBN-978-0-7506-6526-1.

[21] Hveem, S. Lydisolasjonegenskaper til lette innervegger. Oslo, Norway: Norges byggforskningsinstitut, 2000. (Byggforskserien, Byggdetaljer 524.325, Sendning 2-2000).

[22] http://www.ecophon.fi. Read 24.6.2009.

[23] http://www.euro.who.int/Noise. Read 24.6.2009.

[24] ISO 140-2:1991. Acoustics – Measurement of sound insulation in buildings and of building elements – Part 2: Determination, verification and application of precision data. Genève, Switzerland: International Organizarion for Standardization, 1991.

[25] ISO 140-4:1998. Acoustics – Measurement of sound insulation in buildings and of building elements – Part 4: Field measurements of airborne sound insulation of building elements. Genève, Switzerland: International Organizarion for Standardization, 1998.

[26] ISO 354:2003. Acoustics – Measurement of sound absorption in a reverberation room. Genève, Switzerland: International Organizarion for Standardization, 2003.

[27] ISO 717-1:1996. Acoustics – Rating of sound insulation in buildings and of building elements – Part 1: Airborne sound insulation. Genève, Switzerland: International Organizarion for Standardization, 1996.

[28] Kaarlela, A., Jokitulppo, J., Helenius, R., Keskinen, E., Hongisto, V. Meluhaitat toimistotyössä - pilottitutkimus. Helsinki, Finland: Työterveyslaitos, 2004. (Työympäristötutkimuksen raporttisarja 9). 36 pp. ISBN 951-802-588-6.

[29] Kristensen, K., Rindel, J. Bygningsakustik – Teori og praksis. Hørsholm, Norway: Statens byggefoskningsinstitut, 1989. (SBI-anvisning 166). 223 pp. ISBN 87-563-0736-5.

[30] Kroemer, K. H. E., Kroemer, A. D. Office Ergonomics. London, UK: Taylor & Francis, 2001. 258 pp. ISBN 0-7484-0952-1 (hbk).

[31] Kryter, K. The Effects of Noise on Man. New York, USA: Academic Press, 1970. 633 pp. ISBN 0-12-427450-1.

[32] Kylliäinen, M. Talonrakentamisen akustiikka. Tampere, Finland: Tampere University of Technology, Department of Civil Engineering, 2006. (Research report 137). 205 pp. ISBN 952-15-1650-X.

[33] Larm, P., Hakala, J., Hongisto, V. Sound insulation of Finnish building boards. Helsinki, Finland: Finnish Institute of Occupational Health, 2006. (Work Environment Research Report Series 22). 34 pp.

[34] Lawrence, A. Architectural Acoustics. Barging, Essex, England: Elsevier publishing company Ltd, 1970. 219 pp. ISBN 444-20059-2.

[35] Lian, M., Kristensen T. (ed.) Innvendige skillevegger av tre. Oslo, Norway: SINTEF Byggforsk, 2006. (Byggforskserien, Byggdetaljer 524.213 2-2006).

[36] National Building Code of Finland, section D2: Indoor Climate and Ventilation of Buildings – Regulations and Guidelines 2003 (unofficial translation). Helsinki, Finland: Ministry of the Environment, 2002.

[37] Nightingale, T. R. T. Application of the CEN draft building acoustics prediction model to a lightweight double leaf construction. Applied Acoustics, 1995. Vol 46. pp. 265-284.

[38] Sala, E. & Viljanen V. Improvement of acoustic conditions for speech communication in classrooms. Applied Acoustics, 1995. Vol 45. pp. 81-91.

[39] Salter, M. Acoustics – Architecture, Engineering, the Environment. San Francisco, USA: William Stout Publishers, 1998. 344 pp. ISBN 0-9651144-6-5.

[40] SFS 5907:2004. Acoustic Classification of Buildings. Helsinki, Finland: Finnish Standards Association SFS, 2004.

[41] Siikanen, U. Puurakennusten suunnittelu. $4^{th}$ edition. Helsinki, Finland: Rakennustieto Oy, 1998. 259 pp. ISBN 951-682-436-6.

[42] United States Department of Agriculture. Wood Handbook – Wood as an engineering material. Madison, Wisconsin, USA, 1999. (Forest Products Laboratory, General Technical Report FPL-GTR-113). 486 pp.

[43] Uris, A., Bravo, J. M., Gomes-Lozano, V., Ramirez, P., Llinares, J. Sound insulation of double frame partitions with an internal gypsum board layer. Applied Acoustics, 2006. Vol 67. pp. 918-925.

[44] Uris, A., Bravo, J. M., Llinares, J., Estelles, H. The influence of slits on sound transmission through a lightweight partition. Applied Acoustics, 2004. Vol 65. pp. 421-430.

[45] Veistinen, J., Pennala, E. Finnforest plywood handbook. Lahti, Finland: Kirjapaino Markprint Oy, 1999. 201 pp. ISBN 951-97765-1-6.

# Appendix A

## Measurement Results of Typical Partition and New Partitions

| | |
|---|---|
| **Measurement location:** | Idea-Puu Oy, office space |
| **Date of measurement:** | 18.2.2009 |
| **Measurement method:** | ISO 140-4 |
| **Measurer:** | Matias Remes |

| | |
|---|---|
| **Measurement from:** | Room 1 |
| **to:** | Room 2 |
| **Separating structure:** | MDF 12 mm (11 % of the surface perforated panel, perforation ratio 6,7 %), timber studding + mineral wool 92 mm, MDF 12 mm (solid surface), MDF-panels attached to studs via aluminum rails |

| | | | |
|---|---|---|---|
| **Area of the separating structure:** | $S$ = | 6,6 | $m^2$ |
| **Volume of the source room:** | $V_1$ = | 22,5 | $m^3$ |
| **Volume of the receiving room:** | $V_2$ = | 20,2 | $m^3$ |

| ***f* [Hz]** | ***R`* [dB]** |
|---|---|
| 50 | 16,3 |
| 63 | 14,1 |
| 80 | 12,6 |
| 100 | 17,8 |
| 125 | 15,8 |
| 160 | 15,2 |
| 200 | 18,2 |
| 250 | 20,7 |
| 315 | 22,8 |
| 400 | 24,4 |
| 500 | 26,3 |
| 630 | 25,8 |
| 800 | 26,7 |
| 1000 | 26,5 |
| 1250 | 29,6 |
| 1600 | 29,3 |
| 2000 | 29,0 |
| 2500 | 30,6 |
| 3150 | 31,5 |
| 4000 | 33,8 |
| 5000 | 33,8 |

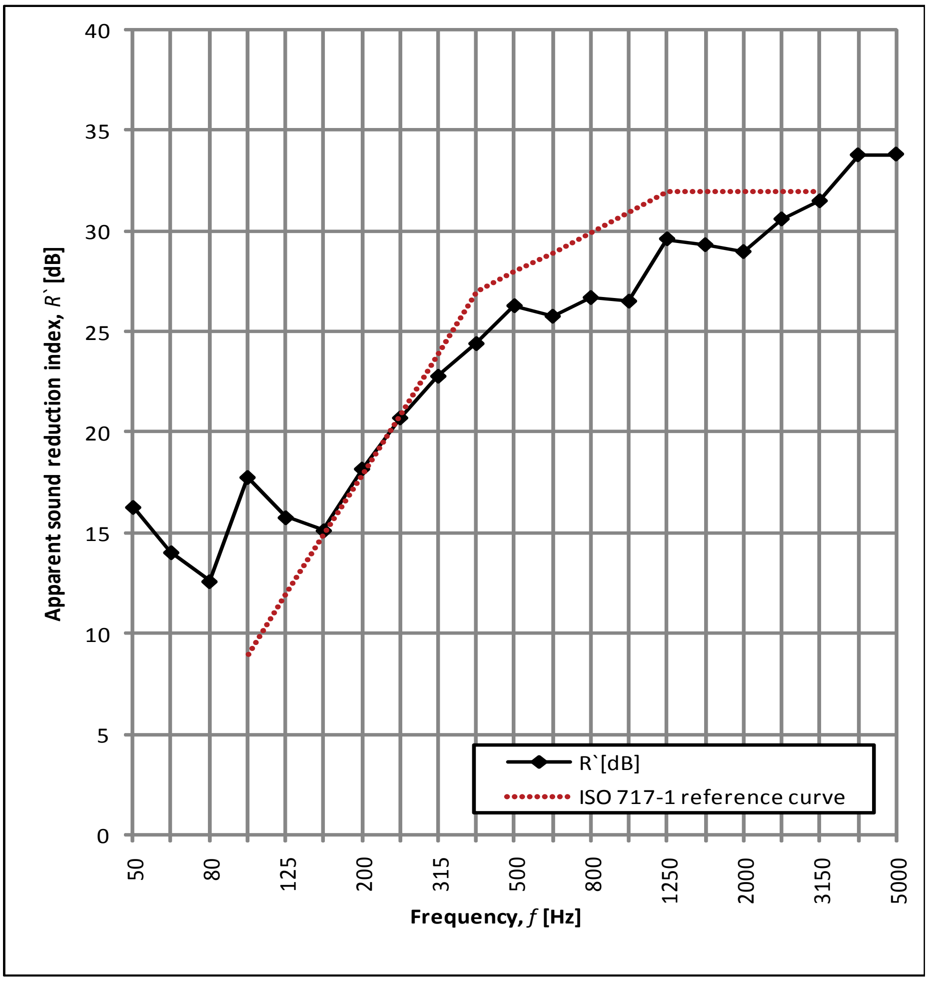


Apparent weighted sound reduction index according to ISO 717-1:

***R`*** $_w$ **(*C* ; *C*** $_{tr}$ **)** = **28** ( -1 ; -3 ) **dB**

| | |
|---|---|
| **Measurement location:** | Idea-Puu Oy, office space |
| **Date of measurement:** | 18.2.2009 |
| **Measurement method:** | ISO 140-4 |
| **Measurer:** | Matias Remes |
| **Measurement from:** | Corridor |
| **to:** | Room 1 |
| **Separating structure:** | MDF 12 mm attached to timber studs, door opening (830 x 2100 mm) sealed with plywood board 15 mm |

**Area of the separating structure:** $S$ = 8,8 $m^2$

**Volume of the source room:** $V_1$ = 41,2 $m^3$

**Volume of the receiving room:** $V_2$ = 22,5 $m^3$

| ***f*** **[Hz]** | ***R`*** **[dB]** |
|---|---|
| 50 | 6,2 |
| 63 | 9,5 |
| 80 | 8,2 |
| 100 | 11,1 |
| 125 | 13,4 |
| 160 | 13,6 |
| 200 | 16,9 |
| 250 | 18,6 |
| 315 | 17,8 |
| 400 | 16,3 |
| 500 | 16,2 |
| 630 | 16,6 |
| 800 | 17,7 |
| 1000 | 19,6 |
| 1250 | 19,3 |
| 1600 | 18,1 |
| 2000 | 17,9 |
| 2500 | 18,8 |
| 3150 | 20,0 |
| 4000 | 21,3 |
| 5000 | 23,0 |

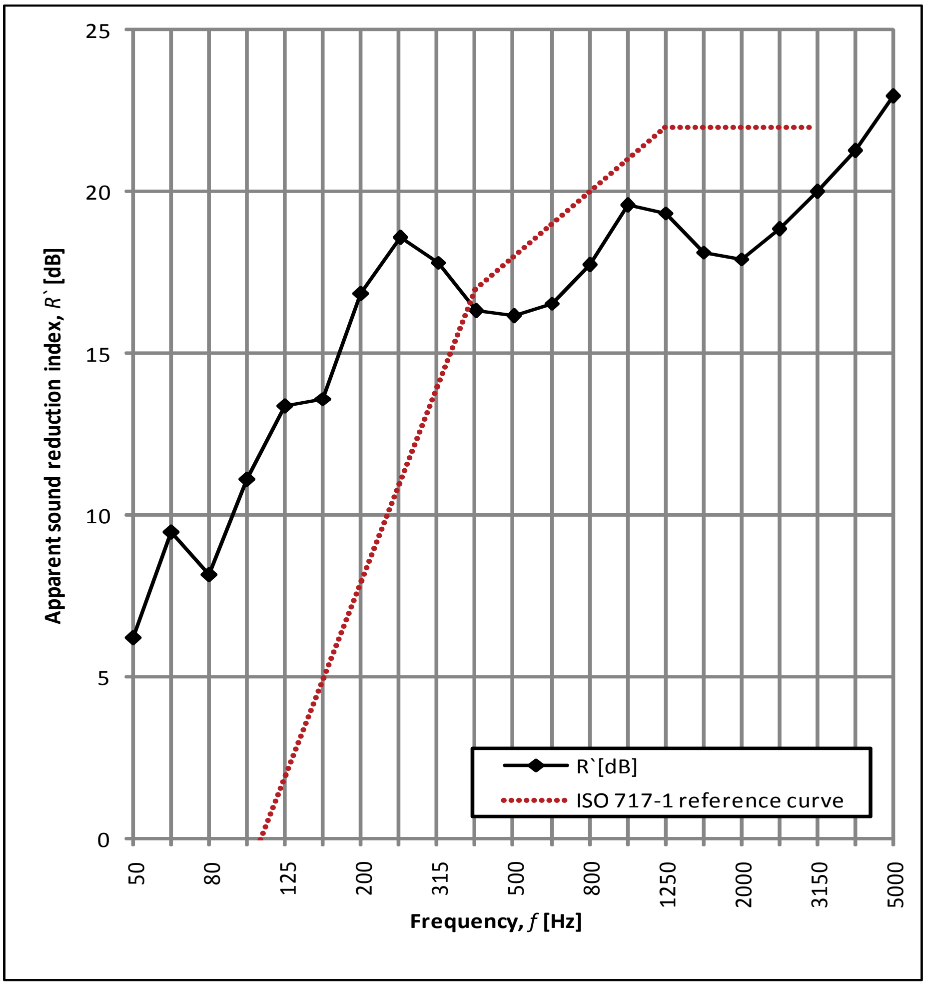


**Apparent weighted sound reduction index according to ISO 717-1:**

**$R`_w$ ($C$ ; $C_{tr}$) = 18 ( 0 ; 0 ) dB**

| | |
|---|---|
| **Measurement location:** | Idea-Puu Oy, office space |
| **Date of measurement:** | 18.2.2009 |
| **Measurement method:** | ISO 140-4 |
| **Measurer:** | Matias Remes |
| **Measurement from:** | Corridor |
| **to:** | Room 2 |
| **Separating structure:** | Laminated glass sheets 3+3 mm attached to timber studs, door (manufacturer Fiskars, no decibel rating) 900 x 2100 mm |

**Area of the separating structure:** $S$ = 7,4 $m^2$

**Volume of the source room:** $V_1$ = 41,2 $m^3$

**Volume of the receiving room:** $V_2$ = 20,2 $m^3$

| ***f*** **[Hz]** | ***R`*** **[dB]** |
|---|---|
| 50 | 15,2 |
| 63 | 10,8 |
| 80 | 12,4 |
| 100 | 10,7 |
| 125 | 12,0 |
| 160 | 13,8 |
| 200 | 16,9 |
| 250 | 19,1 |
| 315 | 18,0 |
| 400 | 17,5 |
| 500 | 17,5 |
| 630 | 18,3 |
| 800 | 17,5 |
| 1000 | 17,6 |
| 1250 | 17,3 |
| 1600 | 19,7 |
| 2000 | 20,8 |
| 2500 | 19,4 |
| 3150 | 19,5 |
| 4000 | 21,0 |
| 5000 | 20,1 |

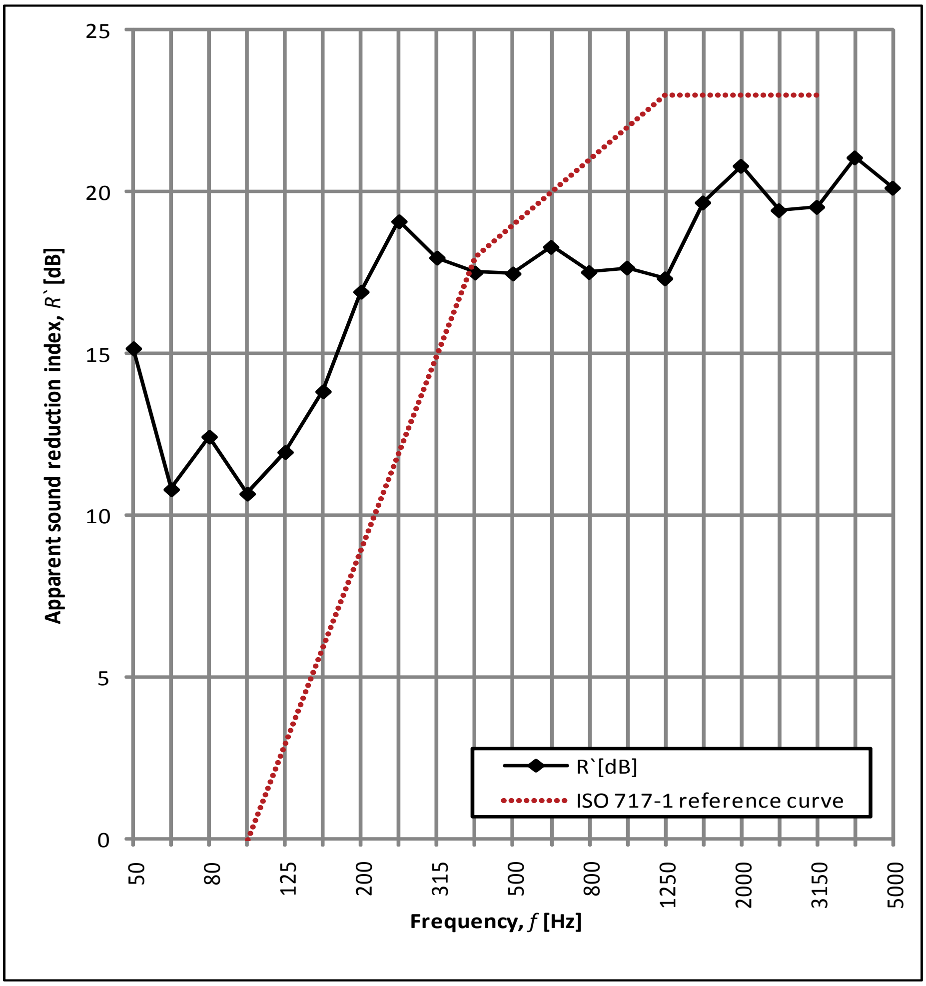


**Apparent weighted sound reduction index according to ISO 717-1:**

***R`$_w$* (*C* ; *C$_{tr}$*)** = **19** ( -1 ; -1 ) **dB**

**Measurement location:** Idea-Puu Oy, test room
**Date of measurement:** 13.5.2009
**Measurement method:** ISO 140-4
**Measurer:** Matias Remes

**Measurement from:** Room 1
**to:** Room 2
**Separating structure:** 2 x chipboard 11 mm (screw fastening), timber studs + mineral wool 50 mm, airspace 20 mm, timber studs + mineral wool 50 mm, 2 x MDF 12 mm (screw fastening)

**Area of the separating structure:** $S$ = 7,5 $m^2$
**Volume of the source room:** $V_1$ = 18,0 $m^3$
**Volume of the receiving room:** $V_2$ = 17,8 $m^3$

| ***f*** **[Hz]** | ***R`*** **[dB]** |
|---|---|
| 50 | 20,8 |
| 63 | 20,6 |
| 80 | 30,8 |
| 100 | 33,5 |
| 125 | 38,4 |
| 160 | 36,9 |
| 200 | 40,3 |
| 250 | 42,1 |
| 315 | 44,6 |
| 400 | 46,7 |
| 500 | 48,9 |
| 630 | 48,9 |
| 800 | 49,9 |
| 1000 | 50,1 |
| 1250 | 49,5 |
| 1600 | 51,1 |
| 2000 | 50,8 |
| 2500 | 52,1 |
| 3150 | 52,6 |
| 4000 | 53,6 |
| 5000 | 53,1 |

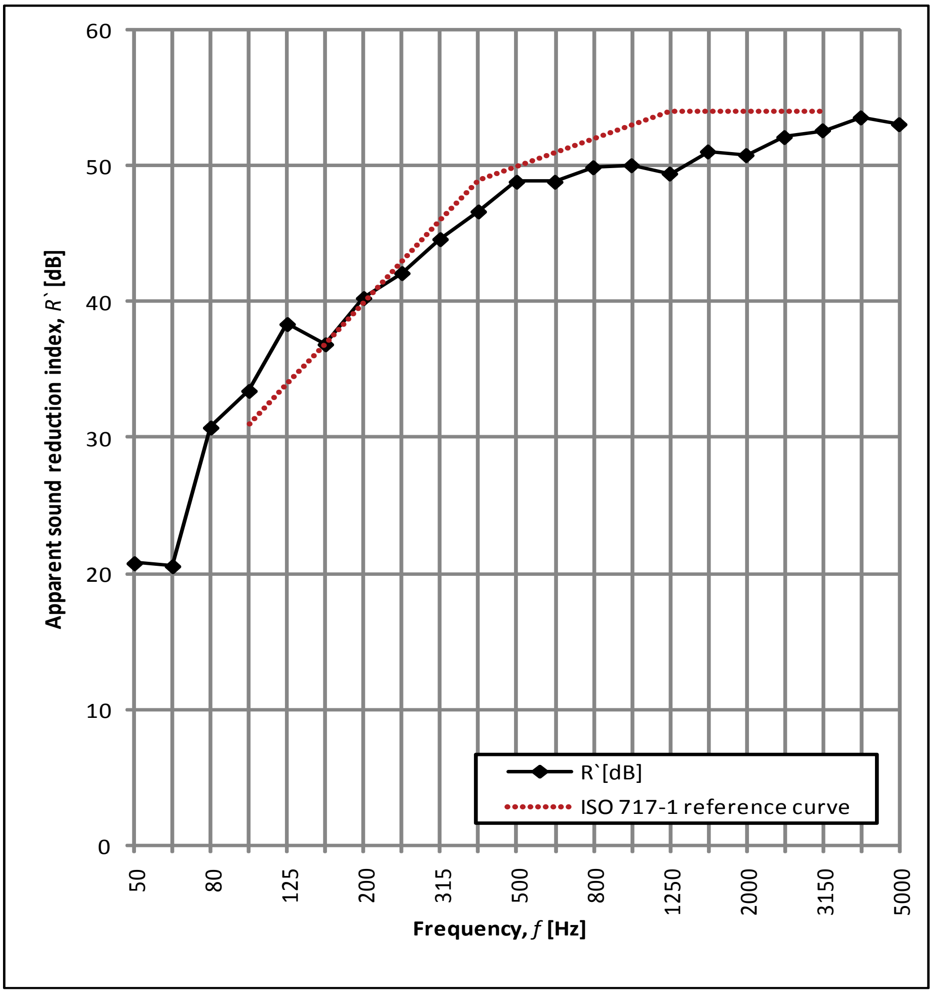


**Apparent weighted sound reduction index according to ISO 717-1:**

**$R`_w$ ($C$ ; $C_{tr}$) = 50 ( -1 ; -4 ) dB**

| | |
|---|---|
| **Measurement location:** | Idea-Puu Oy, test room |
| **Date of measurement:** | 13.5.2009 |
| **Measurement method:** | ISO 140-4 |
| **Measurer:** | Matias Remes |

| | |
|---|---|
| **Measurement from:** | Room 1 |
| **to:** | Room 2 |
| **Separating structure:** | Chipboard 11 mm, timber studs + mineral wool 50 mm, airspace 20 mm, timber studs + mineral wool 50 mm, MDF 19 mm |

**Area of the separating structure:** $S$ = 7,5 $m^2$

**Volume of the source room:** $V_1$ = 18,0 $m^3$

**Volume of the receiving room:** $V_2$ = 17,8 $m^3$

| ***f*** **[Hz]** | ***R`*** **[dB]** |
|---|---|
| 50 | 13,3 |
| 63 | 11,3 |
| 80 | 15,1 |
| 100 | 23,6 |
| 125 | 32,6 |
| 160 | 31,8 |
| 200 | 35,6 |
| 250 | 39,3 |
| 315 | 42,0 |
| 400 | 46,0 |
| 500 | 47,2 |
| 630 | 48,7 |
| 800 | 48,5 |
| 1000 | 48,8 |
| 1250 | 48,7 |
| 1600 | 48,3 |
| 2000 | 48,8 |
| 2500 | 49,2 |
| 3150 | 49,5 |
| 4000 | 50,6 |
| 5000 | 51,2 |

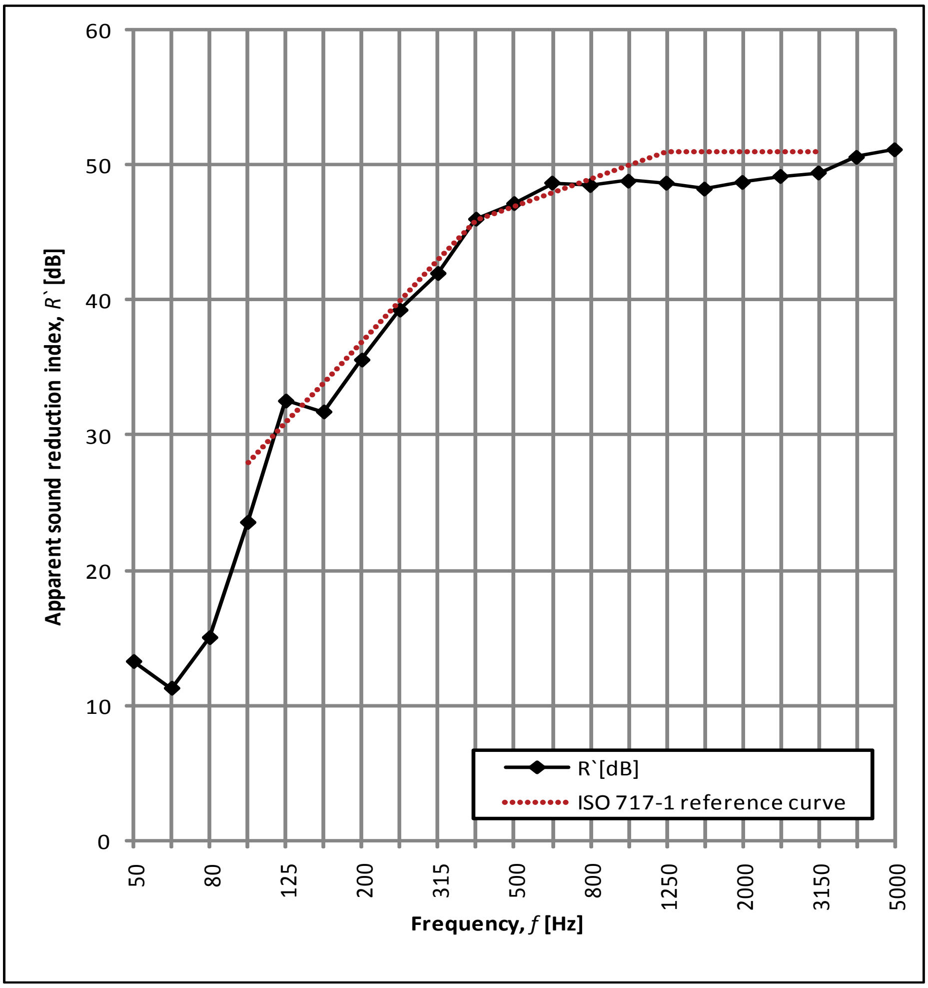


**Apparent weighted sound reduction index according to ISO 717-1:**

**$R`_w$ ($C$ ; $C_{tr}$) = 47 ( -2 ; -6 ) dB**

| | |
|---|---|
| **Measurement location:** | Idea-Puu Oy, test room |
| **Date of measurement:** | 20.5.2009 |
| **Measurement method:** | ISO 140-4 |
| **Measurer:** | Matias Remes |

| | |
|---|---|
| **Measurement from:** | Room 1 |
| **to:** | Room 2 |
| **Separating structure:** | Chipboard 11 mm, 2 x timber studs 50 mm attached with screws, 100% mineral wool filling, chipboard 11 mm |

| | | | |
|---|---|---|---|
| **Area of the separating structure:** | $S$ = | 7,5 | $m^2$ |
| **Volume of the source room:** | $V_1$ = | 18,0 | $m^3$ |
| **Volume of the receiving room:** | $V_2$ = | 17,8 | $m^3$ |

| *f* [Hz] | *R*` [dB] |
|---|---|
| 50 | 21,3 |
| 63 | 15,6 |
| 80 | 16,8 |
| 100 | 19,0 |
| 125 | 27,3 |
| 160 | 27,8 |
| 200 | 29,9 |
| 250 | 32,7 |
| 315 | 35,2 |
| 400 | 40,9 |
| 500 | 44,7 |
| 630 | 45,0 |
| 800 | 44,6 |
| 1000 | 46,4 |
| 1250 | 46,5 |
| 1600 | 47,2 |
| 2000 | 47,0 |
| 2500 | 47,0 |
| 3150 | 45,7 |
| 4000 | 48,1 |
| 5000 | 50,1 |

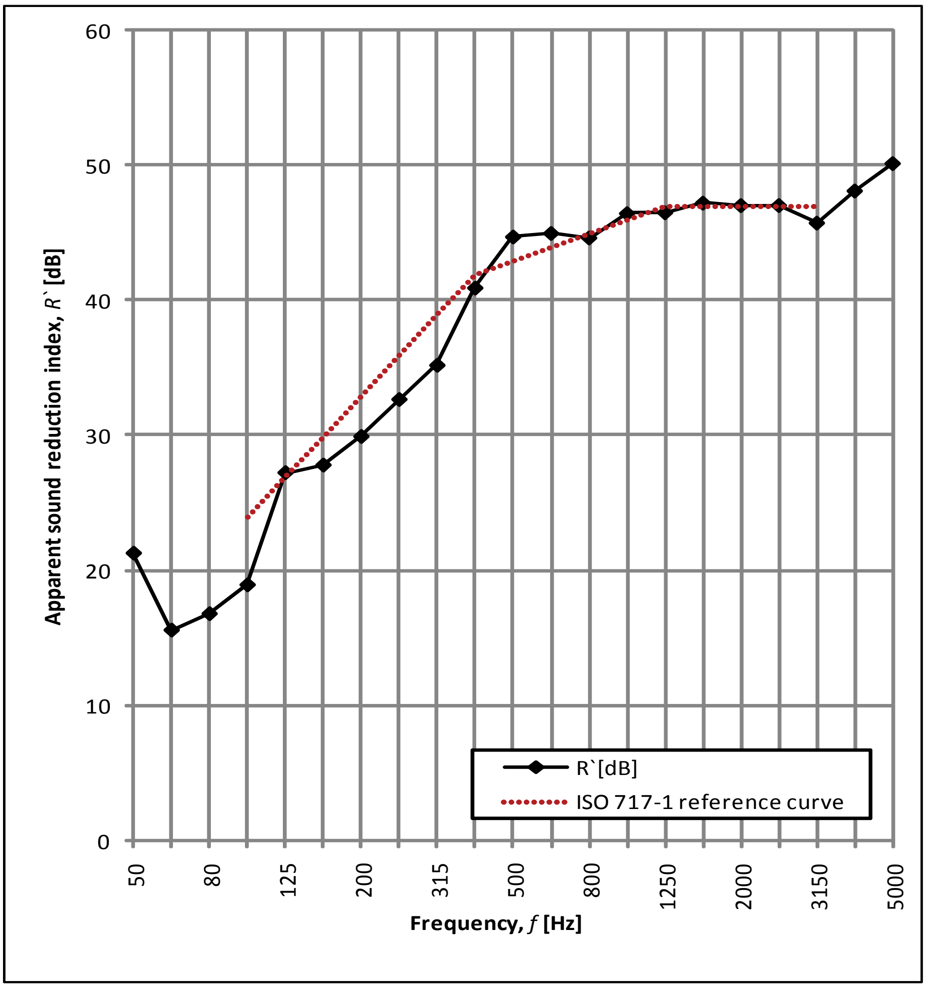


**Apparent weighted sound reduction index according to ISO 717-1:**

**$R`_w$ ($C$ ; $C_{tr}$) = 43 ( -2 ; -7 ) dB**

| | |
|---|---|
| **Measurement location:** | Idea-Puu Oy, test room |
| **Date of measurement:** | 13.5.2009 |
| **Measurement method:** | ISO 140-4 |
| **Measurer:** | Matias Remes |

| | |
|---|---|
| **Measurement from:** | Corridor |
| **to:** | Room 2 |
| **Separating structure:** | MDF 12 mm + chipboard 11 mm (screw fastening), timber studs + mineral wool 92 mm, MDF 12 mm + chipboard 11 mm (screw fastening), door 900 x 2100 mm ($R_w$ = 37 dB) |

| | | | |
|---|---|---|---|
| **Area of the separating structure:** | $S$ = | 6,8 | $m^2$ |
| **Volume of the source room:** | $V_1$ = | 246,9 | $m^3$ |
| **Volume of the receiving room:** | $V_2$ = | 17,8 | $m^3$ |

| ***f*** **[Hz]** | ***R`*** **[dB]** |
|---|---|
| 50 | 19,6 |
| 63 | 17,4 |
| 80 | 18,2 |
| 100 | 24,5 |
| 125 | 22,2 |
| 160 | 29,8 |
| 200 | 27,9 |
| 250 | 28,3 |
| 315 | 25,2 |
| 400 | 29,9 |
| 500 | 31,1 |
| 630 | 31,5 |
| 800 | 33,0 |
| 1000 | 32,9 |
| 1250 | 32,3 |
| 1600 | 30,3 |
| 2000 | 30,7 |
| 2500 | 31,5 |
| 3150 | 32,9 |
| 4000 | 34,8 |
| 5000 | 36,7 |

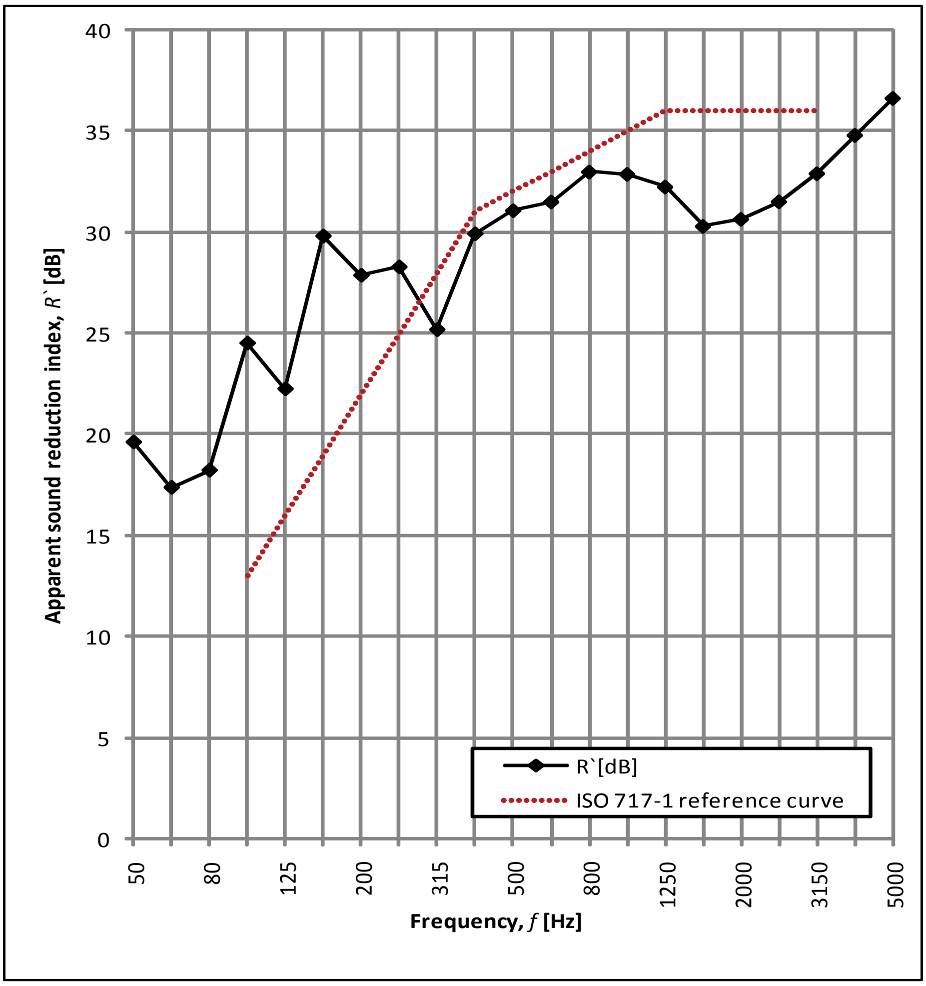


**Apparent weighted sound reduction index according to ISO 717-1:**

$R`_w\ (C\ ;\ C_{tr})$ = **32** ( -1 ; -2 ) **dB**

| | |
|---|---|
| **Measurement location:** | Idea-Puu Oy, test room |
| **Date of measurement:** | 13.5.2009 |
| **Measurement method:** | ISO 140-4 |
| **Measurer:** | Matias Remes |

| | |
|---|---|
| **Measurement from:** | Corridor |
| **to:** | Room 2 |
| **Separating structure:** | Chipboard 11 mm, timber studs + mineral wool 92 mm, chipboard 11 mm, door 900 x 2100 mm ($R_w$ = 37 dB) |

| | | | |
|---|---|---|---|
| **Area of the separating structure:** | $S$ = | 6,8 | $m^2$ |
| **Volume of the source room:** | $V_1$ = | 246,9 | $m^3$ |
| **Volume of the receiving room:** | $V_2$ = | 17,8 | $m^3$ |

| ***f*** **[Hz]** | ***R`*** **[dB]** |
|---|---|
| 50 | 15,7 |
| 63 | 17,7 |
| 80 | 17,6 |
| 100 | 17,6 |
| 125 | 27,7 |
| 160 | 26,4 |
| 200 | 26,0 |
| 250 | 26,5 |
| 315 | 25,0 |
| 400 | 27,5 |
| 500 | 30,9 |
| 630 | 32,0 |
| 800 | 32,7 |
| 1000 | 32,8 |
| 1250 | 31,0 |
| 1600 | 29,3 |
| 2000 | 29,0 |
| 2500 | 31,4 |
| 3150 | 32,3 |
| 4000 | 34,7 |
| 5000 | 35,6 |

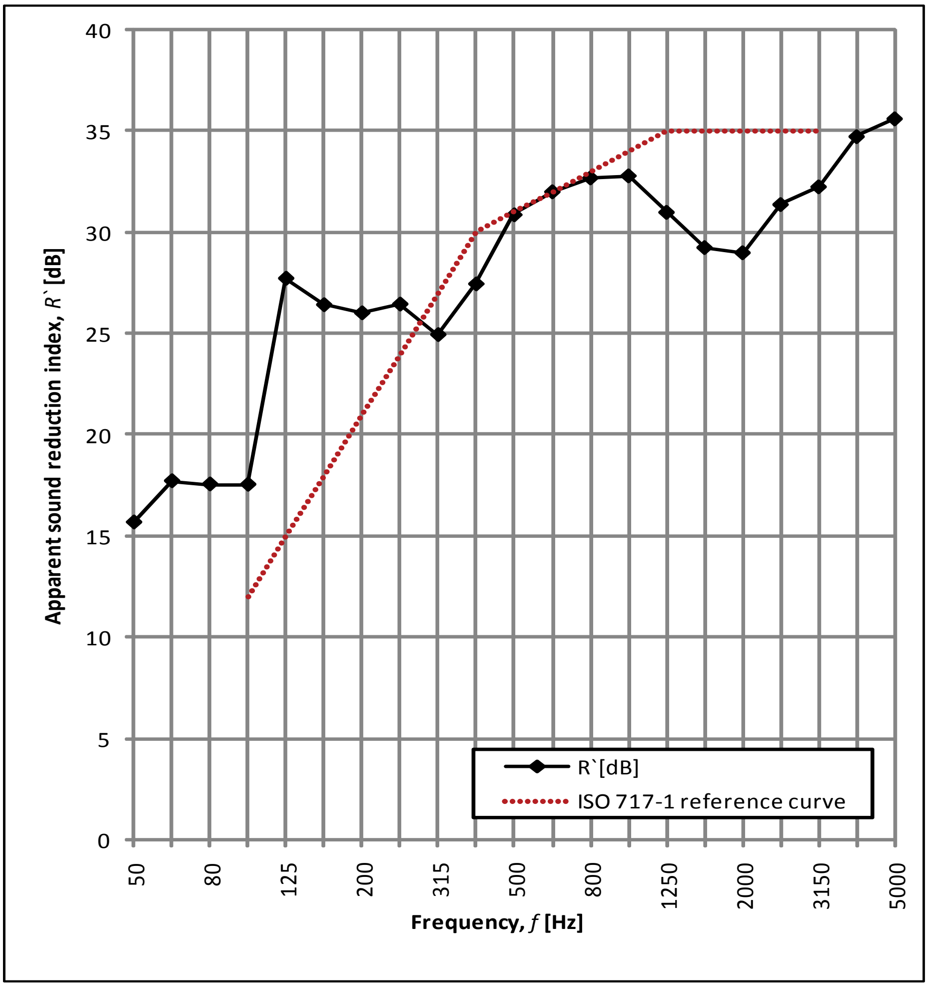


**Apparent weighted sound reduction index according to ISO 717-1:**

$\boldsymbol{R`_w\ (C\,;C_{tr})}$ = **31** ( -1 ; -2 ) **dB**

# APPENDIX B

## MEASUREMENT RESULTS OF PARTITION WITH PERFORATED PANELS

**Measurement location:** Idea-Puu Oy, test room
**Date of measurement:** 2.6.2009
**Measurement method:** ISO 140-4
**Measurer:** Matias Remes

**Measurement from:** Room 2
**to:** Room 1
**Separating structure:** Chipboard 11 mm (solid surface), 2 x timber studs 50 mm (attached with screws) + mineral wool 100 mm, MDF 12 mm (0% of the wall surface perforated)

**Area of the separating structure:** $S$ = 7,5 $m^2$
**Volume of the source room:** $V_1$ = 17,8 $m^3$
**Volume of the receiving room:** $V_2$ = 18,0 $m^3$

| *f* [Hz] | *R*` [dB] |
|---|---|
| 50 | 20,9 |
| 63 | 16,3 |
| 80 | 14,4 |
| 100 | 18,0 |
| 125 | 24,3 |
| 160 | 23,8 |
| 200 | 30,1 |
| 250 | 31,3 |
| 315 | 34,9 |
| 400 | 41,2 |
| 500 | 45,1 |
| 630 | 45,6 |
| 800 | 42,7 |
| 1000 | 42,9 |
| 1250 | 43,9 |
| 1600 | 44,1 |
| 2000 | 42,5 |
| 2500 | 42,8 |
| 3150 | 43,4 |
| 4000 | 43,9 |
| 5000 | 46,1 |

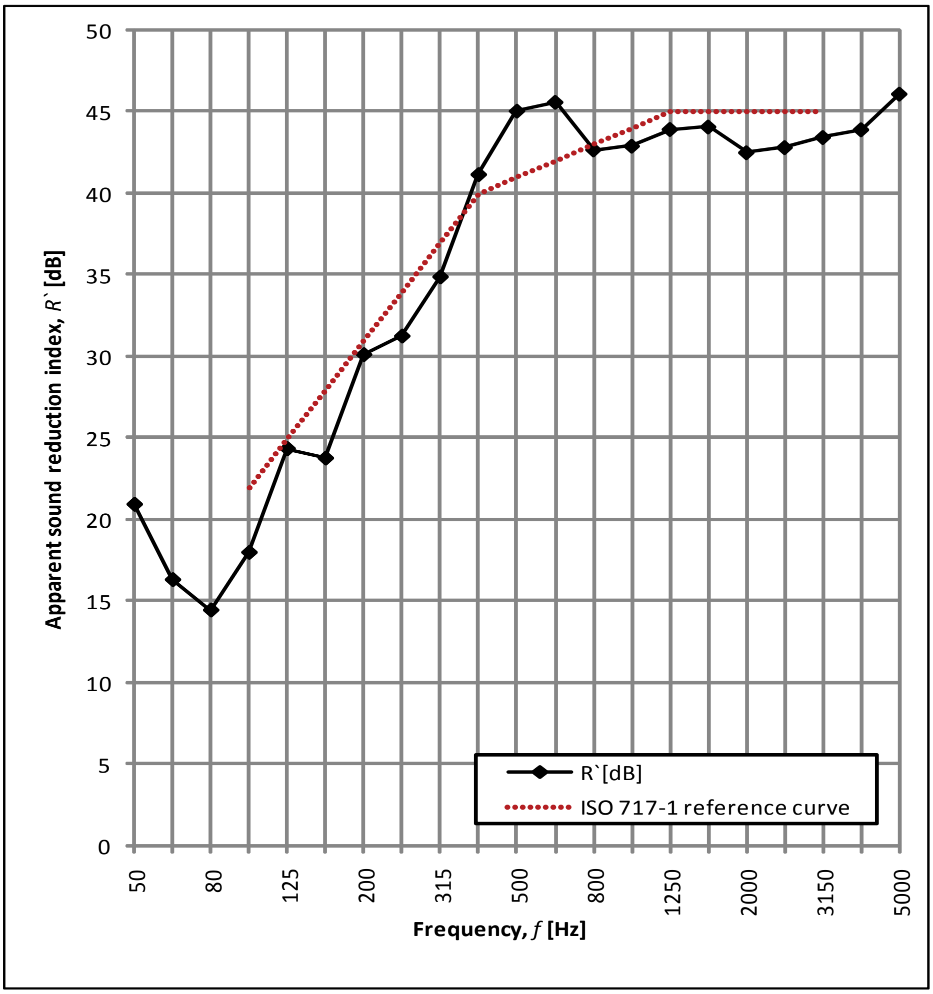


**Apparent weighted sound reduction index according to ISO 717-1:**
**$R`_w$ ($C$ ; $C_{tr}$) = 41 ( -5 ; -9 ) dB**

**Measurement location:** Idea-Puu Oy, test room
**Date of measurement:** 2.6.2009
**Measurement method:** ISO 140-4
**Measurer:** Matias Remes

**Measurement from:** Room 2
**to:** Room 1
**Separating structure:** Chipboard 11 mm (solid surface), 2 x timber studs 50 mm (attached with screws) + mineral wool 100 mm, MDF 12 mm (19% of the wall surface perforated panel, perf. ratio 17,1%)

**Area of the separating structure:** $S$ = 7,5 $m^2$
**Volume of the source room:** $V_1$ = 17,8 $m^3$
**Volume of the receiving room:** $V_2$ = 18,0 $m^3$

| *f* [Hz] | *R*` [dB] |
|---|---|
| 50 | 21,2 |
| 63 | 17,8 |
| 80 | 16,4 |
| 100 | 17,4 |
| 125 | 20,3 |
| 160 | 19,7 |
| 200 | 23,3 |
| 250 | 29,1 |
| 315 | 30,3 |
| 400 | 35,7 |
| 500 | 39,1 |
| 630 | 42,4 |
| 800 | 42,4 |
| 1000 | 41,8 |
| 1250 | 43,8 |
| 1600 | 43,3 |
| 2000 | 42,4 |
| 2500 | 42,8 |
| 3150 | 43,3 |
| 4000 | 44,2 |
| 5000 | 46,6 |

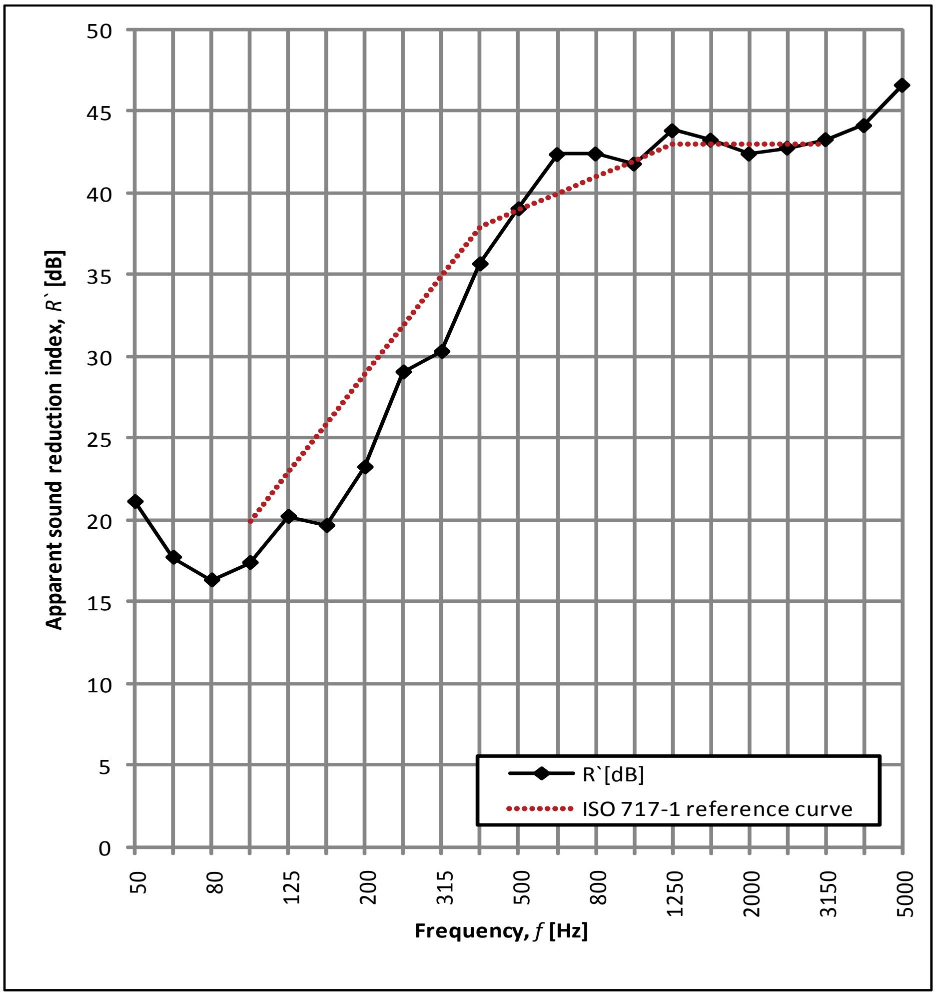


**Apparent weighted sound reduction index according to ISO 717-1:**

**$R`_w$ ($C$ ; $C_{tr}$) = 39 ( -3 ; -7 ) dB**

| | |
|---|---|
| **Measurement location:** | Idea-Puu Oy, test room |
| **Date of measurement:** | 2.6.2009 |
| **Measurement method:** | ISO 140-4 |
| **Measurer:** | Matias Remes |
| **Measurement from:** | Room 2 |
| **to:** | Room 1 |
| **Separating structure:** | Chipboard 11 mm (solid surface), 2 x timber studs 50 mm (attached with screws) + mineral wool 100 mm, MDF 12 mm (38% of the wall surface perforated panel, perf. ratio 17,1%) |

| | | | |
|---|---|---|---|
| **Area of the separating structure:** | $S$ = | 7,5 | $m^2$ |
| **Volume of the source room:** | $V_1$ = | 17,8 | $m^3$ |
| **Volume of the receiving room:** | $V_2$ = | 18,0 | $m^3$ |

| ***f*** **[Hz]** | ***R`*** **[dB]** |
|---|---|
| 50 | 16,3 |
| 63 | 17,8 |
| 80 | 14,4 |
| 100 | 19,0 |
| 125 | 18,4 |
| 160 | 21,6 |
| 200 | 20,9 |
| 250 | 25,9 |
| 315 | 28,1 |
| 400 | 33,1 |
| 500 | 34,9 |
| 630 | 40,5 |
| 800 | 40,5 |
| 1000 | 41,6 |
| 1250 | 42,8 |
| 1600 | 43,0 |
| 2000 | 42,6 |
| 2500 | 42,3 |
| 3150 | 42,7 |
| 4000 | 43,9 |
| 5000 | 46,4 |

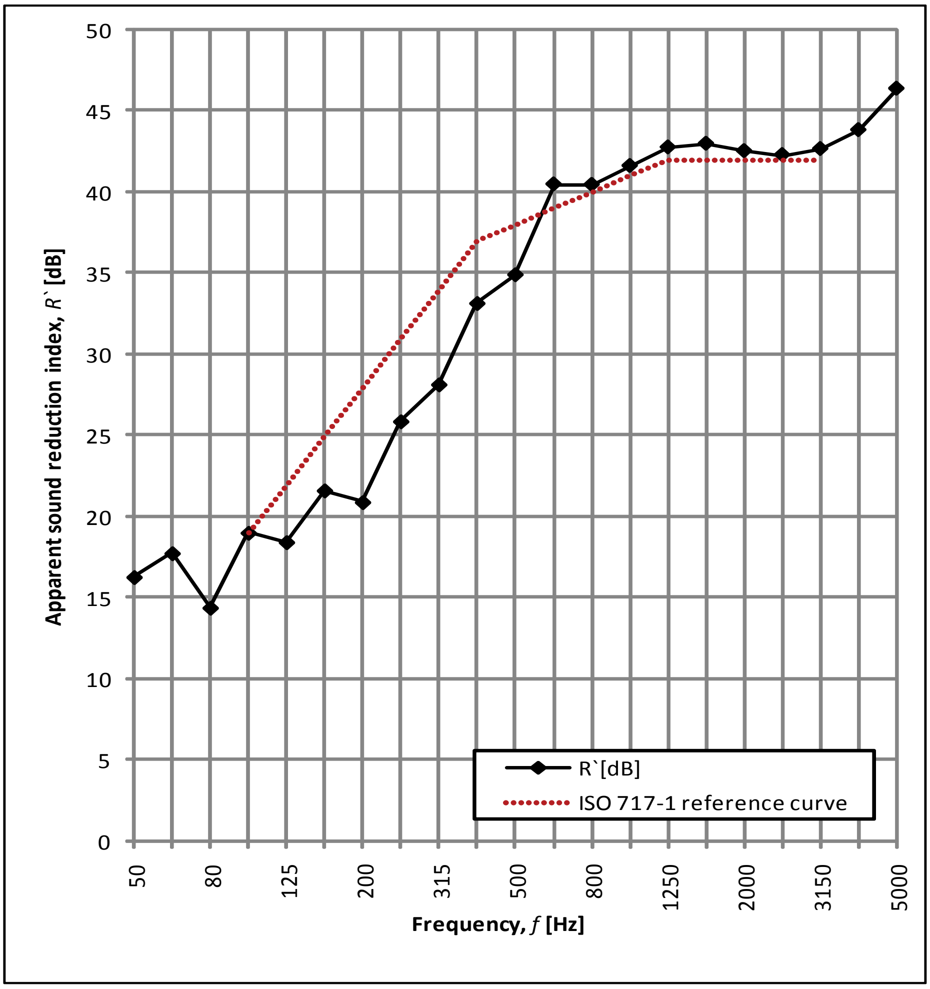


**Apparent weighted sound reduction index according to ISO 717-1:**

$R`_w$ **(*C* ; $C_{tr}$) = 38 ( -3 ; -7 ) dB**

**Measurement location:** Idea-Puu Oy, test room
**Date of measurement:** 2.6.2009
**Measurement method:** ISO 140-4
**Measurer:** Matias Remes

**Measurement from:** Room 2
**to:** Room 1
**Separating structure:** Chipboard 11 mm (solid surface), 2 x timber studs 50 mm (attached with screws) + mineral wool 100 mm, MDF 12 mm (57% of the wall surface perforated panel, perf. ratio 17,1%)

**Area of the separating structure:** $S$ = 7,5 $m^2$
**Volume of the source room:** $V_1$ = 17,8 $m^3$
**Volume of the receiving room:** $V_2$ = 18,0 $m^3$

| *f* [Hz] | *R*` [dB] |
|---|---|
| 50 | 19,1 |
| 63 | 15,8 |
| 80 | 12,7 |
| 100 | 17,4 |
| 125 | 18,5 |
| 160 | 20,5 |
| 200 | 19,5 |
| 250 | 23,4 |
| 315 | 27,1 |
| 400 | 28,9 |
| 500 | 34,4 |
| 630 | 38,4 |
| 800 | 40,1 |
| 1000 | 41,5 |
| 1250 | 42,2 |
| 1600 | 43,0 |
| 2000 | 42,6 |
| 2500 | 42,7 |
| 3150 | 42,8 |
| 4000 | 43,5 |
| 5000 | 46,0 |

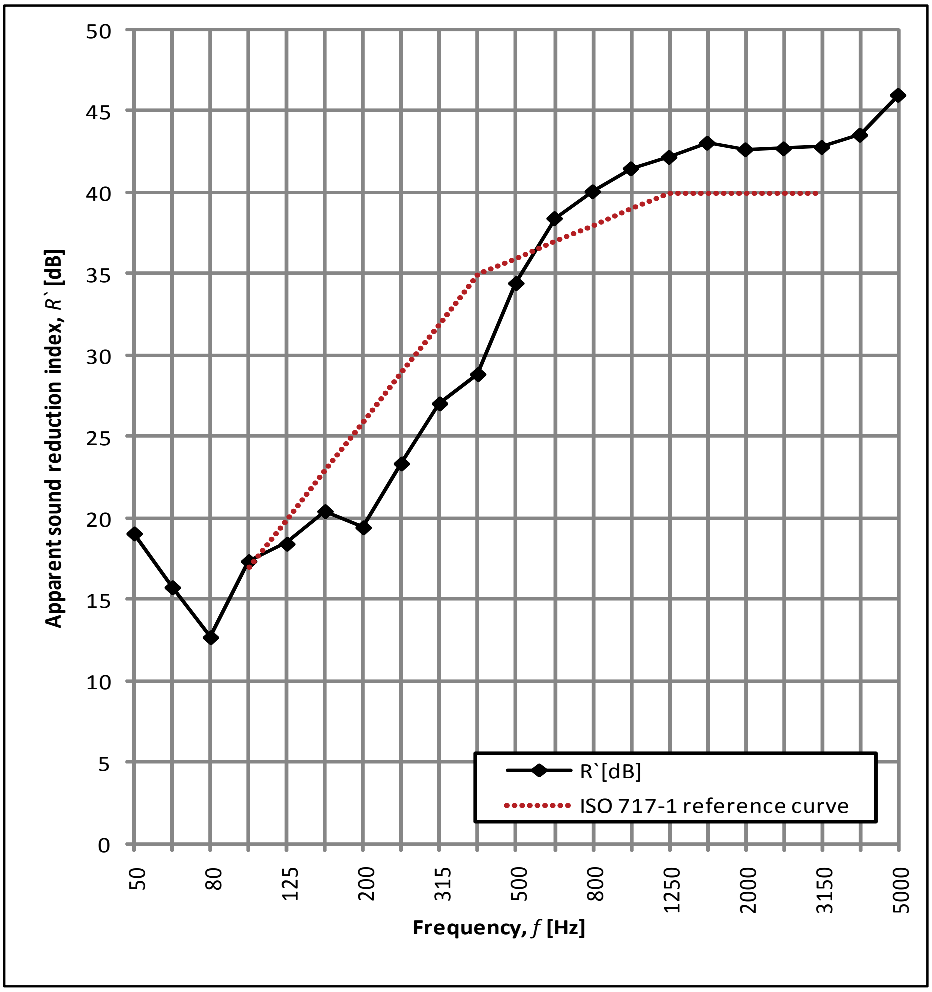


**Apparent weighted sound reduction index according to ISO 717-1:**

***R`$_w$* (*C* ; *C$_{tr}$*)  =  36  (  -2  ;  -6  )  dB**

| | |
|---|---|
| **Measurement location:** | Idea-Puu Oy, test room |
| **Date of measurement:** | 2.6.2009 |
| **Measurement method:** | ISO 140-4 |
| **Measurer:** | Matias Remes |
| **Measurement from:** | Room 2 |
| **to:** | Room 1 |
| **Separating structure:** | Chipboard 11 mm (solid surface), 2 x timber studs 50 mm (attached with screws) + mineral wool 100 mm, MDF 12 mm (90% of the wall surface perforated panel, perf. ratio 17,1%) |

**Area of the separating structure:** $S$ = 7,5 $m^2$
**Volume of the source room:** $V_1$ = 17,8 $m^3$
**Volume of the receiving room:** $V_2$ = 18,0 $m^3$

| *f* [Hz] | *R`* [dB] |
|---|---|
| 50 | 19,8 |
| 63 | 17,8 |
| 80 | 17,4 |
| 100 | 15,6 |
| 125 | 13,0 |
| 160 | 13,0 |
| 200 | 15,8 |
| 250 | 21,4 |
| 315 | 23,9 |
| 400 | 27,8 |
| 500 | 32,5 |
| 630 | 36,2 |
| 800 | 38,8 |
| 1000 | 39,9 |
| 1250 | 42,8 |
| 1600 | 42,2 |
| 2000 | 41,6 |
| 2500 | 41,9 |
| 3150 | 42,4 |
| 4000 | 43,6 |
| 5000 | 45,9 |

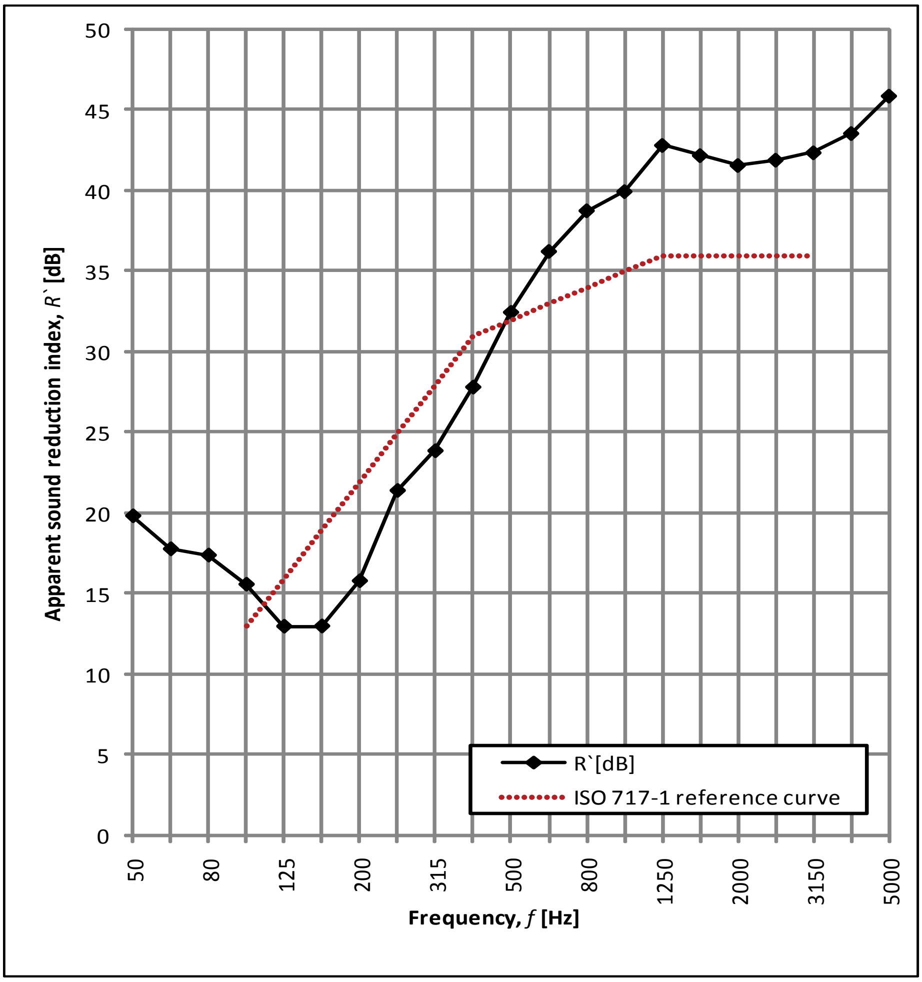


**Apparent weighted sound reduction index according to ISO 717-1:**

$\boldsymbol{R`_w\ (C\,;C_{tr})}$ = **32** ( -2 ; -6 ) **dB**

# Appendix C

## Measurement Data

## Measurements of typical partitions 18.2.2009

| Frequency [Hz] | 50 | 63 | 80 | 100 | 125 | 160 | 200 | 250 | 315 | 400 | 500 | 630 | 800 | 1000 | 1250 | 1600 | 2000 | 2500 | 3150 | 4000 | 5000 |
|---|---|---|---|---|---|---|---|---|---|---|---|---|---|---|---|---|---|---|---|---|---|
| Rev. time in room 1, T [s] | 0,11 | 0,38 | 0,34 | 0,30 | 0,28 | 0,28 | 0,29 | 0,31 | 0,30 | 0,30 | 0,29 | 0,31 | 0,30 | 0,32 | 0,32 | 0,34 | 0,35 | 0,36 | 0,35 | 0,36 | 0,35 |
| Rev. time in room 2, T [s] | 0,32 | 0,48 | 0,32 | 0,33 | 0,40 | 0,38 | 0,63 | 0,71 | 0,77 | 0,84 | 0,83 | 0,80 | 0,79 | 0,75 | 0,72 | 0,70 | 0,67 | 0,60 | 0,58 | 0,59 | 0,38 |
| **1) R`$_w$ room 1 -> room 2** | | | | | | | | | | | | | | | | | | | | | |
| SPL in room 1, $L_{p1\_tot}$ [dB] | 75,0 | 79,4 | 80,6 | 83,8 | 89,5 | 89,7 | 86,0 | 88,4 | 87,8 | 86,7 | 88,2 | 91,9 | 97,1 | 95,3 | 97,3 | 96,2 | 93,8 | 93,4 | 86,9 | 83,2 | 79,0 |
| SPL in room 2, $L_{p2\_tot}$ [dB] | 56,9 | 65,3 | 66,1 | 64,3 | 72,9 | 73,5 | 68,9 | 69,4 | 66,9 | 64,6 | 64,2 | 68,2 | 72,5 | 70,6 | 69,3 | 68,5 | 66,2 | 63,7 | 56,2 | 50,2 | 44,1 |
| **2) R`$_w$ corridor -> room 1** | | | | | | | | | | | | | | | | | | | | | |
| SPL in room 1, $L_{p1\_tot}$ [dB] | 67,9 | 76,1 | 78,7 | 84,5 | 90,2 | 92,7 | 88,8 | 90,7 | 90,4 | 90,4 | 91,7 | 93,7 | 99,9 | 97,9 | 99,3 | 97,0 | 94,9 | 94,3 | 88,2 | 84,6 | 80,2 |
| SPL in room 2, $L_{p2\_tot}$ [dB] | 56,0 | 66,3 | 69,7 | 72,1 | 75,2 | 77,5 | 70,5 | 71,0 | 71,2 | 72,8 | 74,1 | 76,0 | 80,9 | 77,3 | 78,9 | 78,0 | 76,3 | 74,9 | 67,6 | 62,7 | 56,6 |
| **3) R`$_w$ corridor -> room 2** | | | | | | | | | | | | | | | | | | | | | |
| SPL in room 1, $L_{p1\_tot}$ [dB] | 68,8 | 75,6 | 77,2 | 79,0 | 88,5 | 90,8 | 90,2 | 89,1 | 88,6 | 88,9 | 91,1 | 93,7 | 99,1 | 97,2 | 98,8 | 97,3 | 95,1 | 93,4 | 87,1 | 84,0 | 79,1 |
| SPL in room 2, $L_{p2\_tot}$ [dB] | 52,3 | 65,2 | 63,4 | 67,1 | 76,2 | 76,5 | 74,9 | 72,2 | 73,2 | 74,3 | 76,5 | 78,0 | 84,1 | 82,0 | 83,7 | 79,8 | 76,2 | 75,4 | 68,8 | 64,3 | 58,5 |
| **Background noise level [dB]** | | | | | | | | | | | | | | | | | | | | | |
| Room 1 | 27,2 | 26,7 | 27,4 | 32,4 | 28,7 | 26,5 | 29,3 | 24,8 | 25,1 | 25,1 | 25,6 | 25,7 | 25,7 | 26,2 | 26,4 | 27,0 | 27,3 | 27,2 | 27,2 | 27,5 | 29,2 |
| Room 2 | 43,5 | 42,4 | 41,2 | 40,0 | 39,2 | 38,1 | 36,5 | 35,1 | 34,1 | 32,8 | 31,9 | 30,7 | 29,6 | 28,5 | 27,5 | 26,5 | 25,6 | 24,4 | 23,4 | 22,3 | 21,4 |
| Corridor | 38,7 | 25,7 | 24,4 | 27,0 | 28,1 | 28,9 | 27,9 | 15,0 | 16,8 | 14,0 | 15,5 | 13,2 | 11,8 | 13,0 | 12,9 | 11,1 | 9,9 | 8,0 | 7,3 | 7,4 | 7,3 |

## Measurements of new partitions 13.5.2009

| Frequency [Hz] | 50 | 63 | 80 | 100 | 125 | 160 | 200 | 250 | 315 | 400 | 500 | 630 | 800 | 1000 | 1250 | 1600 | 2000 | 2500 | 3150 | 4000 | 5000 |
|---|---|---|---|---|---|---|---|---|---|---|---|---|---|---|---|---|---|---|---|---|---|
| Rev. time in room 2, T [s] | 0,35 | 0,57 | 0,51 | 0,50 | 0,91 | 0,68 | 0,56 | 0,77 | 0,58 | 0,56 | 0,50 | 0,49 | 0,49 | 0,46 | 0,41 | 0,41 | 0,40 | 0,42 | 0,40 | 0,40 | 0,39 |
| **1) R`$_w$ room 1 -> room 2 (class 1 partition)** | | | | | | | | | | | | | | | | | | | | | |
| SPL in room 1, $L_{p1\_tot}$ [dB] | 60,9 | 65,8 | 67,5 | 68,4 | 79,3 | 83,9 | 86,1 | 86,0 | 86,7 | 85,7 | 90,7 | 91,9 | 96,5 | 94,7 | 96,1 | 94,8 | 91,5 | 91,5 | 85,5 | 81,8 | 76,9 |
| SPL in room 2, $L_{p2\_tot}$ [dB] | 39,7 | 47,0 | 38,0 | 36,1 | 44,8 | 49,5 | 47,6 | 46,9 | 43,9 | 40,7 | 43,1 | 44,2 | 47,6 | 45,5 | 47,0 | 44,1 | 41,0 | 39,8 | 33,2 | 28,4 | 23,9 |
| **2) R`$_w$ corridor -> room 2 (class 1 corridor partition)** | | | | | | | | | | | | | | | | | | | | | |
| SPL in room 1, $L_{p1\_tot}$ [dB] | 64,0 | 69,8 | 73,3 | 78,7 | 87,4 | 90,0 | 90,7 | 88,9 | 88,7 | 88,5 | 90,9 | 93,3 | 97,2 | 94,4 | 96,8 | 95,5 | 93,0 | 92,6 | 85,9 | 82,4 | 78,4 |
| SPL in room 2, $L_{p2\_tot}$ [dB] | 43,6 | 53,7 | 56,0 | 55,0 | 68,6 | 62,3 | 64,1 | 63,3 | 64,9 | 59,9 | 60,6 | 62,5 | 64,9 | 62,0 | 64,4 | 65,1 | 62,2 | 61,0 | 52,8 | 47,4 | 41,4 |
| **3) R`$_w$ room 1 -> room 2 (class 2 partition)** | | | | | | | | | | | | | | | | | | | | | |
| SPL in room 1, $L_{p1\_tot}$ [dB] | 59,8 | 64,3 | 63,4 | 67,5 | 81,0 | 84,4 | 87,3 | 87,3 | 87,2 | 88,4 | 91,8 | 93,7 | 98,7 | 96,7 | 98,3 | 96,0 | 93,8 | 93,3 | 86,7 | 83,1 | 78,1 |
| SPL in room 2, $L_{p2\_tot}$ [dB] | 46,1 | 54,7 | 49,6 | 45,1 | 52,2 | 55,2 | 53,4 | 51,1 | 47,0 | 44,1 | 45,8 | 46,1 | 51,3 | 48,8 | 49,9 | 48,1 | 45,3 | 44,5 | 37,5 | 32,7 | 27,0 |
| **4) R`$_w$ corridor -> room 2 (class 2/3 corridor partition)** | | | | | | | | | | | | | | | | | | | | | |
| SPL in room 1, $L_{p1\_tot}$ [dB] | 64,2 | 69,6 | 71,7 | 74,2 | 86,5 | 85,1 | 85,2 | 84,0 | 84,7 | 86,0 | 88,1 | 90,6 | 94,6 | 92,2 | 93,1 | 91,7 | 89,1 | 88,8 | 82,5 | 78,9 | 73,7 |
| SPL in room 2, $L_{p2\_tot}$ [dB] | 47,7 | 53,1 | 54,9 | 57,3 | 62,1 | 60,7 | 60,5 | 60,1 | 61,1 | 59,7 | 58,0 | 59,3 | 62,6 | 59,9 | 61,9 | 62,4 | 59,9 | 57,4 | 50,0 | 43,9 | 37,7 |
| **Background noise level [dB]** | | | | | | | | | | | | | | | | | | | | | |
| Room 1 | 48,9 | 48,3 | 38,6 | 38,0 | 37,8 | 38,4 | 42,2 | 33,0 | 33,1 | 30,9 | 27,2 | 25,3 | 21,3 | 19,1 | 16,2 | 11,9 | 10,9 | 9,0 | 6,8 | 6,1 | 6,8 |
| Room 2 | 31,5 | 33,3 | 41,4 | 29,7 | 24,7 | 27,1 | 27,7 | 28,9 | 34,2 | 30,8 | 28,3 | 30,0 | 22,2 | 26,1 | 29,3 | 27,7 | 24,7 | 22,3 | 18,4 | 12,3 | 11,9 |
| Corridor | 39,5 | 38,8 | 27,2 | 27,4 | 28,4 | 30,0 | 33,5 | 26,9 | 29,6 | 24,1 | 21,9 | 25,2 | 18,1 | 22,2 | 27,0 | 27,5 | 27,0 | 22,8 | 18,7 | 13,7 | 10,9 |

## Measurements of new partitions (continued) 20.5.2009

| Frequency [Hz] | 50 | 63 | 80 | 100 | 125 | 160 | 200 | 250 | 315 | 400 | 500 | 630 | 800 | 1000 | 1250 | 1600 | 2000 | 2500 | 3150 | 4000 | 5000 |
|---|---|---|---|---|---|---|---|---|---|---|---|---|---|---|---|---|---|---|---|---|---|
| Rev. time in room 2, T [s] | | | | | | | | | | | | | | | | | | | | | |
| **1) R`w room 1 -> room 2 (class 3 partition)** | | | | | | | | | | | | | | | | | | | | | |
| SPL in room 1, $L_{p1\_tot}$ [dB] | 64,0 | 68,4 | 66,1 | 70,9 | 83,7 | 86,8 | 89,4 | 89,5 | 90,7 | 91,2 | 94,8 | 95,4 | 100,4 | 98,1 | 98,3 | 96,9 | 93,9 | 93,3 | 86,9 | 82,7 | 77,8 |
| SPL in room 2, $L_{p2\_tot}$ [dB] | 46,9 | 56,4 | 52,7 | 54,5 | 58,3 | 61,0 | 61,1 | 59,8 | 57,1 | 52,1 | 52,1 | 52,3 | 57,5 | 53,4 | 53,2 | 51,0 | 48,2 | 47,3 | 42,0 | 35,3 | 28,2 |
| **Background noise level [dB]** | | | | | | | | | | | | | | | | | | | | | |
| Room 1 | 35,8 | 23,0 | 16,6 | 20,1 | 15,7 | 11,2 | 13,4 | 18,2 | 17,8 | 18,8 | 15,2 | 7,8 | 5,4 | 6,8 | 7,8 | 6,7 | 8,0 | 6,1 | 5,5 | 5,7 | 7,0 |
| Room 2 | 33,1 | 31,8 | 26,9 | 19,3 | 25,8 | 28,3 | 24,6 | 28,2 | 33,8 | 25,7 | 22,7 | 25,9 | 21,2 | 22,9 | 24,8 | 24,8 | 21,0 | 18,9 | 12,8 | 10,7 | 10,7 |

## Measurements of partition with perforated panels 2.6.2009

| Frequency [Hz] | 50 | 63 | 80 | 100 | 125 | 160 | 200 | 250 | 315 | 400 | 500 | 630 | 800 | 1000 | 1250 | 1600 | 2000 | 2500 | 3150 | 4000 | 5000 |
|---|---|---|---|---|---|---|---|---|---|---|---|---|---|---|---|---|---|---|---|---|---|
| Rev. time in room 1, T [s] | 0,57 | 0,83 | 0,78 | 0,56 | 0,38 | 0,49 | 0,48 | 0,59 | 0,68 | 0,69 | 0,76 | 0,76 | 0,73 | 0,77 | 0,72 | 0,71 | 0,68 | 0,64 | 0,58 | 0,55 | 0,53 |
| **1) R`$_w$ room 2 -> room 1 (90% of the wall surface in room 2 perforated)** | | | | | | | | | | | | | | | | | | | | | |
| SPL in room 1, $L_{p1\_tot}$ [dB] | 74,9 | 82,4 | 82,0 | 83,7 | 89,2 | 87,9 | 88,7 | 88,2 | 87,9 | 89,2 | 91,7 | 94,1 | 100,0 | 97,0 | 99,6 | 97,8 | 95,1 | 95,0 | 88,7 | 86,1 | 81,8 |
| SPL in room 2, $L_{p2\_tot}$ [dB] | 56,8 | 68,0 | 67,7 | 69,8 | 76,2 | 75,9 | 73,9 | 68,6 | 66,5 | 63,9 | 62,2 | 60,9 | 64,0 | 60,1 | 59,5 | 58,3 | 56,1 | 55,3 | 48,1 | 44,2 | 37,3 |
| **2) R`$_w$ room 2 -> room 1 (57% of the wall surface in room 2 perforated)** | | | | | | | | | | | | | | | | | | | | | |
| SPL in room 1, $L_{p1\_tot}$ [dB] | 72,9 | 81,1 | 78,1 | 84,2 | 93,6 | 93,5 | 90,8 | 88,1 | 89,0 | 89,2 | 93,2 | 95,5 | 100,8 | 98,1 | 100,5 | 98,6 | 96,2 | 96,1 | 89,4 | 86,6 | 82,4 |
| SPL in room 2, $L_{p2\_tot}$ [dB] | 55,6 | 68,6 | 68,5 | 68,5 | 75,1 | 74,1 | 72,3 | 66,6 | 64,4 | 62,9 | 61,7 | 60,1 | 63,5 | 59,7 | 61,1 | 58,3 | 56,0 | 55,7 | 48,5 | 44,7 | 37,8 |
| **3) R`$_w$ room 2 -> room 1 (38% of the wall surface in room 2 perforated)** | | | | | | | | | | | | | | | | | | | | | |
| SPL in room 1, $L_{p1\_tot}$ [dB] | 73,7 | 80,9 | 78,5 | 83,4 | 93,5 | 94,6 | 93,3 | 89,3 | 87,2 | 92,4 | 92,8 | 96,0 | 101,2 | 98,2 | 100,5 | 99,2 | 96,5 | 96,2 | 89,6 | 86,8 | 82,5 |
| SPL in room 2, $L_{p2\_tot}$ [dB] | 59,2 | 66,5 | 67,2 | 66,1 | 75,1 | 74,1 | 73,4 | 65,3 | 61,5 | 61,8 | 60,9 | 58,5 | 63,5 | 59,7 | 60,4 | 58,8 | 56,4 | 56,2 | 48,8 | 44,5 | 37,5 |
| **4) R`$_w$ room 2 -> room 1 (19% of the wall surface in room 2 perforated)** | | | | | | | | | | | | | | | | | | | | | |
| SPL in room 1, $L_{p1\_tot}$ [dB] | 75,7 | 82,1 | 81,7 | 84,9 | 91,8 | 91,0 | 91,7 | 91,1 | 91,0 | 93,9 | 94,6 | 97,3 | 103,0 | 99,7 | 102,5 | 100,6 | 97,9 | 97,5 | 91,1 | 87,7 | 83,4 |
| SPL in room 2, $L_{p2\_tot}$ [dB] | 56,2 | 67,7 | 68,5 | 69,1 | 71,6 | 72,3 | 69,4 | 63,9 | 63,1 | 60,8 | 58,5 | 57,9 | 63,4 | 61,0 | 61,4 | 60,0 | 58,0 | 56,9 | 49,6 | 45,1 | 38,2 |
| **5) R`$_w$ room 2 -> room 1 (0% of the wall surface in room 2 perforated)** | | | | | | | | | | | | | | | | | | | | | |
| SPL in room 1, $L_{p1\_tot}$ [dB] | 67,5 | 74,4 | 73,6 | 77,7 | 86,2 | 87,0 | 89,9 | 86,1 | 85,4 | 88,8 | 91,5 | 92,2 | 97,4 | 95,0 | 97,0 | 95,1 | 92,0 | 91,4 | 85,1 | 81,5 | 77,0 |
| SPL in room 2, $L_{p2\_tot}$ [dB] | 48,3 | 61,5 | 62,3 | 61,4 | 61,9 | 64,3 | 60,8 | 56,8 | 53,0 | 50,2 | 49,4 | 49,6 | 57,5 | 55,2 | 55,8 | 53,7 | 52,0 | 50,8 | 43,5 | 39,2 | 32,3 |
| **Background noise level [dB]** | | | | | | | | | | | | | | | | | | | | | |
| Room 1 | 31,0 | 28,7 | 21,7 | 24,7 | 25,9 | 29,4 | 26,7 | 23,1 | 23,7 | 29,0 | 26,3 | 25,5 | 19,0 | 15,2 | 12,4 | 13,1 | 16,3 | 18,4 | 10,8 | 7,2 | 7,6 |
| Room 2 | 36,9 | 29,0 | 17,3 | 20,8 | 28,7 | 34,4 | 27,4 | 25,6 | 24,2 | 33,4 | 24,6 | 22,9 | 17,6 | 16,8 | 20,3 | 17,7 | 12,5 | 11,5 | 9,5 | 8,1 | 7,5 |

Each sound pressure level (SPL) is an energy average of 10 measurements, calculated with the formula

$$L_{p\_tot} = 10 \log_{10}\left( \sum_{i=1}^{n} 10^{L_{p\_i}/10} \right)$$

where $L_{p\_i}$ is the sound pressure level [dB].

# Appendix D

## Modelling results of new partitions

**Modelled structure:**

2 x chipboard 11 mm (attached with screws), timber studs + mineral wool 50 mm, airspace 20 mm, timber studs + mineral wool 50 mm, 2 x MDF 12 mm (attached with screws)

**Calculation parameters:**

| **Plates** | **Plate 1 :** 2 x chipboard 11 mm | | | **Plate 2:** 2 x MDF 12 mm | | |
|---|---|---|---|---|---|---|
| Num. of plates (screwed) | N = | 2 | - | N = | 2 | - |
| Thickness | $h_1$ = | 0,011 | m | $h_2$ = | 0,012 | m |
| Density | $\rho_1$ = | 640 | $kg/m^3$ | $\rho_2$ = | 760 | $kg/m^3$ |
| Surface mass | $m_1$` = | 7,0 | $kg/m^2$ | $m_2$` = | 9,1 | $kg/m^2$ |
| Poisson`s ratio | $\mu_1$ = | 0,28 | - | $\mu_2$ = | 0,28 | - |
| Modulus of elasticity | $E_1$ = | 2900 | MPa | $E_2$ = | 6300 | MPa |
| Internal loss factor | $\eta_{int1}$ = | 0,01 | - | $\eta_{int2}$ = | 0,01 | - |

**Cavity / absorbing material /studs**

| | | | | | | | |
|---|---|---|---|---|---|---|---|
| Cavity thickness | d = | 0,120 | m | Cavity filling ratio | FR = | 0,90 | - |
| Cavity, x-dimension | $L_{x,c}$ = | 0,580 | m | Absorption coefficient | $\alpha_c$ = | 0,90 | - |
| Cavity, y-dimension | $L_{y,c}$ = | 2,400 | m | Centers distance of studs | b = | 0,600 | m |

Area of the structure in the calculation is 10 $m^2$. Connections between plates and studs are assumed to act as line couplings.

| *f* [Hz] | *R* [dB] |
|---|---|
| 50 | 22,0 |
| 63 | 23,7 |
| 80 | 24,6 |
| 100 | 33,4 |
| 125 | 38,6 |
| 160 | 44,5 |
| 200 | 49,9 |
| 250 | 55,2 |
| 315 | 60,7 |
| 400 | 66,4 |
| 500 | 71,0 |
| 630 | 74,1 |
| 800 | 76,8 |
| 1000 | 78,7 |
| 1250 | 79,0 |
| 1600 | 73,5 |
| 2000 | 65,9 |
| 2500 | 59,1 |
| 3150 | 61,5 |
| 4000 | 67,5 |
| 5000 | 73,1 |

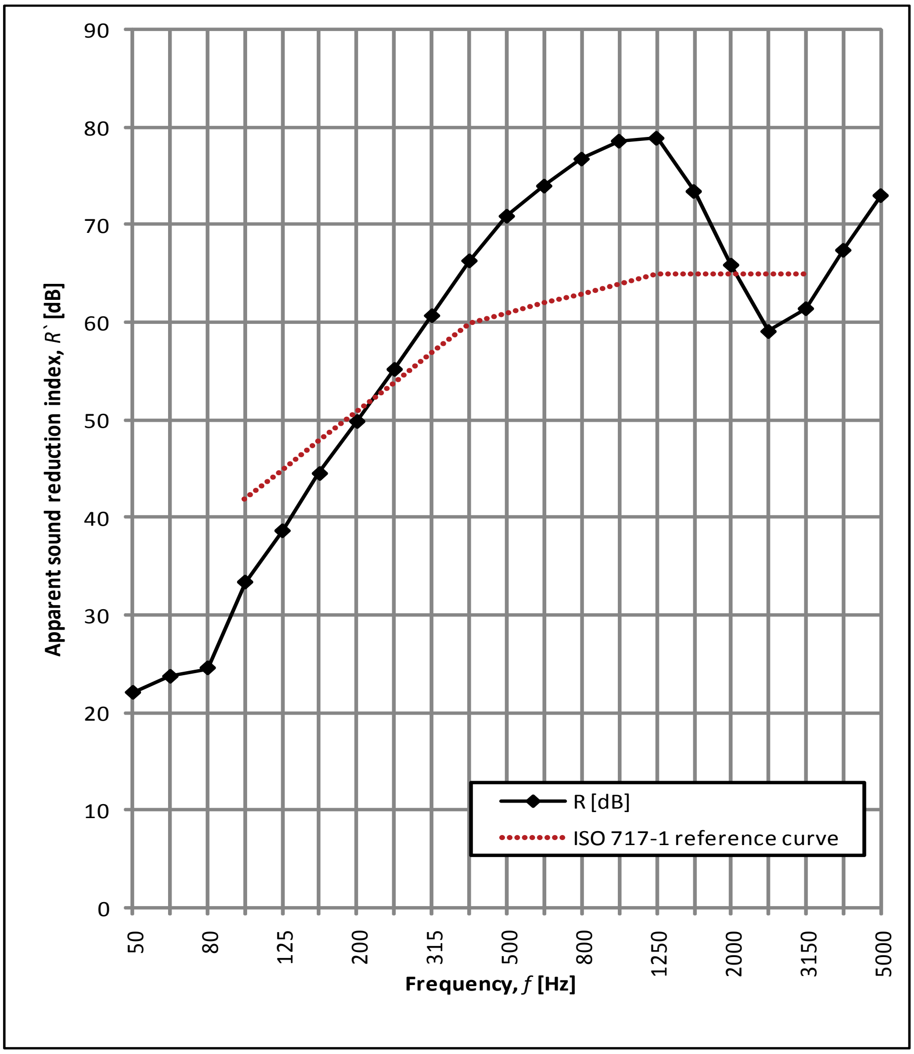


**Weighted sound reduction index according to ISO 717-1:**

***R*** $_w$ **= 61 dB**

**Modelled structure:**

Chipboard 11 mm, timber studs + mineral wool 50 mm, airspace 20 mm, timber studs + mineral wool 50 mm, MDF 19 mm

**Calculation parameters:**

| **Plates** | **Plate 1 :** chipboard 11 mm | | | **Plate 2:** MDF 19 mm | | |
|---|---|---|---|---|---|---|
| Num. of plates (screwed) | N = | 1 | - | N = | 1 | - |
| Thickness | $h_1$ = | 0,011 | m | $h_2$ = | 0,019 | m |
| Density | $\rho_1$ = | 640 | kg/m$^3$ | $\rho_2$ = | 760 | kg/m$^3$ |
| Surface mass | $m_1$` = | 7,0 | kg/m$^2$ | $m_2$` = | 14,4 | kg/m$^2$ |
| Poisson`s ratio | $\mu_1$ = | 0,28 | - | $\mu_2$ = | 0,28 | - |
| Modulus of elasticity | $E_1$ = | 2900 | MPa | $E_2$ = | 4800 | MPa |
| Internal loss factor | $\eta_{int1}$ = | 0,01 | - | $\eta_{int2}$ = | 0,01 | - |

**Cavity / absorbing material /studs**

| | | | | | | | |
|---|---|---|---|---|---|---|---|
| Cavity thickness | d = | 0,120 | m | Cavity filling ratio | FR = | 0,90 | - |
| Cavity, x-dimension | $L_{x,c}$ = | 0,580 | m | Absorption coefficient | $\alpha_c$ = | 0,90 | - |
| Cavity, y-dimension | $L_{y,c}$ = | 2,400 | m | Centers distance of studs | b = | 0,600 | m |

Area of the structure in the calculation is 10 m$^2$. Connections between plates and studs are assumed to act as line couplings.

| *f* [Hz] | *R* [dB] |
|---|---|
| 50 | 21,3 |
| 63 | 19,7 |
| 80 | 21,2 |
| 100 | 23,0 |
| 125 | 30,6 |
| 160 | 36,4 |
| 200 | 41,7 |
| 250 | 47,0 |
| 315 | 52,4 |
| 400 | 57,9 |
| 500 | 62,2 |
| 630 | 64,8 |
| 800 | 66,6 |
| 1000 | 66,1 |
| 1250 | 54,8 |
| 1600 | 58,1 |
| 2000 | 59,4 |
| 2500 | 52,6 |
| 3150 | 54,9 |
| 4000 | 60,9 |
| 5000 | 66,5 |

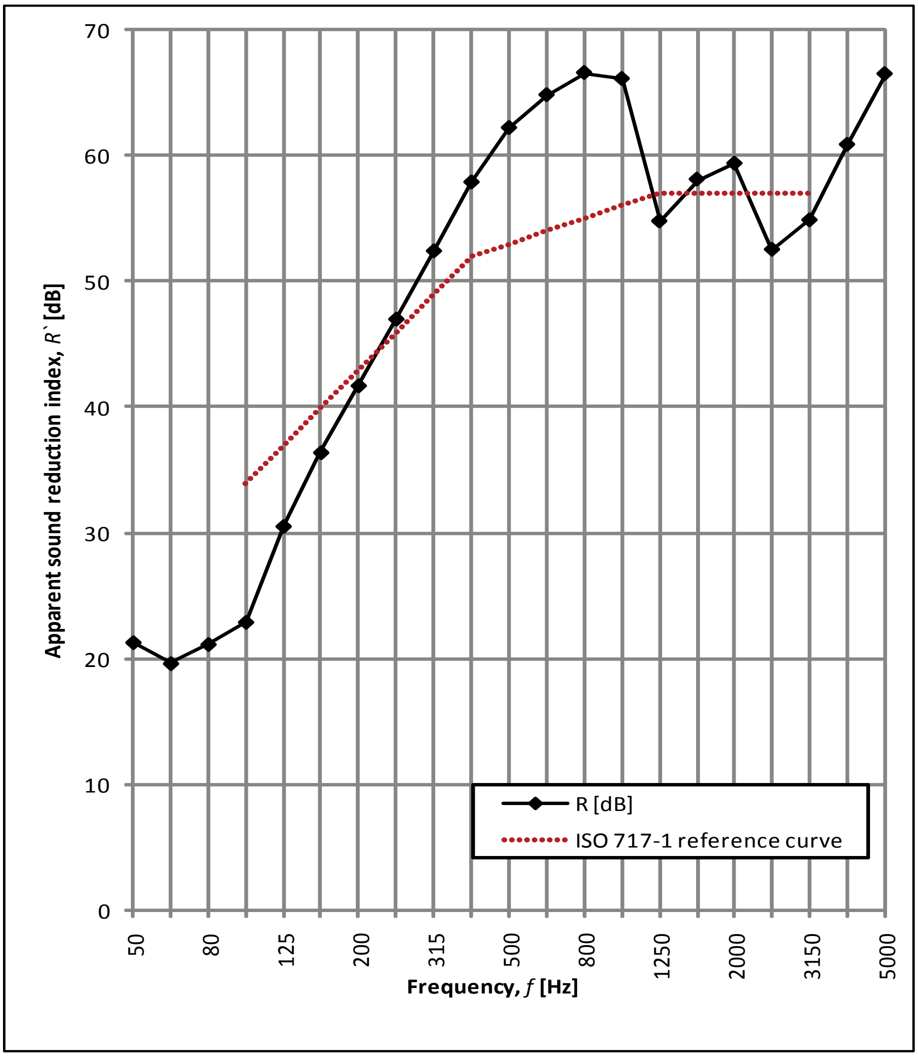


**Weighted sound reduction index according to ISO 717-1:**

***R*** $_w$ **= 53 dB**

**Modelled structure:**

Chipboard 11 mm, timber studs + mineral wool 92 mm, chipboard 11 mm

**Calculation parameters:**

| **Plates** | **Plate 1 :** chipboard 11 mm | | | **Plate 2:** chipboard 11 mm | | |
|---|---|---|---|---|---|---|
| Num. of plates (screwed) | N = | 1 | - | N = | 1 | - |
| Thickness | $h_1$ = | 0,011 | m | $h_2$ = | 0,011 | m |
| Density | $\rho_1$ = | 640 | $kg/m^3$ | $\rho_2$ = | 640 | $kg/m^3$ |
| Surface mass | $m_1$` = | 7,0 | $kg/m^2$ | $m_2$` = | 7,0 | $kg/m^2$ |
| Poisson`s ratio | $\mu_1$ = | 0,28 | - | $\mu_2$ = | 0,28 | - |
| Modulus of elasticity | $E_1$ = | 2900 | MPa | $E_2$ = | 2900 | MPa |
| Internal loss factor | $\eta_{int1}$ = | 0,01 | - | $\eta_{int2}$ = | 0,01 | - |

**Cavity / absorbing material /studs**

| | | | | | | | |
|---|---|---|---|---|---|---|---|
| Cavity thickness | d = | 0,092 | m | Cavity filling ratio | FR = | 1,00 | - |
| Cavity, x-dimension | $L_{x,c}$ = | 0,580 | m | Absorption coefficient | $\alpha_c$ = | 0,90 | - |
| Cavity, y-dimension | $L_{y,c}$ = | 2,400 | m | Centers distance of studs | b = | 0,600 | m |

Area of the structure in the calculation is 10 $m^2$. Connections between plates and studs are assumed to act as line couplings.

| ***f*** **[Hz]** | ***R*** **[dB]** |
|---|---|
| 50 | 14,8 |
| 63 | 16,4 |
| 80 | 17,7 |
| 100 | 19,4 |
| 125 | 21,1 |
| 160 | 28,4 |
| 200 | 33,2 |
| 250 | 35,0 |
| 315 | 36,8 |
| 400 | 38,7 |
| 500 | 40,4 |
| 630 | 42,1 |
| 800 | 43,8 |
| 1000 | 45,1 |
| 1250 | 46,2 |
| 1600 | 46,5 |
| 2000 | 45,0 |
| 2500 | 35,4 |
| 3150 | 34,9 |
| 4000 | 38,0 |
| 5000 | 40,8 |

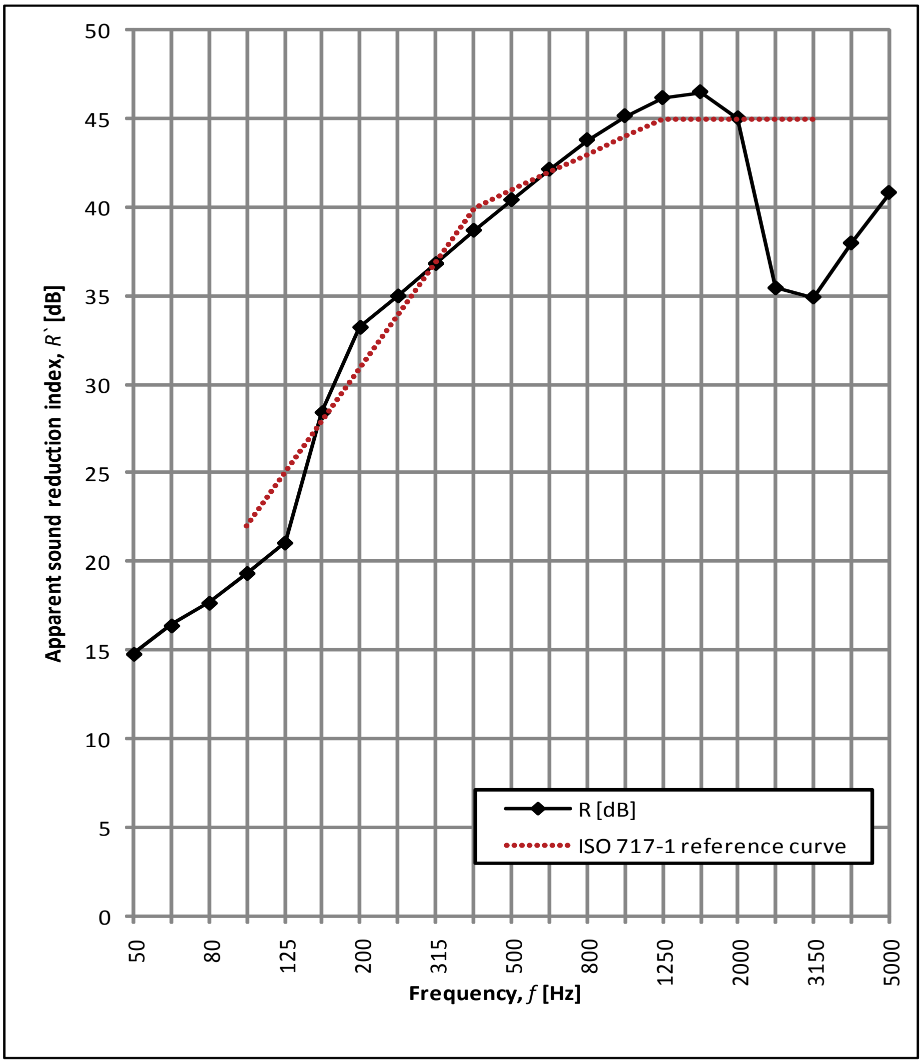


**Weighted sound reduction index according to ISO 717-1:**

$R_w$ = **41 dB**

**Modelled structure:**

2 x chipboard 11 mm (attached with screws), timber studs + mineral wool 92 mm, 2 x MDF 12 mm (attached with screws)

**Calculation parameters:**

| **Plates** | | **Plate 1 :** 2 x chipboard 11 mm | | | **Plate 2:** 2 x MDF 12 mm | |
|---|---|---|---|---|---|---|
| Num. of plates (screwed) | N = | 2 | - | N = | 2 | - |
| Thickness | $h_1$ = | 0,011 | m | $h_2$ = | 0,012 | m |
| Density | $\rho_1$ = | 640 | $kg/m^3$ | $\rho_2$ = | 760 | $kg/m^3$ |
| Surface mass | $m_1$` = | 7,0 | $kg/m^2$ | $m_2$` = | 9,1 | $kg/m^2$ |
| Poisson`s ratio | $\mu_1$ = | 0,28 | - | $\mu_2$ = | 0,28 | - |
| Modulus of elasticity | $E_1$ = | 2900 | MPa | $E_2$ = | 6300 | MPa |
| Internal loss factor | $\eta_{int1}$ = | 0,01 | - | $\eta_{int2}$ = | 0,01 | - |

**Cavity / absorbing material /studs**

| | | | | | | | |
|---|---|---|---|---|---|---|---|
| Cavity thickness | d = | 0,092 | m | Cavity filling ratio | FR = | 1,00 | - |
| Cavity, x-dimension | $L_{x,c}$ = | 0,580 | m | Absorption coefficient | $\alpha_c$ = | 0,90 | - |
| Cavity, y-dimension | $L_{y,c}$ = | 2,400 | m | Centers distance of studs | b = | 0,600 | m |

Area of the structure in the calculation is 10 $m^2$. Connections between plates and studs are assumed to act as line couplings.

| ***f*** **[Hz]** | ***R*** **[dB]** |
|---|---|
| 50 | 22,0 |
| 63 | 23,7 |
| 80 | 25,0 |
| 100 | 26,7 |
| 125 | 28,5 |
| 160 | 37,7 |
| 200 | 39,4 |
| 250 | 41,2 |
| 315 | 43,0 |
| 400 | 44,8 |
| 500 | 46,5 |
| 630 | 48,0 |
| 800 | 49,4 |
| 1000 | 50,2 |
| 1250 | 50,1 |
| 1600 | 47,0 |
| 2000 | 43,6 |
| 2500 | 40,6 |
| 3150 | 42,7 |
| 4000 | 45,7 |
| 5000 | 48,6 |

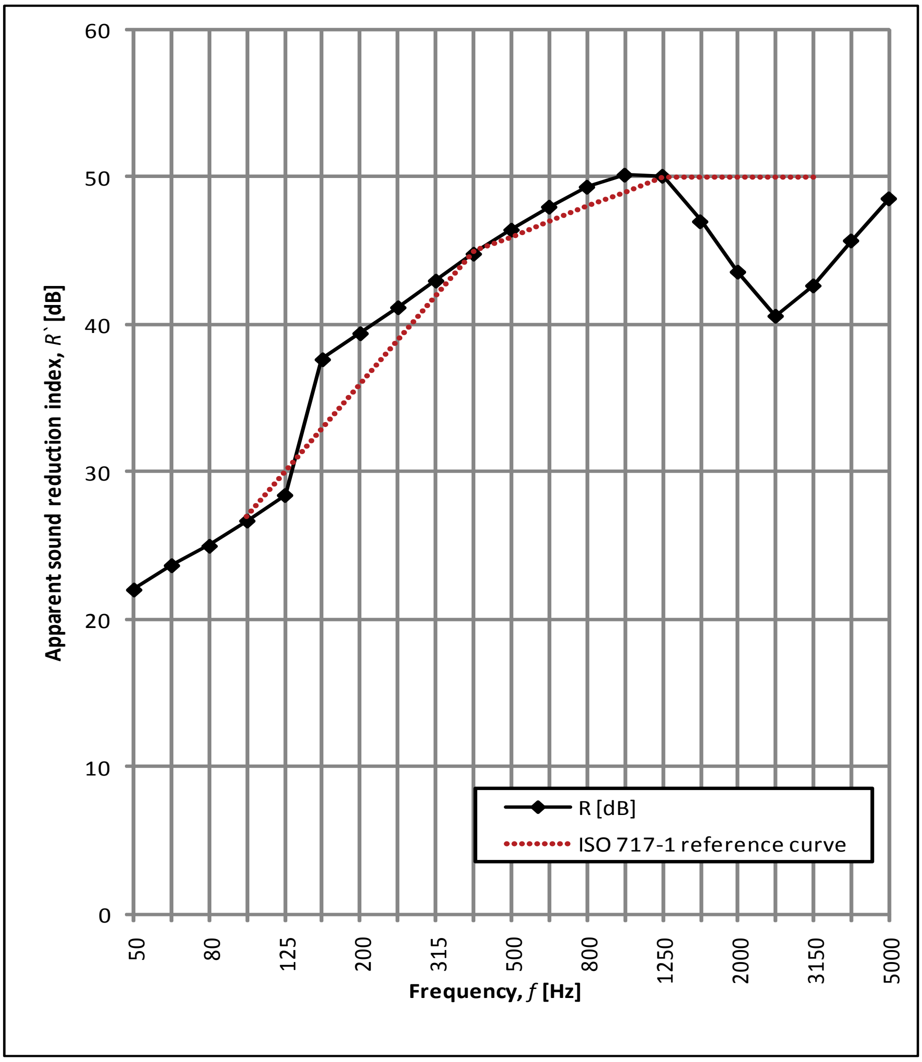


**Weighted sound reduction index according to ISO 717-1:**

***R*** ***w*** **= 46 dB**

## Calculation of apparent weighted sound reduction index

### Test room at Idea-Puu Oy, Class I partitions

Formulas used in the prediction model:

$$F_n = R_{fn} + K_{ij} + 10\log\left(\frac{S_{sn}}{S_{rn}}\right)$$

$$R'_w = R_w - 10\log\left[1+\left(\frac{1}{S}\right)\sum_{n=1}^{4}\left(S_{sn}\cdot 10^{(R_{w,0}-F_n)/10}\right)\right]$$

Schematic illustration of flanking paths:

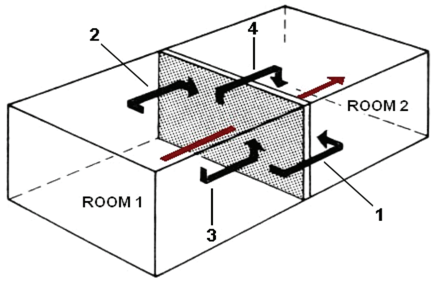


### Partition separating adjacent rooms: Class I partition

| | | | |
|---|---|---|---|
| Weighted SRI of separating partition | $R_w$ = | 61 | dB |
| Area of the separating partition | $S$ = | 7,5 | $m^2$ |

### Flanking path 1: Class I corridor partition

| | | | |
|---|---|---|---|
| Weighted SRI of flanking structure 1 | $R_{w1}$ = | 46 | dB |
| Correction term [1)] | | -5 | dB |
| Corrected SRI of flanking structure 1 | $R_{f1}$ = | 41 | dB |
| Vibration reduction index of junction | $K_{ij\_1}$ = | 25 | dB |
| Area of flanking structure 1 in the source room | $S_{s1}$ = | 6,8 | $m^2$ |
| Area of flanking structure 1 in the receiving room | $S_{r1}$ = | 6,8 | $m^2$ |

$$10\log\left(\frac{S_{s1}}{S_{r1}}\right) = 0 \text{ dB}$$

$$F_1 = R_{f1} + K_{ij\_1} + 10\log\left(\frac{S_{s1}}{S_{r1}}\right) = 66 \text{ dB}$$

$$C_1 = \frac{1}{S}\cdot S_{s1}\cdot 10^{(R_w-F_1)/10} = 0{,}29$$

### Flanking path 2: flanking side wall[2)] (double-leaf partition, continuous plate layers)

| | | | |
|---|---|---|---|
| Weighted SRI of flanking structure 2 | $R_{w2}$ = | 54 | dB |
| Correction term [1)] | | -5 | dB |
| Corrected SRI of flanking structure 2 | $R_{f2}$ = | 49 | dB |
| Vibration reduction index of junction | $K_{ij\_2}$ = | 0 | dB |
| Area of flanking structure 2 in the source room | $S_{s2}$ = | 6,8 | $m^2$ |
| Area of flanking structure 2 in the receiving room | $S_{r2}$ = | 6,8 | $m^2$ |

$$10\log\left(\frac{S_{s2}}{S_{r2}}\right) = 0 \text{ dB}$$

$$F_2 = R_{f2} + K_{ij\_2} + 10\log\left(\frac{S_{s2}}{S_{r2}}\right) = 49 \text{ dB}$$

$$C_2 = \frac{1}{S}\cdot S_{s2}\cdot 10^{(R_w-F_2)/10} = 14{,}37$$

### Flanking path 3: base- / intermediate floor (concrete slab 150 mm, continuous)

| | | | |
|---|---|---|---|
| Weighted SRI of flanking structure 3 | $R_{w3}$ = | 58 | dB |
| Correction term [1)] | | 0 | dB |
| Corrected SRI of flanking structure 3 | $R_{f3}$ = | 58 | dB |
| Vibration reduction index of junction | $K_{ij\_3}$ = | 0 | dB |
| Area of flanking structure 3 in the source room | $S_{s3}$ = | 6,2 | $m^2$ |
| Area of flanking structure 3 in the receiving room | $S_{r3}$ = | 6,2 | $m^2$ |

$$10\log\left(\frac{S_{s3}}{S_{r3}}\right) = 0 \text{ dB}$$

$$F_3 = R_{f3} + K_{ij\_3} + 10\log\left(\frac{S_{s3}}{S_{r3}}\right) = 58 \text{ dB}$$

$$C_3 = \frac{1}{S}\cdot S_{s3}\cdot 10^{(R_w-F_3)/10} = 1{,}65$$

### Flanking path 4: roof / intermediate floor (hollow core slab 265 mm, continuous)

| | | | |
|---|---|---|---|
| Weighted SRI of flanking structure 4 | $R_{w4}$ = | 61 | dB |
| Correction term [1)] | | 0 | dB |
| Corrected SRI of flanking structure 4 | $R_{f4}$ = | 61 | dB |
| Vibration reduction index of junction | $K_{ij\_4}$ = | 0 | dB |
| Area of flanking structure 4 in the source room | $S_{s4}$ = | 6,2 | $m^2$ |
| Area of flanking structure 4 in the receiving room | $S_{r4}$ = | 6,2 | $m^2$ |

$$10\log\left(\frac{S_{s4}}{S_{r4}}\right) = 0 \text{ dB}$$

$$F_4 = R_{f4} + K_{ij\_4} + 10\log\left(\frac{S_{s4}}{S_{r4}}\right) = 61 \text{ dB}$$

$$C_4 = \frac{1}{S}\cdot S_{s4}\cdot 10^{(R_w-F_4)/10} = 0{,}83$$

## Apparent weighted sound reduction index

Apparent SRI from room 1 to room 2

$$R'_w = R_w - 10\log\left(C_1 + C_2 + C_3 + C_4 + 1\right) = \mathbf{48\ dB}$$

[1)] Correction terms according to Homb et al. [14]

[2)] Structure of the flanking side wall: chipboard 12 mm + gypsum board 15 mm (screw fastening), MDF 12 mm (glue fastening), timber studs + mineral wool 90 mm, chipboard 12 mm + perforated MDF 12 mm (screw fastening)

## Calculation of apparent weighted sound reduction index

### Test room at Idea-Puu Oy, Class 2 partitions

Formulas used in the prediction model:

$$F_n = R_{fn} + K_{ij} + 10\log\left(\frac{S_{sn}}{S_{rn}}\right)$$

$$R_w^{'} = R_w - 10\log\left[1 + \left(\frac{1}{S}\right)\sum_{n=1}^{4}\left(S_{sn}\cdot 10^{(R_{w,0}-F_n)/10}\right)\right]$$

Schematic illustration of flanking paths:

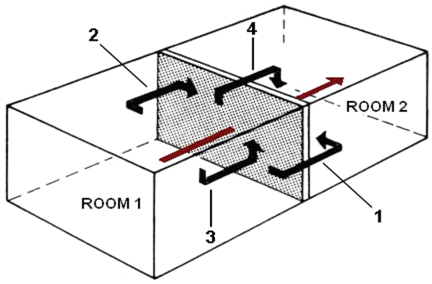


### Partition separating adjacent rooms: Class 2 partition

| | | | |
|---|---|---|---|
| Weighted SRI of separating partition | $R_w$ = | 53 | dB |
| Area of the separating partition | $S$ = | 7,5 | $m^2$ |

### Flanking path 1: Class 2 corridor partition

| | | | |
|---|---|---|---|
| Weighted SRI of flanking structure 1 | $R_{w1}$ = | 41 | dB |
| Correction term *) | | -5 | dB |
| Corrected SRI of flanking structure 1 | $R_{f1}$ = | 36 | dB |
| Vibration reduction index of junction | $K_{ij\_1}$ = | 25 | dB |
| Area of flanking structure 1 in the source room | $S_{s1}$ = | 6,8 | $m^2$ |
| Area of flanking structure 1 in the receiving room | $S_{r1}$ = | 6,8 | $m^2$ |

$$10\log\left(\frac{S_{s1}}{S_{r1}}\right) = 0 \text{ dB}$$

$$F_1 = R_{f1} + K_{ij\_1} + 10\log\left(\frac{S_{s1}}{S_{r1}}\right) = 61 \text{ dB}$$

$$C_1 = \frac{1}{S}\cdot S_{s1}\cdot 10^{(R_w-F_1)/10} = 0{,}14$$

### Flanking path 2: flanking side wall (double-leaf partition, continuous plate layers)

| | | | |
|---|---|---|---|
| Weighted SRI of flanking structure 2 | $R_{w2}$ = | 54 | dB |
| Correction term *) | | -5 | dB |
| Corrected SRI of flanking structure 2 | $R_{f2}$ = | 49 | dB |
| Vibration reduction index of junction | $K_{ij\_2}$ = | 0 | dB |
| Area of flanking structure 2 in the source room | $S_{s2}$ = | 6,8 | $m^2$ |
| Area of flanking structure 2 in the receiving room | $S_{r2}$ = | 6,8 | $m^2$ |

$$10\log\left(\frac{S_{s2}}{S_{r2}}\right) = 0 \text{ dB}$$

$$F_2 = R_{f2} + K_{ij\_2} + 10\log\left(\frac{S_{s2}}{S_{r2}}\right) = 49 \text{ dB}$$

$$C_2 = \frac{1}{S}\cdot S_{s2}\cdot 10^{(R_w-F_2)/10} = 2{,}28$$

### Flanking path 3: base- / intermediate floor (concrete slab 150 mm, continuous)

| | | | |
|---|---|---|---|
| Weighted SRI of flanking structure 3 | $R_{w3}$ = | 58 | dB |
| Correction term *) | | 0 | dB |
| Corrected SRI of flanking structure 3 | $R_{f3}$ = | 58 | dB |
| Vibration reduction index of junction | $K_{ij\_3}$ = | 0 | dB |
| Area of flanking structure 3 in the source room | $S_{s3}$ = | 6,2 | $m^2$ |
| Area of flanking structure 3 in the receiving room | $S_{r3}$ = | 6,2 | $m^2$ |

$$10\log\left(\frac{S_{s3}}{S_{r3}}\right) = 0 \text{ dB}$$

$$F_3 = R_{f3} + K_{ij\_3} + 10\log\left(\frac{S_{s3}}{S_{r3}}\right) = 58 \text{ dB}$$

$$C_3 = \frac{1}{S}\cdot S_{s3}\cdot 10^{(R_w-F_3)/10} = 0{,}26$$

### Flanking path 4: roof / intermediate floor (hollow core slab 265 mm, continuous)

| | | | |
|---|---|---|---|
| Weighted SRI of flanking structure 4 | $R_{w4}$ = | 61 | dB |
| Correction term *) | | 0 | dB |
| Corrected SRI of flanking structure 4 | $R_{f4}$ = | 61 | dB |
| Vibration reduction index of junction | $K_{ij\_4}$ = | 0 | dB |
| Area of flanking structure 4 in the source room | $S_{s4}$ = | 6,2 | $m^2$ |
| Area of flanking structure 4 in the receiving room | $S_{r4}$ = | 6,2 | $m^2$ |

$$10\log\left(\frac{S_{s4}}{S_{r4}}\right) = 0 \text{ dB}$$

$$F_4 = R_{f4} + K_{ij\_4} + 10\log\left(\frac{S_{s4}}{S_{r4}}\right) = 61 \text{ dB}$$

$$C_4 = \frac{1}{S}\cdot S_{s4}\cdot 10^{(R_w-F_4)/10} = 0{,}13$$

## Apparent weighted sound reduction index

Apparent SRI from room 1 to room 2

$$R_w^{'} = R_w - 10\log\left(C_1 + C_2 + C_3 + C_4 + 1\right) = \mathbf{47\ dB}$$

*) Correction terms according to Homb et al. [14]

## Calculation of apparent weighted sound reduction index

### Test room at Idea-Puu Oy, Class 3 partitions

Formulas used in the prediction model:

$$F_n = R_{fn} + K_{ij} + 10\log\left(\frac{S_{sn}}{S_{rn}}\right)$$

$$R_w^{'} = R_w - 10\log\left[1 + \left(\frac{1}{S}\right)\sum_{n=1}^{4}\left(S_{sn}\cdot 10^{(R_{w,0}-F_n)/10}\right)\right]$$

Schematic illustration of flanking paths:

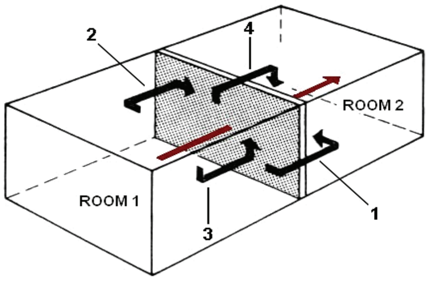


### Partition separating adjacent rooms: Class 3 partition

| | | | |
|---|---|---|---|
| Weighted SRI of separating partition | $R_w$ = | 41 | dB |
| Area of the separating partition | $S$ = | 7,5 | $m^2$ |

### Flanking path 1: Class 3 corridor partition

| | | | |
|---|---|---|---|
| Weighted SRI of flanking structure 1 | $R_{w1}$ = | 41 | dB |
| Correction term *) | | -5 | dB |
| Corrected SRI of flanking structure 1 | $R_{f1}$ = | 36 | dB |
| Vibration reduction index of junction | $K_{ij\_1}$ = | 25 | dB |
| Area of flanking structure 1 in the source room | $S_{s1}$ = | 6,8 | $m^2$ |
| Area of flanking structure 1 in the receiving room | $S_{r1}$ = | 6,8 | $m^2$ |

$$10\log\left(\frac{S_{s1}}{S_{r1}}\right) = 0 \text{ dB}$$

$$F_1 = R_{f1} + K_{ij\_1} + 10\log\left(\frac{S_{s1}}{S_{r1}}\right) = 61 \text{ dB}$$

$$C_1 = \frac{1}{S}\cdot S_{s1}\cdot 10^{(R_w-F_1)/10} = 0{,}01$$

### Flanking path 2: flanking side wall (double-leaf partition, continuous plate layers)

| | | | |
|---|---|---|---|
| Weighted SRI of flanking structure 2 | $R_{w2}$ = | 54 | dB |
| Correction term *) | | -5 | dB |
| Corrected SRI of flanking structure 2 | $R_{f2}$ = | 49 | dB |
| Vibration reduction index of junction | $K_{ij\_2}$ = | 0 | dB |
| Area of flanking structure 2 in the source room | $S_{s2}$ = | 6,8 | $m^2$ |
| Area of flanking structure 2 in the receiving room | $S_{r2}$ = | 6,8 | $m^2$ |

$$10\log\left(\frac{S_{s2}}{S_{r2}}\right) = 0 \text{ dB}$$

$$F_2 = R_{f2} + K_{ij\_2} + 10\log\left(\frac{S_{s2}}{S_{r2}}\right) = 49 \text{ dB}$$

$$C_2 = \frac{1}{S}\cdot S_{s2}\cdot 10^{(R_w-F_2)/10} = 0{,}14$$

### Flanking path 3: base- / intermediate floor (concrete slab 150 mm, continuous)

| | | | |
|---|---|---|---|
| Weighted SRI of flanking structure 3 | $R_{w3}$ = | 58 | dB |
| Correction term *) | | 0 | dB |
| Corrected SRI of flanking structure 3 | $R_{f3}$ = | 58 | dB |
| Vibration reduction index of junction | $K_{ij\_3}$ = | 0 | dB |
| Area of flanking structure 3 in the source room | $S_{s3}$ = | 6,2 | $m^2$ |
| Area of flanking structure 3 in the receiving room | $S_{r3}$ = | 6,2 | $m^2$ |

$$10\log\left(\frac{S_{s3}}{S_{r3}}\right) = 0 \text{ dB}$$

$$F_3 = R_{f3} + K_{ij\_3} + 10\log\left(\frac{S_{s3}}{S_{r3}}\right) = 58 \text{ dB}$$

$$C_3 = \frac{1}{S}\cdot S_{s3}\cdot 10^{(R_w-F_3)/10} = 0{,}02$$

### Flanking path 4: roof / intermediate floor (hollow core slab 265 mm, continuous)

| | | | |
|---|---|---|---|
| Weighted SRI of flanking structure 4 | $R_{w4}$ = | 61 | dB |
| Correction term *) | | 0 | dB |
| Corrected SRI of flanking structure 4 | $R_{f4}$ = | 61 | dB |
| Vibration reduction index of junction | $K_{ij\_4}$ = | 0 | dB |
| Area of flanking structure 4 in the source room | $S_{s4}$ = | 6,2 | $m^2$ |
| Area of flanking structure 4 in the receiving room | $S_{r4}$ = | 6,2 | $m^2$ |

$$10\log\left(\frac{S_{s4}}{S_{r4}}\right) = 0 \text{ dB}$$

$$F_4 = R_{f4} + K_{ij\_4} + 10\log\left(\frac{S_{s4}}{S_{r4}}\right) = 61 \text{ dB}$$

$$C_4 = \frac{1}{S}\cdot S_{s4}\cdot 10^{(R_w-F_4)/10} = 0{,}01$$

## Apparent weighted sound reduction index

Apparent SRI from room 1 to room 2

$$R_w^{'} = R_w - 10\log\left(C_1 + C_2 + C_3 + C_4 + 1\right) = \mathbf{40\ dB}$$

*) Correction terms according to Homb et al. [14]

# APPENDIX E

## MODELLING RESULTS OF APPARENT SOUND REDUCTION INDEX IN TYPICAL OFFICE BUILDING

## Calculation of apparent weighted sound reduction index

### Typical office building, Class I partitions

### Flanking path 2: concrete inner envelope of exterior wall (continuous)

Formulas used in the prediction model:

$$F_n = R_{fn} + K_{ij} + 10\log\left(\frac{S_{sn}}{S_{rn}}\right)$$

$$R'_w = R_w - 10\log\left[1 + \left(\frac{1}{S}\right)\sum_{n=1}^{4}\left(S_{sn}\cdot 10^{(R_{w,0}-F_n)/10}\right)\right]$$

Schematic illustration of flanking paths:

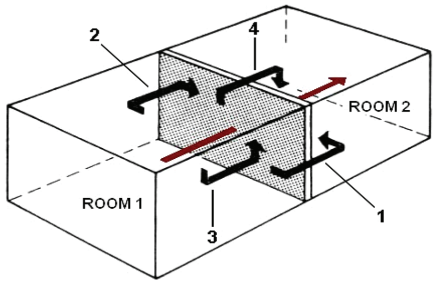


### Partition separating adjacent rooms: Class I partition

| | | | |
|---|---|---|---|
| Weighted SRI of separating partition | $R_w$ = | 61 | dB |
| Area of the separating partition | $S$ = | 7,5 | $m^2$ |

### Flanking path 1: Class I corridor partition

| | | | |
|---|---|---|---|
| Weighted SRI of flanking structure 1 | $R_{w1}$ = | 46 | dB |
| Correction term *) | | -5 | dB |
| Corrected SRI of flanking structure 1 | $R_{f1}$ = | 41 | dB |
| Vibration reduction index of junction | $K_{ij\_1}$ = | 25 | dB |
| Area of flanking structure 1 in the source room | $S_{s1}$ = | 6,8 | $m^2$ |
| Area of flanking structure 1 in the receiving room | $S_{r1}$ = | 6,8 | $m^2$ |

$$10\log\left(\frac{S_{s1}}{S_{r1}}\right) = 0 \text{ dB}$$

$$F_1 = R_{f1} + K_{ij\_1} + 10\log\left(\frac{S_{s1}}{S_{r1}}\right) = 66 \text{ dB}$$

$$C_1 = \frac{1}{S}\cdot S_{s1}\cdot 10^{(R_w-F_1)/10} = 0{,}29$$

### Flanking path 2: concrete inner envelope of exterior wall (continuous)

| | | | |
|---|---|---|---|
| Weighted SRI of flanking structure 2 | $R_{w2}$ = | 59 | dB |
| Correction term *) | | 0 | dB |
| Corrected SRI of flanking structure 2 | $R_{f2}$ = | 59 | dB |
| Vibration reduction index of junction | $K_{ij\_2}$ = | 0 | dB |
| Area of flanking structure 2 in the source room | $S_{s2}$ = | 6,8 | $m^2$ |
| Area of flanking structure 2 in the receiving room | $S_{r2}$ = | 6,8 | $m^2$ |

$$10\log\left(\frac{S_{s2}}{S_{r2}}\right) = 0 \text{ dB}$$

$$F_2 = R_{f2} + K_{ij\_2} + 10\log\left(\frac{S_{s2}}{S_{r2}}\right) = 59 \text{ dB}$$

$$C_2 = \frac{1}{S}\cdot S_{s2}\cdot 10^{(R_w-F_2)/10} = 1{,}44$$

### Flanking path 3: base- / intermediate floor (e.g. hollow core slab ≥ 265 mm / 380 kg/$m^2$)

| | | | |
|---|---|---|---|
| Weighted SRI of flanking structure 3 | $R_{w3}$ = | 61 | dB |
| Correction term *) | | 0 | dB |
| Corrected SRI of flanking structure 3 | $R_{f3}$ = | 61 | dB |
| Vibration reduction index of junction | $K_{ij\_3}$ = | 0 | dB |
| Area of flanking structure 3 in the source room | $S_{s3}$ = | 6,2 | $m^2$ |
| Area of flanking structure 3 in the receiving room | $S_{r3}$ = | 6,2 | $m^2$ |

$$10\log\left(\frac{S_{s3}}{S_{r3}}\right) = 0 \text{ dB}$$

$$F_3 = R_{f3} + K_{ij\_3} + 10\log\left(\frac{S_{s3}}{S_{r3}}\right) = 61 \text{ dB}$$

$$C_3 = \frac{1}{S}\cdot S_{s3}\cdot 10^{(R_w-F_3)/10} = 0{,}83$$

### Flanking path 4: roof / intermediate floor (e.g. hollow core slab ≥ 265 mm / 380 kg/$m^2$)

| | | | |
|---|---|---|---|
| Weighted SRI of flanking structure 4 | $R_{w4}$ = | 61 | dB |
| Correction term *) | | 0 | dB |
| Corrected SRI of flanking structure 4 | $R_{f4}$ = | 61 | dB |
| Vibration reduction index of junction | $K_{ij\_4}$ = | 0 | dB |
| Area of flanking structure 4 in the source room | $S_{s4}$ = | 6,2 | $m^2$ |
| Area of flanking structure 4 in the receiving room | $S_{r4}$ = | 6,2 | $m^2$ |

$$10\log\left(\frac{S_{s4}}{S_{r4}}\right) = 0 \text{ dB}$$

$$F_4 = R_{f4} + K_{ij\_4} + 10\log\left(\frac{S_{s4}}{S_{r4}}\right) = 61 \text{ dB}$$

$$C_4 = \frac{1}{S}\cdot S_{s4}\cdot 10^{(R_w-F_4)/10} = 0{,}83$$

## Apparent weighted sound reduction index

Apparent SRI from room 1 to room 2

$$R'_w = R_w - 10\log\left(C_1 + C_2 + C_3 + C_4 + 1\right) = \mathbf{55\ dB}$$

*) Correction terms according to Homb et al. [14]

## Calculation of apparent weighted sound reduction index

### Typical office building, Class I partitions

### Flanking path 2: concrete inner envelope of exterior wall (truncated)

Formulas used in the prediction model:

$$\boxed{F_n = R_{fn} + K_{ij} + 10\log\left(\frac{S_{sn}}{S_{rn}}\right)}$$

$$\boxed{R_w^{'} = R_w - 10\log\left[1 + \left(\frac{1}{S}\right)\sum_{n=1}^{4}\left(S_{sn}\cdot 10^{(R_{w,0}-F_n)/10}\right)\right]}$$

Schematic illustration of flanking paths:

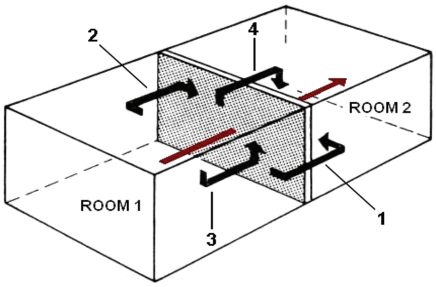


#### Partition separating adjacent rooms: Class I partition

| | | | |
|---|---|---|---|
| Weighted SRI of separating partition | $R_w$ = | 61 | dB |
| Area of the separating partition | $S$ = | 7,5 | $m^2$ |

#### Flanking path I: Class I corridor partition

| | | | |
|---|---|---|---|
| Weighted SRI of flanking structure 1 | $R_{w1}$ = | 46 | dB |
| Correction term *) | | -5 | dB |
| Corrected SRI of flanking structure 1 | $R_{f1}$ = | 41 | dB |
| Vibration reduction index of junction | $K_{ij\_1}$ = | 25 | dB |
| Area of flanking structure 1 in the source room | $S_{s1}$ = | 6,8 | $m^2$ |
| Area of flanking structure 1 in the receiving room | $S_{r1}$ = | 6,8 | $m^2$ |

$$10\log\left(\frac{S_{s1}}{S_{r1}}\right) = 0 \text{ dB}$$

$$F_1 = R_{f1} + K_{ij\_1} + 10\log\left(\frac{S_{s1}}{S_{r1}}\right) = 66 \text{ dB}$$

$$C_1 = \frac{1}{S}\cdot S_{s1}\cdot 10^{(R_w - F_1)/10} = 0{,}29$$

#### Flanking path 2: concrete inner envelope of exterior wall (truncated)

| | | | |
|---|---|---|---|
| Weighted SRI of flanking structure 2 | $R_{w2}$ = | 44 | dB |
| Correction term *) | | 0 | dB |
| Corrected SRI of flanking structure 2 | $R_{f2}$ = | 44 | dB |
| Vibration reduction index of junction | $K_{ij\_2}$ = | 15 | dB |
| Area of flanking structure 2 in the source room | $S_{s2}$ = | 6,8 | $m^2$ |
| Area of flanking structure 2 in the receiving room | $S_{r2}$ = | 6,8 | $m^2$ |

$$10\log\left(\frac{S_{s2}}{S_{r2}}\right) = 0 \text{ dB}$$

$$F_2 = R_{f2} + K_{ij\_2} + 10\log\left(\frac{S_{s2}}{S_{r2}}\right) = 59 \text{ dB}$$

$$C_2 = \frac{1}{S}\cdot S_{s2}\cdot 10^{(R_w - F_2)/10} = 1{,}44$$

#### Flanking path 3: base- / intermediate floor (e.g. hollow core slab ≥ 265 mm / 380 kg/$m^2$)

| | | | |
|---|---|---|---|
| Weighted SRI of flanking structure 3 | $R_{w3}$ = | 61 | dB |
| Correction term *) | | 0 | dB |
| Corrected SRI of flanking structure 3 | $R_{f3}$ = | 61 | dB |
| Vibration reduction index of junction | $K_{ij\_3}$ = | 0 | dB |
| Area of flanking structure 3 in the source room | $S_{s3}$ = | 6,2 | $m^2$ |
| Area of flanking structure 3 in the receiving room | $S_{r3}$ = | 6,2 | $m^2$ |

$$10\log\left(\frac{S_{s3}}{S_{r3}}\right) = 0 \text{ dB}$$

$$F_3 = R_{f3} + K_{ij\_3} + 10\log\left(\frac{S_{s3}}{S_{r3}}\right) = 61 \text{ dB}$$

$$C_3 = \frac{1}{S}\cdot S_{s3}\cdot 10^{(R_w - F_3)/10} = 0{,}83$$

#### Flanking path 4: roof / intermediate floor (e.g. hollow core slab ≥ 265 mm / 380 kg/$m^2$)

| | | | |
|---|---|---|---|
| Weighted SRI of flanking structure 4 | $R_{w4}$ = | 61 | dB |
| Correction term *) | | 0 | dB |
| Corrected SRI of flanking structure 4 | $R_{f4}$ = | 61 | dB |
| Vibration reduction index of junction | $K_{ij\_4}$ = | 0 | dB |
| Area of flanking structure 4 in the source room | $S_{s4}$ = | 6,2 | $m^2$ |
| Area of flanking structure 4 in the receiving room | $S_{r4}$ = | 6,2 | $m^2$ |

$$10\log\left(\frac{S_{s4}}{S_{r4}}\right) = 0 \text{ dB}$$

$$F_4 = R_{f4} + K_{ij\_4} + 10\log\left(\frac{S_{s4}}{S_{r4}}\right) = 61 \text{ dB}$$

$$C_4 = \frac{1}{S}\cdot S_{s4}\cdot 10^{(R_w - F_4)/10} = 0{,}83$$

### Apparent weighted sound reduction index

Apparent SRI from room 1 to room 2 $R_w^{'} = R_w - 10\log\left(C_1 + C_2 + C_3 + C_4 + 1\right) =$ **55 dB**

*) Correction terms according to Homb et al. [14]

## Calculation of apparent weighted sound reduction index

### Typical office building, Class I partitions

### Flanking path 2: panel facing installed over masonry exterior wall structure

Formulas used in the prediction model:

$$F_n = R_{fn} + K_{ij} + 10\log\left(\frac{S_{sn}}{S_{rn}}\right)$$

$$R'_w = R_w - 10\log\left[1+\left(\frac{1}{S}\right)\sum_{n=1}^{4}\left(S_{sn}\cdot 10^{(R_{w,0}-F_n)/10}\right)\right]$$

Schematic illustration of flanking paths:

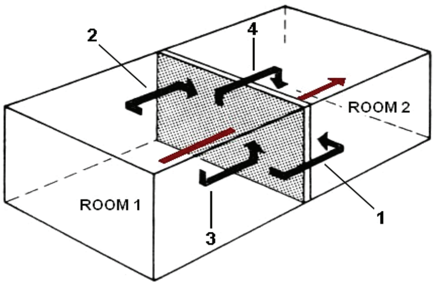


### Partition separating adjacent rooms: Class I partition

| | | | |
|---|---|---|---|
| Weighted SRI of separating partition | $R_w$ = | 61 | dB |
| Area of the separating partition | $S$ = | 7,5 | $m^2$ |

### Flanking path 1: Class I corridor partition

| | | | |
|---|---|---|---|
| Weighted SRI of flanking structure 1 | $R_{w1}$ = | 46 | dB |
| Correction term *) | | -5 | dB |
| Corrected SRI of flanking structure 1 | $R_{f1}$ = | 41 | dB |
| Vibration reduction index of junction | $K_{ij\_1}$ = | 25 | dB |
| Area of flanking structure 1 in the source room | $S_{s1}$ = | 6,8 | $m^2$ |
| Area of flanking structure 1 in the receiving room | $S_{r1}$ = | 6,8 | $m^2$ |

$$10\log\left(\frac{S_{s1}}{S_{r1}}\right) = 0 \text{ dB}$$

$$F_1 = R_{f1} + K_{ij\_1} + 10\log\left(\frac{S_{s1}}{S_{r1}}\right) = 66 \text{ dB}$$

$$C_1 = \frac{1}{S}\cdot S_{s1}\cdot 10^{(R_w - F_1)/10} = 0{,}29$$

### Flanking path 2: panel facing over masonry ext. wall structure (continuous panel truncated)

| | | | |
|---|---|---|---|
| Weighted SRI of flanking structure 2 | $R_{w2}$ = | 24 | dB |
| Correction term *) | | 10 | dB |
| Corrected SRI of flanking structure 2 | $R_{f2}$ = | 34 | dB |
| Vibration reduction index of junction | $K_{ij\_2}$ = | 25 | dB |
| Area of flanking structure 2 in the source room | $S_{s2}$ = | 6,8 | $m^2$ |
| Area of flanking structure 2 in the receiving room | $S_{r2}$ = | 6,8 | $m^2$ |

$$10\log\left(\frac{S_{s2}}{S_{r2}}\right) = 0 \text{ dB}$$

$$F_2 = R_{f2} + K_{ij\_2} + 10\log\left(\frac{S_{s2}}{S_{r2}}\right) = 59 \text{ dB}$$

$$C_2 = \frac{1}{S}\cdot S_{s2}\cdot 10^{(R_w - F_2)/10} = 1{,}44$$

### Flanking path 3: base- / intermediate floor (e.g. hollow core slab ≥ 265 mm / 380 kg/m²)

| | | | |
|---|---|---|---|
| Weighted SRI of flanking structure 3 | $R_{w3}$ = | 61 | dB |
| Correction term *) | | 0 | dB |
| Corrected SRI of flanking structure 3 | $R_{f3}$ = | 61 | dB |
| Vibration reduction index of junction | $K_{ij\_3}$ = | 0 | dB |
| Area of flanking structure 3 in the source room | $S_{s3}$ = | 6,2 | $m^2$ |
| Area of flanking structure 3 in the receiving room | $S_{r3}$ = | 6,2 | $m^2$ |

$$10\log\left(\frac{S_{s3}}{S_{r3}}\right) = 0 \text{ dB}$$

$$F_3 = R_{f3} + K_{ij\_3} + 10\log\left(\frac{S_{s3}}{S_{r3}}\right) = 61 \text{ dB}$$

$$C_3 = \frac{1}{S}\cdot S_{s3}\cdot 10^{(R_w - F_3)/10} = 0{,}83$$

### Flanking path 4: roof / intermediate floor (e.g. hollow core slab ≥ 265 mm / 380 kg/m²)

| | | | |
|---|---|---|---|
| Weighted SRI of flanking structure 4 | $R_{w4}$ = | 61 | dB |
| Correction term *) | | 0 | dB |
| Corrected SRI of flanking structure 4 | $R_{f4}$ = | 61 | dB |
| Vibration reduction index of junction | $K_{ij\_4}$ = | 0 | dB |
| Area of flanking structure 4 in the source room | $S_{s4}$ = | 6,2 | $m^2$ |
| Area of flanking structure 4 in the receiving room | $S_{r4}$ = | 6,2 | $m^2$ |

$$10\log\left(\frac{S_{s4}}{S_{r4}}\right) = 0 \text{ dB}$$

$$F_4 = R_{f4} + K_{ij\_4} + 10\log\left(\frac{S_{s4}}{S_{r4}}\right) = 61 \text{ dB}$$

$$C_4 = \frac{1}{S}\cdot S_{s4}\cdot 10^{(R_w - F_4)/10} = 0{,}83$$

## Apparent weighted sound reduction index

Apparent SRI from room 1 to room 2

$$R'_w = R_w - 10\log\left(C_1 + C_2 + C_3 + C_4 + 1\right) = \mathbf{55\ dB}$$

*) Correction terms according to Homb et al. [14]

## Calculation of apparent weighted sound reduction index

### Typical office building, Class I partitions

### Flanking path 2: lightweight plate structure of exterior wall (truncated)

Formulas used in the prediction model:

$$F_n = R_{fn} + K_{ij} + 10\log\left(\frac{S_{sn}}{S_{rn}}\right)$$

$$R'_w = R_w - 10\log\left[1+\left(\frac{1}{S}\right)\sum_{n=1}^{4}\left(S_{sn}\cdot 10^{(R_{w,0}-F_n)/10}\right)\right]$$

Schematic illustration of flanking paths:

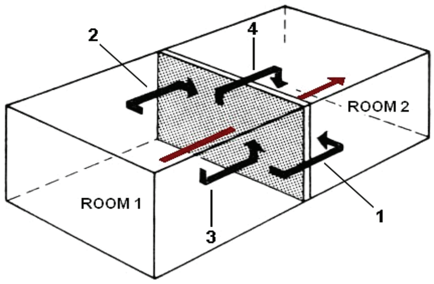


### Partition separating adjacent rooms: Class I partition

| | | | |
|---|---|---|---|
| Weighted SRI of separating partition | $R_w$ = | 61 | dB |
| Area of the separating partition | $S$ = | 7,5 | m$^2$ |

### Flanking path I: Class I corridor partition

| | | | |
|---|---|---|---|
| Weighted SRI of flanking structure 1 | $R_{w1}$ = | 46 | dB |
| Correction term *) | | -5 | dB |
| Corrected SRI of flanking structure 1 | $R_{f1}$ = | 41 | dB |
| Vibration reduction index of junction | $K_{ij\_1}$ = | 25 | dB |
| Area of flanking structure 1 in the source room | $S_{s1}$ = | 6,8 | m$^2$ |
| Area of flanking structure 1 in the receiving room | $S_{r1}$ = | 6,8 | m$^2$ |

$$10\ \log\left(\frac{S_{s1}}{S_{r1}}\right) = 0 \text{ dB}$$

$$F_1 = R_{f1} + K_{ij\_1} + 10\log\left(\frac{S_{s1}}{S_{r1}}\right) = 66 \text{ dB}$$

$$C_1 = \frac{1}{S}\cdot S_{s1}\cdot 10^{(R_w - F_1)/10} = 0{,}29$$

### Flanking path 2: lightweight exterior wall structure (truncated)

| | | | |
|---|---|---|---|
| Weighted SRI of flanking structure 2 | $R_{w2}$ = | 49 | dB |
| Correction term *) | | -5 | dB |
| Corrected SRI of flanking structure 2 | $R_{f2}$ = | 44 | dB |
| Vibration reduction index of junction | $K_{ij\_2}$ = | 15 | dB |
| Area of flanking structure 2 in the source room | $S_{s2}$ = | 6,8 | m$^2$ |
| Area of flanking structure 2 in the receiving room | $S_{r2}$ = | 6,8 | m$^2$ |

$$10\ \log\left(\frac{S_{s2}}{S_{r2}}\right) = 0 \text{ dB}$$

$$F_2 = R_{f2} + K_{ij\_2} + 10\log\left(\frac{S_{s2}}{S_{r2}}\right) = 59 \text{ dB}$$

$$C_2 = \frac{1}{S}\cdot S_{s2}\cdot 10^{(R_w - F_2)/10} = 1{,}44$$

### Flanking path 3: base- / intermediate floor (e.g. hollow core slab ≥ 265 mm / 380 kg/m$^2$)

| | | | |
|---|---|---|---|
| Weighted SRI of flanking structure 3 | $R_{w3}$ = | 61 | dB |
| Correction term *) | | 0 | dB |
| Corrected SRI of flanking structure 3 | $R_{f3}$ = | 61 | dB |
| Vibration reduction index of junction | $K_{ij\_3}$ = | 0 | dB |
| Area of flanking structure 3 in the source room | $S_{s3}$ = | 6,2 | m$^2$ |
| Area of flanking structure 3 in the receiving room | $S_{r3}$ = | 6,2 | m$^2$ |

$$10\ \log\left(\frac{S_{s3}}{S_{r3}}\right) = 0 \text{ dB}$$

$$F_3 = R_{f3} + K_{ij\_3} + 10\log\left(\frac{S_{s3}}{S_{r3}}\right) = 61 \text{ dB}$$

$$C_3 = \frac{1}{S}\cdot S_{s3}\cdot 10^{(R_w - F_3)/10} = 0{,}83$$

### Flanking path 4: roof / intermediate floor (e.g. hollow core slab ≥ 265 mm / 380 kg/m$^2$)

| | | | |
|---|---|---|---|
| Weighted SRI of flanking structure 4 | $R_{w4}$ = | 61 | dB |
| Correction term *) | | 0 | dB |
| Corrected SRI of flanking structure 4 | $R_{f4}$ = | 61 | dB |
| Vibration reduction index of junction | $K_{ij\_4}$ = | 0 | dB |
| Area of flanking structure 4 in the source room | $S_{s4}$ = | 6,2 | m$^2$ |
| Area of flanking structure 4 in the receiving room | $S_{r4}$ = | 6,2 | m$^2$ |

$$10\ \log\left(\frac{S_{s4}}{S_{r4}}\right) = 0 \text{ dB}$$

$$F_4 = R_{f4} + K_{ij\_4} + 10\log\left(\frac{S_{s4}}{S_{r4}}\right) = 61 \text{ dB}$$

$$C_4 = \frac{1}{S}\cdot S_{s4}\cdot 10^{(R_w - F_4)/10} = 0{,}83$$

## Apparent weighted sound reduction index

Apparent SRI from room 1 to room 2 $\quad R'_w = R_w - 10\log\left(C_1 + C_2 + C_3 + C_4 + 1\right) =$ **55 dB**

*) Correction terms according to Homb et al. [14]

## Calculation of apparent weighted sound reduction index

### Typical office building, Class 2 partitions

### Flanking path 2: concrete inner envelope of exterior wall (continuous)

Formulas used in the prediction model:

$$F_n = R_{fn} + K_{ij} + 10\log\left(\frac{S_{sn}}{S_{rn}}\right)$$

$$R'_w = R_w - 10\log\left[1 + \left(\frac{1}{S}\right)\sum_{n=1}^{4}\left(S_{sn}\cdot 10^{(R_{w,0}-F_n)/10}\right)\right]$$

Schematic illustration of flanking paths:

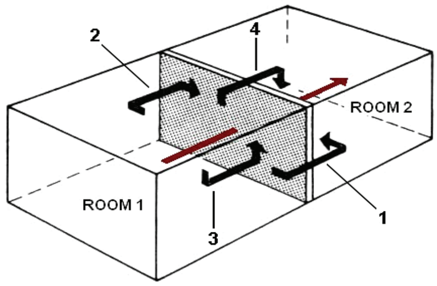


### Partition separating adjacent rooms: Class 2 partition

| | | | |
|---|---|---|---|
| Weighted SRI of separating partition | $R_w$ = | 53 | dB |
| Area of the separating partition | $S$ = | 7,5 | $m^2$ |

### Flanking path 1: Class 2/3 corridor partition

| | | | |
|---|---|---|---|
| Weighted SRI of flanking structure 1 | $R_{w1}$ = | 41 | dB |
| Correction term *) | | -5 | dB |
| Corrected SRI of flanking structure 1 | $R_{f1}$ = | 36 | dB |
| Vibration reduction index of junction | $K_{ij\_1}$ = | 25 | dB |
| Area of flanking structure 1 in the source room | $S_{s1}$ = | 6,8 | $m^2$ |
| Area of flanking structure 1 in the receiving room | $S_{r1}$ = | 6,8 | $m^2$ |

$$10\ \log\left(\frac{S_{s1}}{S_{r1}}\right) = 0 \text{ dB}$$

$$F_1 = R_{f1} + K_{ij\_1} + 10\log\left(\frac{S_{s1}}{S_{r1}}\right) = 61 \text{ dB}$$

$$C_1 = \frac{1}{S}\cdot S_{s1}\cdot 10^{(R_w-F_1)/10} = 0{,}14$$

### Flanking path 2: concrete inner envelope of exterior wall (continuous)

| | | | |
|---|---|---|---|
| Weighted SRI of flanking structure 2 | $R_{w2}$ = | 46 | dB |
| Correction term *) | | 0 | dB |
| Corrected SRI of flanking structure 2 | $R_{f2}$ = | 46 | dB |
| Vibration reduction index of junction | $K_{ij\_2}$ = | 0 | dB |
| Area of flanking structure 2 in the source room | $S_{s2}$ = | 6,8 | $m^2$ |
| Area of flanking structure 2 in the receiving room | $S_{r2}$ = | 6,8 | $m^2$ |

$$10\ \log\left(\frac{S_{s2}}{S_{r2}}\right) = 0 \text{ dB}$$

$$F_2 = R_{f2} + K_{ij\_2} + 10\log\left(\frac{S_{s2}}{S_{r2}}\right) = 46 \text{ dB}$$

$$C_2 = \frac{1}{S}\cdot S_{s2}\cdot 10^{(R_w-F_2)/10} = 4{,}54$$

### Flanking path 3: base- / intermediate floor (e.g. hollow core slab ≥ 265 mm / 380 kg/$m^2$)

| | | | |
|---|---|---|---|
| Weighted SRI of flanking structure 3 | $R_{w3}$ = | 61 | dB |
| Correction term *) | | 0 | dB |
| Corrected SRI of flanking structure 3 | $R_{f3}$ = | 61 | dB |
| Vibration reduction index of junction | $K_{ij\_3}$ = | 0 | dB |
| Area of flanking structure 3 in the source room | $S_{s3}$ = | 6,2 | $m^2$ |
| Area of flanking structure 3 in the receiving room | $S_{r3}$ = | 6,2 | $m^2$ |

$$10\ \log\left(\frac{S_{s3}}{S_{r3}}\right) = 0 \text{ dB}$$

$$F_3 = R_{f3} + K_{ij\_3} + 10\log\left(\frac{S_{s3}}{S_{r3}}\right) = 61 \text{ dB}$$

$$C_3 = \frac{1}{S}\cdot S_{s3}\cdot 10^{(R_w-F_3)/10} = 0{,}13$$

### Flanking path 4: roof / intermediate floor (e.g. hollow core slab ≥ 265 mm / 380 kg/$m^2$)

| | | | |
|---|---|---|---|
| Weighted SRI of flanking structure 4 | $R_{w4}$ = | 61 | dB |
| Correction term *) | | 0 | dB |
| Corrected SRI of flanking structure 4 | $R_{f4}$ = | 61 | dB |
| Vibration reduction index of junction | $K_{ij\_4}$ = | 0 | dB |
| Area of flanking structure 4 in the source room | $S_{s4}$ = | 6,2 | $m^2$ |
| Area of flanking structure 4 in the receiving room | $S_{r4}$ = | 6,2 | $m^2$ |

$$10\ \log\left(\frac{S_{s4}}{S_{r4}}\right) = 0 \text{ dB}$$

$$F_4 = R_{f4} + K_{ij\_4} + 10\log\left(\frac{S_{s4}}{S_{r4}}\right) = 61 \text{ dB}$$

$$C_4 = \frac{1}{S}\cdot S_{s4}\cdot 10^{(R_w-F_4)/10} = 0{,}13$$

## Apparent weighted sound reduction index

Apparent SRI from room 1 to room 2

$$R'_w = R_w - 10\log\left(C_1 + C_2 + C_3 + C_4 + 1\right) = \mathbf{45\ dB}$$

*) Correction terms according to Homb et al. [14]

## Calculation of apparent weighted sound reduction index

### Typical office space, Class 2 partitions

### Flanking path 2: lightweight plate structure of exterior wall (truncated)

Formulas used in the prediction model:

$$F_n = R_{fn} + K_{ij} + 10\log\left(\frac{S_{sn}}{S_{rn}}\right)$$

$$R'_w = R_w - 10\log\left[1+\left(\frac{1}{S}\right)\sum_{n=1}^{4}\left(S_{sn}\cdot 10^{(R_{w,0}-F_n)/10}\right)\right]$$

Schematic illustration of flanking paths:

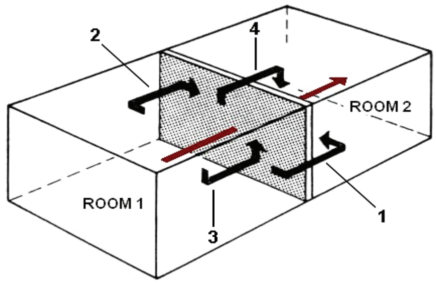


### Partition separating adjacent rooms: Class 2 partition

| | | | |
|---|---|---|---|
| Weighted SRI of separating partition | $R_w$ = | 53 | dB |
| Area of the separating partition | $S$ = | 7,5 | $m^2$ |

### Flanking path I: Class 2/3 corridor partition

| | | | |
|---|---|---|---|
| Weighted SRI of flanking structure 1 | $R_{w1}$ = | 41 | dB |
| Correction term *) | | -5 | dB |
| Corrected SRI of flanking structure 1 | $R_{f1}$ = | 36 | dB |
| Vibration reduction index of junction | $K_{ij\_1}$ = | 25 | dB |
| Area of flanking structure 1 in the source room | $S_{s1}$ = | 6,8 | $m^2$ |
| Area of flanking structure 1 in the receiving room | $S_{r1}$ = | 6,8 | $m^2$ |

$$10\log\left(\frac{S_{s1}}{S_{r1}}\right) = 0 \text{ dB}$$

$$F_1 = R_{f1} + K_{ij\_1} + 10\log\left(\frac{S_{s1}}{S_{r1}}\right) = 61 \text{ dB}$$

$$C_1 = \frac{1}{S}\cdot S_{s1}\cdot 10^{(R_w-F_1)/10} = 0{,}14$$

### Flanking path 2: lightweight exterior wall structure (truncated)

| | | | |
|---|---|---|---|
| Weighted SRI of flanking structure 2 | $R_{w2}$ = | 36 | dB |
| Correction term *) | | -5 | dB |
| Corrected SRI of flanking structure 2 | $R_{f2}$ = | 31 | dB |
| Vibration reduction index of junction | $K_{ij\_2}$ = | 15 | dB |
| Area of flanking structure 2 in the source room | $S_{s2}$ = | 6,8 | $m^2$ |
| Area of flanking structure 2 in the receiving room | $S_{r2}$ = | 6,8 | $m^2$ |

$$10\log\left(\frac{S_{s2}}{S_{r2}}\right) = 0 \text{ dB}$$

$$F_2 = R_{f2} + K_{ij\_2} + 10\log\left(\frac{S_{s2}}{S_{r2}}\right) = 46 \text{ dB}$$

$$C_2 = \frac{1}{S}\cdot S_{s2}\cdot 10^{(R_w-F_2)/10} = 4{,}54$$

### Flanking path 3: base- / intermediate floor (e.g. hollow core slab ≥ 265 mm / 380 kg/$m^2$)

| | | | |
|---|---|---|---|
| Weighted SRI of flanking structure 3 | $R_{w3}$ = | 61 | dB |
| Correction term *) | | 0 | dB |
| Corrected SRI of flanking structure 3 | $R_{f3}$ = | 61 | dB |
| Vibration reduction index of junction | $K_{ij\_3}$ = | 0 | dB |
| Area of flanking structure 3 in the source room | $S_{s3}$ = | 6,2 | $m^2$ |
| Area of flanking structure 3 in the receiving room | $S_{r3}$ = | 6,2 | $m^2$ |

$$10\log\left(\frac{S_{s3}}{S_{r3}}\right) = 0 \text{ dB}$$

$$F_3 = R_{f3} + K_{ij\_3} + 10\log\left(\frac{S_{s3}}{S_{r3}}\right) = 61 \text{ dB}$$

$$C_3 = \frac{1}{S}\cdot S_{s3}\cdot 10^{(R_w-F_3)/10} = 0{,}13$$

### Flanking path 4: roof / intermediate floor (e.g. hollow core slab ≥ 265 mm / 380 kg/$m^2$)

| | | | |
|---|---|---|---|
| Weighted SRI of flanking structure 4 | $R_{w4}$ = | 61 | dB |
| Correction term *) | | 0 | dB |
| Corrected SRI of flanking structure 4 | $R_{f4}$ = | 61 | dB |
| Vibration reduction index of junction | $K_{ij\_4}$ = | 0 | dB |
| Area of flanking structure 4 in the source room | $S_{s4}$ = | 6,2 | $m^2$ |
| Area of flanking structure 4 in the receiving room | $S_{r4}$ = | 6,2 | $m^2$ |

$$10\log\left(\frac{S_{s4}}{S_{r4}}\right) = 0 \text{ dB}$$

$$F_4 = R_{f4} + K_{ij\_4} + 10\log\left(\frac{S_{s4}}{S_{r4}}\right) = 61 \text{ dB}$$

$$C_4 = \frac{1}{S}\cdot S_{s4}\cdot 10^{(R_w-F_4)/10} = 0{,}13$$

## Apparent weighted sound reduction index

Apparent SRI from room 1 to room 2 $\quad R'_w = R_w - 10\log\left(C_1 + C_2 + C_3 + C_4 + 1\right) =$ **45 dB**

*) Correction terms according to Homb et al. [14]

## Calculation of apparent weighted sound reduction index

### Typical office building, Class 3 partitions

### Flanking path 2: concrete inner envelope of exterior wall (continuous)

Formulas used in the prediction model:

$$\boxed{F_n = R_{fn} + K_{ij} + 10\log\left(\frac{S_{sn}}{S_{rn}}\right)}$$

$$\boxed{R_w^{`} = R_w - 10\log\left[1+\left(\frac{1}{S}\right)\sum_{n=1}^{4}\left(S_{sn}\cdot 10^{(R_{w,0}-F_n)/10}\right)\right]}$$

Schematic illustration of flanking paths:

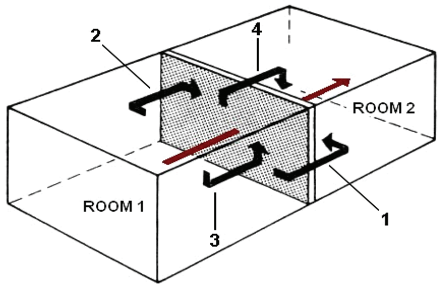


### Partition separating adjacent rooms: Class 3 partition

| | | | |
|---|---|---|---|
| Weighted SRI of separating partition | $R_w$ = | 41 | dB |
| Area of the separating partition | $S$ = | 7,5 | $m^2$ |

### Flanking path 1: Class 3 corridor partition

| | | | |
|---|---|---|---|
| Weighted SRI of flanking structure 1 | $R_{w1}$ = | 41 | dB |
| Correction term *) | | -5 | dB |
| Corrected SRI of flanking structure 1 | $R_{f1}$ = | 36 | dB |
| Vibration reduction index of junction | $K_{ij\_1}$ = | 25 | dB |
| Area of flanking structure 1 in the source room | $S_{s1}$ = | 6,8 | $m^2$ |
| Area of flanking structure 1 in the receiving room | $S_{r1}$ = | 6,8 | $m^2$ |

$$10\log\left(\frac{S_{s1}}{S_{r1}}\right) = 0 \text{ dB}$$

$$F_1 = R_{f1} + K_{ij\_1} + 10\log\left(\frac{S_{s1}}{S_{r1}}\right) = 61 \text{ dB}$$

$$C_1 = \frac{1}{S}\cdot S_{s1}\cdot 10^{(R_w-F_1)/10} = 0{,}01$$

### Flanking path 2: concrete inner envelope of exterior wall (continuous)

| | | | |
|---|---|---|---|
| Weighted SRI of flanking structure 2 | $R_{w2}$ = | 36 | dB |
| Correction term *) | | 0 | dB |
| Corrected SRI of flanking structure 2 | $R_{f2}$ = | 36 | dB |
| Vibration reduction index of junction | $K_{ij\_2}$ = | 0 | dB |
| Area of flanking structure 2 in the source room | $S_{s2}$ = | 6,8 | $m^2$ |
| Area of flanking structure 2 in the receiving room | $S_{r2}$ = | 6,8 | $m^2$ |

$$10\log\left(\frac{S_{s2}}{S_{r2}}\right) = 0 \text{ dB}$$

$$F_2 = R_{f2} + K_{ij\_2} + 10\log\left(\frac{S_{s2}}{S_{r2}}\right) = 36 \text{ dB}$$

$$C_2 = \frac{1}{S}\cdot S_{s2}\cdot 10^{(R_w-F_2)/10} = 2{,}87$$

### Flanking path 3: base- / intermediate floor (e.g. hollow core slab ≥ 265 mm / 380 kg/m²)

| | | | |
|---|---|---|---|
| Weighted SRI of flanking structure 3 | $R_{w3}$ = | 61 | dB |
| Correction term *) | | 0 | dB |
| Corrected SRI of flanking structure 3 | $R_{f3}$ = | 61 | dB |
| Vibration reduction index of junction | $K_{ij\_3}$ = | 0 | dB |
| Area of flanking structure 3 in the source room | $S_{s3}$ = | 6,2 | $m^2$ |
| Area of flanking structure 3 in the receiving room | $S_{r3}$ = | 6,2 | $m^2$ |

$$10\log\left(\frac{S_{s3}}{S_{r3}}\right) = 0 \text{ dB}$$

$$F_3 = R_{f3} + K_{ij\_3} + 10\log\left(\frac{S_{s3}}{S_{r3}}\right) = 61 \text{ dB}$$

$$C_3 = \frac{1}{S}\cdot S_{s3}\cdot 10^{(R_w-F_3)/10} = 0{,}01$$

### Flanking path 4: roof / intermediate floor (e.g. hollow core slab ≥ 265 mm / 380 kg/m²)

| | | | |
|---|---|---|---|
| Weighted SRI of flanking structure 4 | $R_{w4}$ = | 61 | dB |
| Correction term *) | | 0 | dB |
| Corrected SRI of flanking structure 4 | $R_{f4}$ = | 61 | dB |
| Vibration reduction index of junction | $K_{ij\_4}$ = | 0 | dB |
| Area of flanking structure 4 in the source room | $S_{s4}$ = | 6,2 | $m^2$ |
| Area of flanking structure 4 in the receiving room | $S_{r4}$ = | 6,2 | $m^2$ |

$$10\log\left(\frac{S_{s4}}{S_{r4}}\right) = 0 \text{ dB}$$

$$F_4 = R_{f4} + K_{ij\_4} + 10\log\left(\frac{S_{s4}}{S_{r4}}\right) = 61 \text{ dB}$$

$$C_4 = \frac{1}{S}\cdot S_{s4}\cdot 10^{(R_w-F_4)/10} = 0{,}01$$

## Apparent weighted sound reduction index

Apparent SRI from room 1 to room 2 $\quad R_w^{`} = R_w - 10\log\left(C_1 + C_2 + C_3 + C_4 + 1\right) =$ **35 dB**

*) Correction terms according to Homb et al. [14]

## Calculation of apparent weighted sound reduction index

### Typical office building, Class 3 partitions

### Flanking path 2: lightweight plate structure of exterior wall (truncated)

Formulas used in the prediction model:

$$F_n = R_{fn} + K_{ij} + 10\log\left(\frac{S_{sn}}{S_{rn}}\right)$$

$$R_w^{'} = R_w - 10\log\left[1 + \left(\frac{1}{S}\right)\sum_{n=1}^{4}\left(S_{sn} \cdot 10^{(R_{w,0}-F_n)/10}\right)\right]$$

Schematic illustration of flanking paths:

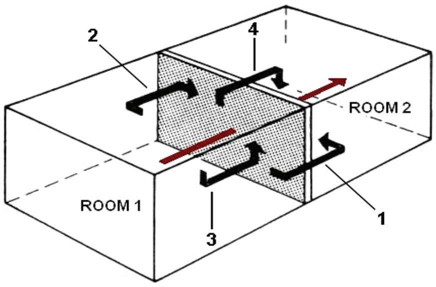


### Partition separating adjacent rooms: Class 3 partition

| | | | |
|---|---|---|---|
| Weighted SRI of separating partition | $R_w$ = | 41 | dB |
| Area of the separating partition | $S$ = | 7,5 | $m^2$ |

### Flanking path I: Class 2/3 corridor partition

| | | | |
|---|---|---|---|
| Weighted SRI of flanking structure 1 | $R_{w1}$ = | 41 | dB |
| Correction term *) | | -5 | dB |
| Corrected SRI of flanking structure 1 | $R_{f1}$ = | 36 | dB |
| Vibration reduction index of junction | $K_{ij\_1}$ = | 25 | dB |
| Area of flanking structure 1 in the source room | $S_{s1}$ = | 6,8 | $m^2$ |
| Area of flanking structure 1 in the receiving room | $S_{r1}$ = | 6,8 | $m^2$ |

$$10\log\left(\frac{S_{s1}}{S_{r1}}\right) = 0 \text{ dB}$$

$$F_1 = R_{f1} + K_{ij\_1} + 10\log\left(\frac{S_{s1}}{S_{r1}}\right) = 61 \text{ dB}$$

$$C_1 = \frac{1}{S} \cdot S_{s1} \cdot 10^{(R_w - F_1)/10} = 0{,}01$$

### Flanking path 2: lightweight exterior wall structure (truncated)

| | | | |
|---|---|---|---|
| Weighted SRI of flanking structure 2 | $R_{w2}$ = | 26 | dB |
| Correction term *) | | -5 | dB |
| Corrected SRI of flanking structure 2 | $R_{f2}$ = | 21 | dB |
| Vibration reduction index of junction | $K_{ij\_2}$ = | 15 | dB |
| Area of flanking structure 2 in the source room | $S_{s2}$ = | 6,8 | $m^2$ |
| Area of flanking structure 2 in the receiving room | $S_{r2}$ = | 6,8 | $m^2$ |

$$10\log\left(\frac{S_{s2}}{S_{r2}}\right) = 0 \text{ dB}$$

$$F_2 = R_{f2} + K_{ij\_2} + 10\log\left(\frac{S_{s2}}{S_{r2}}\right) = 36 \text{ dB}$$

$$C_2 = \frac{1}{S} \cdot S_{s2} \cdot 10^{(R_w - F_2)/10} = 2{,}87$$

### Flanking path 3: base- / intermediate floor (e.g. hollow core slab ≥ 265 mm / 380 kg/m²)

| | | | |
|---|---|---|---|
| Weighted SRI of flanking structure 3 | $R_{w3}$ = | 61 | dB |
| Correction term *) | | 0 | dB |
| Corrected SRI of flanking structure 3 | $R_{f3}$ = | 61 | dB |
| Vibration reduction index of junction | $K_{ij\_3}$ = | 0 | dB |
| Area of flanking structure 3 in the source room | $S_{s3}$ = | 6,2 | $m^2$ |
| Area of flanking structure 3 in the receiving room | $S_{r3}$ = | 6,2 | $m^2$ |

$$10\log\left(\frac{S_{s3}}{S_{r3}}\right) = 0 \text{ dB}$$

$$F_3 = R_{f3} + K_{ij\_3} + 10\log\left(\frac{S_{s3}}{S_{r3}}\right) = 61 \text{ dB}$$

$$C_3 = \frac{1}{S} \cdot S_{s3} \cdot 10^{(R_w - F_3)/10} = 0{,}01$$

### Flanking path 4: roof / intermediate floor (e.g. hollow core slab ≥ 265 mm / 380 kg/m²)

| | | | |
|---|---|---|---|
| Weighted SRI of flanking structure 4 | $R_{w4}$ = | 61 | dB |
| Correction term *) | | 0 | dB |
| Corrected SRI of flanking structure 4 | $R_{f4}$ = | 61 | dB |
| Vibration reduction index of junction | $K_{ij\_4}$ = | 0 | dB |
| Area of flanking structure 4 in the source room | $S_{s4}$ = | 6,2 | $m^2$ |
| Area of flanking structure 4 in the receiving room | $S_{r4}$ = | 6,2 | $m^2$ |

$$10\log\left(\frac{S_{s4}}{S_{r4}}\right) = 0 \text{ dB}$$

$$F_4 = R_{f4} + K_{ij\_4} + 10\log\left(\frac{S_{s4}}{S_{r4}}\right) = 61 \text{ dB}$$

$$C_4 = \frac{1}{S} \cdot S_{s4} \cdot 10^{(R_w - F_4)/10} = 0{,}01$$

## Apparent weighted sound reduction index

Apparent SRI from room 1 to room 2

$$R_w^{'} = R_w - 10\log\left(C_1 + C_2 + C_3 + C_4 + 1\right) = \mathbf{35 \text{ dB}}$$

*) Correction terms according to Homb et al. [14]

# APPENDIX F

## DRAWINGS OF NEW PARTITIONS

# Class I partition

Drawing I-I:
Section; sealing to intermediate floor / base floor / roof. Sealing to side walls accordingly.

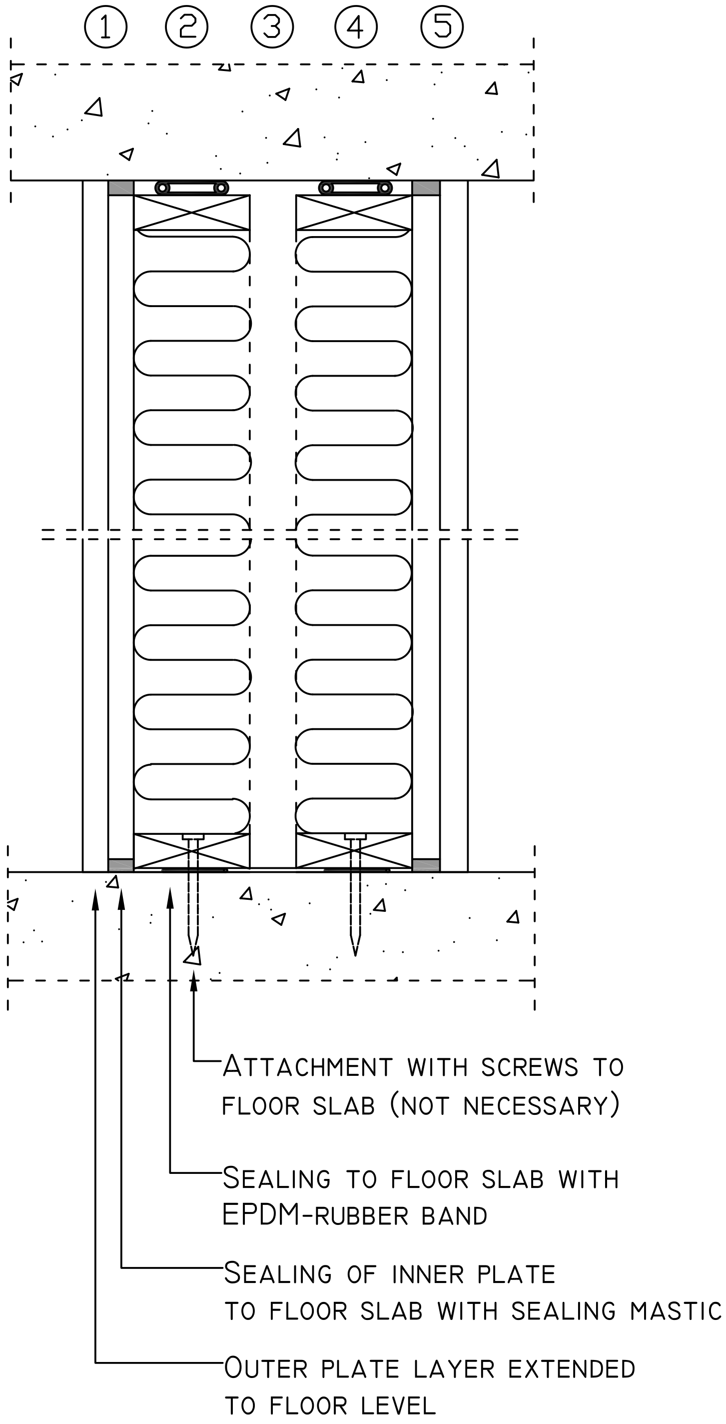


1. 2 x chipboard 11 mm (screw fastening)
2. Timber studding + mineral wool 50 mm
3. Air space 20 mm (empty, no connection between studs)
4. Timber studding + mineral wool 50 mm
5. 2 x Medium density fiberboard 12 mm (screw fastening)

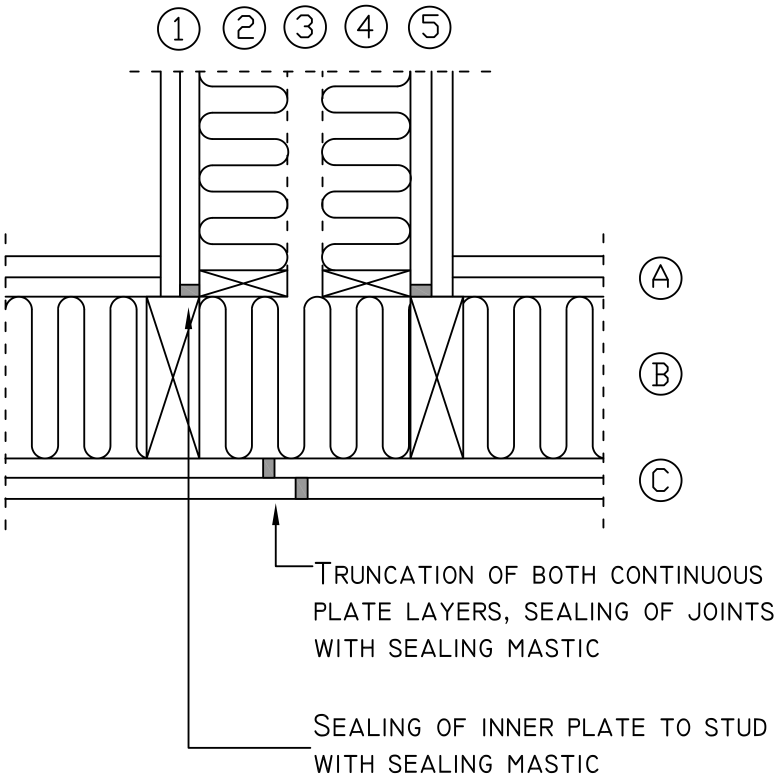


1. 2 x Chipboard 11 mm (screw fastening)
2. Timber studding + mineral wool 50 mm
3. Air space 20 mm (empty, no connection between studs)
4. Timber studding + mineral wool 50 mm
5. 2 x Medium density fiberboard 12 mm (screw fastening)

A. Chipboard 11 mm + MDF 12 mm (screw fastening)
B. Timber studding + mineral wool 92 mm (100% filling)
C. Chipboard 11 mm + MDF 12 mm (screw fastening)

# Class I partition

Drawing I-3:
Junction to exterior wall (principle). Alternative I: truncated lightweight structure.

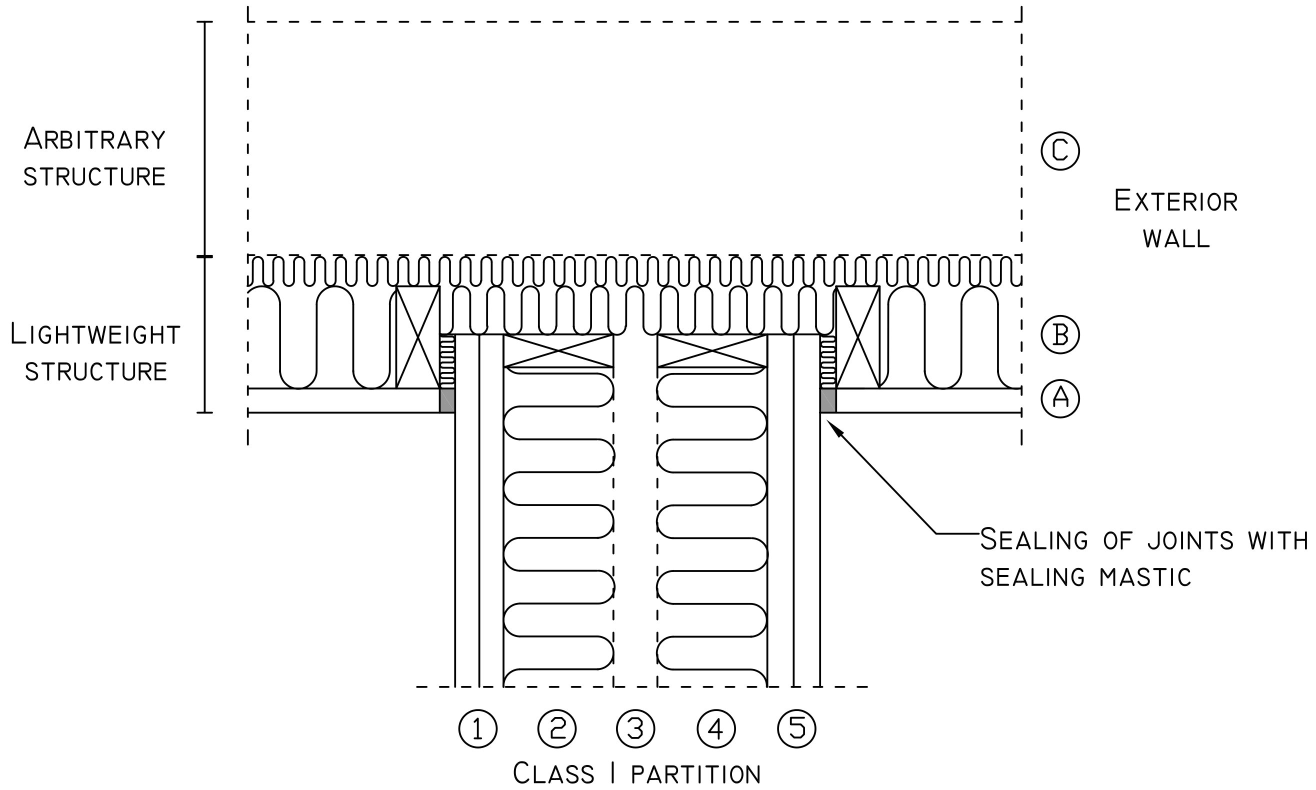


1. 2 x chipboard 11 mm (screw fastening)
2. Timber studding + mineral wool 50 mm
3. Air space 20 mm (empty, no connection between studs)
4. Timber studding + mineral wool 50 mm
5. 2 x medium density fiberboard 12 mm (screw fastening)

A. Arbitrary building board
B. Studding + mineral wool
C. Arbitrary structure

# Class I partition

**Drawing I-4:**
Junction to exterior wall (principle). Alternative 2: continuous concrete inner envelope.

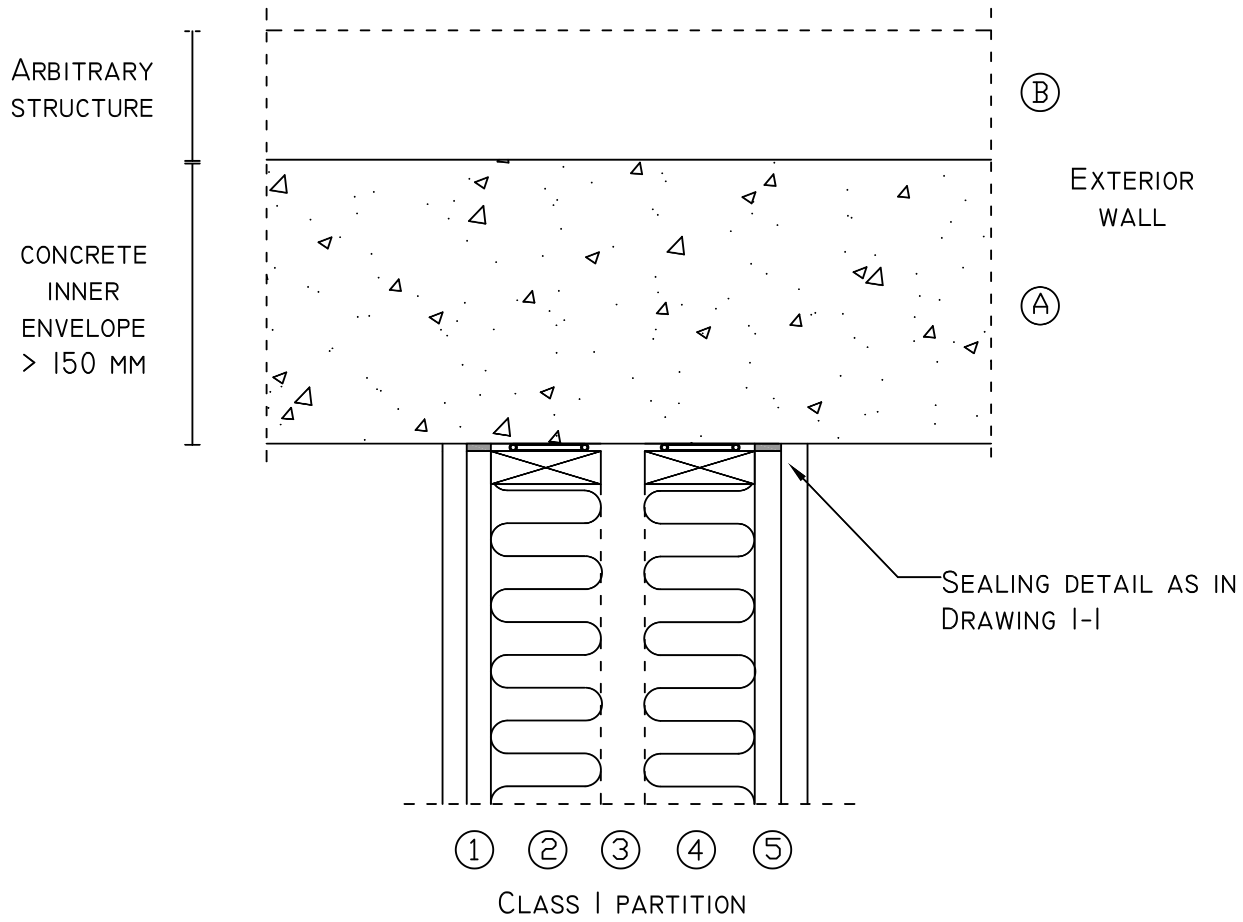


1. 2 x chipboard 11 mm (screw fastening)
2. Timber studding + mineral wool 50 mm
3. Air space 20 mm (empty, no connection between studs)
4. Timber studding + mineral wool 50 mm
5. 2 x medium density fiberboard 12 mm (screw fastening)

A. Massive concrete slab, thickness at least 150 mm
B. Arbitrary structure

# Class I partition

Drawing I-5:
Junction to exterior wall (principle). Alternative 3: panel facing installed against masonry structure.

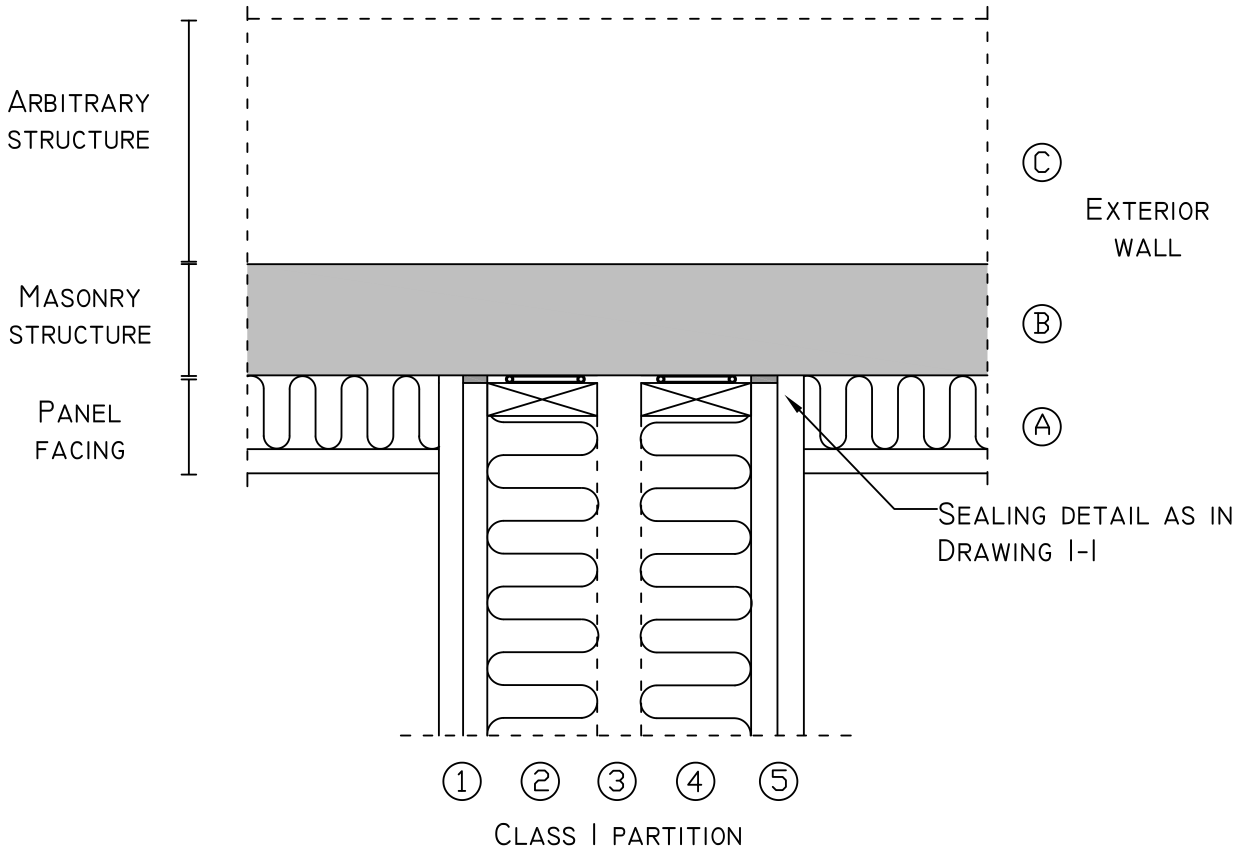


1. 2 x chipboard 11 mm (screw fastening)
2. Timber studding + mineral wool 50 mm
3. Air space 20 mm (empty, no connection between studs)
4. Timber studding + mineral wool 50 mm
5. 2 x medium density fiberboard 12 mm (screw fastening)

A. Panel facing: arbitrary building board over studding + mineral wool
B. Masonry structure: concrete or brick > 120 mm / lightweight concrete > 150 mm
C. Arbitrary structure

# Class I partition

Drawing I-6:
Junction to exterior wall (principle). Alternative 4: truncated concrete inner envelope.

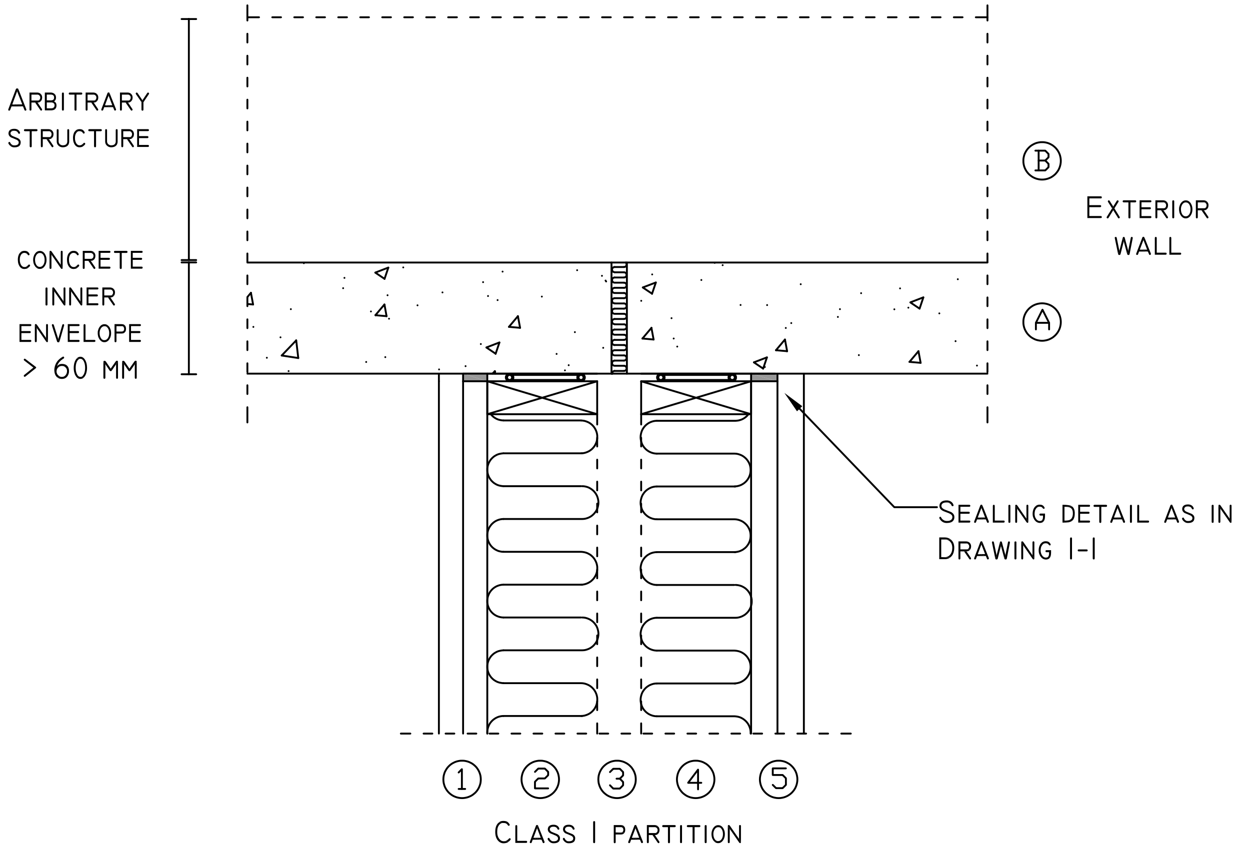


1. 2 x chipboard 11 mm (screw fastening)
2. Timber studding + mineral wool 50 mm
3. Air space 20 mm (empty, no connection between studs)
4. Timber studding + mineral wool 50 mm
5. 2 x medium density fiberboard 12 mm (screw fastening)

A. Massive concrete slab (truncated), thickness at least 60 mm
B. Arbitrary structure

# Class 2 partition

Drawing 2-1:
Section; sealing to intermediate floor / base floor / roof. Sealing to side walls accordingly.

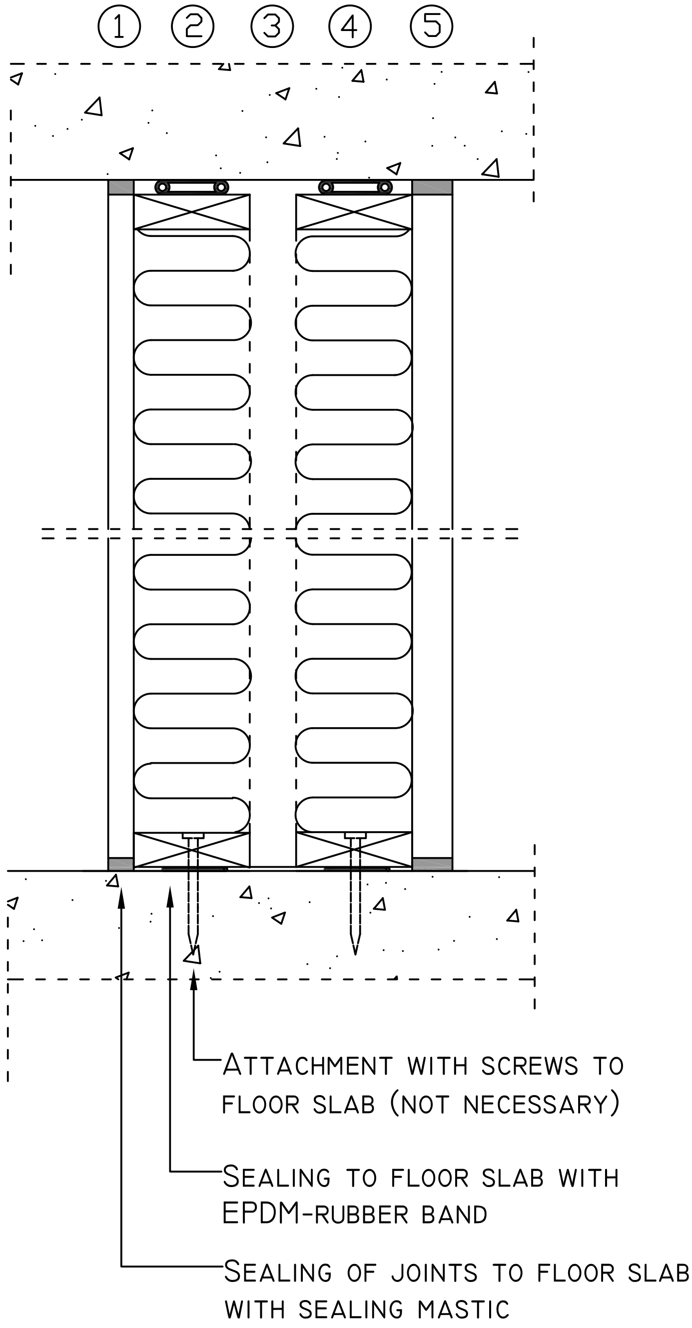


1. Chipboard 11 mm
2. Timber studding + mineral wool 50 mm
3. Air space 20 mm (empty, no connection between studs)
4. Timber studding + mineral wool 50 mm
5. Medium density fiberboard 19 mm

# Class 2 partition

Drawing 2-2:
T-junction between class 2 partition and lightweight side wall structure.

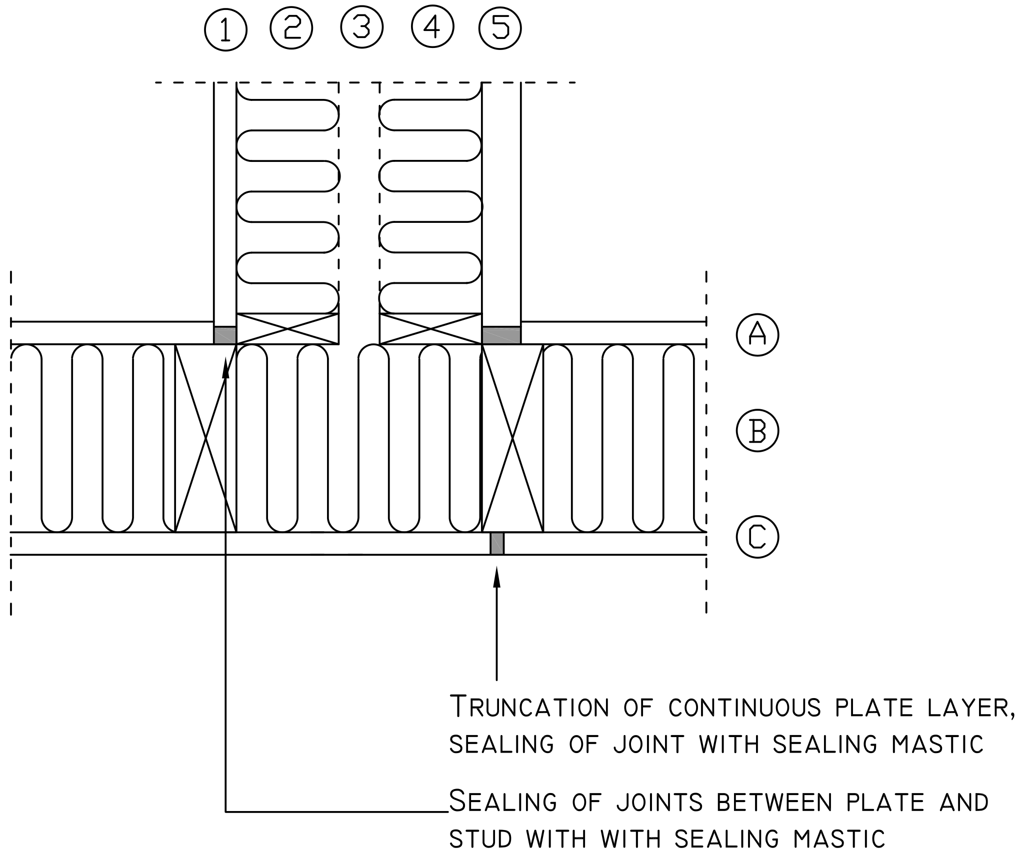


1. Chipboard 11 mm
2. Timber studding + mineral wool 50 mm
3. Air space 20 mm (empty no connection between studs)
4. Timber studding + mineral wool 50 mm
5. Medium density fiberboard 19 mm

A. Chipboard 11 mm
B. Timber studding + mineral wool 92 mm (100% filling)
C. Chipboard 11 mm

# Class 2 partition

Drawing 2-3:
Junction to exterior wall (principle). Alternative I: truncated lightweight structure.

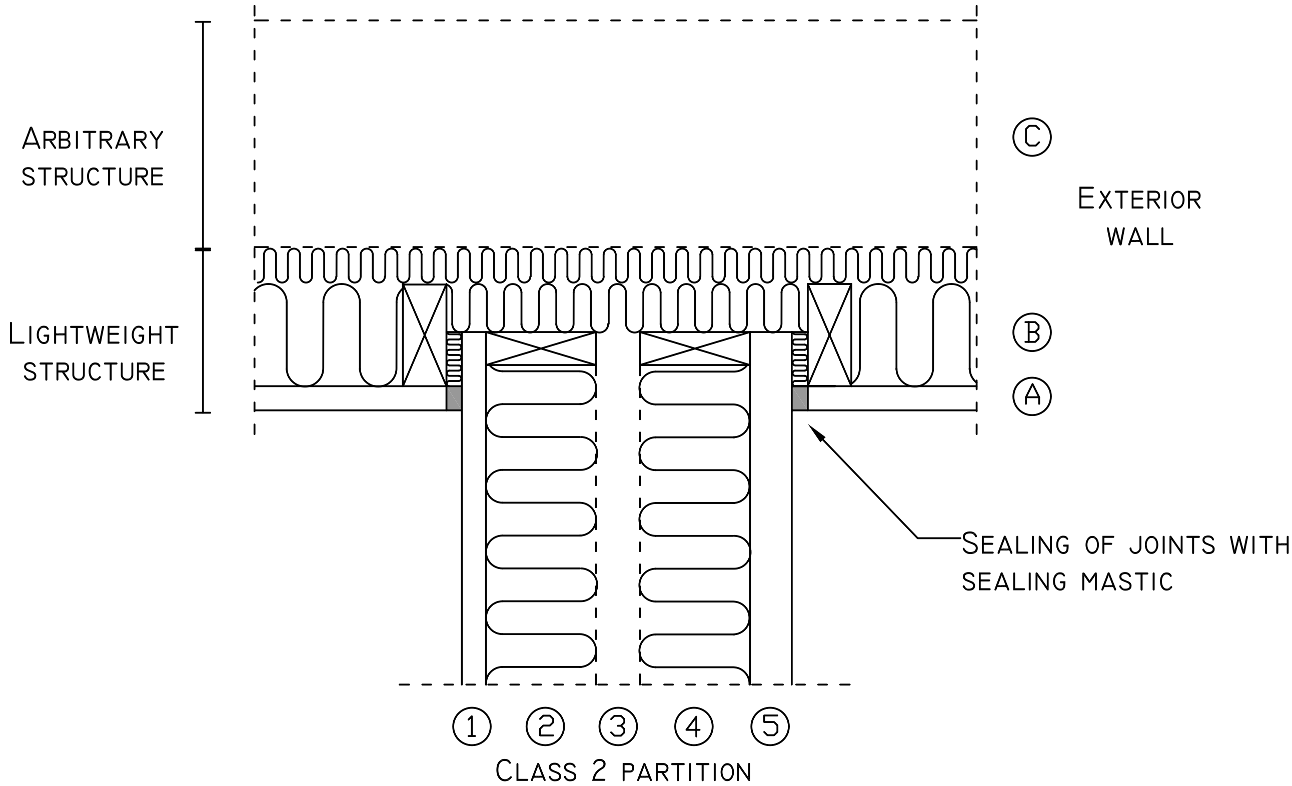


1. Chipboard 11 mm
2. Timber studding + mineral wool 50 mm
3. Air space 20 mm (empty, no connection between studs)
4. Timber studding + mineral wool 50 mm
5. Medium density fiberboard 19 mm

A. Arbitrary building board
B. Studding + mineral wool
C. Arbitrary structure

# Class 2 partition

Drawing 2-4:
Junction to exterior wall (principle). Alternative 2: continuous concrete inner envelope.

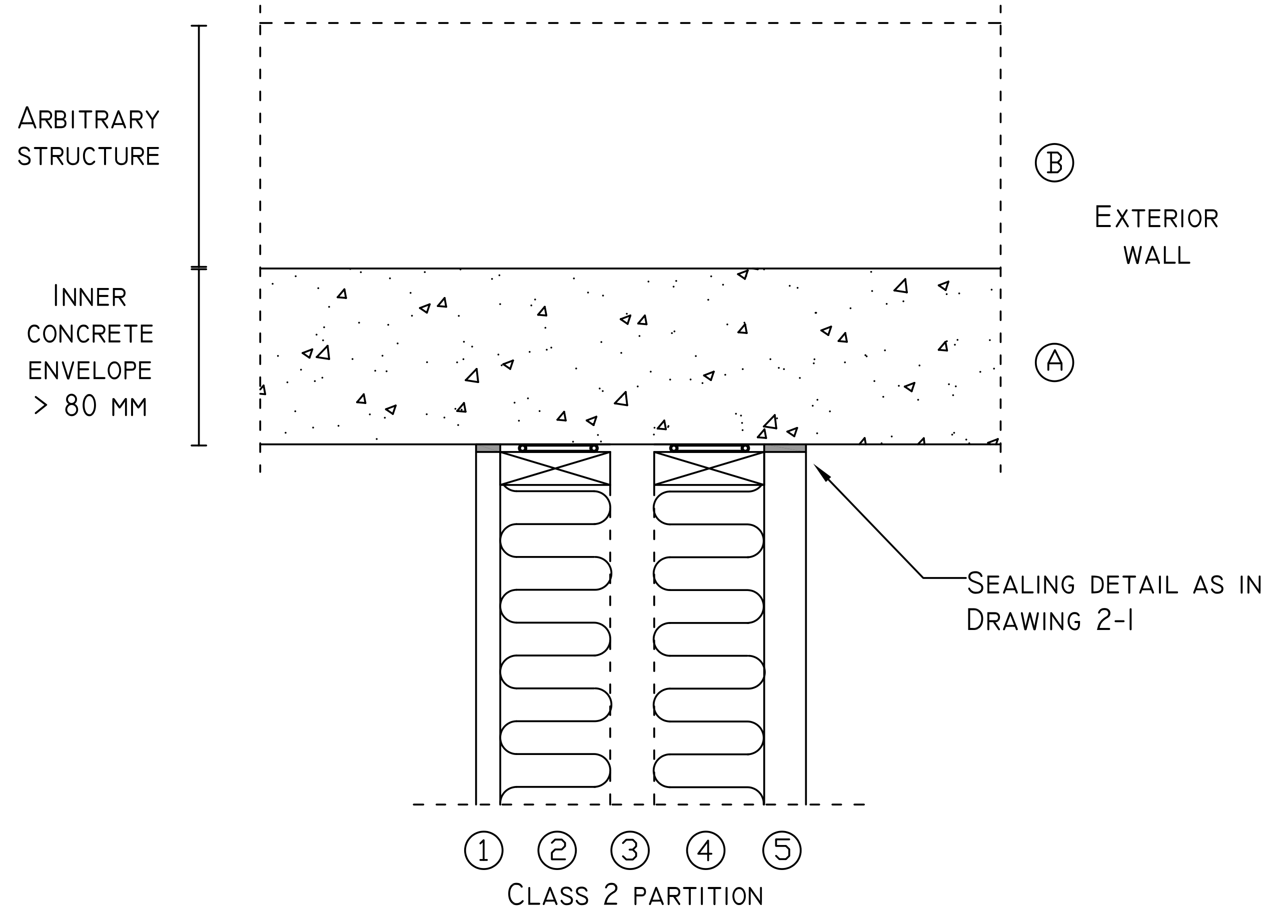


1. Chipboard 11 mm
2. Timber studding + mineral wool 50 mm
3. Air space 20 mm (empty, no connection between studs)
4. Timber studding + mineral wool 50 mm
5. Medium density fiberboard 19 mm

A. Massive concrete slab, thickness at least 80 mm
B. Arbitrary structure

# CLASS 3 PARTITION

DRAWING 3-1:
SECTION; SEALING TO INTERMEDIATE FLOOR / BASE FLOOR / ROOF. SEALING TO SIDE WALLS ACCORDINGLY.

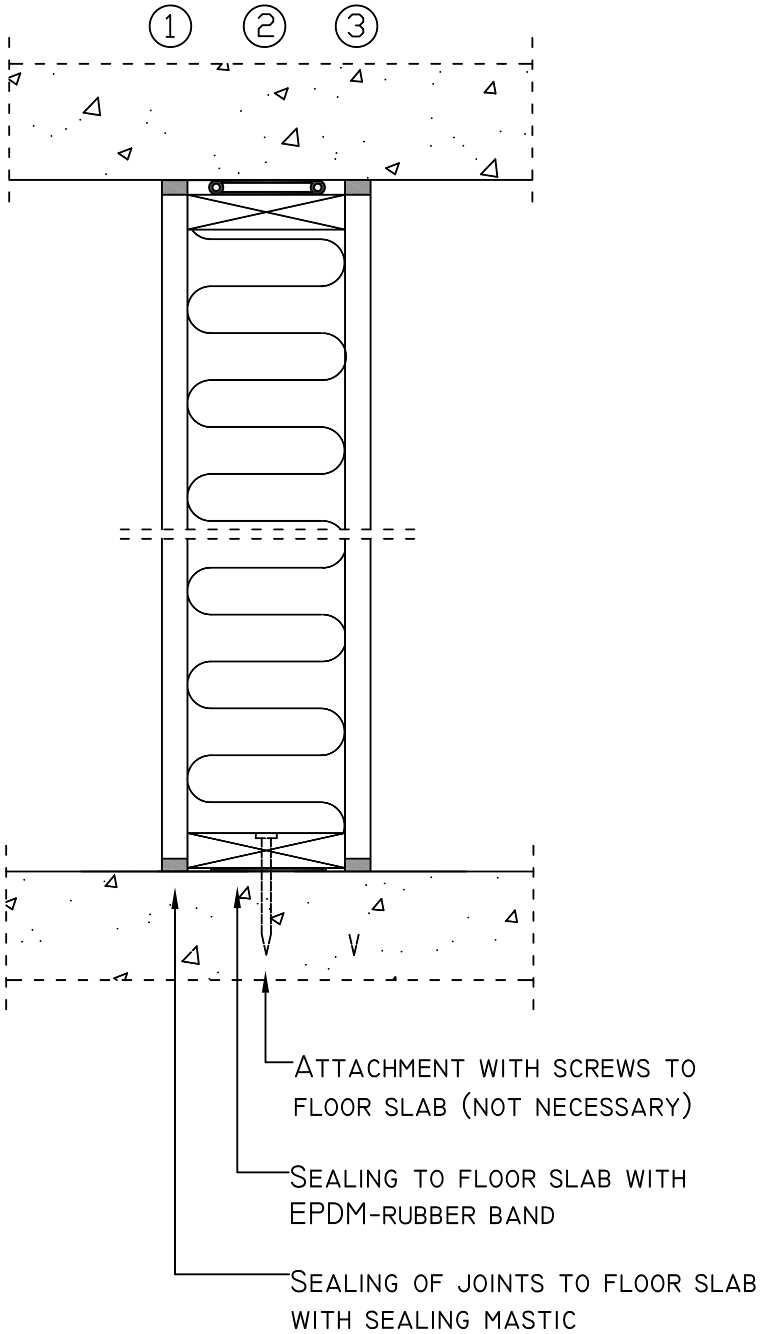


1. CHIPBOARD 11 MM
2. TIMBER STUDDING + MINERAL WOOL 92 MM (100% FILLING)
3. CHIPBOARD 11 MM

# CLASS 3 PARTITION

DRAWING 3-2:
T-JUNCTION BETWEEN CLASS 3 PARTITION AND LIGHTWEIGHT SIDE WALL STRUCTURE.

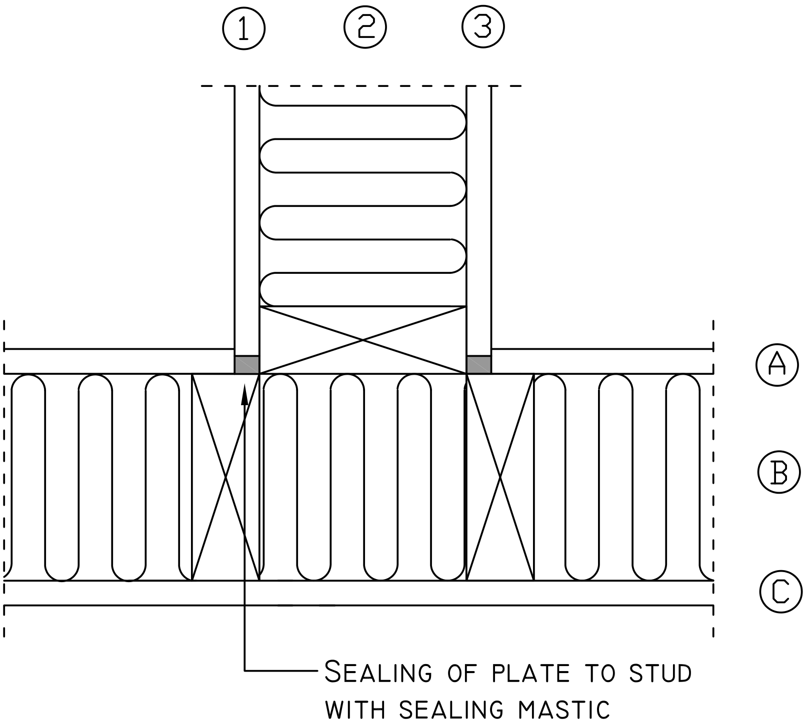


1. CHIPBOARD 11 MM
2. TIMBER STUDDING + MINERAL WOOL 92 MM (100% FILLING)
3. CHIPBOARD 11 MM

A. CHIPBOARD 11 MM
B. TIMBER STUDDING + MINERAL WOOL 92 MM (100% FILLING)
C. CHIPBOARD 11 MM

# Class 3 partition

Drawing 3-3:
Junction to exterior wall. Alternative 1: continuous concrete inner envelope.

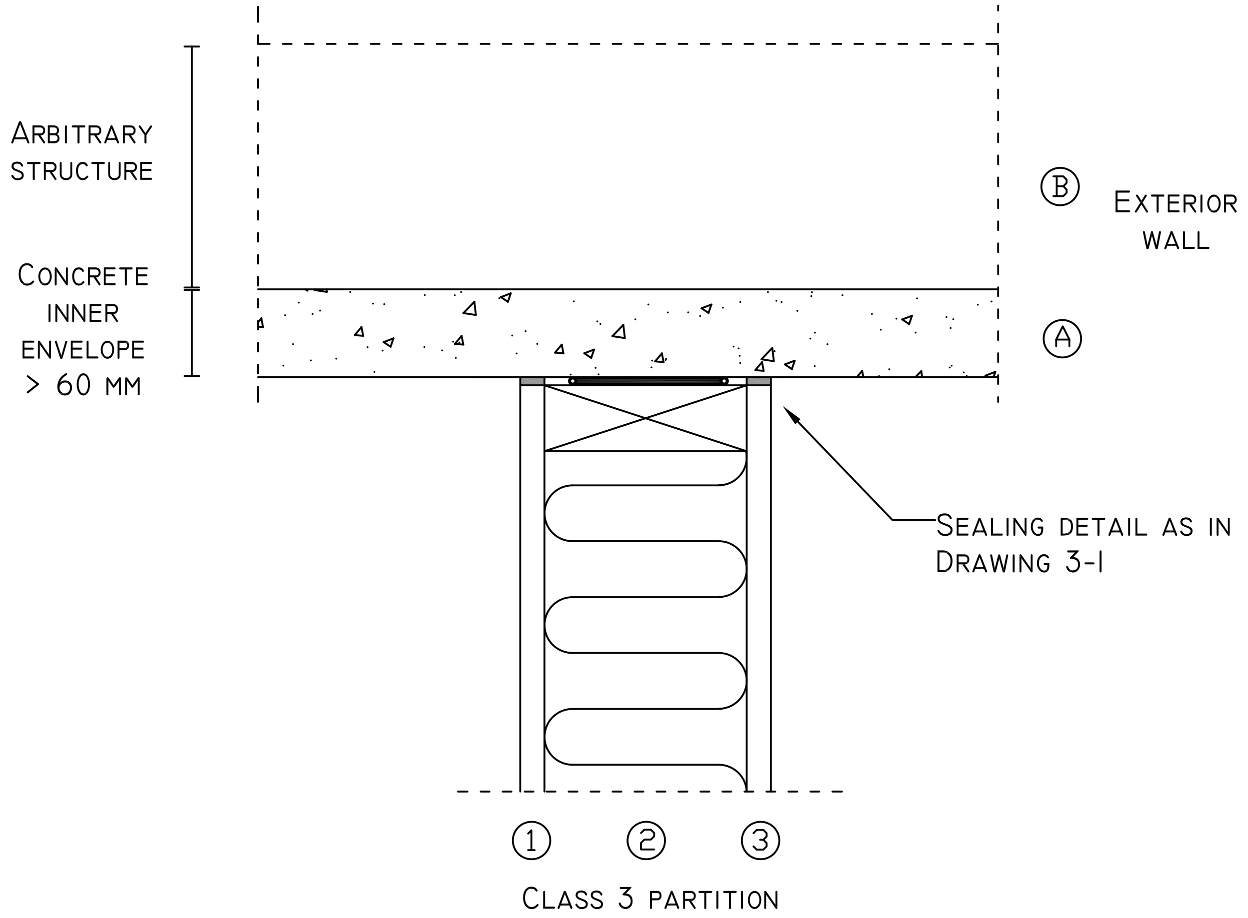


1. Chipboard 11 mm
2. Timber studding + mineral wool 50 mm (100 % filling)
3. Chipboard 11 mm

A. Massive concrete slab, thickness at least 60 mm
B. Arbitrary structure

# Class 3 partition

**Drawing 3-4:**
Junction to exterior wall (principle). Alternative 2: truncated lightweight structure.

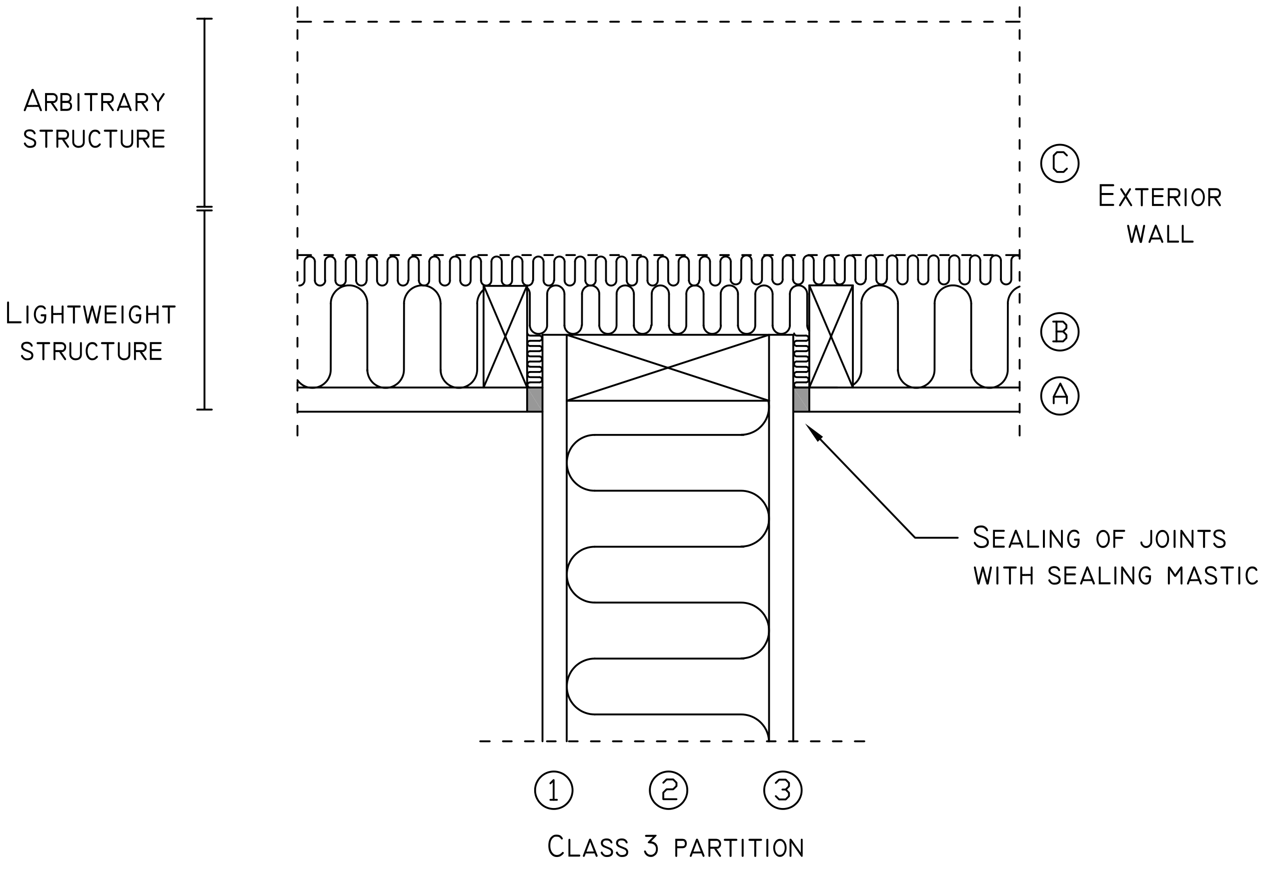


1. Chipboard 11 mm
2. Timber studding + mineral wool 92 mm (100% filling)
3. Chipboard 11 mm

A. Arbitrary building board
B. Studding + mineral wool
C. Arbitrary structure